

Formation and CD-Spectroscopic Characterization of antigenic
Protein/Polyanion Complexes

Inauguraldissertation

zur

Erlangung des akademischen Grades eines

Doktors der Naturwissenschaften (Dr. rer. nat.)

der

Mathematisch-Naturwissenschaftlichen Fakultät

der

Ernst-Moritz-Arndt-Universität Greifswald

vorgelegt von

Sven Brandt

geboren am 21.08.1982

in Rostock

Greifswald, September 2014

Dekan: Prof. Dr. Klaus Fesser

1. Gutachter: Prof. Dr. Christiane A. Helm
2. Gutachter: Prof. Dr. Gerald Brezesinski

Tag der Promotion: 19.12.2014

Optimism is merely a lack of information.

Heiner Müller (1929-1995)

Table of Contents

TABLE OF CONTENTS	1
LIST OF APPENDED PAPERS	3
CONTRIBUTION TO THE APPENDED PAPERS	4
ABBREVIATIONS	5
1. INTRODUCTION	7
1.1 PAPER I (PF4 EVOLUTIONARY ANALYSIS)	9
1.2 PAPER II (PF4/POLYANIONS)	11
1.3 PAPER III (PF4/DEFINED HEPARINS)	15
1.4 PAPER IV (PF4/POLYPHOSPHATES)	18
1.5 PAPER V (PF4/APTAMER)	23
1.6 PAPER VI (PROTAMINE/HEPARIN)	25
2. PROTEINS, POLYANIONS, REAGENTS	27
2.1 PROTEINS	27
2.1.1 PLATELET FACTOR 4	32
2.1.2 PROTAMINE	34
2.2 POLYANIONS	36
2.2.1 UNFRACTIONATED HEPARIN (UFH)	37
2.2.2 LOW-MOLECULAR-WEIGHT HEPARIN (LMWH) – REVIPARIN	38
2.2.3 2-O, 3-O DESULFATED HEPARIN (ODSH)	39
2.2.4 HEPARIN OLIGOSACCHARIDES (HO06, HO08, HO16)	40
2.2.5 FONDAPARINUX	40
2.2.6 CHONDROITIN SULFATE	41
2.2.7 DEXTRAN SULFATE	41
2.2.8 HYALURONIC ACID (HA)	42
2.2.9 DEXTRAN	43
2.2.10 DNA – PROTEIN C-APTAMER	44
2.2.11 POLYPHOSPHATES – P3, P45, P75	45
2.3 REAGENTS, MATERIALS	46
2.4 DEVICES AND SOFTWARES	47
3. BACTERIA	48
3.1 ESCHERICHIA COLI (E. COLI JM109-FITC)	52
3.2 FITC LABELING	52
4. EXPERIMENTAL TECHNIQUES	54
4.1 CIRCULAR DICHROISM (CD) SPECTROSCOPY	54

4.2	ENZYME IMMUNOASSAY (EIA)	64
4.3	ISOTHERMAL TITRATION CALORIMETRY (ITC)	67
4.4	FLOW CYTOMETRY	71
4.4.1	PF4 BINDING TO GRAM-NEGATIVE BACTERIAL SURFACE	72
4.4.2	PHAGOCYTOSIS OF PF4-MARKED BACTERIA BY POLYMORPHONUCLEAR LEUKOCYTES (PMNs)	73
5.	ABSTRACT	75
5.1	EVOLUTIONARY CONSERVATION OF PF4 (PAPER I – PF4/EVOLUTION)	75
5.2	PF4 INTERACTION WITH POLYANIONS (PA) OF VARYING LENGTH AND DEGREE OF SULFATION (PAPER II – PF4/PA)	76
5.3	PF4 INTERACTION WITH DEFINED OLIGOMERIC HEPARINS (PAPER III – PF4/DEFINED HEPARINS)	76
5.4	PF4/POLYPHOSPHATES (POLYP) COMPLEX ANTIGENICITY AND INTERACTION WITH <i>ESCHERICHIA COLI</i> (<i>E. COLI</i>, PAPER IV – PF4/POLYP)	77
5.5	NUCLEIC ACID BASED APTAMERS INDUCE STRUCTURAL CHANGES IN THE PF4 MOLECULE (PAPER V – PF4/APTAMER)	77
5.6	PROTAMINE INTERACTION WITH HEPARIN (PAPER VI – PS/HEPARIN)	78
5.7	CONCLUSION AND OUTLOOK	78
6.	PAPERS	79
6.1	PAPER I: PLATELET FACTOR 4 BINDING TO LIPID A OF GRAM-NEGATIVE BACTERIA EXPOSES PF4/HEPARIN-LIKE EPITOPES	79
6.2	PAPER II: CHARACTERISATION OF THE CONFORMATIONAL CHANGES IN PLATELET FACTOR 4 INDUCED BY POLYANIONS: TOWARDS IN VITRO PREDICTION OF ANTIGENICITY	88
6.3	PAPER III: BINDING OF ANTI-PLATELET FACTOR 4/HEPARIN ANTIBODIES DEPENDS ON THE THERMODYNAMICS OF CONFORMATIONAL CHANGES IN PLATELET FACTOR 4	101
6.4	PAPER IV: POLYPHOSPHATE CHAIN LENGTH DETERMINES THE ANTIGENICITY OF THE COMPLEXES FORMED WITH PLATELET FACTOR 4 (PF4) AND THE BINDING OF PF4 TO BACTERIA	110
6.5	PAPER V: COMPLEX FORMATION WITH NUCLEIC ACIDS AND APTAMERS ALTERS THE ANTIGENIC PROPERTIES OF PLATELET FACTOR 4	124
6.6	PAPER VI: ANTI-PROTAMINE-HEPARIN ANTIBODIES: INCIDENCE, CLINICAL RELEVANCE, AND PATHOGENESIS	135
7.	REFERENCES	144
8.	STATUTORY DECLARATION	152
9.	CURRICULUM VITAE	153
	ACKNOWLEDGEMENT	155

List of appended Papers

This thesis is based on the work contained in the following papers:

	Platelet factor 4 binding to lipid A of Gram-negative bacteria exposes PF4/heparin-like epitopes
I. PF4/evolution	Krystin Krauel, Claudia Weber, <u>Sven Brandt</u> , Ulrich Zähringer, Uwe Mamat, Andreas Greinacher, Sven Hammerschmidt Blood, 2012 Oct 18;120(16):3345-52
	Characterization of the Conformational Changes in Platelet Factor 4 Induced By Polyanions: Towards In-Vitro Prediction of Antigenicity
II. PF4/PA	<u>Sven Brandt</u> , Krystin Krauel, Kay E. Gottschalk, Thomas Renné, Christiane A. Helm, Andreas Greinacher, Stephan Block Thrombosis Haemostasis 2014; 112: 53-64
	Interaction between Platelet Factor 4 and Heparins: Thermodynamics determines Conformational Changes required for binding of Anti-Platelet Factor 4/Heparin Antibodies
III. PF4/defined heparins	Martin Kreimann, <u>Sven Brandt</u> , Stephan Block, Krystin Krauel, Andreas Greinacher, Mihaela Delcea Blood, 2014 Aug 22; poi: blood-2014-03-559518
	The impact of polyphosphate chain length on the antigenicity of PF4/polyP complexes
IV. PF4/polyP	<u>Sven Brandt</u> , Krystin Krauel, Miriam Jaax, Thomas Renné, Christiane Helm, Sven Hammerschmidt, Mihaela Delcea, Andreas Greinacher submitted to Blood
	Complex formation with nucleic acids and aptamers alters the antigenic properties of platelet factor 4
V. PF4/aptamer	Miriam E. Jaax, Krystin Krauel, Thomas Marschall, <u>Sven Brandt</u> , Julia Gansler, Birgitt Füll, Bettina Appel, Silvia Fischer, Stephan Block, Christiane A. Helm, Sabine Müller, Klaus T. Preissner, Andreas Greinacher Blood, 2013 Jul 11;122(2):272-81
	Anti-protamine-heparin antibodies: incidence, clinical relevance, and pathogenesis
VI. PS/heparin	Tamam Bakchoul, Heike Zöllner, Jean Amiral, Simon Panzer, Sixten Selleng, Thomas Kohlmann, <u>Sven Brandt</u> , Mihaela Delcea, Theodore E. Warkentin, Ulrich J. Sachs, Andreas Greinacher Blood, 2013 Apr 11;121(15):2821-7
<hr/> Publication not included in the thesis <hr/>	
	Vaccination with anti-idiotypic antibody ganglidiomab mediates a GD2-specific anti-neuroblastoma immune response
VII. anti-idiotypic Ab	Holger N. Lode, Manuela Schmidt, Diana Seidel, Nicole Huebener, Diana Brackrock, Matthias Bleeke, Daniel Reker, <u>Sven Brandt</u> , Hans-Peter Müller, Christiane A. Helm, Nikolai Siebert Cancer Immunology and Immunotherapy, 2013 Jun;62(6):999-1010

Contribution to the appended Papers

paper I – PF4/evolution	I planned and carried out the amino acid sequence survey for the evolution analysis of PF4. I wrote related parts of the paper.
paper II – PF4/PA paper IV – PF4/polyP	I had the main responsibility for writing the paper.
paper II – PF4/PA paper III – PF4/defined heparins paper IV – PF4/polyP paper V – PF4/aptamer paper VI – PS/heparin	I planned, performed and analyzed the circular dichroism measurements.
paper III – PF4/defined heparins paper IV – PF4/polyP	I planned, carried out and analyzed the enzyme immuno assay measurements.
paper IV – PF4/polyP	I planned, carried out and analyzed the isothermal titration calorimetry and the flow cytometry measurements.
Publication not included in the thesis	
paper VI – anti-idiotypic Ab	I planned, carried out and did the analysis of the Surface plasmon resonance measurements. I wrote related parts of the paper.

Abbreviations

AA	amino acids	PA	polyanions
Ab	antibody	PBS	phosphate buffered saline
AG	antigen	PDI	polydispersity
CD	circular dichroism	PF4	platelet factor 4
DNA	deoxyribonucleic acid	polyP	polyphosphates
EIA	enzyme immunoassay	PS	protamin sulfate
fpx	fondaparinux	RCP	right circularly polarized
g_i	weight of sample at MW M_i	RT	room temperatur
HA	hyaluronic acid	TMB	3,3', 5,5' tetramethyl- benzidin
hep	heparin	UFH	unfractionated heparin
HIPA	heparin-induced platelet activation assay		
HIT	heparin-induced thrombocytopenia		
IgG	immunglobulin G		
ITC	isothermal titration calorimetry		
LCP	left circularly polarized		
LPS	lipopolysaccharide		
LMWH	low molecular weight heparin		
M_i	certain molecular weight i		
\overline{M}_n	number average MW		
\overline{M}_w	weight average MW		
MW	molecular weight		
N_i	number of molecules at MW M_i		
ODSH	2-O, 3-O desulfated heparin		
P3	triphosphate		
P45	45mer polyphosphate		
P75	5mer polyphosphate		

1. Introduction

Almost all processes that take place in an organism are mediated by proteins with a broad diversity of functions. The properties of a protein depend mainly on its tertiary and quaternary structure (see chapter 2.1 Protein) while the amino acid sequence, the so-called primary structure is the base of the folding. Proteins are designed to do their functions and are adapted to the surrounding they are acting in. In the latter regard, hydrophilicity or hydrophobicity plays an important role. For the expression of soluble proteins, the amino acid chain folds in a way that charged as well as polar amino acids are exposed to the aqueous solution and apolar uncharged amino acids are hidden or shielded from it. Vice versa, in case of insoluble proteins like membrane proteins, it is crucial to have at least apolar regions on the surface to be anchored in the hydrophobic part of the lipid bilayer. Platelet factor 4 (PF4) the central

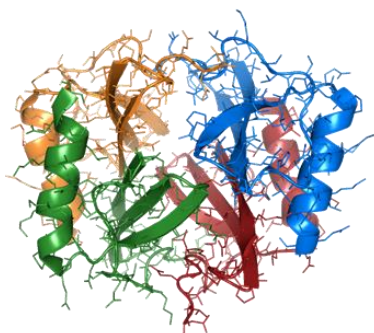


Figure 1.0.1: Cartoon of the homotetramer platelet factor 4 (PF4) based on crystallographic data (PDB code: 1RHP) with the four subunits colored in blue, green, orange, and red.

protein in this thesis belongs to the fraction of soluble proteins. In the majority of mammalian organisms, PF4 and homologous proteins (e.g. interleukin 8 and sequenced but so far undescribed proteins) are found, but not in plants or bacteria.¹

The homotetrameric chemokine PF4 (see figure 1.0.1) was initially described as a platelet-derived heparin-neutralizing factor.² Later it was found that it is involved in hemostasis,^{3,4} platelet coagulation interference,^{3,4} angiogenesis,^{3,5,6} host inflammatory response

promotion,² and that it is a chemoattractant for immune cells like neutrophils and monocytes.^{2,7-9} PF4 gained wide interest because of its central role in the life-threatening, immune-driven, adverse drug effect heparin-induced thrombocytopenia (HIT, see Figure 1.0.2),^{10,11} which occurs in up to 3% of patients receiving unfractionated heparin (UFH) after major surgery.¹² Here, PF4 forms complexes with the polyanion (PA) heparin, which is administered to avoid blood clotting during and after surgeries. By the

complex formation, PF4 competes with antithrombin for the binding sites on the heparin chain and neutralizes the anticoagulatory effect of the latter.

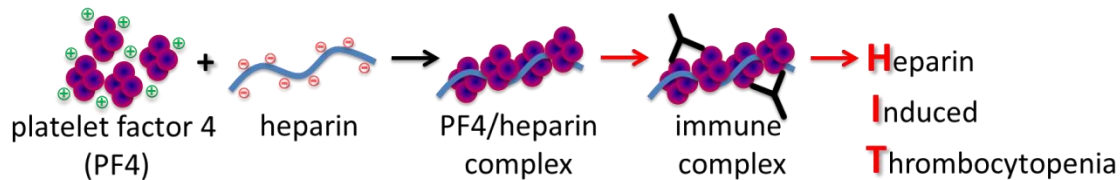


Figure 1.0.2: Platelet factor 4 (PF4) with an equator of positively charged amino acids forms complexes with the negatively charged drug heparin.¹³ Some patients develop antibodies or are already pre-immunized against an epitope that is formed when PF4 aligns on the PA strand. The resulting immune reaction induces the opposite of what is intended by the administration of heparin – rather than preventing thrombosis during surgeries, blood clots are formed in the life-threatening adverse drug effect heparin-induced thrombocytopenia (HIT).

Some patients develop antibodies directed against these multimolecular PF4/heparin complexes.¹⁵ The

antibodies that are formed after administration of heparin are mostly of the IgG class. This type of anti-

bodies and the time of the early onset are not charac-

teristic for a primary immune response where IgM is

formed first followed by IgG after two weeks (see

figure 1.0.3). The early onset of IgG is a hint towards a

secondary immune response meaning that the

patient's immune system has 'seen' an antigen similar

to what is exposed on the PF4/heparin complexes.

The formation of PF4/heparin/antibody complexes

(immune complexes) leads to the release of further

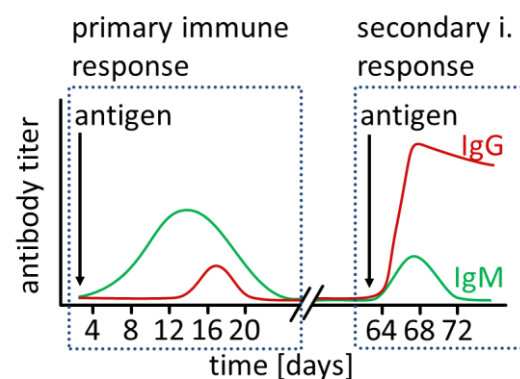


Figure 1.0.3: Classes of antibodies occurring after first antigen contact during primary immune response and after second contact with the same antigen in secondary immune response. Adapted from *Grundwissen Immunologie* by Schütt and Bröker.¹⁴

PF4, formation of multimolecular complexes to which even more antibodies can bind.^{10,13,16} When the

immune complexes bind to platelets *via* the Fc-parts of the antibodies, Fcγ1a-receptors on the platelets

surface get cross-linked, which induces platelet activation, leading to further aggregation and formation

of blood clots.^{15,17} Additionally, PF4 and PF4/heparin/IgG immune complexes then bind to endothelial

cells, leading to severe damage of the cells.^{13,18-20} The prevailing prothrombotic state bares an increased

risk for thrombosis.^{21,22}

It is widely accepted that anti-PF4/heparin antibodies recognize an antigen exposed on PF4²³ at a certain PF4/heparin molar ratio^{13,24} at which the opposite charges of PF4 and heparin are neutralized.^{16,25} Epitope expression on PF4 is not limited to sulfated PA like heparins. Complexes of PF4 with DNA containing phosphate groups and bacterial phospholipids also showed cross-reaction with PF4/heparin antibodies,²⁶⁻²⁸ meaning that a similar epitope is formed on the protein while the PA can be exchanged and antibody recognition as well as immune response persist.^{1,26-28} At the mentioned optimal ratio, PF4 tetramers are aligned on the heparin strand and forced into close approximation.¹⁹ Understanding why an endogenous protein turns immunogenic when forming a complex with a PA is of fundamental interest in basic science as well as in the medical and pharmaceutical field. Knowing the underlying mechanism will be helpful for the development of polyanionic drugs not bearing the risk of an immune reaction induction and may also give hints towards the general mechanism of antibody induction.

1.1 Paper I (PF4 Evolutionary Analysis)

As aforementioned, PF4 binds to bacterial surfaces. There is a cross-reaction with PF4/heparin antibodies when PF4 binds to a bacterial surface, suggesting that it has the function of a marker for potential pathogens.²⁶ To explore if PF4 may also be a part of an ancient immune system against bacteria, we investigated the binding of PF4 to bacterial surface in detail in **paper I** (*PF4 evolutionary analysis*). We found that PF4 binds *via* its positively charged amino acids to the negatively charged phospholipid lipid A, the innermost and highly conserved part of the lipopolysaccharide (LPS) of Gram negative bacteria (see chapter 3. Bacteria).¹ The less lipid A was covered with outer core and O-antigen, the more PF4 bound to the bacterial surface. The knowledge of PF4 binding to potential pathogens like bacteria and exerting a similar epitope on the bacterial surface like in PF4/heparin complexes, supports the hypothesis that PF4 is part of an ancient host defense mechanism.²⁶ LPS is conserved in the envelope of Gram negative bacteria. The question to be answered was whether the structures on the PF4 surface required for the binding to lipid A are also conserved. By executing an amino acid sequence survey, we

found indeed that the mainly positively charged amino acids contributing to the heparin binding site on the PF4 surface or on similar proteins (e.g. PF4 like, interleukin-8 and so far uncharacterized proteins; see figure 1.1.1) are highly conserved in different vertebrate species (**paper I (PF4/evolution)**).¹ PF4 being expressed in miscellaneous vertebrates additionally supports the idea of PF4 as an ancient host defense mechanism. Bacteria covered with PF4 are recognized by sera originating from HIT patients and known to contain anti-PF4/heparin antibodies. It is very likely that PF4 forms a similar epitope on the bacterial surface and in the PF4/heparin complex which is recognized by the same antibodies contained in the aforementioned sera. This is supported by the fact that PF4-covered bacteria were able to induce an immune reaction.²⁹ The finding let us speculate why the lipid A is covalently linked with a polysaccharide chain. When PF4 easily marks bacteria via binding to lipid A, bacteria might have covered the structure that made it vulnerable to the immune system of its host. By the usage of several Gram negative mutants with different O-antigen chain lengths, Krystin Krauel showed that the longer polysaccharide chain of the mutant was, the less PF4 bound to the bacterial surface and the lower was the possibility of an immune reaction.

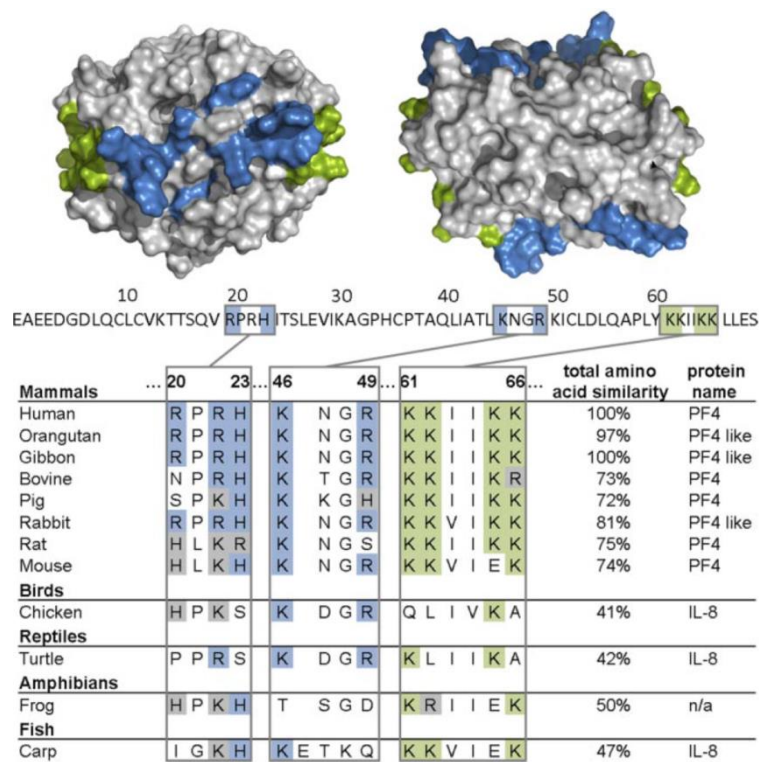


Figure 1.1.1: Amino acids of PF4 important for heparin binding are largely conserved among species. Alignment of the heparin binding region (R20, R22, H23, K46, R49, K61, K62, K65, and K66) of PF4, IL-8, and an uncharacterized protein (n/a) and total amino acid similarity of various species in percentages compared with human (100%) is shown. Above the amino acid sequence of 1 PF4 monomer (70 amino acids, primary structure without signal sequence, UniProt P02776), the crystal structure of a PF4 tetramer (quaternary structure, PDB code 1f9q) is depicted from the front (left) and from the top view (right). Lysine residues of the C-terminus (K61, K62, K65, and K66) are highlighted in green; arginine (R20, R22, and R49), histidine (H23), and other lysine residues (K46) are highlighted in blue. The pictures of the crystal structure of PF4 were made using PyMOLMolecular Graphics System Version 1.3 Schrödinger LLC.

1.2 Paper II (PF4/Polyanions)

At the time the work of this thesis started, it was believed that repetitive structures formed by PF4 on a heparin chain, form an epitope to which antibodies bind inducing the adverse drug effect HIT. It was believed that these repetitive structures might exhibit similarities with capsids of viruses and are therefore, recognized by the immune system of some patients.¹⁹ NMR studies suggested that the complex formation is accompanied by changes in the secondary and tertiary structure of PF4.³⁰ The NMR measurements were done with PF4-M2, a symmetric variant of PF4. It cannot be ruled out that this mutant with slightly different primary structure behaves differently, when forming a complex with PA like heparin. The direct experimental proof for secondary structure changes of PF4 upon complex formation with PA was lacking.

To investigate the structure and potential structural changes of PF4, I used circular dichroism (CD) spectroscopy. Investigating the PF4/PA system with CD spectroscopy is advantageous in many respects. CD spectroscopic measurements have proven to be correct for direct interpretation of structural changes in a protein upon binding to heparin (antithrombin III/heparin system).³¹ In general, CD spectroscopy is not very expensive with respect to protein consumption and also not very time consuming. For NMR studies, which give more detailed information about the protein structure, the asymmetry of PF4 is a problem. This drawback does not play a role in CD spectroscopy, because the signal that is measured arises from the monomer and not from the entire tetrameric protein. The PA that were tested for complex formation with PF4 did not interfere with the measurements, as they did not exhibit a CD signal at all or only at very high concentrations. By carrying out a deconvolution of a protein CD spectrum, it is possible to determine its secondary structure composition. The deconvolution of a protein CD spectrum is most reliable when the protein has a certain α -helical content. PF4 has one α -helix per monomer, which makes it especially suitable for the usage of CD spectroscopy deconvolution. Carrying out a deconvolution only gives secondary structure composition of a protein but from crystallographic data we

know the location of the secondary structures in the PF4 molecule (PDB code: 1f9q). Their distribution is beneficial for working with CD spectroscopy. Secondary structures like the antiparallel β -sheets are agglomerated in the center of the tetramer and all four α -helices are located on the surface of the protein. If the deconvolution of the protein spectra suggests an increase or decrease in a respective secondary structure, the location of structural change is known and it is possible to make an educated guess of the amino acids involved.

In **paper II** (PF4/PA) complex formation between PF4 and different PA was investigated (see table 1.2.1).²⁸ It is believed that the PA wrap around the PF4, forming an interface between the equatorial ring of positively charged amino acids and the sulfate groups of the PA.

Table 1.2.1: List of the PA investigated in **paper II** (PF4/PA). **left:** The PA investigated regarding the degree of polymerization. **right:** The PA assessed regarding degree of polymerization. (* no sulfate groups but carboxy groups, **no sulfate groups)

PA investigated in paper II (PF4/PA)			
degree of polymerization		degree of sulfation	
unfractionated heparin (UFH)	long	dextran sulfate	high
	↓	unfractionated heparin (UFH)	↓
	short	2-O, 3-O desulfated heparin (ODSH)	low
fondaparinux (pentasaccharide)	short	hyaluronic acid*	low
		dextran**	

Clinical studies reveal that three factors have an influence on the immunogenicity of PF4/PA complexes:

i. the molar PF4/PA ratio, ii. the degree of polymerization of the PA and iii. their degree of sulfation. By assessing clinically relevant PA of varying length and degree of sulfation, using the established PF4/PA solid phase enzyme immunoassay (EIA)³² (see chapter 4.2) and CD spectroscopy, we were able to show in **paper II** (PF4/PA) that PF4 changes its secondary structure when forming an immunogenic complex with certain PA. We thereby built the basis of a prediction system just looking at CD data to judge whether a

PA has the potential to form antigenic complexes without the need for (sometimes strongly deviating) patients sera used in the EIA. The deconvolution of the CD spectroscopic data revealed that there is a decrease in α -helical and β -turn content, which is balanced by a remarkable increase in the antiparallel β -sheet content.

In case of PF4, the antiparallel β -sheet is a good measure for the overall change in the structure of PF4. This is because it is the secondary structure that changed the most during titration with a PA and it is the only secondary structure whose content increased. Additionally, it is unlikely that an antibody binds to a disappearing structure, but rather recognizes a neoepitope, meaning a structure that is newly developed. Therefore, in the following, an increase in antiparallel β -sheet, changes in CD signal and secondary structural changes of the protein have essentially the same meaning (for the PF4/PA system).

When comparing the antigenicity, meaning antibody binding measured with the PF4/PA solid phase EIA, with the structural changes in the protein measured by CD spectroscopy it was found:

- i. PF4/PA complexes showing high antibody recognition also showed remarkable changes in the CD signal.
- ii. A correlation between the degree of sulfation and the amount of structural changes as well as in degree of antigenicity exists. The

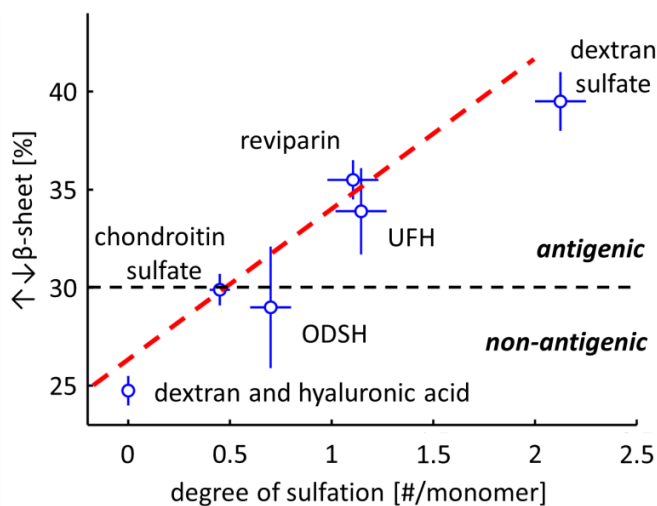


Figure 1.2.1: Correlation between the degree of sulfation and the maximally induced antiparallel β -sheet in the PF4 molecule.

higher the number of negative charges per repeating unit of the PA was, the higher were the secondary structural changes in the protein (see figure 1.2.1). Based on the empirically

- determined antigenicity threshold in the EIA, we were able to define an extent of changes in the antiparallel β -sheet that has to be exceeded (>30%) to turn a PF4/PA complex antigenic. This formed the basis of the antigenicity prediction with the help of CD spectroscopy.
- iii. In case of the degree polymerization a certain chain length had to be exceeded to observe structural changes or antigenicity (yes/no question). A polyanionic pentamer such as fondaparinux does not induce any change in the protein structure and the PF4/fondaparinux complex is also not recognized in the EIA. We propose a model in which at least two PF4 tetramers have to be brought into close approximation to undergo structural changes to form the neoepitope that is recognized by antibodies. The pentamer binds probably to PF4, but it is too short to hold two PF4 tetramers together.
- iv. Antibody binding and secondary structural changes as observed by CD spectroscopy show the same dependence on the PF4:PA ratio (see figure 1.2.2). The course of the curve of antigenicity and antiparallel β -sheet content is very similar. We observed a fast onset in both, antigenicity as well as an antiparallel β -sheet content, which is followed by a distinct peak at a certain PA dependent PF4:PA ratio and ends in a less steep decrease in both antigenicity and antiparallel β -sheet content. The raw CD signal as well as its deconvolution tends to a native-like state again at higher PA concentration.

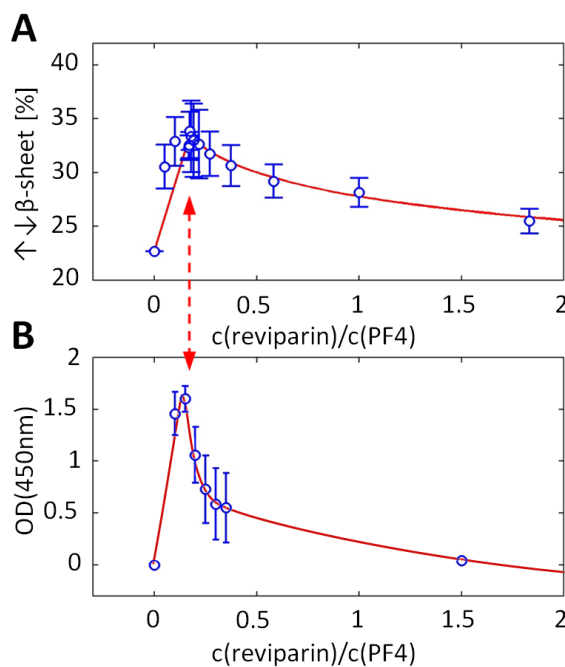


Figure 1.2.2: Structural changes observed by CD spectroscopy (A) and antibody binding in EIA (B) show the same molar PF4:PA ratio dependency with similar onset, decrease and matching peak position.

Therefore, we conclude that the changes were reversible in most cases. Exceptions from this behavior were the aforementioned pentamer fondaparinux, showing no changes over the whole titration and the highly sulfated dextran sulfate where the antigenicity and the structural changes remained even at very high PA concentrations, indicating that the changes were irreversible.

- v. Notably, the peak position of maximum antibody binding and maximum antiparallel β -sheet matched (see figure 1.2.2) with the only exception unfractionated heparin (UFH), where a correction factor had to be introduced to get matching peak positions for prediction of antigenicity based on the CD measurements. We speculate this is due the polydispersity of UFH and that the formed complexes are therefore quite heterogeneous in size, which might lead to deviations in the read-out of the two used techniques.

After observing that PF4 binds to lipid A with a phospholipid anchor in **paper I** (*PF4 evolutionary analysis*) and thus, finding that the binding of PF4 is not restricted to negative charges deriving from sulfate groups present in all heparins, pure phosphates in form of inorganic polyphosphates (polyP) were also tested for complex formation, structural changes and antigenicity. It was found that complexes of PF4 and polyP chains also induce structural changes in the PF4 molecule and even surpassing the threshold of 30% to be antigenic. Further, it turned out that polyP are beneficial for CD measurements as they do not add absorption in the measured wavelength range for far-UV CD spectra like for example, heparins do (see chapter 4.1 Circular dichroism).

1.3 Paper III (PF4/defined Heparins)

After testing clinically relevant but relatively undefined glycosaminoglycans (GAG, see chapter 2.2 Polyanions) in terms of size distribution in **paper II** (*PF4/PA*), the focus was laid on highly purified, monodisperse heparins. In **paper III** (*PF4/defined heparins*) additional physicochemical techniques were introduced by Martin Kreimann to characterize more in detail the complexes formed between PF4 and

defined heparins purchased from Iduron Ltd. (Manchester/UK).³³ Additionally to the heparin oligomers (HO) consisting of 6 (HO06), 8 (HO08) und 16 (HO16) subunits, UFH and the pentamer fondaparinux were tested with the additional methods: isothermal titration calorimetry (ITC, see chapter 4.3 Isothermal titration calorimetry) to analyze the thermodynamics of the complex formation, and atomic force microscopy (AFM) to investigate the complex sizes as well as the occurrence of multimolecular complexes. The relatively clear picture of clinically relevant heparins is put into perspective in **paper II** (PF4/PA). The model that a certain extent of structural change has to be exceeded to turn complexes antigenic had to be extended in case of the defined heparin oligomers. We found that the structural changes are necessary but not sufficient to form antigenic complexes. The three required characteristics were:

- i. An increase in antiparallel β -sheet exceeding $\sim 30\%$ was achieved by UFH, HO16, HO08, and HO06, but not by fondaparinux as shown by CD spectroscopy.
- ii. Multimolecular complexes have to be formed. This requirement was fulfilled by UFH, HO16, and HO08 as shown by AFM.
- iii. A negative entropy during complex formation has to be achieved. The necessity was only fulfilled by UFH and HO16 as shown by ITC.

The increase in antiparallel β -sheet was sufficient ($>30\%$) for all tested PA except for fondaparinux. Nonetheless, the course was different for each PA (see figure 1.3.1). For the complex formation of PF4 with UFH, the curve progression with its steep onset and flat decrease (see figure 1.3.1 A) was already known from **paper II** (PF4/PA). The curve for the complexes formed between PF4 and HO16 is very similar but with the differences that the maximum antiparallel β -sheet is $\sim 5\%$ higher and that the maximum change was observed at a lower concentration ratio (see figure 1.3.1 B), suggesting a more efficient complex formation due to the lower polydispersity. Further, the peak of maximum secondary

structural change is much narrower for HO16. Continuing with the complexes formed between HO08 (figure 1.3.1 C), the peak broadened again and its position was shifted to a slightly higher concentration.

However, the main difference to the PA investigated before is the reduced reversibility of the secondary structural change. The antiparallel β -sheet content stays nearly constant around 36% at higher PA concentrations. As a continuation, of the stepwise change in curve progression from the longer to the shorter heparin oligomers, the curve of the PF4/HO06 complexes is lacking a peak and directly goes into saturation at a certain PF4:HO06 ratio (see figure 1.3.1 D). With ~36.5%, the maximum antiparallel β -sheet content is lower compared to the other heparin oligomers. From the CD results it can be concluded that not only the amount of antiparallel β -sheet has to exceed 30%, but also these changes have to be reversible. The necessity of reversibility is not fulfilled in case of the short heparin oligomers HO08 and HO06 being close to the pentamer fondaparinux, not in-

cluding any structural changes in the PF4 molecule (see figure 1.3.1 E). In **paper II (PF4/PA)** we found, that the secondary structural changes in PF4 induced by the highly charged dextran sulfate were also not reversible. Obviously, it has to be discriminated between the irreversibility of structural changes induced

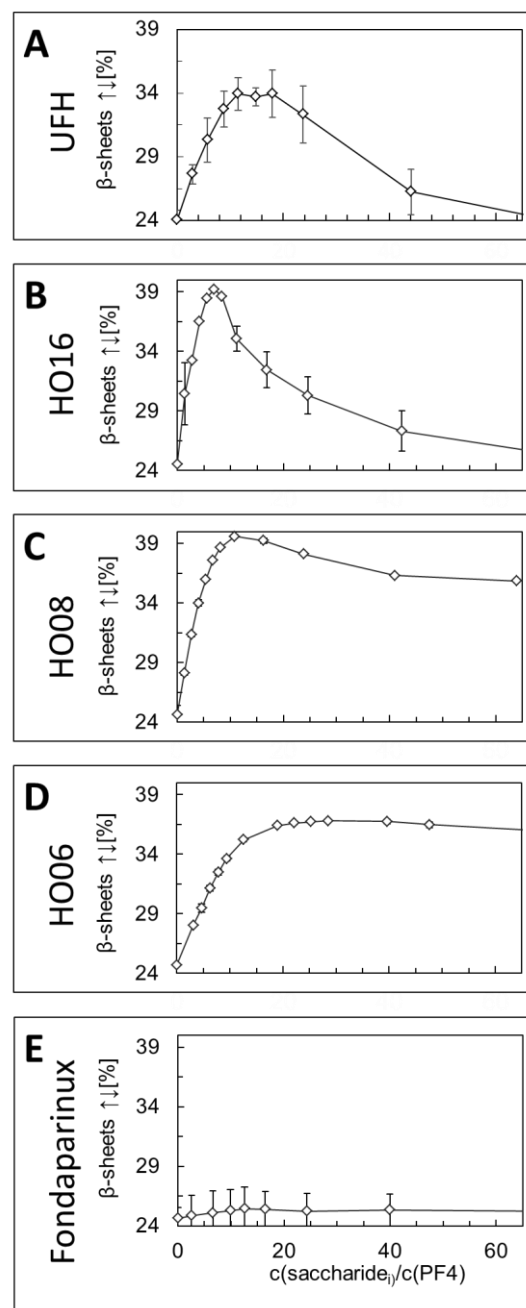


Figure 1.3.1: Deconvolution of CD spectra for PF4 titrated with: a – UFH, b – HO16, c – HO08, d – HO06, e – fondaparinux.

by short PA chains and the irreversible changes of highly sulfated PA of sufficient chain length like dextran sulfate (see **paper II – PF4/PA**).

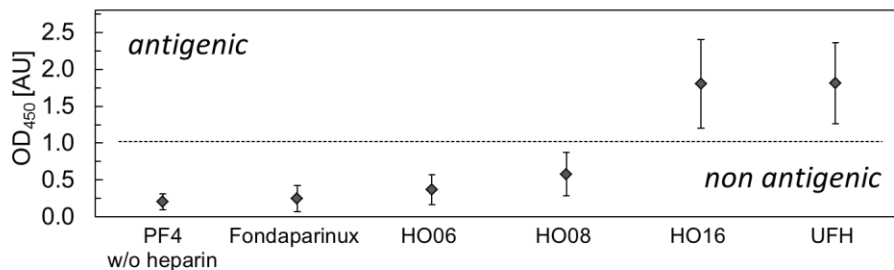


Figure 1.3.2: The PF4/PA EIA revealed antibody binding above the antigenicity threshold for complexes of PF4 with HO16 or UFH, respectively. PF4/HO08 complexes showed only insufficient antibody binding, being therefore non-antigenic.

The requirement of multimolecular complex formation was tested by Martin Kreimann using AFM imaging in liquid. He also carried out the ITC measurements and found that the negative entropy is balanced by a large binding enthalpy between PF4 and the respective heparins and therefore, the enthalpy provides the energy to induce conformational changes in PF4, which are needed for the formation of the neoepitope recognized by the anti-PF4/heparin antibodies. By this finding, the CD results suggesting structural changes were supported. The results were proven by EIA showing that only complexes formed by PF4 with UFH and HO16 consistently exhibited high antibody binding (see figure 1.3.2).

1.4 Paper IV (PF4/Polyphosphates)

After showing in **paper II (PF4/PA)** that PF4 exerts the same features like secondary structural changes and antigenicity in complex with the polyP P75 (chain of 75 phosphates), we studied this system in more detail in **paper IV (PF4/polyP)**. We investigated the complex formation of PF4 of polyP with three different chain lengths (P3, P45, and P75) and the influence of polyP on the binding of PF4 to a Gram-negative bacterial surface. The characterization included techniques that were used before (CD spectroscopy, EIA and ITC) supplemented by a new technique (flow cytometry, see chapter: 4.4 Flow

Cytometry). By CD spectroscopy it was found that, in contrast to the short P3, the two longer polyP P45 and P75 induced secondary structural changes in the PF4 molecule. We observed slight differences in curve progression between the complex formation of PF4 with P45 and P75 which are not only represented in the raw CD spectra but also in the deconvolution of the CD spectra (see figure 1.4.1 A). The onset of increase in antiparallel β -sheet and the peak position is nearly the same for P45 and P75. Further, for both polyP, the secondary structural changes are irreversible. There is only a partial

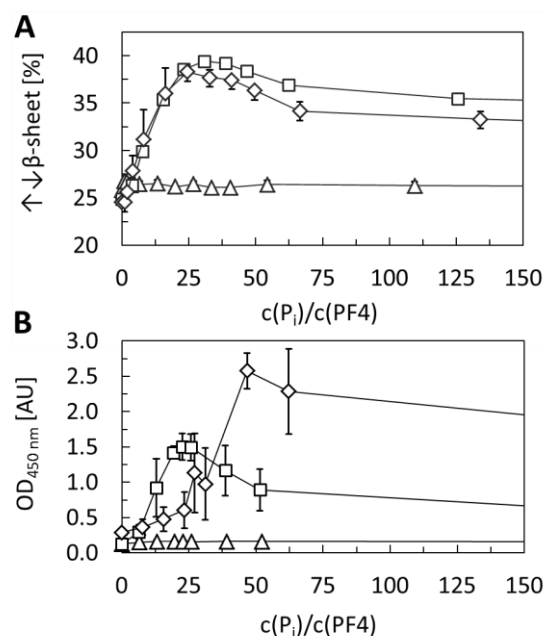


Figure 1.4.1: A - Deconvolution of CD spectra of PF4 in complex with P3 (\triangle), P45 (\square), P75 (\diamond) and B - antibody binding measured by EIA.

folding back to the initial secondary structure which is slightly more pronounced for P75. Whereas the structural changes in the protein upon complex formation with the two longer polyP are quite similar, there are pronounced differences in antibody recognition between PF4/P45 and PF4/P75 complexes (see figure 1.4.1 B). PF4/P75 complexes show very high antibody binding with its maximum shifted to a higher concentration compared to the peak position found by CD spectroscopy. In the case of UFH, we also observed the shifting in peak position and discussed that this might come from the polydispersity. Here, the same feature was observed again, but the P75 has a very low polydispersity index, so the peak shift might have another reason. It may very well be that complexes with longer chains behave differently on the surfaces of EIA plates. Complexes between PF4 and P45 are also antigenic (OD higher than one, see figure 1.4.1 B) but the peak position matches the one found by CD spectroscopy. Complexes between PF4/P3 were not recognized by anti-PF4 heparin antibodies at any PF4:P3 ratio.

The energetic characteristics of the PF4/polyP binding interactions were assessed by ITC. The energies exerted by the complex formation between PF4 and P3 were either too small to be measured or no

complexes were formed at all. The latter is rather unlikely, assuming that the binding mechanism is the same as for P45 and P75, where the binding was already proven with the techniques before. But it may very well be that five charges exerted by the triphosphate are not sufficient to form stable complexes. However, P45 and P75 showed characteristic negative peaks indicating an exothermic reaction. After peak integration, data was fitted with a *One Set Sites* model (included in the Origin-based analysis software provided by MicroCal, LLC, Northampton, MA) to obtain the values of the change in enthalpy (ΔH), dissociation constant (K), the stoichiometry (N), and the Gibbs free energy. As expected for a reaction that runs spontaneously, negative values were found for the ΔG . Moreover, the values were quite similar for P45 and P75. The enthalpies for the PF4/P45 and PF4/P75 calculated per mole of polyP and per mole of PF4 were also found to be negative. When comparing the enthalpies calculated per mole of polyP for P45 and P75 the difference matches quite nicely the difference in size. P75 is three times longer (3.1), meaning that it provides also three times more charges for the electrostatic interaction with PF4. The enthalpy differs by a slightly higher factor of 3.7 (see table 1.4.1). When calculating the enthalpy per mole of PF4, the small difference becomes more evident. Here, the enthalpy of the reaction between PF4 and P75 is higher than for the PF4/P45 complex.

Table 1.4.1: Thermodynamic parameters for the interaction of PF4 with P3, P45 and P75.

Complex	Enthalpy, ΔH^a [kcal/mol]	Enthalpy, ΔH^b [kcal/mol]	Dissociation constant ^b [M]	Stoichio- metry [polyP/PF4]	Gibbs Free Energy, ΔG^b [kcal/mol]	Entropy, $-T\Delta S^a$ [kcal/mol]
PF4/P3	n.d.	n.d.	n.d.	n.d.	n.d.	n.d.
PF4/P45	-8.21±2.31	-4.07±0.49	$1.7 \cdot 10^{-7} \pm 6.7 \cdot 10^{-8}$	0.51±0.1	-9.25±0.22	1.04±2.47
PF4/P75	-16.6±0.46	-7.06±0.33	$8.4 \cdot 10^{-6} \pm 1.4 \cdot 10^{-7}$	0.43±0.01	-8.28±0.09	-8.36±0.55

Note: Thermodynamic parameters calculated: a) per mole of polyP chain or b) per mole of PF4 tetramer. n.d. – not defined (energies for PF4/P3 complex formation too low to be measured)

The stoichiometry indicated that more than one (1.3 ± 0.25) P45 strand binds to one PF4 tetramer, whereas approximately two PF4 molecules bind to one P75 strand ($P75/PF4 = 0.6 \pm 0.01$). The difference in enthalpy, together with the difference in stoichiometry, might already be an indicator for dissimilar mechanism in complex formation. This may also be the explanation for the different antibody binding behavior seen before. Interestingly, a slightly higher affinity was suggested for P45 compared to P75. After the physico-chemical characterization of the PF4/polyP complexes, we assessed the issue of PF4 as a part of an ancient host defense mechanism, extended this time by polyP, which are ubiquitously found in pathogenic bacteria but also in platelets. It is not unlikely that PolyP and PF4 interact. They are released during platelet activation and also after bacterial death. Flow cytometry (see chapter: 4.4 Flow cytometry) was used to show that polyP ratio dependently increases the amount of PF4 that binds to the surface of the Gram-negative bacterium

Escherichia coli (*E. coli* JM109). Therefore, FITC-labeled bacteria and biotinylated PF4 were coincubated with increasing concentrations of polyP to obtain different PF4:polyP molar ratios. P3 did not induce any changes, the amount of bound PF4 remained at baseline over tested polyP concentration range of 0 to

40 $\mu\text{g/ml}$. In contrast, P45 and P75 increased the PF4- coating of the bacterial surface in a PF4:polyP ratio dependent manner by more than two-fold (see figure 1.4.2 A). The maximum binding for both

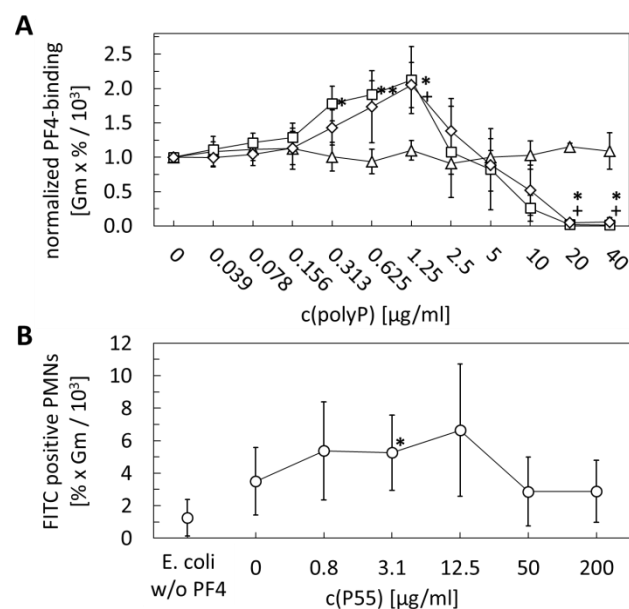


Figure 1.4.2: Flow cytometry experiments showing A – that the amount of PF4 bound to a bacterial surface can be PF4:polyP ratio dependently increased by P45 (□), P75 (◇) but not by P3 (△) and B – that the phagocytosis of bacteria by polymorphonuclear leukocytes is already increased by the addition of PF4 but is further increased when polyP is also present at a certain concentration. At high polyP concentrations both, the PF4 bound to the surface and the phagocytosis decrease. (Significance levels: * - $p < 0.05$, ** - $p < 0.01$)

polyP was achieved at the same concentration. Also, the dissolution of PF4 from the bacterial surface occurred at the same high polyP concentration.

Additionally, we show that PF4 binding to the bacterial surface improves the anti-PF4/heparin antibody-mediated phagocytosis of bacteria by polymorphonuclear leukocytes (PMNs), see figure 1.4.2 B.

Therefore, we again coincubated *E. coli* with PF4 and different concentrations of P75. Additionally, PF4/P75-coated bacteria were incubated with anti-heparin antibodies and afterwards, with PMNs freshly purified from whole blood donated on the same day. In figure 1.4.2 B it can be seen that the phagocytosis is even more efficient when adding P75. At concentrations of P75 higher than 50 µg/ml, the phagocytosis is again inhibited.

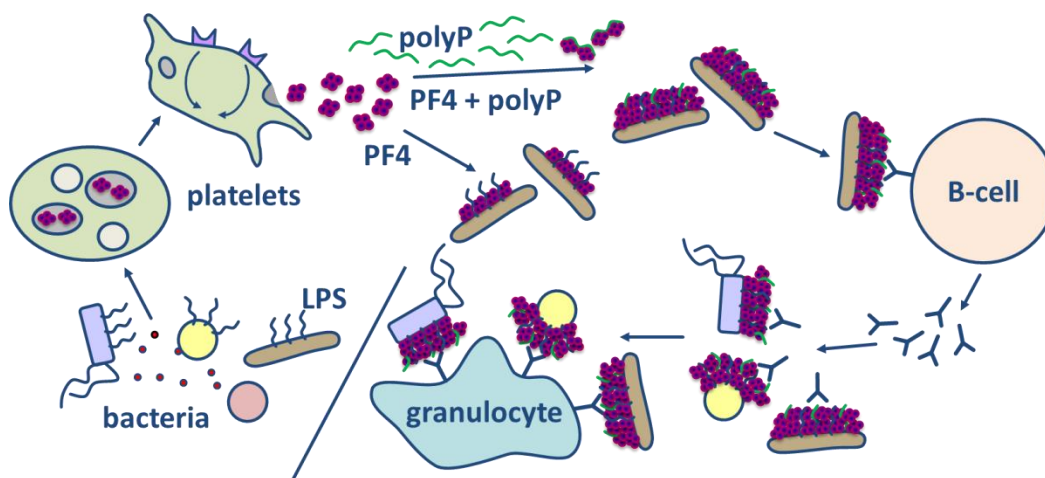


Figure 1.4.3: Schematic representation of the mechanism how polyP might mediate antibacterial host defense. Activated platelets release charged PF4 which interacts with polyP increasing the amount of PF4 attached to the bacterial surface. The formation antigenic multimolecular PF4 clusters initiates antibody formation by B-cells. These antibodies will bind to all bacterial species forming PF4 clusters on the surface. The antibody recognition finally facilitates phagocytosis of the bacteria by leukocytes.

Figure 1.4.3 shows a schematic representation of how polyP might contribute to the ancient host defense mechanism. Bacteria can activate platelets via direct and indirect interaction, respectively. Upon activation, platelets release alpha granules containing PF4 which binds to lipid A on the surface of Gram negative bacteria. The binding is enhanced by polyP, which are also released from platelets upon stronger activation from their dense granules. Due to PF4/polyP interaction, multimolecular complexes are formed exerting more antibody binding sites on the bacterial surface which are additionally in a

greater distance from the outer membrane. The latter might be crucial because the glycosamino chains of the LPS might impede the epitope recognition by the antibody and also the recognition of the Fc part of the antibody by granulocytes.

The highly variable O-antigen of the LPS can reach up to 37 nm.³⁴ An immunoglobulin G with a length of 8.5 nm together with a PF4 tetramer of 6 nm could be hidden in the *lawn* of sugar chains. In contrast, multimolecular PF4/PA complexes in contrast can reach sizes up to about 30 nm in globular form^{13,33} and up to 200 nm in linear form.¹⁹ Therefore, an antibody attached to a multimolecular complex would reach out of the *lawn* and could be recognized by leucocytes via the Fc-part which facilitates the phagocytosis of Gram negative bacteria.

1.5 Paper V (PF4/Aptamer)

We showed that PF4 binds to the phosphate groups of lipid A and to pure inorganic polyP chains. Another class of molecules containing phosphate groups is represented by nucleic acids (DNA and RNA). The concentration of extracellular nucleic acids in plasma ranges from 0 to >1000 ng/ml in healthy individuals.³⁵ Under pathological conditions, upon release of nucleic acids, due to cell death, tissue damage or the breakdown of viruses and bacteria, the concentration can be locally quite high (up to 2 mg/ml)^{36,37} but only for a limited time, as it is cleared from plasma within 4-30 minutes.³⁸ Concluding the aforementioned, naturally the possibility is given, that the positively charged PF4 can interact with DNA and RNA. Another potential contact point between PF4 and nucleic acids arises when the recently introduced therapeutic oligonucleotides called aptamers (see chapter: 2.2.10 DNA – Protein C-aptamer) are administered to patients.³⁹ Here, the interaction between PF4 and nucleic acids becomes relevant in terms of drug safety. Aptamers are designed to have a certain secondary structure to bind a target. A DNA or RNA construct by chance forming complexes with PF4 might be on the one hand less effective because of potential competition for the binding sites. On the other hand, the risk of the adverse drug

effect HIT might prevent the usage of aptamers.

Indeed in **paper V** (*PF4/aptamer*) we show that certain aptamers form complexes with PF4 and induce anti-PF4/aptamer antibodies which cross-react with PF4/heparin complexes. Moreover, by CD spectroscopy we showed that the protein C-

aptamer caused secondary structural changes in

the PF4 molecule similar to those induced by

heparin and even higher (see figure 1.5.1). Further,

the same amount of changes maximally induced by

heparin, were induced by much lower concentration of the protein C-aptamer. For heparin we always

observed distinct peaks of maximum changes, but for PF4 in complex with the protein C-aptamer, the

changes persisted over a quite wide range of concentrations (5 to 20 $\mu\text{g/ml}$) forming a plateau before a

refolding occurred (not shown). Concluding the results of **paper V** (*PF4/aptamer*), some aptamers not

designed to bind to PF4 bear the risk of inducing an immune reaction similar to HIT. The handling of the

data was a bit more challenging for the complex formation of PF4 with an aptamer, as the latter in

contrast to the PA before, exhibits its own CD spectrum. Even though the main signal of DNA and RNA is

observed in the near-UV range, there was a minor signal in the far-UV sensitive for protein secondary

structures. By the stepwise increase of the aptamer concentration, the amplitude of its CD spectrum

became more pronounced, reached the amplitude of the protein and was even higher at the end of the

titration. We classified each aptamer spectrum with a maximum amplitude smaller than the amplitude of

the corresponding PF4 spectrum as reliable and rejected the spectra of higher concentrations (amplitude

of aptamer spectrum higher than amplitude of PF4 spectrum) from the analysis.

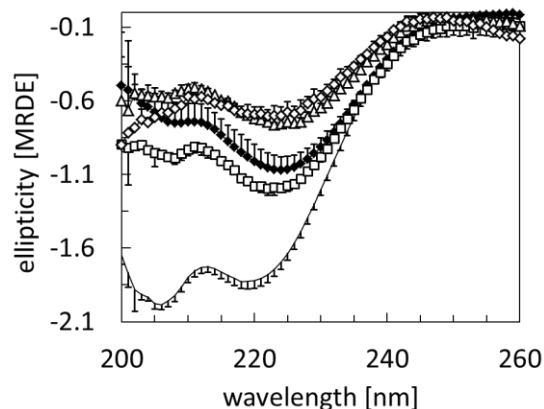


Figure 1.5.1: Changes in the CD spectrum of native PF4 (—) induced by the 44mer-DNA protein C aptamer ($c_{\text{aptamer}}=2.5 \mu\text{g/ml}$ \square , $c_{\text{aptamer}}=5 \mu\text{g/ml}$ \triangle , $c_{\text{aptamer}}=20 \mu\text{g/ml}$ \diamond) compared with the maximum changes induced by UFH ($c_{\text{UFH}}=6.9 \mu\text{g/ml}$ \blacklozenge). Note that the changes in PF4 spectra are rather similar, regardless whether heparin or the aptamer was used.

1.6 Paper VI (Protamine/Heparin)

After the intensive investigation of the complex formation between PF4 and many different classes of PA, we asked the question whether structural changes of endogenous proteins per se may be recognized by antibodies, and whether there may be a general underlying mechanism. It was already shown that PA like heparin can modify the immunogenicity of positively charged proteins.¹⁶ To answer the question, we focused on protamine, a protein routinely used in post-cardiac surgery to reverse the anticoagulant effects of heparin.⁴⁰⁻⁴³ Electrostatically attached to insulin, protamine functions as a stabilizer and also prolongs its function.⁴⁴ As for HIT where an immunization against PF4/heparin complexes is observed, platelet-activating anti-protamine/heparin antibodies are formed in some patients.^{11,43-45} The formation of the immune complexes leads as well to an increased risk for thrombosis and thrombocytopenia.

Protamines are small proteins that condense the DNA in mature spermatozoa.⁴⁶ As the majority of the amino acids contained are arginines (60-80% depending on the source specimen),⁴⁷ protamine is a positively charged protein which is mostly purified from fish sperm (especially salmon). It is accepted that DNA-bound protamine has no β -sheets and an α -helical content of approximately 20% in salmon or 40% in squid.⁴⁷ However, for unbound protamine, an α -helical content of approximately 2-5% is suggested which can be increased by 2,2,2-trifluor-ethanol (TFE) to 34-65%.⁴⁷ Awotwe-Otoo et al.

investigated protamine of five different sources and found that the CD spectrum of all tested protamines adopts the shape of the random coil spectrum (see figure 4.1.1 B).⁴⁸ Although their measurements are quite noisy and the negative band at 198 nm even seems to be cut due to high absolute absorption, it made changes in our experimental setup necessary to

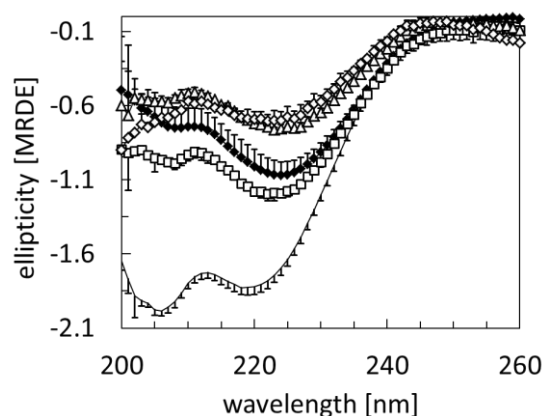


Figure 1.6.1: Upon binding to heparin the CD spectrum of protamine changes to lower ellipticity values, indicating an unfolding of the protein.

also access the wavelength range below 200 nm. Therefore, the protamine was dissolved in water, resulting in a wider accessible nm range (185 to 260 nm). It was necessary to measure below 200 nm to resolve the negative band of protamine at 198 nm (see figure 1.6.1). As PF4, protamine also changes its secondary structure upon binding to heparin. However, the courses of structural changes are different. While for PF4, we observed kind of a forth-and-back reaction with maximum of structural changes in between, there was only a one-directional reaction for protamine. When titrating protamine with heparin, the protein unfolded the more, the higher the heparin concentration was.

2. Proteins, Polyanions, Reagents

2.1 Proteins

"Proteins are at the center of the action in biologic processes."

Donald Voet⁴⁹

The biologic processes described in this thesis involve proteins. When heparin, a chain like polyanion (PA), is administered to prevent blood clotting during surgery, platelets activate and release the protein platelet factor 4 (PF4).⁵⁰ PF4 which is the strongest heparin binder known,⁵¹ competes with other proteins like antithrombin III⁵²⁻⁵⁴ or thrombin⁵⁴ for the binding sites on the heparin chain and decreases the antithrombotic effect of heparin.³⁰ Interestingly, some patients have already or develop after heparin administration antibodies against PF4/heparin complexes. These antibodies (immunoglobulin G, IgG), which are proteins themselves, can then trigger the adverse drug effect heparin-induced thrombocytopenia (HIT).⁵⁵⁻⁵⁷ HIT has been studied for several decades but relatively little is known about the mechanisms leading to antigenic structures.⁵⁸ It is widely accepted that the epitopes recognized by IgG are located on PF4, as heparin can be replaced by other PA. Investigations on the primary structure of PF4 were done in paper I (PF4 evolutionary analysis). Special focus was given to the secondary and to the tertiary structure in paper II (PF4/PA), paper III (PF4/defined heparins), paper IV (PF4/polyP), and paper V (PF4/aptamer).

To neutralize the anticoagulant activity of heparin, protamine sulfate is administered.⁵⁵ Protamine also forms complexes with heparin and, as mentioned above for PF4, some patients develop or have already anti-protamine-heparin antibodies.⁵⁹ As well as for the PF4/heparin complexes, only little was known about the complex formation between protamine sulfate and heparin. Secondary structure investigations were done in paper VI (PS/heparin).

Proteins are amides build-up by amino acids (AA) which are organic zwitterionic compounds containing two functional groups (an amine group (NH₂) and a carboxyl group (COOH)) and a specific side chain (R in figure 2.1). There are about 500 AA known,⁶⁰ but only the 22 proteinogenic α-AA, where both functional groups are attached to the α-carbon, contribute to the formation of proteins.^{61,62} The only exception to the general formula of α-AA (figure 2.1, bottom) is proline, where due to cyclization the NH₂-group is lacking. Depending on the side



Figure 2.1: Structure of an α-amino acid (AA) in its unionized form is shown with an amine group (green) and a carboxyl group (red) attached to C_α. R denotes for the different side chains (residues) that can be at that position, which determine the properties of the AA. The general formula of α-AA is shown at the bottom.

chain, AAs have different properties and can therefore be grouped into several classes: a) nonpolar AA with aliphatic R-groups – are contributing to hydrophobic interactions in proteins structures. In this class, small glycine, for example, allows high flexibility of structures, whereas proline increases the rigidity of the structures containing it. b) polar AA with uncharged R-groups – are hydrophilic and form hydrogen bonds to other polar compounds (e.g. other AA, water). Cysteine residues often form disulfide bonds stabilizing proteins intra- and intermolecularly. c) AA with aromatic R-groups – have on the one hand hydrophobic side chains and on the other hand nitrogen in the tryptophan ring or a hydroxyl group of tyrosine forming hydrogen bonds. Aromatic AA are often situated in active centers of enzymes and catalyze reactions. d) AA with positively charged R-groups as well as e) AA with negatively charged R-groups – include AA which are also often involved in catalytic mechanisms and contribute to the protein structure as they often exposed on the surface of soluble proteins. f) Pyrrolysine is a special AA considered as the 22nd AA and is only present in methanogenic *Archea* and one *Bacterium*.

The fact that the two functional groups (NH₃, COOH), the side chain and a hydrogen (H) are attached to the α-carbon, makes it asymmetric or chiral (exception: glycine where R is a H) meaning that there is no superimposable mirror image. Chirality leads to optical activity which is also called optical rotation. Chiral

molecules turn linear polarized light or absorb right and left circularly polarized light to different degrees (for further information see 4.1 Circular dichroism spectroscopy). With some exceptions in bacterial envelopes and some antibiotics, all proteins are composed of L-stereoisomers. During the reaction between the carboxyl group of one AA and the amino group of another AA, water is released and hence, the reaction is a dehydration (or condensation, figure 2.2).

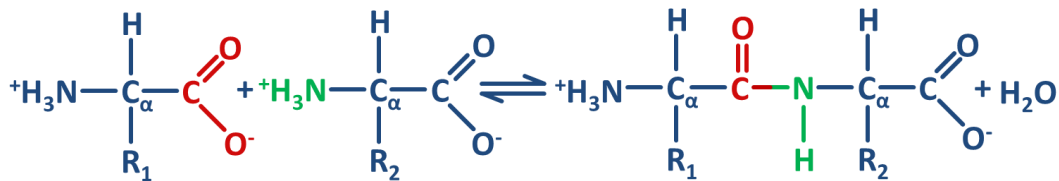


Figure 2.2: The dehydration reaction (=condensation) between the carboxyl group of one AA and the amino group of another AA is shown. The carboxyl group of one AA reacts with the amino group of another AA forming a peptide bond. Once an AA is part of a peptide chain, its side chain is called residue (R_1 and R_2).

The backbone, of a protein is shown in figure 2.3. The α -carbons of the AAs and the peptide bond form the corners of a plane. There is no rotation around the peptide bond, due to its partial double bond character (two resonance forms). The so-called dihedral angles ϕ and ψ indicate to which extent neighboring planes are twisted against each other. The end of the peptide chain with the free amine group is the so-called N-terminus. The counterpart with the free carboxyl group is called C-terminus. The AA sequence of a protein is always given from N- to C-terminus.

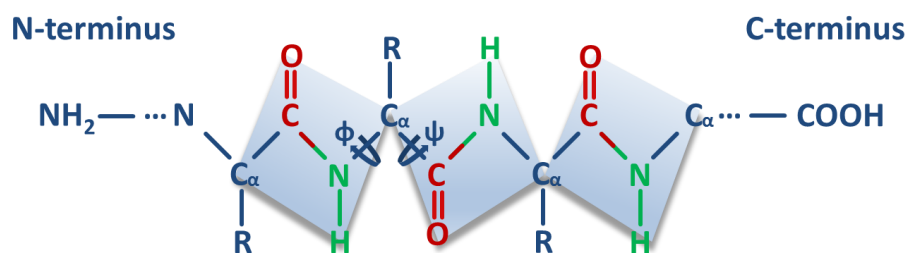


Figure 2.3: The backbone of a protein: with the residues R attached to C_α . The six atoms with blue background are in the same plane. Rotation is only possible around the C_α atoms, because the peptide bond, as marked in red and green letters (Figure 2.1.2), has partial double bond character. The angles describing the torsion of the planes are named phi (ϕ) and psi (ψ).

Proteins are characterized by their primary, secondary, tertiary, and quaternary structure. Their relationship is depicted in figure 2.4. The primary structure of a biological molecule describes the exact

specification of the atomic composition, the chemical bounds or, for unbranched biopolymers like proteins, the sequence of monomeric subunits. Proteins are polyamides and the primary structure is the AA sequence. Secondary structures are characterized as the three-dimensional form of local segments that are stabilized by hydrogen bonds. Proteins present secondary structures such as α -helices, β -sheets, β -turns, and random coil. The latter differs from the others as it is mostly not stabilized by hydrogen bonds. Except for the random coil each secondary structure, has its characteristic dihedral angles (ϕ and ψ). Several of these local structures can be present in a protein and arrange to the so-called tertiary structure. It describes the overall shape of a protein molecule and the spatial relationship of its secondary structures. The tertiary structure is stabilized by disulfides bonds, salt bridges, and hydrogen

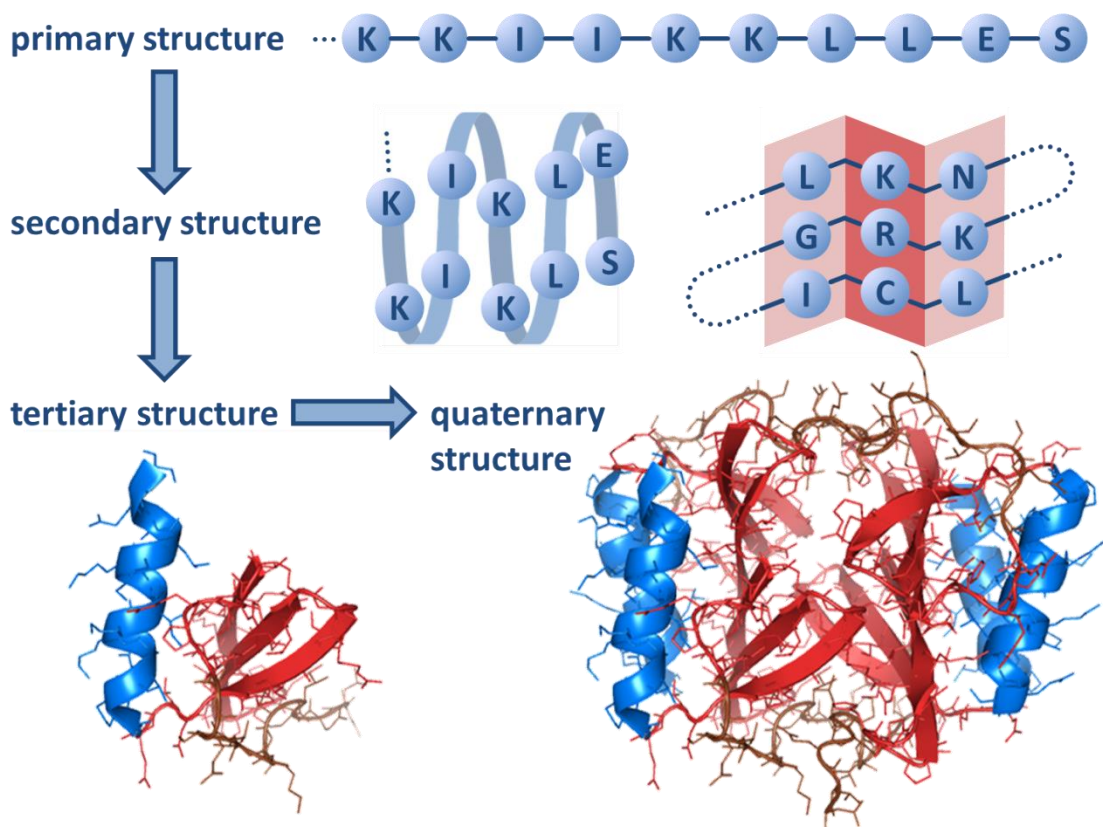


Figure 2.4: A protein is characterized on several levels. It starts with the primary structure describing the AA sequence (shown is the C-terminal end of PF4). Stabilized mostly by hydrogen bonds, the covalently linked AA chain locally folds to secondary structures. Exemplarily, the C-terminal α -helix of PF4 is shown on the left in blue and on the right in red an AA sequence of PF4 forming β -sheets is depicted. The local secondary structures three dimensionally arrange non-covalently to tertiary structures. One of four monomers of PF4 with α -helix in blue, β -sheet structures in red and in brown remaining structures (turn, random coil) are displayed. In many cases, several tertiary structures attach non-covalently to form a quaternary structure. The graphic shows the complete homotetramer of PF4.

bonds. Because the majority of proteins exists and is active in aqueous solution, the charged hydrophilic AA are situated on the surface and the nonpolar hydrophobic AA are not exposed to the surrounding medium forming a hydrophobic core. This hydrophobic interaction is another force that stabilizes the tertiary structure. Tertiary structures can already be functional proteins like in the case of protamine sulfate (paper V – PS/heparin). In many cases, several tertiary structures (also called subunits or monomers) attach through non-covalent interactions, occasionally via disulfide bonds⁶³, to form a quaternary structure (or protein complex). If the subunits of a protein complex are of the same kind, the whole construct is called a homo-XY-mer (XY = 'di' – two subunits, 'tri' – three, 'tetra' – four, etc.). If the subunits are different it is a hetero-XY-mer. Platelet factor 4 (paper I, paper II, paper III, and paper IV) consists of four identical subunits and is therefore, a homotetramer.

The Anfinsen's dogma or thermodynamic hypothesis postulates that for small globular proteins and peptides the amino acid sequence determines the native structure.⁶⁴ For this dogma, Christian B. Anfinsen won the Nobel Prize in chemistry in 1972. It says that under given environmental conditions (temperature, solvent concentration etc.) the folding of a native protein is a unique, stable and a kinetically accessible minimum of the free energy. In contrast the Levinthal's paradox postulated in 1969 by Cyrus Levinthal, states that due to the very large number of degrees of freedom in an unfolded polypeptide chain the number of possible conformations is astronomically large, so large that even a protein of only 100 AA would require 10^{26} seconds to explore every possible conformation for the native one and 10^{26} seconds is actually longer than the universe exists.⁶⁵ Levinthal was aware of the fact that in reality most of the small proteins fold spontaneously within milli- or even microseconds. A possible explanation for the Levinthal paradox was stated by Edward Trifonov and Igor Berezovsky in 2002 who stated that a protein is built up by structurally diverse building blocks of 25 to 30 AA which they call modules or loops.⁶⁶ So-called closed loops were favored during evolution because they provided more stability to the sequence.⁶⁷

2.1.1 Platelet Factor 4

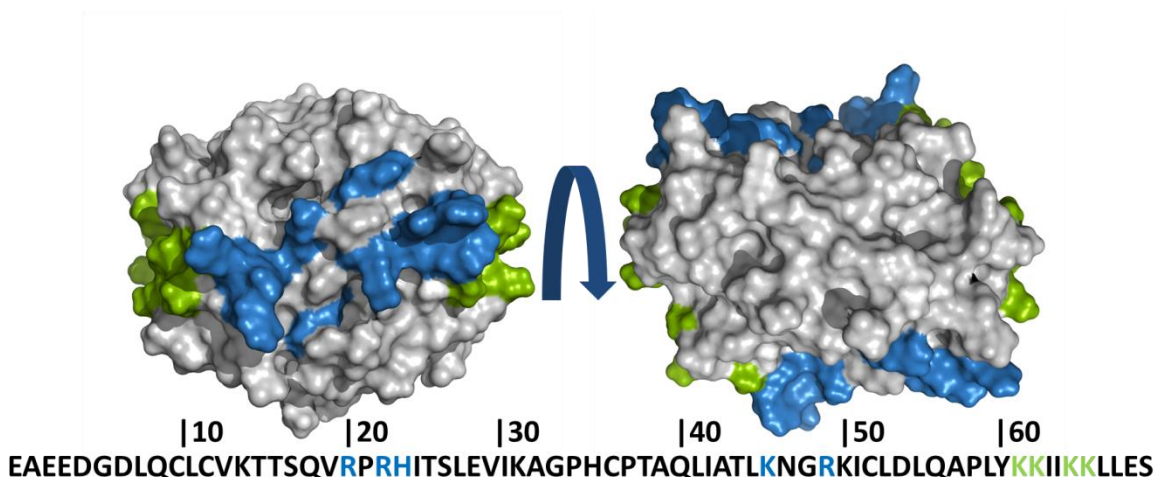


Figure 2.1.1: The PF4 tetramer based on the crystal structure (PDB code: 1f9q) is depicted from the side (left) and in a top view (right). Additionally the primary structure (amino acid sequence) of a monomer without signal sequence (UniProt entry: P02776 – resolved by Zhang et al.⁶⁸) is shown below the images. The positively charged amino acids forming an equator which are important for heparin binding are highlighted in green (C-terminal lysine residues: K61, K62, K65, K66) and blue (arginines: R20, R22, R49; histidine: H23 and another lysine: K46). The figure is partly taken from paper I (PF4/evolution) and was adapted from Ziporen et al.²³ The pictures were made using PyMOL Molecular Graphics System, Version 1.3 Schrödinger, LLC.

Platelet factor 4 (PF4, CXCL4, SCYB4) is a small, homotetrameric chemokine, structurally belonging to the CXC family, where the two N-terminal cysteines are separated by one amino acid. Two asymmetric PF4 dimers form a cylindrical tetramer. The human gene (three exons and two introns) positioned on chromosome four⁶⁹ encodes for a protein that consists of 70 amino acids in its mature monomeric form (101 amino acids including a hydrophobic signal peptide for transmembrane transport⁷⁰) with a molecular weight of 7.8 kDa.⁷¹ PF4 shares 30-90% amino acid identity with other chemokines of the CXC family. The contained four cysteines build up two intramolecular disulfide bonds. The crystal structure of PF4 resolved by Zhang et al. in 1994,⁶⁸ shows that many of the positively charged amino acids are located on the protein's surface to form a positively charged equatorial ring surrounding the tetramer (see figure 2.1.1).^{50,68,71-73} Further can be seen that the four subunits forming the native protein are not attached symmetrically making NMR structure investigations difficult.⁷⁴ It was shown that the tetramer-dimer-monomer equilibrium is pH dependent. Lowering the pH below 4 shifts the equilibrium towards the

monomeric state, while the formation of dimeric and tetrameric structures is favored at increased pH values. The latter is also stabilized by increasing ionic strength.⁷⁵ From figure: 2.1.2, which shows the secondary structures in different colors (top) or the four subunits differently colored (bottom), it can be seen that the three β -sheets per subunit are facing inwards and that the one α -helix per subunit is located on the outside of the protein. Both, the lysine-C-termini at the end of α -helices and the N-termini start and end on the surface of the protein, respectively. The antiparallel β -sheets contain a number of hydrophobic amino acids. In 1955 the anti-heparin activity of PF4 was discovered⁴ which is based on the capability to bind to various chain-like polyanionic molecules via the equator of positive charges.^{74,76}

78

PF4 is synthesized in megakaryocytes⁷⁹ and stored in platelet α -granules but also in mast cells.⁸⁰ Upon injuries of blood vessels, e.g. during surgeries, platelets get activated and

release their content into the blood stream. Once released, PF4 is involved in numerous biological processes including hemostasis, platelet coagulation interference, and host inflammatory response promotion.² As a cytokine, PF4 is a chemoattractant for immune cells like neutrophils and monocytes.⁸ Additionally, PF4 shows similar effects on fibroblasts mediating their migration to vascular lesions and actively participate in the repairing by forming collagen.⁹ Notably PF4 suppresses angiogenesis by

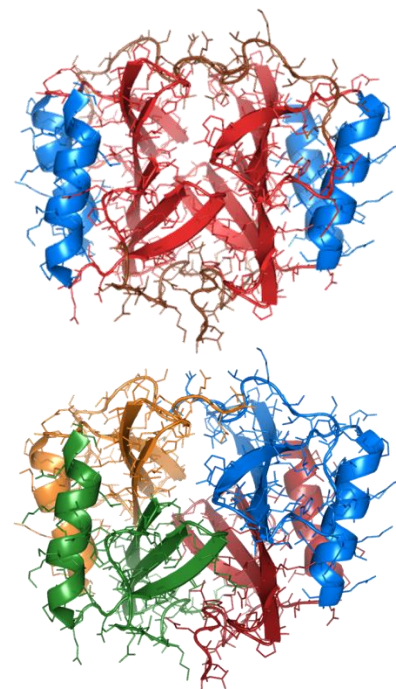


Figure 2.1.2: top – The secondary structure cartoon representatives including the amino acid side chains highlighted in different colors (α -helix – blue, β -sheet – red, turns and random coil – brown) of the PF4 tetramer are depicted. **bottom** – The four subunits differently colored. Both images illustrate the three inward facing β -sheets of each subunit are facing inwards, forming the interface between the subunits. Further the only α -helix (including the C-terminus) per subunit as well as the N-terminus is located on the proteins surface.

inhibiting endothelial cell proliferation and migration which makes PF4 a potential clinical anti-tumor agent because angiogenesis is essential for the growth of primary tumors.^{5,6}

2.1.2 Protamine

Protamine is a small arginine-rich and therefore cationic protein routinely used in post-cardiac surgery to reverse the anticoagulant effects of heparin.⁴⁰⁻⁴³ By forming complexes, protamine makes heparin less accessible for antithrombin and therefore neutralizes its function. It is also used as a stabilizer for insulin. Administered in a complex held together by electrostatic forces, protamine also prolongs the function of insulin.⁴⁴ As for HIT where an immunization against PF4/heparin complexes is observed, platelet-activating anti-protamine/heparin antibodies are formed in some patients.^{11,43-45} Here, as well the formation of the immune complexes leads to an increased risk for thrombosis and thrombocytopenia.



Figure 2.1.3: Primary structure of the protamine used to do the experiments in this thesis (paper VI – PS/heparin). Positively charged arginines depicted in green.

Protamines are small proteins condensing DNA in mature spermatozoa.⁴⁶ Depending on the specimen 60 to 80% of the contained amino acids are arginines.⁴⁷ Sometimes even separate geographical populations of the same species show differences in their primary structure and therefore also in their secondary structure.⁸¹⁻⁸³ Due to the high number of arginines, protamine is a positively charged protein which is mostly purified from fish sperm (especially salmon) for the later use as a drug. The purification process from fish milt consisting of at least 18 steps is rather complicated, involving organic solvents (e.g. alcohol, acetone and picric acid).⁸⁴ The peptide molecular weight of the protamine (Sigma-Aldrich, P4020) used in this thesis was 4250 Da. Since the product was a sulfate salt with approximately 17% sulfate by weight the overall formula weight is 5120 Da. Its primary structure is depicted in figure 2.1.3.1. DNA-bound protamine has no β -sheets and an α -helical content of approximately 20% in salmon or even

40% in squid.⁴⁷ However, for unbound protamine, an α -helical content of approximately 2-5% is suggested which can be increased by 2,2,2-trifluorethanol (TFE) to 34-65%.⁴⁷

2.2 Polyanions

The most carbohydrates found in nature occur as polysaccharides (= glycans) with high molecular weights of more than 20 kDa.⁸⁵ Glycans differ in their reoccurring monosaccharide units, length of chains, types of bonds linking the units, and the degree of branching. They are highly negatively charged molecules and impart high viscosity to a solution by their extended conformation. Their low compressibility makes them ideal molecules for a lubricating fluid in joints. A homopolysaccharide consists of only one kind of monosaccharide unit. Some of them serve as storage forms of monosaccharides used as fuels e.g. starch and glycogen. Others built up structural elements like chitin in exoskeletons or cellulose in plants. In contrast heterosaccharides contain two or more different kinds monosaccharide units. They serve as extracellular support of any kind of organism. The bacterial envelope is made up of the heteropolysaccharide peptide glycan which consists of two alternating monosaccharides (see chapter 3. Bacteria). In animal tissue several types of heteropolysaccharides can be found. They form the matrix holding cells together, provide protection, hold the shape, and give support to cells, tissues, and organs. In contrast to proteins polysaccharides have no template like mRNA. Therefore the enzymes that catalyze their polymerization do not have a stopping point and polysaccharides lack a defined molecular weight. To describe the spread of the molecular weights (MW) in a polysaccharide sample, the polydispersity (PDI, equation 2.2.3), which is the ratio of the number average MW (\overline{M}_n , equation 2.2.1) and the weight average MW (\overline{M}_w , equation 2.2.2), is often used.

$$\overline{M}_n = \frac{\sum_i N_i M_i}{\sum_i N_i} \quad N_i - \text{number of molecules at MW } M_i \quad (2.2.1)$$

$$\overline{M}_w = \frac{\sum_i g_i M_i}{\sum_i g_i} \quad g_i - \text{weight of the sample at MW } M_i \quad (2.2.2)$$

$$PDI = \frac{M_w}{M_n} \quad PDI - \text{polydispersity} \quad (2.2.3)$$

Table 2.2.1: Glycosaminoglycans and their properties (adapted from ref.⁸⁶)

Glycosaminoglycan	constituent sugars	sulfate	approx. M_r [Da]	proteoglycans
hyaluronic acid	glucuronic acid and glucosamine	-	10^5 - 10^7	-
heparin	glucuronic acid or iduronic acid and glucosamine	+	5 - 20×10^3	+
chondroitin 4-(6-) sulfate	glucuronic acid or iduronic acid and galactosamine	+	10 - 50×10^3	+

Other PA investigated in this thesis include deoxyribonucleic acid (DNA, see 2.2.10 DNA – Protein C-aptamer) and polyphosphates (polyP, see 2.2.11 Polyphosphates – P3, P45, P75).

2.2.1 Unfractionated Heparin (UFH)

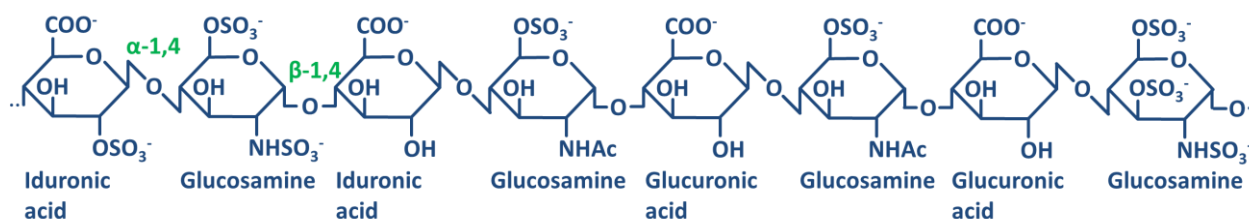


Figure 2.2.1: The four most common disaccharide building blocks, according to Lee et al.⁸⁷, are depicted. The disaccharide unit is composed of glucosamine and an uronic acid (iduronic acid or glucuronic acid, see also table 2.2.1) connected via α -1,4 glucosaminyl and β -1,4 hexuronosyl linkages. As a natural product and due to the nature of polysaccharides the chain length of heparin largely differs, resulting in a PDI of 1.3-1.4.⁸⁸

As a member of the glycosaminoglycan family of carbohydrates heparin consists of a disaccharide repeating unit that is variably sulfated. The name heparin originates from the ancient Greek word $\eta\pi\alpha\rho$ (hepar), meaning liver where it is cleared when circulating through the body.⁸⁹ It was discovered in 1916 and was used in early clinical trials in the 1930 and 1940s.⁹⁰ In the former times porcine mucosal heparin and bovine lung UFH with slightly different molecular weights and polydispersity values were available but the latter is now hardly used after the troubles with bovine spongiform encephalopathy (BSE). The rather high polydispersity of porcine UFH of 1.3-1.4 (\overline{M}_n =12-16 kDa, \overline{M}_w =17-20 kDa^{88,90}, MW_{avg} ~14 kDa⁹¹) makes it challenging to give exact molar ratios or to calculate accurate binding and kinetic constants.⁹⁰ Heparin is a heterosaccharide (see 2.2 Polyanions) with a heterogeneous sequence, consisting of a divers main disaccharide repeating unit of a glucuronic acid or iduronic acid alternating

with a glucosamine (see table 2.2.1) connected via α -1,4 glycosidic linkage and β -1,4 glycosidic linkage, respectively. On the average the disaccharide building blocks have three sulfate groups attached.⁹⁰ The anticoagulant activity of UFH depends on the existence of a specific saccharide sequence with high affinity for antithrombin, containing a pentasaccharide in its center. This pentamer includes the rare 3,6 di-*O*-sulfated, 2-*N*-sulfated glucosamine residue, which is not present in every heparin molecule.⁹² Additional to the pentameric antithrombin binding site a heparin molecule has to be sufficiently long to also bind thrombin to further increase its anticoagulant activity. Both binding sites together are termed C-region, where the C is standing for Choay.⁹³

2.2.2 Low-molecular-Weight Heparin (LMWH) – Reviparin

In the 1980s low-molecular-weight heparins (LMWH) partly replaced its parent compound UFH due to their enhanced usefulness.⁹⁰ LMWH consist of short GAG chains with a molecular weight less than 8 kDa. The rule is that 60% or more of the chains have to have a weight below 8 kDa.⁹⁴ The average molecular weight is 3.5-6 kDa which corresponds to

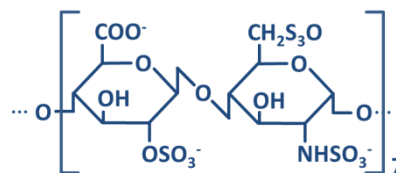


Figure 2.2.2: The chemical structure of the most common disaccharide contained in the defined length heparins is depicted.

6-10 disaccharide units.⁹¹ Several methods are in use to depolymerize the basic product heparin to obtain LMWH. Preparation by fractionation of UFH is not done anymore.⁹⁰ The LMWH which was used in paper II (PF4/PA) and paper III (PF4/defined heparin – in supporting information) was Clivarin with the active component reviparin. Its average molecular weight is 4.4 kDa which corresponds to an average chain length of 7 disaccharide units. It is manufactured via deaminative cleavage with nitrous acid at N-sulfated GAG, which results in an unnatural anhydromannose residue at the reducing end of the oligosaccharide. By the usage of a reducing agent it is converted to anhydromannitol. Further the method forms an unsaturated (C4–C5 double bond) uronate residue on the non-reducing end. LMWH have several advantages compared to UFH. They can be self-administered subcutaneously and have a longer

half-life. Due to these advantages LMWH are the most prescribed heparins in the US.⁹⁵ LMWH can only be incompletely neutralized by protamine sulfate (see chapter: 2.2 Protamine sulfate). To decrease the risk of bleeding reduced doses are administered.⁹⁶ The supply chain of LMWH is vulnerable to contamination and adulteration.⁹⁷

2.2.3 2-O, 3-O Desulfated Heparin (ODSH)

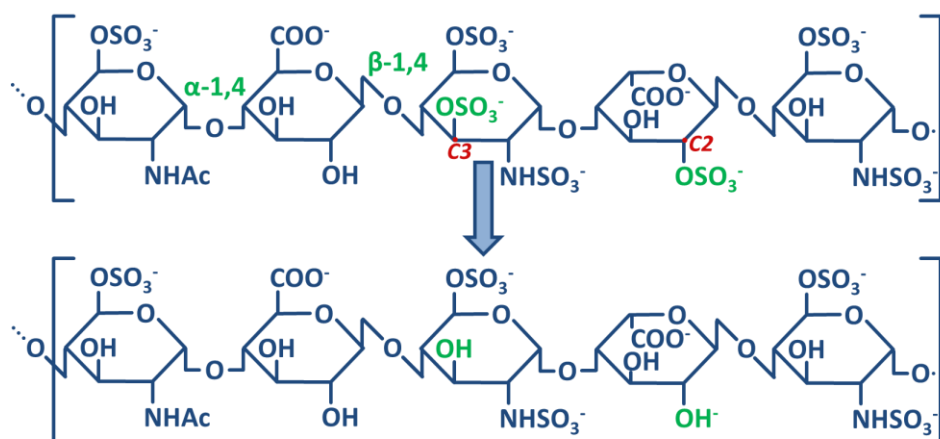


Figure 2.2.3: Chemical structure of ODSH adapted from ref⁹⁸. The 2-oxygen (2-O) on carbon C2 of α-L-iduronic acid and 3-O on carbon C3 of the D-glucosamine-N-sulfate (3,6-disulfate) are selectively removed.

Next to its anticoagulant activity, heparin has other properties like: broad anti-inflammatory activity and mucocatalytic activity. These other pharmacologies are clinically relevant at higher doses than needed for anticoagulation. The risk of bleeding prevents heparin from being used as an anti-inflammatory agent. 2-O, 3-O desulfated heparin (ODSH) is a modified form of heparin. By the selective removal of sulfate groups at the 2-O position on the α-L-iduronic acid and 3-O position of the D-glucosamine-N-sulfate (see figure 2.2.3.1) ODSH has been stripped of its anticoagulation capabilities while retaining the anti-inflammatory and mucolytic properties and has MW ranging from 8 to 14 kDa.^{99,100} Its half-life ranges from 30 to 60 minutes.^{99,100} The ODSH from ParinGenix inc. used in paper II (PF4/PA) retained more than 95% of its anti-inflammatory activity and has less than 3% anticoagulation activity (anti-factor Xa = 0.8-1.7 U/mg) of normal UFH. The anti-inflammatory properties remain due to the retaining sulfate group at the 6-O position. ODSH inhibits complement activation and blocks the two proteases human

leukocyte elastase and cathepsin G activity. Further ODSH is patented to prevent platelet activation and to treat thrombosis in the presence of PF4/heparin complex reactive antibodies^{95,96,98,101} The average MW is 10.5 kDa and the approximate degree of sulfation is 1.0 (5 sulfate groups per pentasaccharide).

^{95,96,98,101}

2.2.4 Heparin Oligosaccharides (HO06, HO08, HO16)

The heparin oligosaccharides (HO) that were used in paper III (PF4/defined heparin) were purchased from Iduron Ltd. (Manchester/UK). The company prepares the HO from high grade porcine heparin which is cleaved using bacterial heparinase and further isolated by high resolution gel filtration. As a result of the endolytic action of the heparinase, the uronic acid on the non-reducing end of the

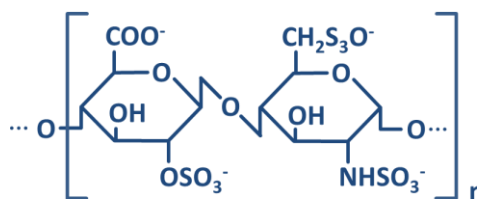


Figure 2.2.4: The chemical structure of the main disaccharide unit contained in the defined length heparins is depicted. For the heparin oligosaccharides used in paper III (PF4/defined heparin) n either denotes for 6, 8, or 16.

polysaccharide has a double bond between C4 and C5. According to the supplier approximately 75% of the HO consist of the main disaccharide unit depicted in figure 2.2.4.

2.2.5 Fondaparinux

Based on the antithrombin binding site of heparin, fondaparinux is a synthesized pentameric saccharide, which is an indirect, selective, and reversible factor Xa inhibitor and is subcutaneously bioavailable. It

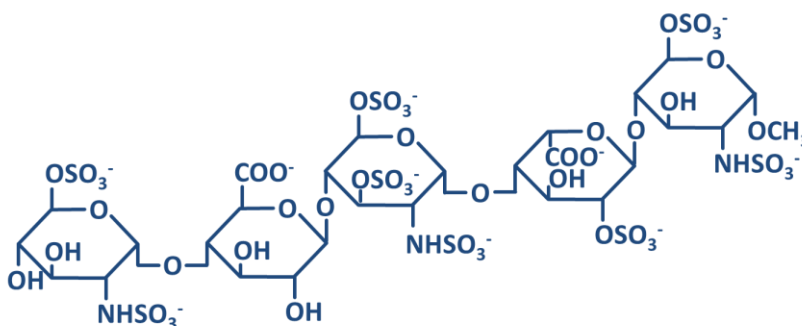


Figure 2.2.5: The chemical structure of the synthetic pentamer fondaparinux is shown.

is extensively studied as well as in use in major orthopedic surgeries and abdominal surgery. It is at least

as effective as low molecular weight heparin and was the first synthesized heparin that was approved for clinical use.^{102,103} Fondaparinux bears a reduced risk of HIT and osteoporosis¹⁰⁴ but at the same time lacks an antidote.

2.2.6 Chondroitin Sulfate

Chondroitin sulfate is the most abundant GAG found in cartilage, bone, heart, skin, tendon and valves. It is the major component of the extracellular matrix of many connective tissues¹⁰⁵ and is usually linked to so called core proteins forming proteoglycans, which is the major component of the extracellular matrix. The mostly C-4 and

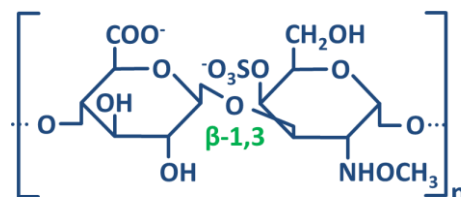


Figure 2.2.6: The chemical structure of chondroitin sulfate with its glucuronic acid and N-acetylgalactosamine units linked by β -1,3 bonds

C-6 sulfated chain of Chondroitin sulfate consists of the alternating sugars glucuronic acid and N-acetylgalactosamine linked by a β -1,3 linkage (see figure 2.2.6) forming an unbranched polysaccharide chain.¹⁰⁵ The chondroitin used in most clinical trials is purified from bovine trachea (95%) naturally having a molecular weight of 50-100 kDa and 10-40 kDa after extraction process.¹⁰⁶ Orally administered, chondroitin sulfate is absorbed increasing the plasma levels over a period of more than 24 hours.¹⁰⁷ Further chondroitin sulfate reduces the effects of proteases, increases the synthesis of proteoglycans, has anti-apoptotic effects and anti-inflammatory properties.¹⁰⁵

2.2.7 Dextran Sulfate

Dextran sulfate is a sulfated variant of dextran and is therefore an anhydroglucose-based polymer. The dextran sulfate used in the experiments included in the thesis contained approximately 17% sulfur. This is equivalent to an degree of sulfation of 2.3 sulfate groups per glycosyl

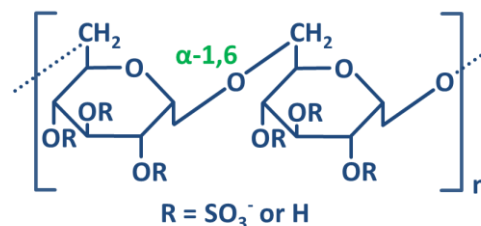


Figure 2.2.7: The chemical structure of dextran sulfate with its α -1,6 linkages is depicted.

residue. 95% of the linkages are of the α -1,6 type. The remaining linkages are responsible for branching of the polymer chain.^{108,109} Conflicting data exists on the lengths of the branches, it is implied that its average length is less than three glucose units¹¹⁰ but branches of more than 50 units length are also reported.^{111,112} The ionic strength affects the conformation of the polymer chain. In low ionic strength solutions dextran sulfate is fully extended due to the repulsion of the negative charges exerted by the sulfate groups. In high ionic strength solutions when all charges are neutralized by counter ions, the polymer is more closely packed.¹¹³

The degree of sulfation is an important factor for colitis induction¹¹⁴ or induction of dysplastic lesions (carcinogenicity).¹¹⁵ The carcinogenic activity differs with administration of dextran sulfate of different molecular weights, whereas the midsize polymers are worse than large and small ones (5 kDa, 40 kDa, 500 kDa)^{115,116}

2.2.8 Hyaluronic Acid (HA)

Hyaluronic acid (hyaluronan or hyaluronate) can be found in all tissues, especially in connective tissues and body fluids of vertebrates (and some bacteria).⁸⁶ Half of the mammalian body's HA is in the skin, a quarter is built in the skeleton and joints, and the rest is equally divided between muscles and viscera.¹¹⁷ However, the lowest concentration is found in blood serum. It has been used in several wound-healing applications like the synthesis of scaffolds functionalized with proteins such as fibronectin to facilitate cell

migration into the wound.¹¹⁸ HA belongs to the group of glycosaminoglycans (GAG, formerly known as acid mucopolysaccharides) which are linear and anionic, but it is quite distinct from other GAG due to

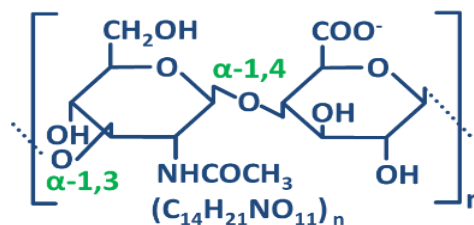


Figure 2.2.8: The chemical structure of the repeating dimer (left: D-N-acetylglucoseamine and right: D-glucuronic acid) of the nonsulfated glycosaminoglycan hyaluronic acid with its alternating α -1,3 and α -1,4 glycosidic linkages and its molecular formula are depicted.

the fact that it lacks any sulfate groups (table 2.2.1) and it is synthesized by a protein (chain growth at the reducing end) in the cellular plasma membrane.⁸⁶ In contrast to other GAGs (<50 kDa, commonly 15-20 kDa) HA chains can be very large, their M_r can reach several million (synovial fluid weight average is about 7×10^6 , >15 μm if it would be straightened).⁸⁶ It was first determined in the laboratory of Karl Meyer in the 1930s.¹¹⁹ The repeating unit of HA is a dimer composed of D-N-acetylglucosamine and D-glucuronic acid, alternatingly connected via α -1,3 and α -1,4 glycosidic linkages. At extracellular pH, the carboxyl groups of HA are fully ionized. Further, the osmotic activity is disproportionately high in relation to its molecular weight. Therefore, it plays a major role in the distribution of water and its homeostasis. A twist in the polysaccharide chain is induced by secondary hydrogen bonds formed along the axis, that impart the stiffness and forms hydrophobic patches that allow the association with other HA chains and extent the capability to bind non-specifically to membranes or other lipid structures.¹²⁰ Overall, the stiffness of the polymer promotes an extended random coil configuration, which overlaps and forms an entangled network at concentration levels of 0.5-1.0 mg/ml.

2.2.9 Dextran

In clinics dextran is used as an antithrombotic, to reduce blood viscosity, and as a volume expander in anemia.¹²¹ Dextran mediates its antithrombotic effect by increasing the surface's electronegativity of vascular endothelium, platelets, or erythrocytes and thereby reducing platelet adhesion or erythrocyte aggregation. Large dextrans (MW > 60 kDa) remain in the blood for weeks, because they are slowly metabolized and poorly excreted by the kidney. In

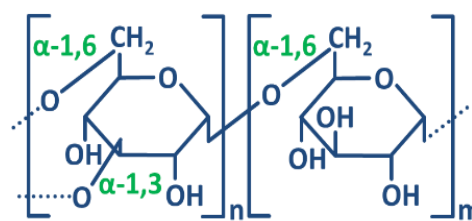


Figure 2.2.9: The chemical structure of dextran with its monomer glucose connected via α -1,6 glycoside linkages on the straight chain and α -1,3 linkages, where polysaccharide chain branches, is shown.

paper II (PF4/PA) complex formation between PF4 and dextran was investigated with the help of circular

dichroism spectroscopy. Dextran is a branched homopolysaccharide present in bacteria and yeast, first discovered by Louis Pasteur.¹²² The straight chain is made up of α -1,6 linked D-glucose and the branches start with α -1,3 glycosidic linkages. Some organisms have α -1,2 or α -1,4 branches. The polymer adopts a random coil structure.¹²³ Dental plaques consist to a great extent of dextrans and are formed by bacteria on the teeth's surface. The plaques are adhesive and allow the organisms to stick to the surface.^{85,124} Dextrans also serve as a source of glucose for bacterial metabolism.

2.2.10 DNA – Protein C-Aptamer

Aptamers (from Latin *aptus* – fit, and Greek *meros* – part) are small DNA or RNA constructs, designed for basic research or as therapeutics to bind to specific target molecules. Due to nuclease degradation, the half-life of nucleic acids in the blood is only 4-30 minutes.³⁸ The clearance of DNA takes a bit longer than of RNA. In healthy individuals, the extracellular concentration of nucleic acids ranges from 0 to > 1000

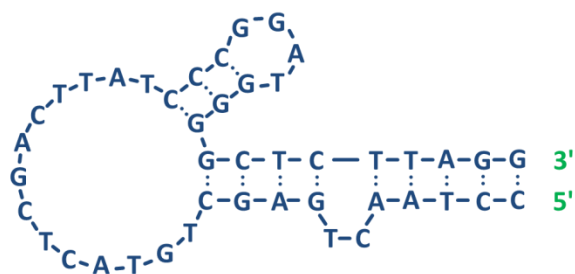


Figure 2.2.10: The nucleotide sequence of the protein C-aptamer including its secondary structure, estimated by mfold DNA database (University of Albany/NY/USA, <http://mfold.rna.albany.edu/?q=mfold/dna-folding-form>) is depicted (A – adenosine T – thymine, C – cytosine, G – guanine). The aptamer was purchased from Purimex (Giebenstein/Germany).

ng/mL.³⁵ However, under pathological conditions like tissue damage, cell apoptosis, breakdown of bacteria and viruses cell-free-nucleic acids can extensively increase. Another source of nucleic acids is represented by neutrophils that form so-called NETS (neutrophil extracellular traps). Several aptamers were investigated in paper V (PF4/aptamer). CD spectroscopic measurements on PF4/aptamer complex formation were conducted with protein C-aptamer (figure: 2.2.10).

2.2.11 Polyphosphates – P3, P45, P75

Inorganic polyphosphates (polyP) are ubiquitous polymers formed by phosphate (P_i) residues linked by high-energy phosphoanhydride bonds and one of the most ancient, conserved and enigmatic molecules in biology.¹²⁵⁻¹²⁷ PolyP are of particular interest in hematology because they are secreted by activated platelets¹²⁸⁻¹³⁰ or mast cells¹³¹ and accumulate in many infectious microorganisms.¹³² It has been shown that polyP are

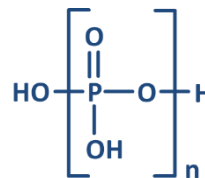


Figure 2.2.11: The chemical structure of polyphosphates, consisting of phosphate (P_i) residues linked by high-energy phosphoanhydride bonds is shown. For the polyP used in this thesis, n denotes for either 3, 45, or 75.

procoagulant,^{130,133,134} prothrombotic,^{130,135} and pro-inflammatory.^{130,133,134} PolyP trigger clotting *via* the contact pathway,^{130,135,136} accelerate factor V activation,¹³⁵ enhance fibrin clot structure,^{137,138} and accelerate factor XI back-activation by thrombin.¹³⁹ The mean chain length of polyP stored in acidocalcisomes together with calcium, ATP, ADP, and serotonin in human platelets is 70-75 P_i ¹²⁸ or 60-100 P_i .¹³⁰ PolyP concentration in plasma ranges from 10-50 μ M, but due to phosphatases, polyP are unstable and have a half-life of about 90 minutes.^{135,137,140} Recently, it was found that polyP act as primordial chaperone stabilizing proteins *in vivo* helping them to withstand proteotoxic stress.¹²⁶

2.3 Reagents, Materials

Reagent, material	Supplier	Catalog number
2-O, 3-O desulfated heparin (ODSH)	ParinGenix Inc., Weston/FL/USA	
anti-human IgG, peroxidase conjugated	Dianova, Hamburg/Germany	
Arixtra® (fondaparinux)	GlaxoSmithKline, Durham/NC/USA	
Calcium chloride (CaCl ₂)	Merck, Darmstadt/Germany	1.02382.0500
Chondroitin 4-sulfate	Sigma-Aldrich, Munich/Germany	27042-10G-F
Clivarin®1.750 (reviparin)	Abott Arzneimittel GmbH, Wiesbaden/Germany	
CovaLink microtiter plate	Nunc, Langenselbold/Germany	
Dextran	Sigma-Aldrich, Munich/Germany	00270-100MG
Dextran sulfate	Sigma-Aldrich, Munich/Germany	D6924-1G
Escherichia coli	Promega GmbH, Mannheim/Germany	
Goat normal serum	Sigma-Aldrich, Munich/Germany	G6767
Heparin-Natrium-25000 (UFH)	ratiopharm®, Ulm/Germany	
heparin oligosaccharides (HO06, HO08, HO16)	Iduron Ltd., Manchester/UK	
Hyaluronic acid	Sigma-Aldrich, Munich/Germany	53747-1G
Hydrogen chloride (HCl)	Carl Roth GmbH, Karlsruhe/Germany	4326.1
Magnesium chloride (MgCl ₂)	Merck, Darmstadt/Germany	1.05833.0250
Monosodium phosphate (NaH ₂ PO ₄)	Merck, Darmstadt/Germany	1.06349.1000
OptEia™ (tetramethylbenzidine)	BD Biosciences, Heidelberg/Germany	
PerCP-Cy5.5 Streptavidin	BD Biosciences, Heidelberg/Germany	551419
Phosphate buffered saline PBS	Invitrogen, Darmstadt/Germany	
Platelet factor 4 (PF4)	Chromatec, Greifswald/Germany	
Potassium chloride	Th. Geyer GmbH, Renningen/Germany	1632.1000
Protamine sulfate	Sigma-Aldrich, Munich/Germany	P4020-1G
Quartz cuvette (10 mm pathlength)	Hellma, Müllheim/Germany	100-10-40 type 100-QS
Quartz cuvette (5 mm pathlength)	Hellma, Müllheim/Germany	110-5-40 type 110-QS
Sodium chloride (NaCl)	Th. Geyer GmbH, Renningen/Germany	1367.1000
Sodium hydroxide (NaOH)	Sigma-Aldrich, Munich/Germany	S8045-1KG
Sulphuric acid (H ₂ SO ₄)	Carl Roth GmbH, Karlsruhe/Germany	X945.1
Tween 20	AppliChem GmbH, Darmstadt/Germany	A4974,0500

2.4 Devices and Softwares

Device	Supplier
Paradigm™ plate reader	Beckman Coulter, Krefeld/Germany
Chirascan CD spectrometer	Applied Photophysics Ltd., Leatherhead/UK
Cytomics FC 500	Beckman Coulter, Krefeld/Germany
MicroCal iTC200	GE Healthcare Europe GmbH, Freiburg/Germany

Software	Supplier
Circular dichroism neural network (CDNN)	developed by Gerald Böhm http://gerald-boehm.de/downloads/category/3-cdnn-software
Origin 7 SR4	OriginLab Cooperation, Northampton/MA/USA
Pro-Data Chirascan (Chirascan Spectrometer Control Panel version 4.2.0)	Applied Photophysics Ltd., Leatherhead/UK
Pro-Data Viewer (version 4.2.0)	Applied Photophysics Ltd., Leatherhead/UK
SoftMax (version 6.2.1)	Molecular Devices (Germany) GmbH, Biberach an d. Riss/GER
Windows Multiple Document Interface (WinMDI 2.8)	developed by Joe Trotter, Scripps Research Institute, San Diego/CA/USA http://facs.scripps.edu/software.html

3. Bacteria

Bacteria are a large kingdom of the Prokaryotes and were among the first life forms on our planet. They appear in different shapes like spheres, rods, or spirals, respectively. With a few micrometers in size not visible with the naked eye, bacteria represent a large fraction of the earth's biomass. It is higher than of all plants and animals together. There are estimated $4\text{--}6 \times 10^{30}$ bacterial cells with a weight of 350-550 petagram ($1 \text{ Pg} = 10^{15} \text{ g}$) that are living in nearly every habitat on earth.¹⁴¹ With estimated 3.5×10^{30} and $0.25\text{--}2.5 \times 10^{30}$ cells most of them are living in oceanic and terrestrial subsurfaces, respectively.¹⁴¹ The soil contains 2.6×10^{29} cells (40 million per gram of soil) and the open ocean is the environment of 1.2×10^{29} cells. Even in fresh water there are still one million cells per milliliter. Prokaryotes also settled at extreme places like acidic hot springs, in deep portions of the earth's crust, and even in nuclear waste they were found.¹⁴²

The fact that bacteria also populate animals and plants and that this cohabitation is not always symbiotic, put evolutionary pressure on both sides. Animals or plants which achieved a defense mechanism against a pathogen had an advantage over others and were more successful in reproduction than those which had not gained the new property. It was the same on the side of the bacteria. Once their host had gained a kind of immunity only those cells survived that were not recognized or could withstand the pressure that was put on them. This evolutionary race is taking place from the very beginning of life on earth. It started with prokaryotes adapting to their environment, continued with the development of animals of higher complexity, and is still ongoing on a new level since the human kind is extensively using antibiotics (e.g. MRSA). Krauel *et al.* found that PF4 binds to bacteria and this feature probably makes it a part of an ancient host defense mechanism.²⁹ As continuation of that idea we found in paper I (PF4 evolutionary analysis) that PF4 binds to the phosphate groups of lipid A and that PF4 is evolutionary conserved over different species (mammals, fish, amphibians, less for birds and reptiles). Several mutants of *E. coli* with differently truncated lipopolysaccharide (LPS) were tested for antibody-

binding. The mutant with the most truncated LPS was found to bind the most PF4. In the view of the evolutionary race we speculate that the LPS-layer covering the outer membrane of Gram-negative *E. coli* could be the reaction of the bacterium to the ancient defense mechanism of its host in which PF4 covered the bacteria and by changing its conformation acted like a danger signal. It might very well be that bacteria got 'invisible' by shielding the structure that is recognized by the immune system with LPS.

Based on the physicochemical properties of their cell walls, bacteria can be grouped into Gram-positive and Gram-negative. With the help of Gram staining, a method first described in 1884 by the Danish scientist Hans Christian Gram, it is possible to distinguish between the two major classes of bacteria.¹⁴³ The envelope of Gram-positive bacteria is composed of a plasma membrane and a 20-80 nm thick mesh-like cell wall made of peptidoglycan (50-90% of envelope) separated by the periplasmic space. The Gram-negative bacteria have two membranes, the inner plasma membrane and the outer membrane which is covered with lipopolysaccharide. Between the membranes there is a thinner layer of peptidoglycan compared to the Gram positive bacteria (10% of envelope).

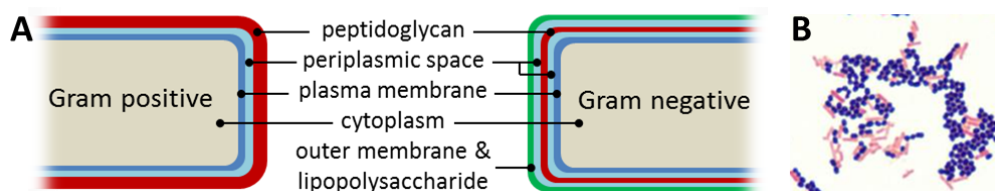


Figure 3.0.1: A – schematic comparing the envelope structure of Gram positive and Gram negative bacteria; B – Gram stain: pink - Gram negative rods (*Escherichia coli*), dark blue: Gram positive cocci (*Enterococcus faecalis*) (stain image: Dave Hanks, 09.09.2013)

The differentiation between Gram-positive and Gram-negative is due to the ability of the envelope to retain either crystal violet stain – Gram-positive (dark blue), or to retain the counterstain by safranin or fuchsin – Gram-negative (pink, red), figure 3.0.1. The staining procedure consists of four steps starting with crystal violet that stains both, Gram negative and Gram positive cells. In a second step iodine is added which forms big complexes with the crystal violet ($CV^+ + I^-/I_3^- \rightarrow CV-I$). Adding alcohol or acetone decolorizes both types of cell within a different time scale. It is faster for Gram negative than for Gram

positive. Gram negative cells lose their outer membrane and the CV-I complexes are washed away from the thinner peptidoglycan layer. Gram positive cells get dehydrated by this treatment and so the complexes are trapped in the thicker peptidoglycan layer. The cells retain the crystal violet and appear deep blue. Finally a counterstain is made with the positively charged safranin or the basic fuchsin to give the Gram-positive cells a pink to red color. Although there is a subset of bacteria that yield a Gram-variable pattern, the method can differentiate most of the microbes by the properties of their cell wall.

To follow the idea of PF4 as an ancient host defense mechanism and because it was found that PF4 binds to lipid A,^{1,26} the innermost part of the lipopolysaccharide (LPS), see figure 3.0.2. Lipid A is a glucosamine disaccharide decorated with multiple fatty acids that build the anchor of the LPS in the outer membrane of Gram-negative bacteria (see figure 3.0.1). The glucosamine residues are phosphorylated and therefore negatively charged. Lipid A is the most conserved part of the LPS¹⁴⁴ and is the main responsible for the toxicity of Gram-negative bacteria. Directly attached to lipid A is the core region consisting of sugars such as 3-deoxy-D-mannooctulosonic acid, also known as keto-deoxyoctulosonate = KDO (figure 3.0.2 – inner core, orange structures)¹⁴⁵ and heptoses (inner core green structures). The inner core of many bacteria is also phosphorylated and can contain other non-carbohydrate components such as amino acids and

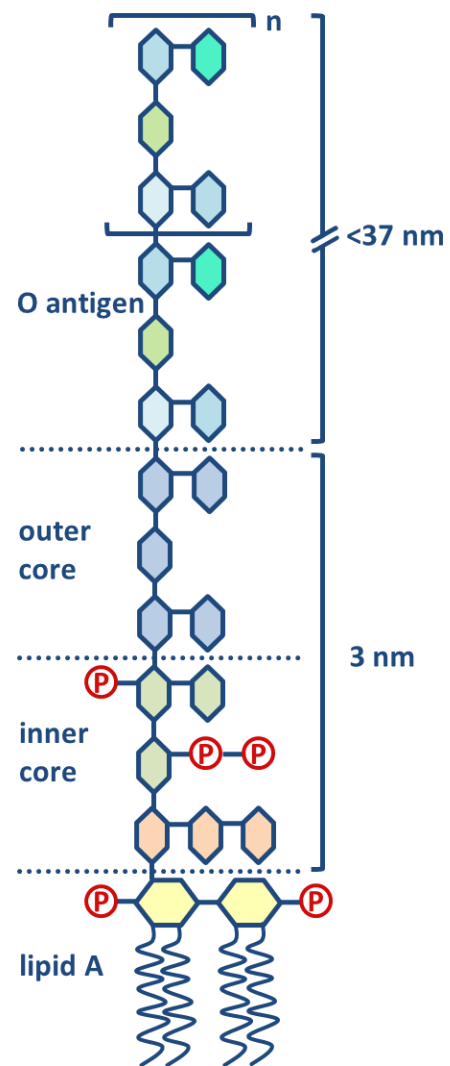


Figure 3.0.2: Schematic of lipopolysaccharide (LPS). The anchor of LPS in the outer membrane is lipid A. Lipid A consists of a phosphorylated glucosamine disaccharide to which several fatty acids are attached. The core region consists of sugars like KDO (orange), heptoses (green) of the inner core and hexoses in the outer core (blue). The O antigen is attached to the third hexose of the inner core and is a repetitive glycan polymer.

ethanolamine substituents. Attached to the last heptose of the inner core, the outer core consists of hexose residues, such as D-glucose, D-mannose, D-galactose, which can also branch forming side chains. The outermost and also most variable part of the LPS, the O antigen, O polysaccharide or O side-chain of bacteria, is usually linked to the third hexose of the outer core. For different *E. coli* strains, over 160 different O antigen structures were found.¹⁴⁶ As the O antigen is exposed on the surface it is the target of host antibodies. The length of the polysaccharide chain also differs between the species and can reach at maximum 37 nm.³⁴ There are also species without or truncated O side-chains, their LPS is called rough. Whereas bacteria with full length LPS are called smooth.

A member of the Gram-negative bacteria was used to investigate the PF4-binding to bacterial surfaces (*Escherichia coli* JM109). The strain was chosen due to the fact that it is very well characterized. It was UV-inactivated and additionally fluorescein isothiocyanate (FITC) labeled to allow discrimination between the microbes and the differently labeled PF4/polyP complexes in flow cytometry. FITC is a fluorescent tracer. The fluorescein functionalized with an isothiocyanate reactive group makes it reactive towards nucleophiles (amine, sulfhydryl groups e.g. of proteins).

3.1 Escherichia coli (E. coli JM109-FITC)

domain	Bacteria
kingdom	Eubacteria
phylum	Proteobacteria
class	Gammaproteobacteria
order	Enterobacteriales
family	Enterobacteriaceae
genus	Escherichia
species	Escherichia coli

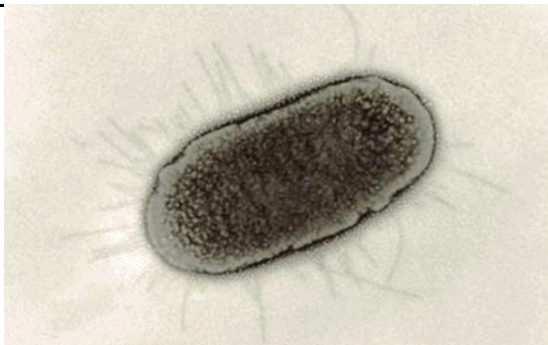


Figure 3.1.1: transmission electron micrograph of *Escherichia coli* (*E.coli*) with projecting pili, negatively stained to enhance contrast

Escherichia coli (*E. coli*; Promega) is a rod-shaped, Gram-negative, facultative anaerobic bacterium which are together with *Streptococcus* the first bacterial genera to colonize the lower intestine of warm-blooded organisms.^{147,148} There are harmless and even beneficial strains that are part of the normal microflora of the gut which prevent potentially pathogenic bacteria from establishing (e.g *Salmonella typhimurium*)^{149,150} or provide their host with nutrition for instance vitamin K₂.¹⁵¹ *E. coli* is the most widely studied prokaryotic organism. The *E. coli* strain K12 subtype JM109 is a special laboratory strain for the selection of plasmids with inserts (white-blue selection).¹⁵² In contrast to the wild type it cannot settle the human intestine and is not viable outside the lab.

3.2 FITC Labeling

Bacteria were cultured in Todd-Hewitt broth supplemented with 0.5% yeast extract until the exponential phase at 37°C.¹⁵³ After washing with PBS they were exposed to UV radiation for two hours on behalf of inactivation. For the labeling 1M 100 μ l NaHCO₃ with a pH of 9 was added to 1 ml of bacteria solution containing 1*10⁹ cells and then 50 μ l fluorescein isothiocyanate (FITC) which was dissolved in dimethylsulfoxide (DMSO) to a final concentration of 7.4 mg/ml was added. Incubation was carried out

for one hour while stirring. Removal of free dye was gained by three washing steps including the resuspension of the bacteria with 10 ml PBS and subsequent centrifugation (4000 rpm, 6 minutes, RT). The final resuspension was adjusted to have the desired number of cells per milliliter.

4. Experimental techniques

4.1 Circular Dichroism (CD) Spectroscopy

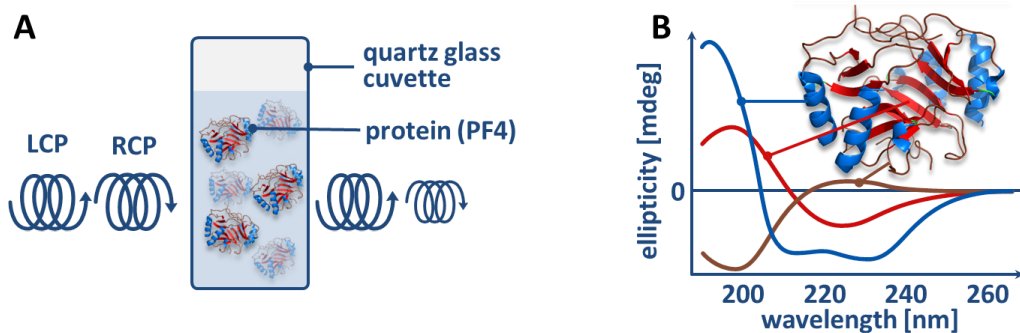


Figure 4.1.1: Schematic of the principle of circular dichroism spectroscopy: The differential absorption of left (LCP) and right circularly polarized light (RCP) when it passes through an optically active solution (e.g. proteins in solution) is depicted in **A**. Although differential absorption is measured, for historical reasons it is mostly expressed in ellipticity [milli degrees]. The sensitivity of far-UV CD spectroscopy for secondary structures is illustrated in **B**. Each secondary structure exhibits a characteristic CD spectrum. The protein in **B** depicts platelet factor 4 with the differently colored secondary structures: α -helix – blue, β -sheets – red, random structures and turns – brown).

The majority of naturally occurring chemical compounds, such as proteins, nucleic acids, hormones, and vitamins exhibit optical activity. There are only very few natural products that are not optically active.

Due to the fact that a mirror image of a compound can have harmful effects on an organism, there was quite early the need for measuring the chiral and optical purity in drug and food related industries. That is why chiroptical measurements were already carried out in the mid-nineteenth century and therefore, these were among the first physical constants measured.¹⁵⁴

Circular dichroism (CD) spectroscopy is a non-destructive tool to study the structure of proteins in solution, which is very economic in terms of sample consumption. Depending on the properties of the protein to investigate, only 15 μ g of protein can be sufficient to run an experiment. Far-UV CD spectroscopy is very accurate when relative changes in secondary structure of proteins have to be measured. It is used to study the influence of the environment, for example by the subsequent change of pH, heat or concentration of denaturants. The work in this thesis focuses on the structural changes of proteins due to interaction with polyanions (PA). The procedure is very similar to that used for the

denaturing of proteins where certain chemicals are titrated to the protein. The only difference is that the denaturant is substituted by different PAs. To obtain optimal results, the usage of dilute or non-absorbing buffers is crucial. Normally, buffers do not exhibit a CD signal but they show absorbance in the lower nanometer range which makes it challenging to detect anything below 200 nm.

The specific characteristic which makes CD spectroscopy suitable for the investigation of protein structures or structural changes of a protein, is the unique CD spectrum each secondary structure exhibits (figure 4.1.1 B). Determining the secondary structure content from CD spectra (deconvolution) is based on the assumption that the CD spectrum of a protein (θ_λ) can be represented by a linear combination of its secondary structural elements (i , their fraction ε_i) which also includes a noise term and the contribution of aromatic chromophores and prosthetic groups (equation 4.1.1).^{155,156} $S_{\lambda i}$ is the ellipticity at each i^{th} secondary structural element.

$$\theta_\lambda = \sum \varepsilon_i S_{\lambda i} + noise \quad (\sum \varepsilon_i = 1, \varepsilon_i \geq 0) \quad (4.1.1)$$

By the usage of softwares that compares the measured spectrum with a database of spectra with known secondary structure composition, it is possible to estimate the fraction of α -helix, β -turns, random coil, antiparallel and parallel β -sheet structures in the investigated protein.

CD spectroscopy is the wavelength dependent differential absorption ($\Delta A(\lambda)$) of left (LCP) and right circularly polarized (RCP) light.

$$\text{Circular dichroism} = \Delta A(\lambda) = A(\lambda)_{LCP} - A(\lambda)_{RCP} \quad (4.1.2)$$

The different extent of absorption of the left and right circularly polarized rays can be quantitatively described by the Beer-Lambert law.

$$A_{\lambda} = \log_{10} \left(\frac{I_0}{I_1} \right) = \varepsilon_{\lambda} \times c \times d \quad (4.1.3)$$

where I_0 is the intensity of the incoming light and I_1 is the intensity of light transmitted through the cell.

The recorded absorption is proportional to the concentration c [mol x L⁻¹], the path length d [cm], and the molar absorption coefficient ε_{ν} [L x cm⁻¹ x L⁻¹]. In CD spectroscopy, alternately LCP and RCP light of the same I_0 ($d=0 \rightarrow I_{LCP,0} = I_{RCP,0}$) is sent into the sample and the intensities I_{RCP} and I_{LCP} are measured after transmission through the sample. The combination of the equations 4.1.2 and 4.1.3 brings the insight that a reference beam is not necessary, due to the fact that (I_0) does not appear in the final equation (4.1.4) anymore. Therefore, most of the devices are of single-beam type (figure 4.1.2).

$$\Delta A(\lambda) = \log_{10} \left(\frac{I_0}{I_{LCP}} \right) - \log_{10} \left(\frac{I_0}{I_{RCP}} \right) = \log_{10} \left(\frac{I_{RCP}}{I_{LCP}} \right) \quad (4.1.4)$$

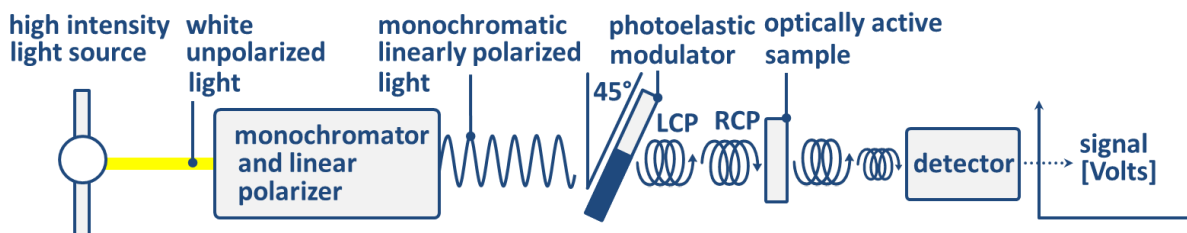


Figure 4.1.2: Schematic of a CD spectrometer: white unpolarized light from a high intensity light source is resolved into a narrow spectral band by a monochromator and converted into plane-polarized light by a polarizer. When passing a photoelastic modulator (PEM) the monochromatic plane-polarized light is alternately converted into right circularly polarized light (RCP) and left circularly polarized light (LCP). During transmission through an optically active sample one of the light beams (RCP or LCP) is absorbed to a greater extent. A detector, usually a photomultiplier, converts the signal into an electrical signal which is then converted into ellipticity values.

Usually, ΔA is measured, but for historical reasons, measurements are mostly reported in (milli)degrees of ellipticity (θ). Geometrically, the ellipticity of an ellipse is the angle described by the following equation:

$$\tan\theta = \frac{E_R - E_L}{E_R + E_L} \quad (4.1.5)$$

where E_R and E_L are the magnitudes of the transmitted electric field vectors of RCP and LCP light. The result of two electric field vectors rotating in opposite directions but with same magnitude and phase is plane polarized light. The red vector in figure 4.1.3 – **A** just oscillates up and downwards in one plane. When, due to absorption, one of the components (LCP or RCP light) is less intense, as shown in figure 4.1.3 – **B**, the resulting vector (red) describes an ellipse. To describe the ellipticity, one can either measure or calculate the angle θ that is formed by semi-minor and semi-major axis and positioned opposite the semi-minor.

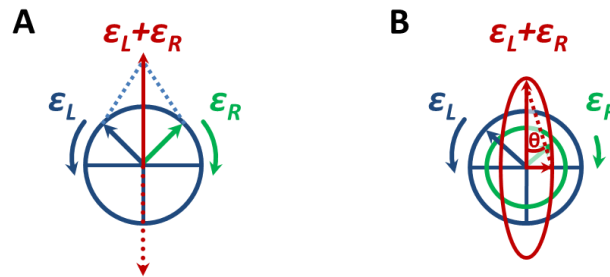


Figure 4.1.3: A – Plane polarized light can be resolved as LCP and RCP light of same amplitude and phase – the electric vector oscillates in a plane. **B** – If one of the intensities is lower, e.g. due to absorption, the electric vector will follow an elliptical path – elliptically polarized light. The semi-major axis and semi-minor axis of an ellipse form a triangle. The angle opposite the semi-minor is the angle θ which is also called ellipticity.

The circular dichroism effect is in general very small leading to a small $\tan\theta$, which is therefore approximated as θ in radians. Based on the knowledge that intensity or irradiance (I) of light is proportional to the square of the electric field vector, the ellipticity becomes:

$$\theta(\text{radians}) = \frac{I_{RCP}^{1/2} - I_{LCP}^{1/2}}{I_{RCP}^{1/2} + I_{LCP}^{1/2}} \quad (4.1.6)$$

By several steps of substitution, simplification, and exponential expanding (Taylor series), one obtains an equation by which the values of ΔA and θ can be simply interconverted.

$$\theta = 3298.2 \times \Delta A(\lambda) [\text{mdeg}] \quad (4.1.7)$$

Changes in the secondary structure of PF4 (papers: II, III, IV, V) and PS (paper: VI) upon interaction with PAs were studied by recording far UV CD spectra (PF4: 200–260 nm, PS: 185–260 nm) using a Chirascan CD spectrometer. The different wavelength ranges for PF4 and PS are due their different solvents. PF4 was dissolved in phosphate buffered saline (PBS: NaCl [139 mmol/L], KCl [2.7 mmol/L], Na₂HPO₄ x 2 H₂O [10 mmol/L], KH₂PO₄ [2 mmol/L], pH 7.4) and PS in ultrapure water from the in-house water purification system (Satorius Arium pro VF). Salts in buffers contribute absorption to the system and set certain limits concerning the lower nm-range. For optimal CD results, the usage of very dilute buffers or water is recommended. In case of PS this recommendation was followed. Water was used to solve PS and it was possible to measure the CD signal down to 190 nm in a cuvette with 5 mm path length. In case of PF4 the solvent constitution was set to match physiologic ion strength. Therefore the measurement with the same path length of 5 mm were limited to approximately to 200 nm in the lower nm range. The initial PF4 concentration was set to 40 µg/mL (1.25 µmol/L, cuvette path length = 10 mm) and 80 µg/mL (2.5 µmol/L, 5 mm), respectively or for PS to 60 µg/mL for PS (12 µmol/L, 5 mm). The formation of the complexes was carried out at 20°C directly within the CD quartz cuvette from Hellma. Each measurement started with a pure protein in solution. Afterward, increasing amounts of a certain PA were sequentially added to the cuvette leading to PF4/PA or PS/UFH mixtures of defined ratio. To reduce the noise, 5–20 CD spectra were first recorded for each protein:PA ratio and later averaged. Additionally, buffer baselines, baselines of each PA concentration step (without PF4 in the solution) were recorded.

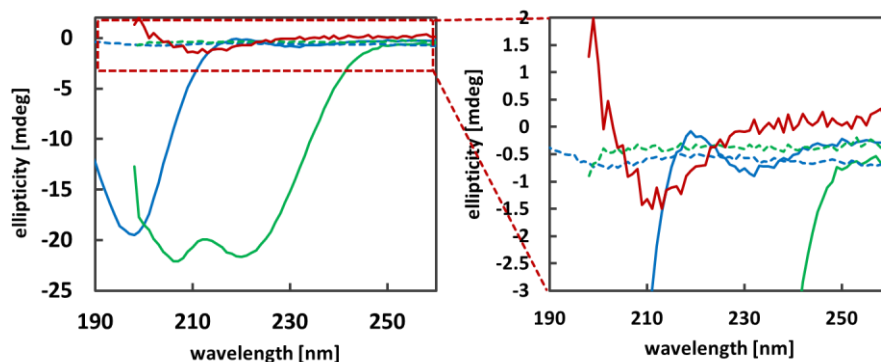


Figure 4.1.4: Comparison of the background corrected (baseline subtracted) CD spectra [mdeg] of the native proteins platelet factor 4 [80 $\mu\text{g/mL}$] (—) and protamine sulfate [60 $\mu\text{g/mL}$] (—) with their respective buffers PBS (---) and water (---). Compared to protein spectra, UFH (—) in the highest used concentration (147 $\mu\text{g/mL}$), does not exhibit a strong CD signal but is nevertheless subtracted in the data processing. All measurements were carried out in cuvettes with a path length of 5 mm.

figure 4.1.4 shows a comparison of the CD spectra of native PF4 and PS. Furthermore, the corresponding baselines by which the proteins are corrected are shown. It is important to highlight that even the highest concentration of heparin which was used, exhibited a signal (—) that was much lower than the ones of the proteins (PF4 —, PS —).

While titrating heparins, which in fact do not exhibit or only a very low CD signal in the accessed range, they add absorption to the measured protein/PA system. This sets limitations for the heparin concentrations that are measurable at a certain setup (combination of cuvette size/path length and protein concentration). The problem of elevated noise at the lower end of the measured wavelength range (200-205 nm in case of the PF4/UFH system, 190 -205 nm for the PS/UFH system) gets more and more evident the higher the heparin concentration gets. To a certain extent this effect is balanced automatically by the CD spectrometer itself by amplifying the power at the sensor to increase its sensitivity. It is also advantageous to increase the number of repetitions per protein:PA in order to reduce the noise of the final averaged CD spectrum.

For the data analysis, the raw spectra of the protein (θ_{protein} , equation 4.1.8), the raw spectra of the protein/PA complexes ($\theta_{\text{protein/PA}}$, equation 4.1.9) and the raw PA baseline spectra (θ_{PA} , equation

4. Experimental techniques

4.1.10) were normalized with respect to the corresponding buffer baseline (baseline subtraction). For the measurements, PF4 was diluted in PBS and PS was solved in water.

$$\theta_{norm}(c_{protein}) = \theta(c_{protein}) - \theta(buffer) [mdeg] \quad (4.1.8)$$

$$\theta_{norm}(c_{protein/PA}) = \theta(c_{protein/PA}) - \theta(buffer) [mdeg] \quad (4.1.9)$$

$$\theta_{norm}(c_{PA}) = \theta(c_{PA}) - \theta(buffer) [mdeg] \quad (4.1.10)$$

Further, the baseline corrected protein/PA complexes ($\theta_{norm}(c_{protein/PA})$) were corrected for the buffer subtracted PA baselines ($\theta_{norm}(c_{PA})$, equation 4.1.11). After this step, the θ values for the protein/PA complexes are corrected for the absorption exhibited by the quartz cuvette and the buffer and for the spectrum that the PA contributed.

$$\theta_{normII}(c_{protein/PA}) = \theta_{norm}(c_{protein/PA}) - \theta_{norm}(c_{PA}) [mdeg] \quad (4.1.11)$$

In the next step $\theta_{protein,norm}$ and $\theta_{protein/PA,normII}$ values are normalized with respect to *path length* [cm], protein concentration $c_{protein}$ [mol x L⁻¹] and number of amino acids ($AA_{protein}$) to obtain the wave-length-dependent mean residue delta epsilon θ_{MRDE} [degrees x cm² x dmol⁻¹] or [degrees x M⁻¹ x m⁻¹].

$$\theta_{MRDE} = \frac{(\theta_{norm}(c_{protein}) [mdeg])}{path\ length\ [cm] \times c_{protein}\ [mol/L] \times AA_{protein}} \quad (4.1.12)$$

$$\theta_{MRDE} = \frac{(\theta_{normII}(c_{protein/PA}) [mdeg])}{path\ length\ [cm] \times c_{protein}\ [mol/L] \times AA_{protein}} \quad (4.1.13)$$

Two different programs were used for the data acquisition with the Chirascan CD spectrometer (Applied Photophysics Ltd., Leatherhead/UK) i) Pro-Data Chirascan (Chirascan Spectrometer Control Panel version 4.2.0) was used to set all the experimental parameters (e.g., wavelength range, shutter, time-per-point etc.) and ii) Pro-Data Viewer version 4.2.0 by Applied Photophysics Ltd. was used to visualize and save

the data. Data preparation introduced in equations 4.1.8-4.1.13, baseline subtraction and normalization were conducted with the help of a home-made Excel template.

To estimate the secondary structure content of PF4, deconvolution of CD-spectra was carried out using CDNN software version 2.1 (Circular Dichroism Neural Networks) using a database of 33 reference proteins.¹⁵⁷ The program was written by Gerald Böhm in the 90's (latest version 1999) and is based on a method called "neural networks". The system is organized into input (CD wavelengths), output (secondary structure information), and hidden layers linked by neurons (nodes), "connections between the neurons are assigned numerical weights (usually via a propagation algorithm) and then trained."¹⁵⁸ The system is trained by feeding it with sets of known proteins (information). The learning process includes the assignment of weights to connected information, iterations between input and output layer and assignment of random weights. The output weights are residual errors and iterations are made until the errors are minimized. The output is a function of the input. For the transfer between the layers, CDNN is using a linear transfer function. The secondary structure determination based on CD data is superior when investigating the conformation of well-folded globular proteins. Absolute values of α -helices can be determined with a precision of 5% and β -sheets and β -turns better than 10%. The overall precision increases to around 1% when structural changes in a protein (relative changes) are investigated.¹⁵⁶ Although a certain amount of α -helices is needed, the quality of the analysis of the structure decreases for proteins with a majority of pure α -helices.¹⁵⁵

For PS, no secondary structure estimation was done due to the fact that the protein does not meet the criteria for deconvolution. PS does not contain any α -helix⁴⁸ or only few (2% or 5%, respectively)⁴⁷, but a certain fraction of α -helix is needed to get reliable results from the deconvolution.¹⁵⁵

From table 4.1.1 it can be seen that the measured range for PF4 was mostly 198 – 260 nm and not 200 – 260 nm. The reason for that is that initially the recommendation was followed to smooth the data prior

to deconvolution. The smoothing procedure is based on a moving average which produces minor artefacts in the first values (low nm values). To overcome this minor issue, two more CD values (199 nm & 198 nm) were measured. Those two values are then the ones that are distorted by the smoothing procedure but are outside the range (200 – 260 nm) used for the deconvolution. There are two exceptions in the table where the measured nm-range was extended. The first exception is PF4/U FH, where the range was 198-470 nm to also cover the near UV-range to gain some insight about the tertiary structure behavior of PF4. In contrast to the far UV-range, where mainly the protein backbone (peptide bond) acts as a chromophore, in the near UV-range aromatic amino acids are the chromophores of interest. If changes in the tertiary structure are connected with structural rearrangements in the vicinity of aromatic amino acids (Tryptophan, Tyrosine, Phenylalanine), their absorption properties change. This can be monitored by near UV CD spectroscopy. The aromatic amino acid with the highest absorption coefficient is Tryptophan ($\epsilon = 5600 \text{ M}^{-1}\text{cm}^{-1}$ at 280 nm) followed by Tyrosine ($\epsilon = 1400 \text{ M}^{-1}\text{cm}^{-1}$ at 274 nm) and Phenylalanine ($\epsilon = 200 \text{ M}^{-1}\text{cm}^{-1}$ at 258 nm) has the lowest. PF4 has only one Tyrosine per monomer positioned next to the C-terminal Lysines and changes in the absorption were not observed. The second exception is the PF4/aptamer measurement where the range was 200 – 350 nm to cover the features of the protein C aptamer which has a pronounced positive band at 275 nm (see figure 4.1.5).

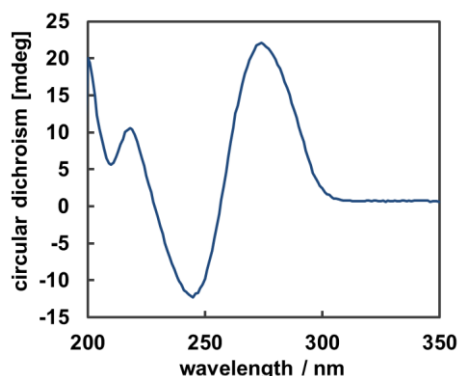


Figure 4.1.5: CD spectrum of the protein C aptamer at a concentration of 40 $\mu\text{g/ml}$ ($2.9 \times 10^{-6} \text{ mol/L}$) showing two pronounced bands at 245 nm and 275 nm

Table 4.1.1: List of the polyanions used in the papers II, III, IV, and V. Their maximum concentration in complex with PF4 in the publication and the measured maximum concentration in brackets is shown. Further the measured wavelength range is listed. *¹ – PF4 concentration [40 µg/mL/1.25x10⁻⁶ mol/L] or *² – PF4 concentration [80 µg/mL; 2.5x10⁻⁶ mol/L]; *³ – Due to their high polydispersity the concentration of the PAs, is given in [monomer mol/L]. *⁴ – In case of heparin the wavelength range was broader to also cover the near-UV range. *⁵ – In case of the protein C aptamer to visualize the features of DNA in the higher nanometer range. *⁶ – According to the supplier Iduron their fractionated heparins (HO06, HO08, HO16) have a PDI very close to one.

	polyanions (PA)	N	PDI	c _{max} (PA)		wavelength range [nm]
				[µg/mL]	[mol/L]	
PF4/PA (paper II)	Unfractionated heparin* ¹	>18	1.4	107 (146.6)	3.46x10 ⁻⁴ * ³	198-260/470* ⁴
	Reviparin (LMWH)* ²	5-7		106.7 (206)	3.45x10 ⁻⁴ * ³	198-260
	Fondaparinux* ²	5	1	119.2 (230)	6.9x10 ⁻⁵	199-260
	Dextran sulfate* ²	45-100		111.1 (311)	2.83x10 ⁻⁴ * ³	199-260
	Dextran* ¹	67	1.43	160 (160)	2.4x10 ⁻³ * ³	198-260
	Chondroitin sulfate* ²			107.7 (159)	2.83x10 ⁻⁴ * ³	198-260
	2-O, 3-O desulfated heparin* ²			106.7 (348)	3.94x10 ⁻⁴ * ³	198-260
	Hyaluronic acid* ²	7223-8667		116.1 (138)	5.98x10 ⁻⁴ * ³	199-260
PF4/defined heparins (paper III)	Unfractionated heparin* ²	>18	1.4	46.6 (146.6)	1.51x10 ⁻⁴ * ³	198-260/470* ⁴
	Fondaparinux* ²	5	1	44.7 (230)	2.59x10 ⁻⁵	198-260
	HO06 (=heparin 6-mer)* ²	6	1* ⁶	40 (100)	2.25x10 ⁻⁵	198-260
	HO08 (=heparin 8-mer)* ²	8	1* ⁶	46.6 (46.6)	1.94x10 ⁻⁵	198-260
	HO16 (=heparin 16-mer)* ²	16	1* ⁶	46.6 (46.6)	1.0x10 ⁻⁵	198-260
PF4/polyP (paper IV)	P3 (=polyP 3-mer)* ²	3		200 (200)	5.44x10 ⁻⁴	198-260
	P45 (=polyP 45-mer)* ²	45		300 (300)	1.34x10 ⁻⁴	198-260
	P75 (=polyP 75-mer)* ²	75		300 (300)	5.45x10 ⁻⁴	198-260
PF4/aptamer (paper V)	Protein C aptamer* ¹	44	1	80 (160)	5.92x10 ⁻⁶	198-260/350* ⁵
PS/UFH (paper VI)	Unfractionated heparin* ¹	>18	1.4	25 (160)	8.1x10 ⁻⁵ * ³	185-260

4.2 Enzyme Immunoassay (EIA)

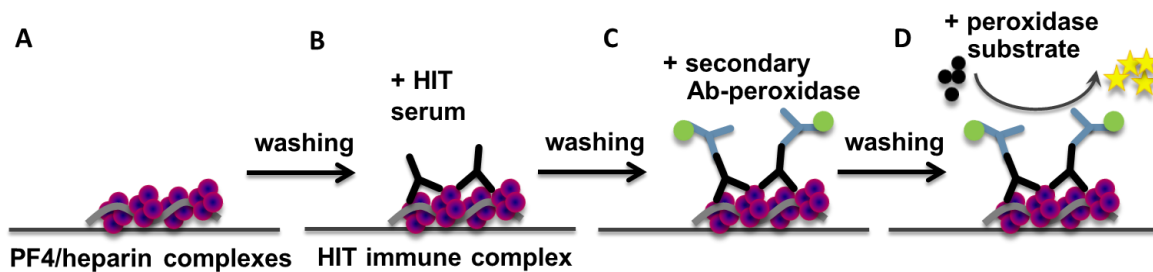


Figure 4.2.1: Schematic of the solid phase PF4/PA EIA, **A** – either PF4 alone or preformed PF4/PA complexes are immobilized on the surface of a microtiter plate, after washing **B** – the complexes are incubated with HIT sera known to contain PF4/heparin Abs, after a second washing step **C** – the PF4/heparin/Ab complexes are incubated with an enzyme-coupled secondary antibody, after the third and last washing step **D** – the PF4/heparin/Ab/secondary Ab complexes are incubated with the substrate for the enzyme that is coupled to the secondary Ab

The enzyme immunoassay (EIA) is a useful diagnostic tool based on the specific reactivity of an antibody against an antigen. The assay used here is a so-called solid phase EIA where a potential antigen (Ag) is non-covalently immobilized on a surface (figure 4.2.1Figure-A), the respective Ab binds to the Ag (figure 4.2.1-B) and a secondary Ab binds to the first Ab (figure 4.2.1-C). The signal amplification and visualization comes from the enzyme that is coupled to the secondary Ab. The more Ab is bound to the Ag, the more enzymes can convert their substrate (hydrogen peroxide, H_2O_2) that is provided in the last step (figure 4.2.1-D).

The PF4/PA enzyme immunoassay (EIA) used in papers II, III, IV, and V was carried out with human sera of patients known to contain anti-PF4/heparin IgG. This was verified by PF4/heparin EIA and heparin-induced platelet activation (HIPA) test, as described with some modifications.³² PF4 (20 μ g/ml) was incubated (60 min, RT) with rising concentrations of the PAs (Table) in coating buffer (0.05 M NaH_2PO_4 , 0.1% NaN_3) to enable complex formation. The aim was to test the antigenicity of PF/PA complexes of different molar ratios (PF4:PA) as investigated in CD spectroscopy. The wells of a Covalink microtiter plate were coated at 4°C overnight with 100 μ l of the corresponding complex solution. On the next day, the plates were washed five times (200 μ L of 0.15 M NaCl, 0.1% Tween 20, pH 7.5) and incubated (60 min, RT) with 100 μ l patient serum (1:200 or 1:1000 in 0.05 M NaH_2PO_4 , 0.15 M NaCl, 7.5% goat normal serum, pH 7.5). Plates were

washed five times and incubated with 100 μl peroxidase-conjugated anti-human IgG (1:20000, Dianova, Hamburg, Germany). Peroxidases are a family of enzymes that mostly have H_2O_2 as substrate and catalyze the following reaction:



Afterward, plates were washed five times and incubated (10 min, RT) with 100 μl with a 1:1 mixture of reagent A containing hydrogen peroxide and reagent B containing 3,3', 5,5' tetramethylbenzidine (TMB) in >25% methanol included in the OptEIA™ substrate reagent set. Whereas hydrogen peroxide is the electron donor (e^- in equation 4.2.1), TMB is the proton donor of the reaction (H^+ in equation 4.2.1). During the reaction TMB is converted into a diimine, which changes the solution from colorless to blue (figure 4.2.2).

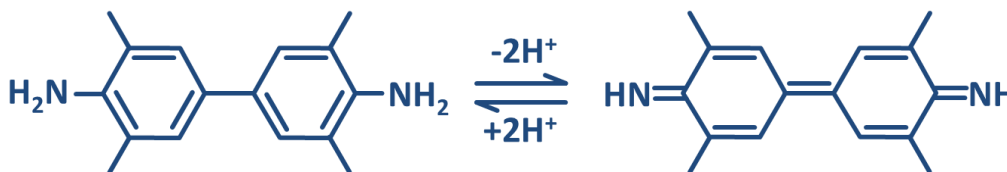


Figure 4.2.2: Conversion from colorless 3,3', 5,5' tetramethylbenzidine (left, TMB) to blue 3,3', 5,5' tetramethylbenzidine diimine (right). When sulfuric acid is added and the pH shifts to lower values, TMB diimine's color changes to yellow.

The color change can already be read out, but the reaction would continue while measuring. Depending on the speed at which the absorption is recorded, this could lead to systematic errors between the first and the last sample. For this reason the reaction is normally stopped. In this case, this was done by adding 100 μl of 1 M sulfuric acid (H_2SO_4). Due to the pH shift, the diimine changes its color from blue to yellow. The absorbance is finally measured at 450 nm.

The optical read out of the EIA bases on Beer-Lambert law (equation: 4.1.1). Here d denotes the filling level of the wells in the microtiter plate, (the value is the same for every sample as equal amounts of TMB and H_2SO_4 were filled in every well) and A denotes absorption coefficient of the converted and stopped

4. Experimental techniques

solution. The concentration c of TMB diimine differs from sample to sample as it is the product of the peroxidase.

Table 4.2.1: Listed are the polyanions tested in the EIA in the publications included in this thesis. Shown are their maximum concentration in the complex ($\mu\text{g/mL}$ and M) and the sera that were used to test the complexes for antigenicity. *¹ Due to the high polydispersity of the PAs, the concentration is given in [monomer mol/L]

	polyanions	max. concentration		patients sera ID
		$\mu\text{g/mL}$	M	
PF4/PA (paper II)	Unfractionated heparin	56	1.81×10^{-4} * ¹	17922, 19660, 26690, 30235
	Reviparin (LMWH)	56	1.81×10^{-4} * ¹	17922, 19660, 30235
	Fondaparinux	56	1.73×10^{-5}	17922, 19660, 30235
	Dextran sulfate	48	1.22×10^{-4} * ¹	17922, 19660, 30235
	Chondroitin sulfate	56	2.25×10^{-4} * ¹	19660, 30235
	2-O, 3-O desulfated heparin	56	2.07×10^{-4} * ¹	17922, 19660, 26690, 30235
PF4/defined heparins (paper III)	Unfractionated heparin	30	9.71×10^{-5} * ¹	17922, 19660, 26690, 30325
	Fondaparinux	30	1.73×10^{-5}	17922, 19660, 30325
	HO06 (= heparin 6-mer)	15	8.33×10^{-6}	17922, 19660, 30325
	HO08 (= heparin 8-mer)	11.7	4.88×10^{-6}	17922, 19660, 30325
	HO16 (= heparin 16-mer)	11.7	2.52×10^{-6}	17922, 19660, 30325
PF4/polyP (paper IV)	P3 (= polyP 3-mer)	16	4.35×10^{-5}	17922, 19660, 30325
	P45 (= polyP 45-mer)	16	7.15×10^{-6}	17922, 19660, 30325
	P75 (= polyP 75-mer)	16	2.22×10^{-6}	17922, 19660, 30325
PF4/aptamer (paper V)	Protein Captamer	80	5.92×10^{-6}	

The absorption measurements were carried out with a Beckman Coulter Paradigm™ plate reader. The software to control the device and save the data was SoftMax (version 6.2.1).

4.3 Isothermal Titration Calorimetry (ITC)

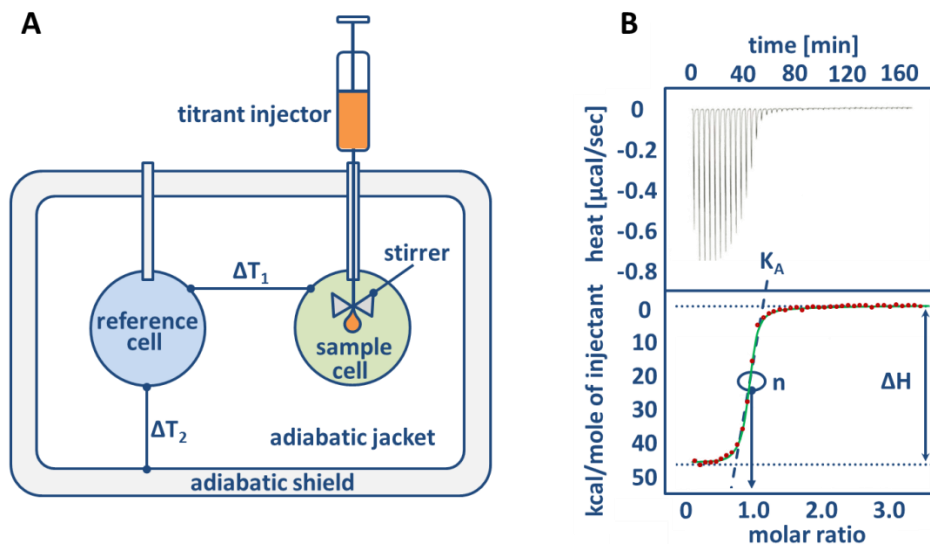


Figure 4.3.1: Schematic shows the principle of power compensation isothermal titration calorimetry. In **A** the general setting of calorimeter is depicted. There are two cells: i) a reference cell filled with buffer or water to which a constant power is supplied to heat it and ii) an active cell filled with sample. Here power is supplied to the sample cell feedback heater that is proportional to ΔT_1 . An injection needle with an attached stirrer dips into the sample cell adding the titrant. Both cells are isolated by an adiabatic shield and an adiabatic jacket. In **B top graph** an ideal thermogram with huge peaks in the beginning which lower when more and more binding sites are saturated is shown. In **B bottom graph** – the peaks are integrated (plotted as dots) and fitted to gain several information about the reaction: i) the K_A from the slope, ii) the stoichiometry from the point of inflection or iii) the mechanism/enthalpy can be read from the difference in energy between the initial and final molar ratio.

Isothermal titration calorimetry (ITC) is a commonly used technique to study thermodynamic parameters of interactions in solution and first described as a method for the simultaneous determination of equilibrium constant (K_{eq}) and enthalpy (ΔH) nearly 50 years ago.^{159,160} Great advantage of ITC is that it is a label free technique and the interaction partners do not need to be immobilized to any matrix or surface. ITC is suitable for different classes of molecules (e.g. proteins, nucleic acids or lipids) and for a wide range of applications (e.g. complex formation, enzyme kinetics or effects of molecular structure changes on binding mechanism). In a single experiment, several thermodynamic parameters such as the affinity of the binding partners (K_A), the stoichiometry of the reaction (n) or enthalpy (ΔH) and entropy (ΔS) can be determined with very high precision. Modern ITC instruments allow the measurement of heat effects as small as 0.1 μcal, binding constants as large as 10^8 - 10^9 M⁻¹, or heat rates as small as 0.1 μcal/sec, making it possible to determine reaction rates in the range of 10^{-12} mol/sec.¹⁶¹ Like the iTC200

used to generate the results in this thesis, the first commercially available titration calorimeter was produced by MicroCal.¹⁶² An isothermal titration calorimeter consists of two cells, a reference cell and a sample cell (figure 4.3.1 **A**). Both cells are of same size and made of same efficient thermal conducting material (Hastelloy™). The cells are surrounded by an adiabatic jacket. A syringe with a stirrer at the tip is used to inject a ligand (or titrant), here polyP and heparin, respectively, to the sample molecule in the cell (PF4). Modern ITC instruments like the used iTC200 are used in a titration mode. Here a defined number of incremental injections are made in a defined interval. The heat change (release or absorption) during an ITC experiment is measured indirectly via the power ($\mu\text{cal/sec}$) that is applied to maintain isothermal conditions between reference and sample cell. For example, if heat is released during titration, indicating that the investigated reaction is exothermic, the temperature in the sample cell is higher than in the reference cell after an injection. The power that is applied to the sample cell heater drops until isothermal conditions are recovered. This power drop reflects in a negative peak in the thermogram (figure 4.3.1 **B** – top graph). The ligand concentration in the syringe has to be set such that there are several peaks of same height (same amount of heat is released/absorbed) in the beginning and at the end of the experiment to obtain two baselines. As more and more binding sites are saturated, the amount of heat that is released/absorbed decreases with every further injection of ligand.

As shown in the bottom graph of figure 4.3.1 – **B**, ΔH is obtained by integrating the peaks and calculating the difference between initial and final baseline. By applying a fit with a matching model (e.g. 1:1 binding) the stoichiometry (n) of the reaction can be obtained from the point of inflection of the binding isotherm. From the slope of the same isotherm, the K_A (and then K_D) can be assessed.

$$K_D = \frac{1}{K_A} \quad [\text{M}] \quad (4.3.1)$$

Based on the obtained K_A , the Gibbs free energy, ΔG can be calculated by the following equation, where RT [Jmol^{-1}] is the product of the molar gas constant, R and the absolute temperature, T .

$$\Delta G = -RT \ln K_A \quad \left[\frac{\text{J}}{\text{mol}} \right] \quad (4.3.2)$$

The change in entropy (ΔS) and enthalpy (ΔH) contribute to the Gibbs free energy (ΔG) as shown in following equation.

$$\Delta G = \Delta H - T\Delta S \quad \left[\frac{\text{J}}{\text{mol}} \right] = \left[\frac{\text{J}}{\text{mol}} \right] - \left[K * \frac{\text{J/mol}}{K} \right] \quad (4.3.3)$$

The change in entropy gives information about the mechanism of the reaction, indicating whether conformational changes and/or changes in hydrophobic interaction occur. According to the second law of thermodynamics, ΔG is always negative in an open system. The formation of many polyanion/polycation complexes is majorly driven by an increase of global entropy due to the release of counterions.¹⁶³⁻¹⁶⁵ The Gibbs free energy is a thermodynamic potential. For $\Delta G < 0$ a reaction starts spontaneously and is favorable. A system is in equilibrium when $\Delta G = 0$, neither forward nor backward reaction is favored. Processes with $\Delta G > 0$ are disfavored and do not start spontaneously. The enthalpy is a measure for the heat of binding. A change in enthalpy (ΔH) indicates alterations in electrostatic interactions, hydrogen bonding, and van der Waals bonding. For $\Delta H > 0$ heat is absorbed during the reaction, the reaction is endotherm. When heat is released during a reaction it is an exothermic reaction and $\Delta H < 0$.

All ITC measurements were conducted with a MicroCal iTC200 purchased from GE Healthcare Life Sciences. Due to its small reaction chamber of only 200 μl , it is quite economic in terms of the amount of protein needed per experiment. The supplier mentions that the smallest amount needed is 10 μg of protein to run an experiment. In order to obtain a good signal-to-noise ratio, the PF4 solution filled in the reaction cell had a concentration of $1.48 \times 10^{-5} \text{ M}$ which corresponds to an amount of 95 μg PF4 per experiment to fill the cell. However, there is also a funnel that needs to be filled. Totally 118 μg ($3.7 \times 10^{-7} \text{ mol}$) PF4 was used per run.

4. Experimental techniques

The ITC was used in paper IV (PF4/polyP) and by Martin Kreimann in paper III (PF4/defined heparins). Experiments were carried out at 25°C. Prior to the experiment, the protein and the polyphosphates (polyP) were first solved in PBS (pH 7.4). The purchased polyP were reported to be essentially salt-free. To avoid buffer mismatch PF4 was additionally dialyzed against PBS overnight. PF4 [1.48×10^{-5} M] was filled into the sample cell, PBS into the reference cell and the syringe was loaded with polyP (P3 [1.41×10^{-3} M], P45 [2.64×10^{-4} M], P75 [1.36×10^{-4} M]) and heparin, respectively. The measurement was started by injecting 0.4 μ l polyP, followed by 18 injections of 2 μ l while stirring at 1000 RPM. Time between two injections was set to 240 seconds, whereas the feedback was low, the filter period was set to five seconds and the reference power to 6 volts. Control measurements involved the titration of PBS into PBS, PBS into PF4 solution, and polyP into PBS.

In the data analysis, the area under each peak was integrated to obtain the amount of heat released during each injection. Data was then normalized for the concentrations and plotted against the molar ratio of polyP to PF4. Calorimetric data were fitted by nonlinear regression using a single-site model to get the change in enthalpy (ΔH), stoichiometry (N), change in entropy (ΔS), Gibbs free energy (ΔG) and the dissociation constant (K_D) using MicroCal-enabled Origin 7 SR4 software (OriginLab Cooperation, Northampton, USA) supplied with the instrument. Equilibrium affinity constant (K_D) was calculated as the reciprocal of K_A . According to the supplier, measuring affinities in the sub-millimolar to picomolar range is possible. The reported thermodynamic parameters are values of triplicate measurements.

4.4 Flow Cytometry

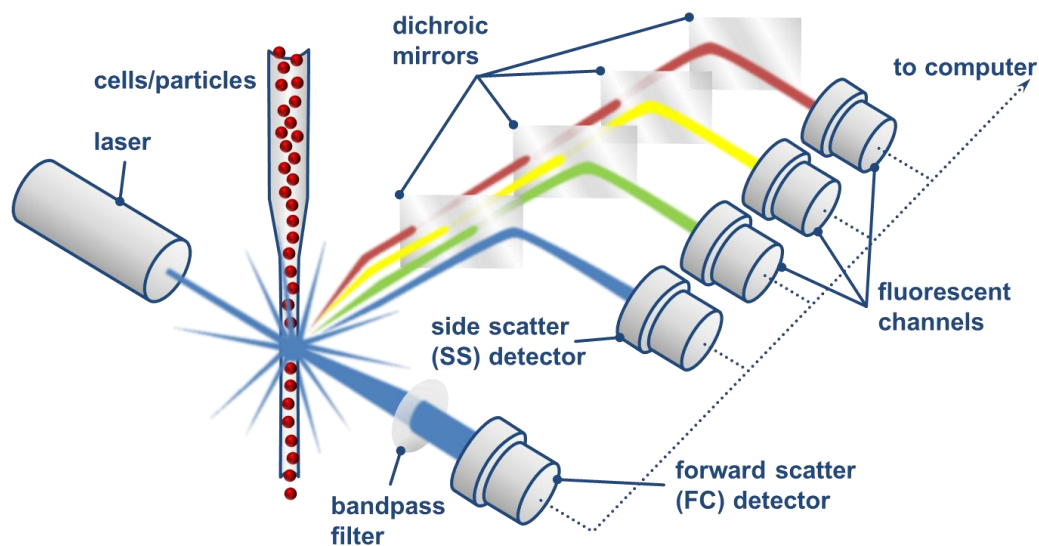


Figure 4.4.1: Schematic of the flow cytometry principle: particles (e.g. cells) mostly fluorescently labeled are aligned in a liquid stream and scatter light when they pass a laser beam. The scattered light and the fluorescence exhibited by excited fluorophores are recorded by detectors positioned in line and orthogonal to the laser beam. Dichroic mirrors deflect the specific wavelengths (depicted as different colors) to the corresponding detector.

Flow cytometry is a technique used to simultaneously analyze multiple physical and chemical characteristics of single cells or particles. The sample of interest is mostly labeled with fluorescent markers, suspended in solution and forced through a nozzle in a liquid stream. The liquid stream passes a laser beam and each particle scatters the light in characteristic manner. There is one detector in line with the laser that records the whole spectrum of forward scattered (FSC) light which is a measure for the volume/size of the particle. Another detector records the whole spectrum of sideward scattered (SSC) light which depends on the complexity of the particle. When measuring cells it is often called granularity. Additionally, there might be one or more detectors recording filtered SSC light emitted from fluorophores. Dichroic mirrors are used to select certain wavelength ranges. In the analysis, the different data sets are plotted against each other to differentiate populations and group specimen with same properties.

Flow cytometry was used in paper I (PF4 evolutionary analysis, by Krystin Krauel) and paper IV (PF4/poly, by myself) to investigate the influence of heparin and polyP on the binding of PF4 to bacterial surfaces (figureFigure). For the latter (paper IV, PF4/polyP) a well characterized lab stem, Gram-negative *Escherichia coli* (*E. coli* JM109), was chosen.

4.4.1 PF4 binding to Gram-negative bacterial Surface

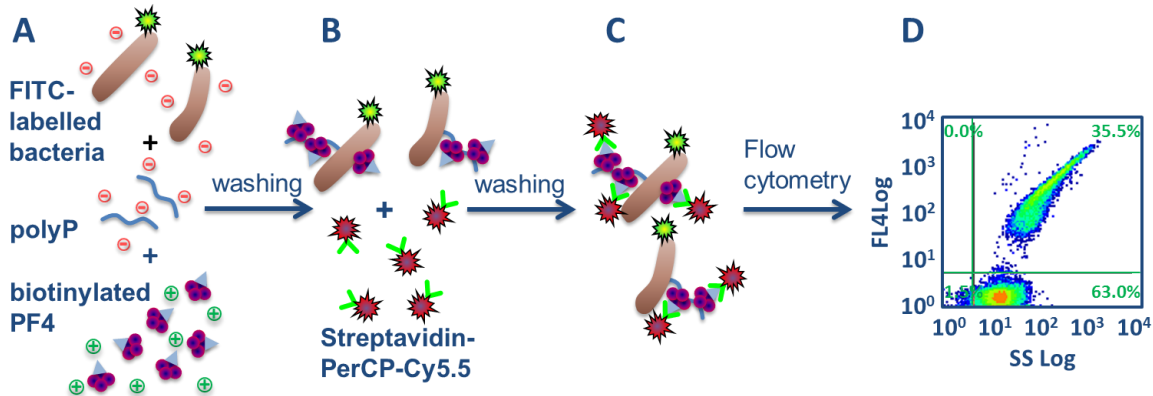


Figure 4.4.1.1: The setup which was used to analyze the influence of polyP on PF4 binding (PF4 partly biotinylated) to bacteria is depicted. FITC labeled and UV deactivated bacteria were incubated with PF4 and different amounts of polyP. After washing the bacteria/PF4/polyP complexes were incubated with Cy5.5 labeled streptavidin to detect the PF4 on the bacterial surface. After another washing step, analysis was carried out with the help of flow cytometry.

For the influence of polyP on PF4 binding to bacterial surfaces (figure 4.4.1.1), UV deactivated and fluorescein (FITC) labeled bacteria were incubated with partly biotinylated PF4 and different amounts of polyP to get different PF4:polyP ratios. UV deactivated and FITC labeled Gram-negative *E. coli* was incubated (30 minutes, 4°C, shaking) with biotinylated PF4 (20 µg/ml, diluted in PBS) together with different concentrations (0-40 µg/ml) of polyP. After washing by adding 3 mL PBS to the 100 µl bacteria:PF4:polyP solution and centrifugation (3000 g, 5 min, 4°C), bacteria were incubated (30 minutes, 4°C) with Streptavidin-PE Cy5.5 (BD Biosciences) and washed as before. PF4 binding to the bacteria was recorded by flow cytometry (Cytomics FC 500, Beckman Coulter). Afterward raw data were exported to carry out the analysis with Windows Multiple Document Interface software (WinMDI 2.8, plots shown in figure 4.4.1.2).

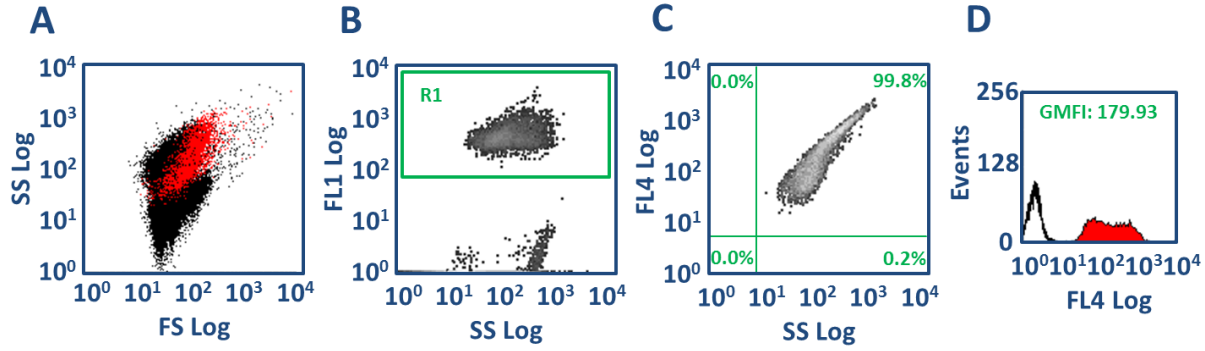


Figure 4.4.1.2: Depicted is the analysis of one PF4/polyP molar ratio measured in flow cytometry. **A** – As a measure of size the forward scatter (FS) against sideward scatter (SS) that gives information about granularity of cells. Each event recorded is represented as a point. **B** – The SS is plotted against the fluorescein (FITC) channel to discriminate intact labeled bacteria from destroyed but also labeled bacterial particles. Cell debris is excluded by setting a region (green frame) around the fluorescein labeled bacteria. By gating on the region R1 only events (FITC-labeled bacteria) located in the frame will be used in further analysis. Here data is visualized as a heat map. **C** – SS is plotted against the Cy5.5 channel and quadrants are set to visualize the labeled PF4 as well as to discriminate bacteria with or without PF4 attached. Here 99.8% of the bacteria were covered with PF4. **D** – A histogram plotting the gated events together with the geometric mean of the fluorescence intensity (GMFI) for Cy5.5 is shown, giving information about the amount of PF4 attached to the bacterial surface. For the final values plotted in the publication the percentage of labeled bacteria is multiplied by GMFI of the Cy5.5 to obtain the binding activity.

The binding activity plotted in the publications is product of geometric mean fluorescence intensity

(GMFI) of the fluorophore Cy5.5 and the percentage of labeled bacteria (equation 4.4.1).

$$\text{binding activity} = \text{GMFI}(\text{Cy5.5}) * \%(\text{labeled bacteria}) \quad (4.4.1)$$

4.4.2 Phagocytosis of PF4-marked Bacteria by polymorphonuclear Leukocytes (PMNs)

For the phagocytosis assay²⁶²⁶, FITC labeled UV-deactivated Gram-negative E. coli were coincubated with PF4 (200 µg/ml) and P75 (0 to 200 µg/ml) in different PF4:polyP molar ratios (figure 4.4.2.1 A). Human sera known to contain anti-PF4/heparin IgG were heat-inactivated (45 minutes, 56°C) and four times pre-adsorbed with non-PF4 coated E. coli (30 minutes, 4°C). PF4/polyP coated bacteria were incubated with the pretreated sera (figure 4.4.2.1 B). These opsonized bacteria were coincubated with whole blood cells, obtained from hirudinized blood of healthy volunteers (10 minutes, 37°C, figure 4.4.2.1 C-1). The

sample is transferred from the water bath to ice to stop the phagocytosis of the bacteria by the polymorphonuclear leukocytes (PMNs). A 0.4% trypan blue solution (Sigma-Aldrich) is added to quench the fluorescence of non-phagocytosed FITC-labeled bacteria (5 minutes, on ice, figure 4.4.2.1 C-2). After washing FACS lysing solution (BD Biosciences) is added to destroy red blood cells as they did not contribute to phagocytosis (7 minutes, RT, figure 4.4.2.1 C-3). After washing, to stain the DNA of the remaining cells a propidium iodide solution (Fluka BioChemica) is added (10 minutes, on ice, figure 4.4.2.1 C-4). The mean fluorescence intensity (MFI) of FITC-positive PMNs was recorded as a measure for bacterial phagocytosis.

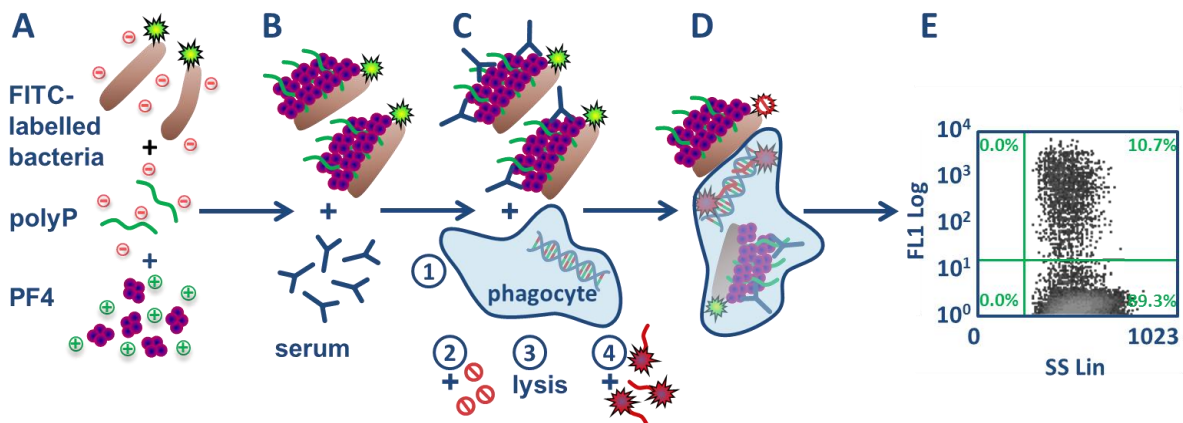


Figure 4.4.2.1: Schematic of the phagocytosis assay. A – FITC labeled bacteria are coincubated with polyP and PF4 in different PF4:P75 molar ratios. B – PF4/P75-labeled bacteria are incubated with sera known to contain anti-PF4/heparin antibodies. C-1 – For phagocytosis, whole blood cells are incubated with PF4/P75/IgG-labeled bacteria. C-2 – Trypan blue is added to quench the fluorescence of unphagocytosed FITC-labeled bacteria. C-3 – Red blood cells are removed by the addition of a lysing solution and washing. C-4 – The DNA of the remaining cells is stained by the addition of propidium iodide. D – PMNs with stained DNA containing FITC-labeled bacteria and quenched unphagocytosed bacteria are transferred to be analyzed by flow cytometry (E).

5. Abstract

The central aim of this thesis was the investigation of protein/polyanion interaction using circular dichroism (CD) spectroscopy, enzyme immune assay (EIA), isothermal titration calorimetry (ITC) and flow cytometry (FC). A further aim was to understand why an endogenous protein becomes immunogenic when forming a complex. The focus was on the protein platelet factor (PF4), which gained wide interest in the clinical field, due to its role in the life-threatening, immune-driven, adverse drug effect heparin-induced thrombocytopenia (HIT). PF4 is a small homotetrameric chemokine with several basic amino acids on its surface, forming a positively charged ring. The antibodies that are formed during HIT recognize an epitope exposed on PF4, when it is in a complex with heparin at a certain molar ratio at which, PF4 tetramers are aligned on the heparin and forced into close approximation.

The main results and conclusions of the thesis are summarized below:

5.1 Evolutionary Conservation of PF4 (Paper I – PF4/Evolution)

By carrying out an amino acid sequence survey we found that the positively charged amino acids contributing to the heparin binding site on the surface of PF4 and related proteins are highly conserved in all vertebrates, including fish species.

PF4 interacts with the phospholipid lipid A, the innermost part of the lipopolysaccharide (LPS) of Gram negative bacteria. We showed that the shorter the sugar chain of the O antigen, outer and inner core of the LPS were the more PF4 was binding. The interaction of PF4 with lipid A is inhibited by heparin, suggesting that the amino acids known to contribute to heparin binding are also involved in binding to lipid A.

5.2 PF4 Interaction with Polyanions (PA) of varying Length and Degree of Sulfation (Paper II – PF4/PA)

CD spectroscopy was found to be a powerful technique to monitor structural changes of PF4 caused by binding to various clinically relevant polyanions. Therefore PF4 was titrated with different PA to investigate the dependencies: i. impact of the PF4:PA molar ratio, ii. degree of polymerization of the PA and iii. degree of sulfation of the PA. In all cases, exposure of HIT-relevant epitope(s) was only observed for PA that also induced changes in secondary structure of PF4. A comparison of results of an immune assay with CD spectroscopic data showed that the extent of complex antigenicity correlates well with the magnitude of changes in PF4 secondary structure, and that the structural changes of PF4 have to exceed a certain threshold to achieve PF4/PA complex antigenicity. These findings allowed us to calculate expectation intervals for complex antigenicity solely using CD spectroscopic data.

To our knowledge, this was the first demonstration that the capability of drugs to induce antigenicity of PF4 can be assessed without the necessity of in vivo studies or the use of antibodies obtained from immunized patients specific for the antigens.

The antigenicity of PF4 in complex is not restricted to negative charges originating from sulfate groups, PA with phosphate groups are also capable (binding to phospholipids). We investigated inorganic polyphosphates (polyP) with a chain length of 75 P_i and showed that the induced secondary structural changes are even higher compared to the changes induced by the different heparins and that the PF4/P75 complexes are antigenic as well.

5.3 PF4 Interaction with defined oligomeric Heparins (Paper III – PF4/defined Heparins)

We tested highly purified, monodisperse heparins. In contrast to the clinically relevant but relatively undefined (high polydispersity index) glycosamino glycans reported in paper II (PF4/PA). The defined heparins induced higher secondary structural changes.

Here we showed for the first time that strong conformational changes during PF4/PA complex formation are necessary but not sufficient for to the expression of the anti-PF4/heparin antibody binding site. Also, the size of the complexes is not the only prerequisite for anti-PF4/heparin antibody binding (tested by atomic force microscopy). By ITC we found that antigenicity is only induced if the PF4/PA complex has a high binding enthalpy and the complex formation leads to a negative change in entropy.

5.4 PF4/Polyphosphates (polyP) Complex Antigenicity and Interaction with *Escherichia coli* (*E. coli*, Paper IV – PF4/polyP)

PolyP with chain lengths of 45 P_i and 75 P_i induced remarkable secondary structural changes in the PF4 molecule, thereby exposing the epitope recognized by anti-PF4/heparin antibodies. The induced conformational changes were similar to the changes induced by the defined heparins. Again a high binding enthalpy was observed but here in connection with a positive change in entropy.

Further we showed that polyP (≥ 45 P_i) enhance PF4 binding to the surface of Gram negative *E. coli* at intermediate concentration and disrupt the binding at elevated polyP concentrations. The increased amounts of PF4 on the bacterial surface also improved the binding of anti-PF4/heparin antibodies and thereby the phagocytosis of the bacteria by polymorphonuclear leucocytes.

5.5 Nucleic acid based Aptamers induce structural Changes in the PF4 Molecule (Paper V – PF4/Aptamer)

Nucleic acids are another class of molecules containing phosphate groups. Especially after cell damage their extracellular concentration can be locally quite high (>2 mg/ml). We found that certain aptamers form complexes with PF4 and thereby inducing anti-PF4/aptamer antibodies which cross-react with PF4/heparin complexes. Moreover by CD spectroscopy we showed that the protein C-aptamer caused similar secondary structural changes of PF4 like heparin, but already at much lower concentration. The maximally induced changes by the protein-C aptamer were even higher and persisted over a broader concentration range.

5.6 Protamine Interaction with Heparin (Paper VI – PS/Heparin)

After the intensive investigation of the complex formation between PF4 and many different classes of PA we assessed another protein for structural changes upon complex formation with heparin. Protamine (PS) a protein in routinely used in post-cardiac surgery to reverse the anticoagulant effects of heparin was found to unfold but not to refold with increasing concentration of PA in solution.

5.7 Conclusion and Outlook

When starting this thesis, it was believed that repetitive structures formed by PF4 on a heparin chain mold the epitope recognized by antibodies inducing HIT. These repetitive structures might exhibit similarities with viral capsids and are therefore recognized by the immune system of some patients. We found that induced by the close approximation PF4 changes its conformation, thereby exposing a neoepitope.

The conserved positively charged amino acids of the heparin binding site and the involvement of these amino acids in the binding to lipid A confirm our hypothesis of PF4 as part of an ancient immune-mediated host defense mechanism. As possible consequence of the “primitive mechanism of defense” the highly variable O-antigens of LPS might have significantly contributed to an efficient escape mechanism by hiding the structures that made the bacteria vulnerable. In turn polyP might be an adaption of the host improve pathogen recognition by PF4 and further by antibodies inducing phagocytosis of the PF4-marked objects.

Although shown only for PF4 and PS, our findings might be applicable to other proteins that also express epitopes upon changes in their secondary structure. Our physicochemical methods may further be applied: i. to drug development for the prediction of antigenicity induced by polyanionic drugs, ii. to guide the development of synthetic heparins and other polyanion based drugs, e.g. aptamers, that do not lead to HIT and iii. to provide relevant aspects for other biological functions of heparins.

6. Papers

6.1 Paper I: Platelet Factor 4 binding to Lipid A of Gram-negative Bacteria exposes PF4/Heparin-like Epitopes

Platelet factor 4 binding to lipid A of Gram-negative bacteria exposes PF4/heparin-like epitopes

*Krystin Krauel,^{1,2} *Claudia Weber,³ Sven Brandt,² Ulrich Zähringer,⁴ Uwe Mamat,⁴ †Andreas Greinacher,¹ and †Sven Hammerschmidt³

¹Institut für Immunologie und Transfusionsmedizin; ²Zentrum für Innovationskompetenz-Humorale Immunreaktionen bei kardiovaskulären Erkrankungen; and ³Abteilung Genetik der Mikroorganismen, Interfakultäres Institut für Genetik und Funktionelle Genomforschung, Ernst-Moritz-Arndt-Universität, Greifswald, Germany; and ⁴Abteilung für Molekulare Infektiologie, Forschungszentrum Borstel, Leibniz-Zentrum für Medizin und Biowissenschaften, Borstel, Germany

The positively charged chemokine platelet factor 4 (PF4) forms immunogenic complexes with heparin and other polyanions. Resulting antibodies can induce the adverse drug effect heparin-induced thrombocytopenia. PF4 also binds to bacteria, thereby exposing the same neoantigen(s) as with heparin. In this study, we identified the negatively charged lipopolysaccharide (LPS) as the PF4 binding structure on Gram-negative bacteria. We demonstrate by flow cytometry that mutant

bacteria with progressively truncated LPS structures show increasingly enhanced PF4 binding activity. PF4 bound strongest to mutants lacking the O-antigen and core structure of LPS, but still exposing lipid A on their surfaces. Strikingly, PF4 bound more efficiently to bisphosphorylated lipid A than to monophosphorylated lipid A, suggesting that phosphate residues of lipid A mediate PF4 binding. Interactions of PF4 with Gram-negative bacteria, where only the lipid A part of LPS is

exposed, induce epitopes on PF4 resembling those on PF4/heparin complexes as shown by binding of human anti-PF4/heparin antibodies. As both the lipid A on the surface of Gram-negative bacteria and the amino acids of PF4 contributing to polyanion binding are highly conserved, our results further support the hypothesis that neoepitope formation on PF4 after binding to bacteria is an ancient host defense mechanism. (*Blood*. 2012; 120(16):3345-3352)

Introduction

Besides their pivotal role in hemostasis, platelets are involved in host defense against pathogens and in modulation of immune reactions. This function of platelets occurs either indirectly through their interaction with endothelial cells and leukocytes^{1,2} or directly by secretion of antimicrobial substances from platelet storage granules and lysosomes.^{3,4}

Recently, we have shown that the chemokine platelet factor 4 (PF4), which is stored within platelet α -granules, plays a role in bacterial host defense by inducing a humoral immune response to PF4-coated bacteria.⁵ During bacterial infections, platelets are activated^{6,7} and release positively charged PF4, which can bind in a charge-dependent manner to the bacterial surface, thereby inducing neoepitopes. The formation of antigenic PF4 clusters is probably the result of neutralization of the positive charge of PF4 by polyanions,⁸ which allows narrowing of the distance between single PF4 tetramers down to 3 to 5 nm. This creates linear, ridge-like complexes and exposes new antigenic epitopes on PF4.⁹ Antibodies to PF4/polyanion complexes bind to PF4 on the bacterial surface, leading to opsonization and increased phagocytosis of PF4-coated bacteria.⁵ As PF4 is capable of binding to a large variety of bacteria, the antibody response to PF4/polyanion complexes constitutes a very broad reactive defense mechanism and could represent an evolutionary interface between innate and specific immunity. Antibodies induced by PF4 clusters would be an example of antibodies with a limited target antigen repertoire that nevertheless could result

in binding to a large variety of bacteria when these bacteria are coated with PF4.⁵

In medicine, research on the immune reaction to PF4/polyanion complexes to date has primarily focused on its role in causing an adverse reaction to the anticoagulant heparin as PF4 forms immunogenic complexes with heparin on platelet surfaces. Anti-PF4/polyanion antibodies bind to these PF4/heparin complex-coated platelets and induce Fc-receptor-dependent platelet activation,^{10,11} leading to intravascular consumption of platelets, associated potentiation of in vivo thrombin generation, and the prothrombotic syndrome, heparin-induced thrombocytopenia (HIT).

We and others have recently demonstrated the prevalence of anti-PF4/heparin antibodies of the IgM class in up to 20% and of the IgG class in up to 6% of the general population and in a slightly lower number of normal blood donors.^{5,12} These antibodies are highly significantly associated with periodontitis, one of the most prevalent human infections, often associated with transient bacteremia.¹³ The major bacterial species in periodontitis are the Gram-negative bacteria *Aggregatibacter actinomycetemcomitans* and *Porphyromonas gingivalis*.¹⁴ Both bacteria bind PF4 and consequently expose epitopes recognized by anti-PF4/heparin antibodies.¹³

The outer leaflet of the outer membrane of Gram-negative bacteria is mainly composed of negatively charged lipopolysaccharide (LPS), interspersed with proteins (Figure 1).¹⁵ LPS, a complex glycolipid, is anchored in the outer membrane by the highly

Submitted June 5, 2012; accepted August 15, 2012. Prepublished online as *Blood* First Edition paper, August 31, 2012; DOI 10.1182/blood-2012-06-434985.

*K.K. and C.W. contributed equally to this study.

†A.G. and S.H. share senior authorship of this study.

The online version of this article contains a data supplement.

The publication costs of this article were defrayed in part by page charge payment. Therefore, and solely to indicate this fact, this article is hereby marked "advertisement" in accordance with 18 USC section 1734.

© 2012 by The American Society of Hematology

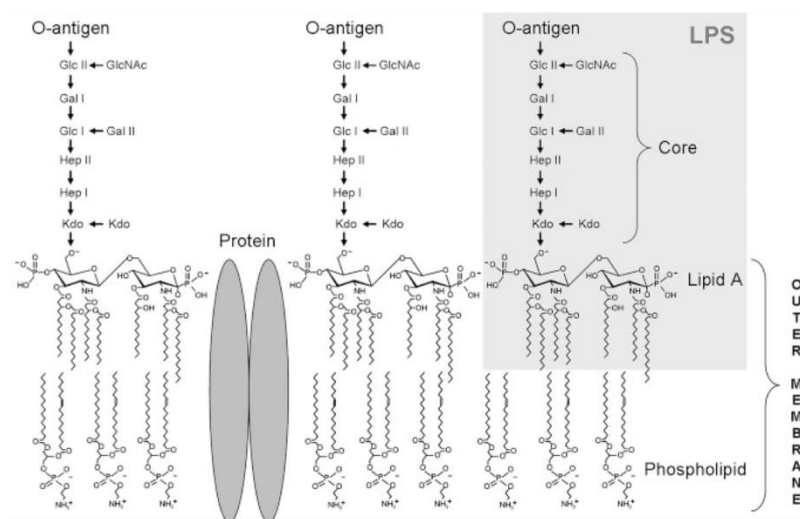


Figure 1. Schematic architecture of the LPS embedded in the outer membrane of Gram-negative bacteria. LPS is a complex glycolipid composed of a highly conserved lipid A anchor, the more variable core oligosaccharide, and the hypervariable antigenic O-polysaccharide (O-antigen) consisting of several copies of oligosaccharide repeating units. Glc indicates glucose; Gal, galactose; GlcNAc, N-acetyl-D-glucosamine; and Hep, heptose.

conserved lipid A. The central core oligosaccharide is linked to lipid A and can be divided into an inner core composed of heptoses and 3-deoxy-D-manno-oct-2-ulosonic acid (Kdo), and an outer core consisting of hexoses, followed by the most variable part of the LPS molecule, the O-specific polysaccharide chain.¹⁶

In this study, we have identified the phosphate groups of the highly conserved lipid A as the binding site for PF4 on the surface of Gram-negative bacteria. In accordance with our hypothesis that opsonization of bacteria by PF4 might represent an ancient host defense mechanism, we found the anion binding site of PF4 and PF4-like proteins conserved among different vertebrate species.

Methods

Bacterial strains

Bacterial strains used in this study are listed in Table 1. *Escherichia coli* K-12 wild-type strain BW30270 and *E coli* K-12 mutant strains^{17,18} were kindly provided by R. W. Woodard (University of Michigan, Ann Arbor, MI). *Salmonella enterica* sv Typhimurium SL3770 *waa*⁺ and the isogenic *Salmonella* LPS mutants were obtained from K. E. Sanderson (*Salmonella* Genetic Stock Center, Calgary, AB). Bacteria were cultured at 37°C to the exponential growth phase (A_{600} of 0.7–1.2) in Todd-Hewitt broth supplemented with 0.5% yeast extract (Roth).¹⁹

Table 1. Bacterial strains used in this study

Strain	Characteristic	Source or reference
<i>S enterica</i> sv Typhimurium wild-type strain		
SL3770	<i>waa</i> ⁺ , smooth LPS (S-form)	SGSC#225
<i>S enterica</i> sv Typhimurium mutant strains		
SL3749	<i>waaL446</i> , lacking LPS O-antigen ligase	SGSC#228
SL3750	<i>waaJ417</i> , lacking LPS glucosyltransferase II	SGSC#229
SL3748	<i>waaI432</i> , lacking LPS galactosyltransferase I	SGSC#227
SL3769	<i>waaG471</i> , lacking LPS glucosyltransferase I	SGSC#231
SL3789	<i>waaF511</i> , lacking LPS heptosyltransferase II	SGSC#230
SL1102	<i>hldE543</i> , lacking LPS heptosyltransferase I	SGSC#258
<i>E coli</i> K-12 wild-type strain		
BW30270	<i>waa</i> ⁺ , rough LPS (R-form)	CGSC#7925
<i>E coli</i> K-12 mutant strains		
KPM53	<i>waaC</i> , lacking LPS heptosyltransferase I	Mamat et al ¹⁸
KPM121	<i>waaA</i> , defective in Kdo transferase of LPS biosynthesis	Mamat et al ¹⁷

SGSC indicates *Salmonella* Genetic Stock Center; and CGSC, *E coli* Genetic Stock Center.

LPS and derivatives

LPS-biotin was purchased from InvivoGen. Lipid A substituted with 2 Kdo residues (Kdo₂-lipid A) and lipid A were isolated from *E coli* F515 (Re chemotype). Separation and purification of lipid A from Kdo was performed as described.²⁰ LPS isolated from *E coli* O55:B5, mono-(4'-P)-phosphoryl lipid A (MPLA) isolated from *E coli* F583 (Rd mutant) and Kdo were purchased from Sigma-Aldrich.

Purification of PF4 and PF4 biotinylation

Human PF4 was isolated from platelets (Chromatec) and biotinylated as described.⁵ The concentration of biotinylated PF4 was determined by a bicinchoninic acid protein assay kit using BSA as standard (Sigma-Aldrich).

Binding of LPS to immobilized PF4 and binding of PF4 to immobilized LPS derivatives

To investigate binding of LPS to immobilized PF4, wells of a microtiter plate (MaxiSorp, Nunc) were coated with PF4 (10 µg/mL), BSA, or buffer (carbonate-bicarbonate buffer, pH 9.6; Mediatec) at 4°C overnight. In the reverse approach, wells (PolySorp, Nunc) were coated with LPS, Kdo₂-lipid A, lipid A (bisphosphorylated), MPLA (monophosphorylated), or Kdo in carbonate-bicarbonate buffer pH 9.6 (each with 50 µg/mL, 4°C, overnight). Before the incubation with increasing concentrations of LPS-biotin (0.6, 1.3, 2.5, 5.0, 10, 20, and 40 µg/mL; 60 minutes, room temperature), PF4-biotin (0.06, 0.13, 0.25, 0.5, 1.0, 2.0, and 4.0 µg/mL; 60 minutes), or

buffer as a control, microtiter plates were washed 5 times with PBS + 0.1% Tween and blocked with PBS + 0.1% Tween + 2% BSA (60 minutes, room temperature). Plates were washed and incubated with peroxidase-conjugated streptavidin (1:4000, 60 minutes, room temperature; Jackson ImmunoResearch Laboratories). After final washing steps, tetramethylbenzidine was added to the wells, the reaction was stopped with 1M H₂SO₄, and absorbance was measured at 450 nm. In addition, binding of PF4-biotin (2 µg/mL) to immobilized lipid A was measured in the presence of increasing concentrations (0.5, 1, 2, 4, and 8 µg/mL) of bacterial permeability increasing protein (BPI; Alpha Diagnostic International), polymyxin B sulfate (Sigma-Aldrich), or buffer.

PF4 binding to bacterial LPS mutants

E coli BW30270, KPM53, and KPM121, and *S enterica* sv Typhimurium strains SL3770, SL3749, SL3750, SL3748, SL3769, SL3789, and SL1102 (Table 1) were incubated (30 minutes, 4°C) with PF4-biotin, 20 µg/mL; or buffer, washed with PBS/0.05% BSA (3000g, 5 minutes, 4°C) and incubated (30 minutes, 4°C) with peridinin chlorophyll protein-Cy5.5 conjugated streptavidin (BD Biosciences). Bacteria were washed and fixed with 1% paraformaldehyde (20 minutes, 4°C). PF4 binding was analyzed by flow cytometry (Cytomics FC 500, Beckman Coulter). The geometric mean fluorescence intensity multiplied by the percentage of labeled bacteria constituted binding activity.

In inhibition assays, PF4-biotin (40 µg/mL) was preincubated (30 minutes, 4°C) with 200 µg/mL LPS, Kdo, Kdo₂-lipid A, lipid A, MPLA, or buffer before assessing PF4 binding to the *E coli* $\Delta waaA$ mutant KPM121 by flow cytometric analysis.

Furthermore, *E coli* strains BW30270, KPM53 and KPM121 (Table 1) were pretreated (15 minutes, 37°C) with pronase E (100 µg/mL; Merck), trypsin (100 µg/mL; Sigma-Aldrich), or buffer, washed 3 times with PBS, pH 7.4 (3700g, 6 minutes, room temperature), incubated (30 minutes, 4°C) with PF4-biotin (20 µg/mL) or buffer and analyzed for PF4 binding. Activity of pronase E and trypsin was controlled by reduction of *E coli* Antigen 43.

Anti-PF4/heparin antibody binding to PF4-coated bacterial LPS mutants

Binding of human anti-PF4/heparin antibodies to bacteria was assessed by adsorption and elution experiments as described.⁵ In brief, LPS mutant strains *E coli* KPM53 and KPM121 were incubated with PF4 (20 µg/5 × 10⁷ bacteria, 30 minutes, 4°C) or buffer (PBS, pH 7.4), washed (3000g, 5 minutes, 4°C) and incubated (30 minutes, 4°C) with diluted human serum of patients known to contain anti-PF4/heparin IgG antibodies (n = 3 per strain), and washed again to remove unbound antibodies. Bound antibodies were eluted with glycine buffer (0.1M, pH 2.7; 5 minutes, room temperature), bacteria removed by centrifugation, and supernatants (eluates: containing the antibodies) neutralized with Tris buffer (1M, pH 9). Untreated sera and eluates were tested by PF4/heparin IgG ELISA,²¹ including inhibition by unfractionated heparin (100 IU/mL; Braun) and binding to PF4 alone. In addition, heparin-induced platelet activation test was performed as described²² to test the ability of eluates to activate platelets.

Phagocytosis assay

Phagocytosis assays were performed as described⁵ with the following modifications. The *E coli* K12 wild-type strain BW30270 and its isogenic $\Delta waaA$ mutant KPM121 were self-labeled with FITC by adding 100mM NaHCO₃, pH 9, and incubating with 370 µg/mL FITC dissolved in DMSO (60 minutes, 37°C; AppliChem). Bacteria were washed 3 times with PBS/0.05% BSA (3000g, 5 minutes, 4°C) and incubated with PF4 (20 µg/5 × 10⁷ bacteria, 30 minutes, 4°C). The washed samples (3000g, 5 minutes, 4°C) were incubated (30 minutes, 4°C) with human serum (1:50) of patients known to contain anti-PF4/heparin IgG antibodies (n = 4 per strain). The sera had been preadsorbed with each of both strains (non-PF4-coated; 15 minutes, 4°C; 4 times). Bacteria were washed again to remove

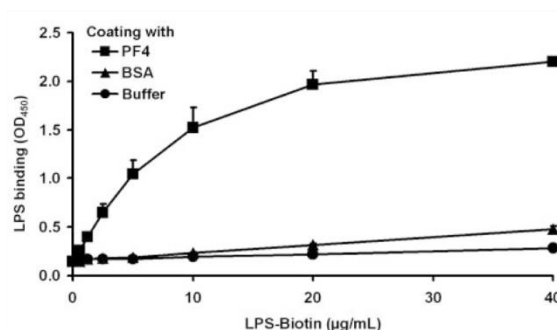


Figure 2. LPS binds dose-dependently to PF4. Binding of biotinylated LPS (0.6, 1.3, 2.5, 5.0, 10, 20, and 40 µg/mL) to immobilized PF4 (10 µg/mL) was detected with peroxidase-conjugated streptavidin, followed by the addition of tetramethylbenzidine. Binding of PF4 to BSA or buffer (each with 10 µg/mL) served as controls to exclude nonspecific binding of LPS-biotin to proteins or to the plastic surface. Data are mean OD₄₅₀ ± SD of 3 independent experiments.

unbound antibodies. Finally, the whole blood phagocytosis assay was performed as described⁵ using pretreated bacteria.

PF4 amino acid sequence survey

For the bioinformatics analysis, different resources, including the Universal Protein Resource (UniProt, <http://www.uniprot.org>), the National Center for Biotechnology Information (NCBI, <http://www.ncbi.nlm.nih.gov>), and the Search Tool for the Retrieval of Interacting Genes/Proteins (STRING, <http://string-db.org/>), were used. The survey was started with BLAST²³ searches, and the complete human PF4 amino acid sequence was used for protein sequence comparisons against the genome sequence databases available for other species. Although the databases generally mirror each other, additional sequences were provided by the databases of NCBI and STRING. The multiple sequence alignment was performed using ClustalW2 (www.ebi.ac.uk).

Statistical analysis

Data are plotted as mean ± SD. We compared samples of bacterial binding studies, affinity purification experiments, and phagocytosis assay by paired Student *t* test. Differences between samples of ELISA data were calculated by paired *t* test, except for PF4 binding to bisphosphorylated lipid A compared with MPLA, which was analyzed by ANOVA test. *P* < .05 was considered statistically significant.

Results

Identification of the PF4 binding site on LPS

A negatively charged microbial component has been suggested to recruit PF4 to the Gram-negative bacterial cell surface. As PF4 binding is a general characteristic for Gram-negative bacteria, a conserved surface structure, such as LPS (Figure 1), may be involved in binding of PF4. To test this hypothesis, binding of LPS to immobilized PF4 was investigated. The results show that LPS binds dose-dependently to PF4 (Figure 2). To decipher in more detail the PF4 binding part in LPS, we performed PF4 binding assays using different mutants of *S enterica* sv Typhimurium with gradually truncated LPS structures. Surprisingly, the wild-type strain SL3770 with smooth (S)-form LPS (*waa*⁺) showed a low degree of PF4 binding (geometric mean fluorescence intensity [GMFI], 8.5 ± 2.9; Figure 3A). However, PF4 binding capacity increased step-wise in mutants with increasing truncations of the LPS outer and inner core oligosaccharides. The first mutant which was able to recruit PF4 in significant amounts was *S enterica* sv

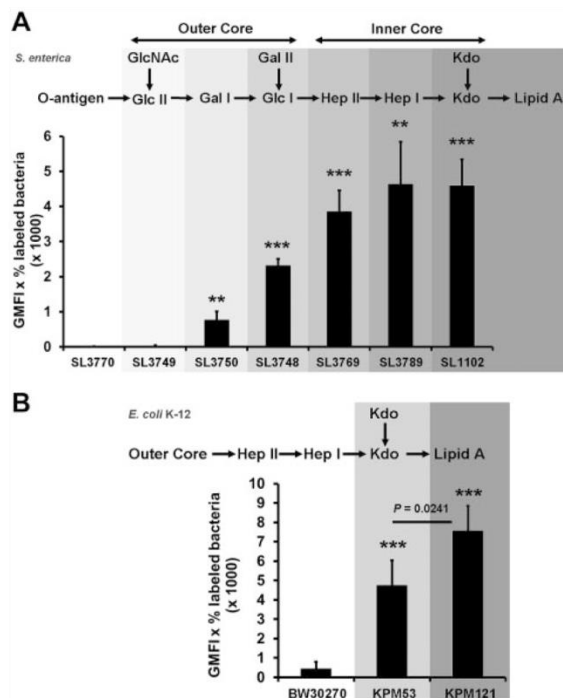


Figure 3. Bacterial mutants with progressively truncated LPS backbones show increasing PF4 binding activity. *S. enterica* sv Typhimurium wild-type strain SL3770 *waa*⁺, the isogenic LPS mutants SL3749 *waaL446*, SL3750 *waaJ417*, SL3748 *waaI432*, SL3769 *waaG471*, SL3789 *waaF511*, and SL1102 *hldE543* (A), the *E. coli* K-12 wild-type strain BW30270, and the LPS mutants KPM53 ($\Delta waaC$) and KPM121 ($\Delta waaA$; B) were incubated with biotinylated PF4 (20 μ g/mL). PF4 binding was detected with peridinin chlorophyll protein-Cy5.5 conjugated streptavidin using flow cytometry and expressed as geometric mean fluorescence intensity (GMFI) multiplied by the percentage of labeled bacteria. Data represent mean \pm SD of at least 3 independent experiments (*S. enterica* sv Typhimurium wild-type and mutants, $n = 3$; *E. coli* BW30270, $n = 5$; *E. coli* KPM53, $n = 5$; and *E. coli* KPM121, $n = 3$). ** $P < .01$ versus wild-type. *** $P < .001$ versus wild-type.

Typhimurium SL3750 (*waaJ417*), lacking the O-antigen and GlcII of the LPS outer core (GMFI, 768.2 ± 243.1 vs *rfa*⁺ GMFI, 8.5 ± 2.9 ; $P = .0056$). Further deletions of consecutive sugars of the outer and inner core to the level of Kdo₂-lipid A, as represented by *S. enterica* sv Typhimurium SL1102 (*hldE543*; GMFI, 4587.3 ± 754.3 ; $P = .0005$), gradually increased PF4 binding (Figure 3A).

To test whether lipid A alone is sufficient for PF4 binding, we switched to *E. coli* KPM121 ($\Delta waaA$), which predominantly expresses the nonglycosylated, tetra-acylated lipid A precursor lipid IV_A.¹⁷ Compared with *S. enterica* sv Typhimurium SL3770, *E. coli* K-12 wild-type strain BW30270 showed at least some PF4 binding (Figure 3B; GMFI, 445.0 ± 359.0). (It is noteworthy that the *E. coli* K-12 is a strain with rough-type LPS, which lacks the O16-antigen because of an IS5 insertion mutation in the *wbbL* gene for a rhamnosyltransferase involved in O-antigen synthesis,²⁴ whereas *S. enterica* sv Typhimurium SL3770 expresses the S-form of LPS.) In accordance with the results obtained for the *S. enterica* sv Typhimurium mutants, the *E. coli* K-12 $\Delta waaC$ mutant KPM53 with 2 Kdo residues attached to lipid A (corresponding to the *hldE543* mutant of *S. enterica* sv Typhimurium SL1102) showed increased PF4 binding compared with the wild-type (GMFI, 4738.5 ± 1304.6 , $P = .0001$). When the 2 Kdo residues were also deleted in the *E. coli* $\Delta waaC$ mutant KPM121 (now exposing predominantly the tetraacylated lipid A precursor lipid IV_A), PF4

binding further increased (GMFI, 7581.3 ± 1285.5 ; $P = .0241$; Figure 3B). This suggests that lipid A is a major PF4 binding partner on the surface of Gram-negative bacteria.

Phosphate groups of lipid A mediate PF4 binding

To assess whether PF4 directly interacts with lipid A, we analyzed binding of PF4 to isolated lipid A and Kdo₂-lipid A. The binding experiments demonstrated that PF4 binds directly and in a dose-dependent manner to lipid A (Figure 4A). To show specificity, we coinubated lipid A with either BPI or polymyxin. These lipid A binding compounds inhibit binding of PF4 to lipid A in a dose-dependent manner, starting at 0.5 μ g/mL and reaching significance at a concentration of 4 μ g/mL ($P = .0096$) and 1 μ g/mL ($P = .0192$), respectively (Figure 4B). PF4 bound to immobilized lipid A, but not to immobilized LPS or Kdo₂-lipid A, probably because of steric hindrance (Figure 4A). This is consistent with the higher PF4 binding activity to nonglycosylated lipid IV_A of *E. coli* KPM121 compared with *E. coli* KPM53 with 2 Kdo residues attached to lipid A (Kdo₂-lipid A; $P = .0241$; Figure 3B). PF4 did not bind to immobilized Kdo (Figure 4A).

However, when the experiments were performed with soluble lipid A, soluble Kdo₂-lipid A, and soluble LPS, all inhibited PF4 binding to *E. coli* KPM121 (GMFI, 143.2 ± 17.5 ; $P = .0002$, 56.4 ± 8.2 ; $P = .0002$ and GMFI, 242.6 ± 74.8 ; $P = .0022$, respectively, vs buffer GMFI, 6071.8 ± 139.0 ; Figure 4C). As expected, soluble Kdo did not inhibit PF4 binding to *E. coli* KPM121 (GMFI, 6213.5 ± 82.9 vs buffer GMFI, 6095.0 ± 435.9 ; $P = .6763$; Figure 4C).

The lipid A backbone [4'-*P*- β -D-GlcN-(1 \rightarrow 6)- α -D-GlcN-1'-*P*] carries 2 phosphate groups in positions 4' and 1'. These negatively charged phosphate groups are important for PF4 binding, as binding of PF4 to immobilized MPLA (monophosphorylated) was significantly lower than to its native (bisphosphorylated) lipid A counterpart (Figure 4A; $P < .0001$). Concordantly, soluble MPLA had reduced inhibitory effects on PF4 binding to *E. coli* KPM121 compared with lipid A (GMFI, 893.9 ± 240.2 vs GMFI, 143.2 ± 17.5 ; $P = .0320$; Figure 4C).

Surface exposed proteins play no major role in PF4 binding

Besides LPS, negatively charged proteins decorate the bacterial surface. Possible binding of PF4 to proteins unmasked by the lack of LPS was not changed by treatment of *E. coli* BW30270, KPM53, and KPM121 with proteolytic enzymes. Pretreatment of the wild-type strain (BW30270), the *waaC* mutant (KPM53), and the *waaA* mutant (KPM121) with pronase E or trypsin did not alter PF4 binding ($P > .2$ for all comparisons; data not shown).

PF4 bound to lipid A of Gram-negative bacteria exposes PF4/heparin-like epitopes

To test whether anti-PF4/heparin antibodies recognize PF4 bound to lipid A of Gram-negative bacteria, we used LPS mutant strains only displaying lipid A and Kdo (*E. coli* KPM53), or lipid IV_A without Kdo (*E. coli* KPM121) in adsorption and elution experiments. Affinity-purified IgG antibodies eluted from PF4-coated *E. coli* strains KPM53 and KPM121 reacted with PF4/heparin complexes in the PF4/heparin-ELISA (Figure 5A), suggesting that PF4 bound to lipid A on bacterial surfaces exposes epitopes, which are also present in PF4/heparin complexes. In contrast, no antibodies with PF4/heparin specificity were eluted from native bacteria (not preincubated with PF4; Figure 5A). As further controls, the affinity-purified antibodies did not react with PF4 alone, and the

6. Appended papers

6.1 Paper I: PF4 evolution

BLOOD, 18 OCTOBER 2012 • VOLUME 120, NUMBER 16

PF4 INTERACTION WITH LIPID A 3349

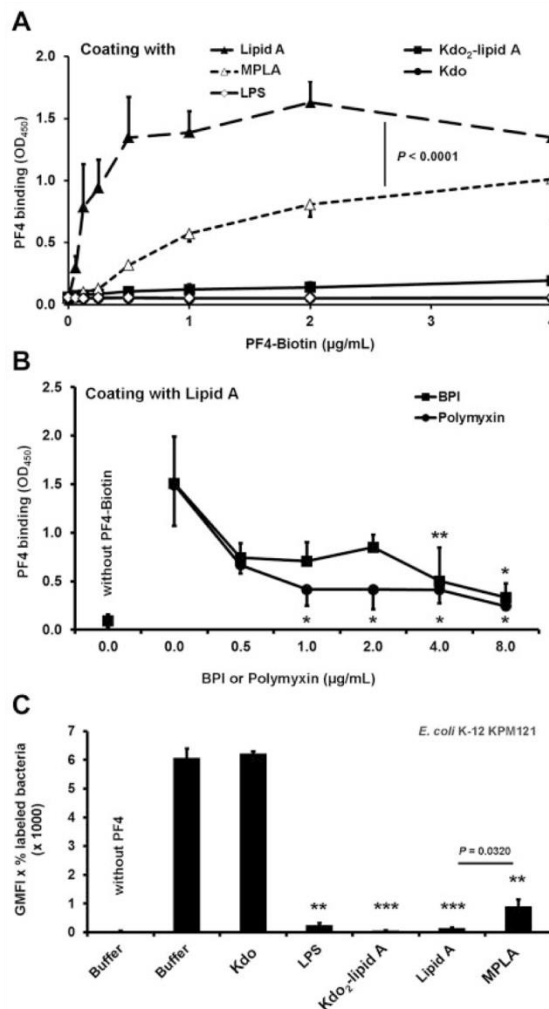


Figure 4. PF4 interaction with isolated lipid A relies on the phosphate groups. (A) PF4 binds dose-dependently to lipid A but not to LPS, Kdo₂-lipid A, or to Kdo alone. Binding of PF4 to MPLA (mono-(4'-P)-phosphoryl lipid) is reduced compared with binding to bisphosphorylated lipid A (Lipid A). Binding of biotinylated PF4 (0.06, 0.13, 0.25, 0.5, 1, 2, and 4 µg/mL) to immobilized LPS, Lipid A, Kdo₂-lipid A, MPLA, or Kdo (50 µg/mL) was detected with peroxidase-conjugated streptavidin followed by addition of tetramethylbenzidine. Data are mean OD ± SD of 3 independent experiments. (B) Binding of PF4 to Lipid A is inhibited by BPI or polymyxin B sulfate. Binding of biotinylated PF4 (2 µg/mL) in the presence of BPI or polymyxin (0.5, 1, 2, 4, and 8 µg/mL each) or buffer to immobilized Lipid A (50 µg/mL) was detected with peroxidase-conjugated streptavidin followed by addition of tetramethylbenzidine. Data are mean OD ± SD of 3 independent experiments. **P* < .05 versus PF4-biotin + buffer. ***P* < .01 versus PF4-biotin + buffer. (C) Preincubation of PF4 with LPS, lipid A, Kdo₂-lipid A, but not Kdo alone, inhibits PF4 binding to the *E. coli* KPM121 displaying only lipid IV_A on its surface, whereas the inhibitory effect of MPLA is reduced. PF4-biotin (40 µg/mL) was preincubated with Kdo, LPS, Kdo₂-lipid A, Lipid A, MPLA (each with 200 µg/mL), or buffer before assessing PF4 binding to *E. coli* KPM121 by flow cytometry. The results are expressed as geometric mean fluorescence intensity (GMFI) multiplied by the percentage of labeled bacteria. Data represent mean ± SD of 3 independent experiments. ***P* < .01 versus PF4-biotin preincubated with buffer. ****P* < .001 versus PF4-biotin preincubated with buffer.

addition of excess of heparin (disrupting PF4/heparin complexes) abrogated binding of eluted anti-PF4/heparin antibodies in the PF4/heparin ELISA, indicating the specificity of antibodies eluted from PF4-coated bacteria for PF4/heparin complexes.

The affinity purified (using PF4-coated *E. coli* K-12 mutants KPM53 and KPM121) anti-PF4/heparin antibodies also activated

platelets at low (0.2 IU/mL) but not at high heparin concentrations (100 IU/mL) in a functional assay for platelet activating anti-PF4/heparin antibodies (heparin-induced platelet activation; 3 of 3 sera, each).

To assess the impact of exposed lipid A on opsonization, bacterial mutants lacking LPS and wild-type bacteria were pre-treated with PF4 and anti-PF4/heparin antibodies, and phagocytosis of these bacteria by polymorphonuclear leukocytes was measured by flow cytometry. *E. coli* K-12 mutant KPM121 was more efficiently phagocytosed than its isogenic wild-type strain BW30270 (MFI, 18 267.4 ± 1449.3 vs wild-type MFI, 6118.5 ± 1449.3; *P* = .0054), demonstrating that the enhanced opsonization resulted in increased phagocytosis (Figure 5B).

Amino acids of PF4 important for polyanion binding are highly conserved among species

Finally, we analyzed the presence of PF4 and PF4-related proteins among vertebrate species in a PF4 amino acid sequence survey. The genomes encoding PF4, PF4-like protein, IL-8, or an uncharacterized protein with high similarities to human PF4 showed highly conserved amino acid residues among species, which represent essential motifs of the heparin binding site in human PF4 (Figure 6). These are lysine residues of the C-terminus (K61, K62, K65,

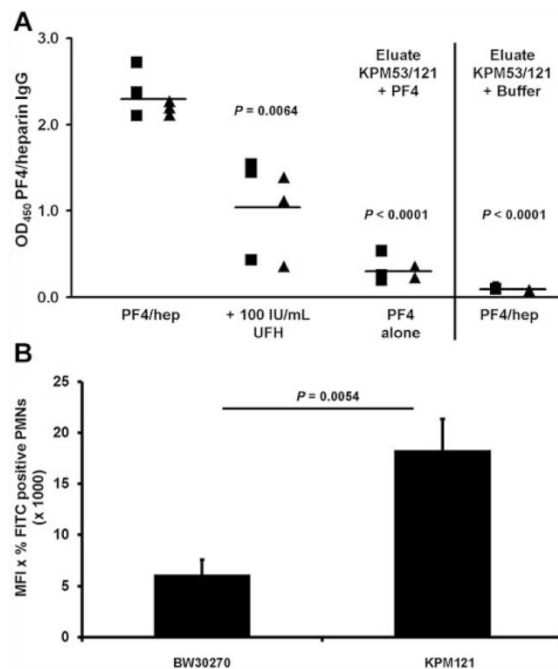
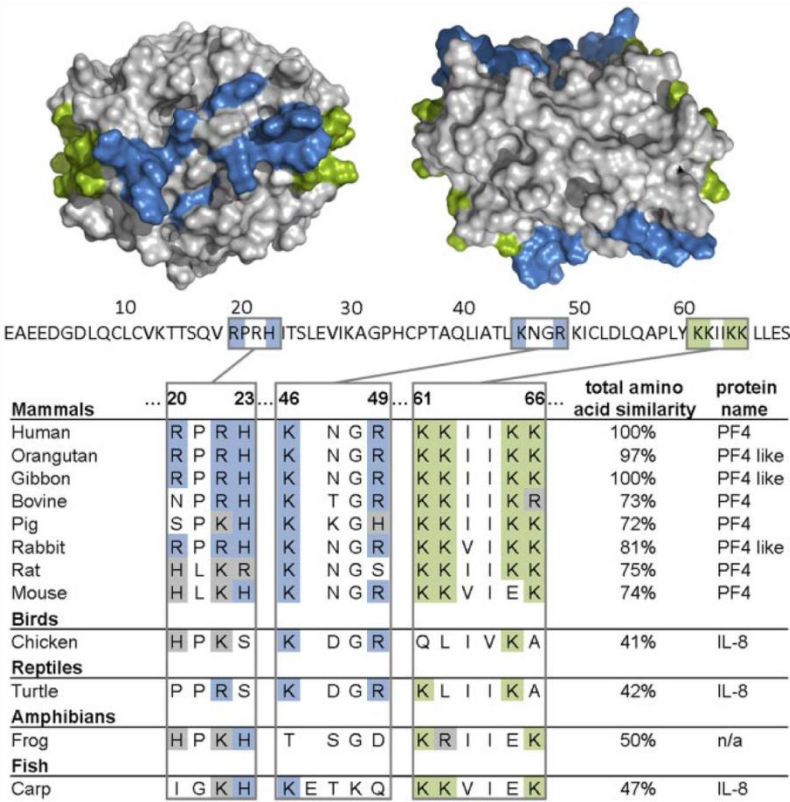


Figure 5. PF4-coated *E. coli* LPS mutants are recognized by anti-PF4/heparin IgG from sera of patients with HIT. (A) PF4-coated *E. coli* LPS mutants $\Delta waaC$ (KPM53) or $\Delta waaA$ (KPM121) were incubated with sera of 3 patients with HIT known to contain anti-PF4/heparin antibodies, and bound IgG was affinity purified. Symbols represent reactivities of IgG antibodies eluted from PF4-coated *E. coli* KPM53 (squares) or KPM121 (triangles); means are presented as horizontal lines. Binding of the purified antibodies to PF4/heparin complexes (first column) was inhibited by excess heparin (100 IU/mL unfractionated heparin [UFH], column 2), which disrupts PF4/heparin complexes. Antibodies did not react with PF4 alone (column 3). PF4-untreated bacteria served as control for unspecific binding of the antibodies to bacteria alone (column 4). (B) *E. coli* K12 wild-type strain BW30270 and its isogenic $\Delta waaA$ mutant KPM121 were labeled with FITC and preincubated with PF4 and additionally with heat-inactivated human serum containing anti-PF4/heparin IgG (preadsorbed with bacteria alone). After preincubation, the bacteria were subjected to phagocytosis. The figure shows the MFI multiplied by the percentage of FITC-positive polymorphonuclear leukocytes (PMNs) as a measure for bacterial phagocytosis. Data are mean ± SD of 4 different sera.



and K66), arginine residues (R20, R22, and R49), histidine residues (H23), and lysine residue (K46).²⁵⁻²⁹ Even in the case of amino acid substitutions, one cationic amino acid is often replaced by another positively charged amino acid (Figure 6).

Discussion

In this study, we identify the negatively charged phosphate groups in lipid A as the major binding sites for PF4 on Gram-negative bacteria and further demonstrate that PF4 bound to lipid A exposes epitopes on PF4 that can be recognized by human anti-PF4/heparin antibodies. The core- and O-polysaccharide structures of LPS appear to be dispensable as they rather protect from PF4 binding, most likely because of steric hindrance of the lipid A moiety.

The lipid A part of LPS is highly conserved among Gram-negative bacteria.³⁰ Similarly, the PF4 residues that mediate PF4-binding to polyanions are conserved throughout vertebrate species, as shown by our comparative analyses of PF4 and PF4 analogues (Figure 6). This is in accordance with our hypothesis that PF4 may label bacteria for destruction by the immune system. By exposing the same neoepitope after binding to a variety of bacteria, PF4 allows an antibody with one specificity to opsonize a large variety of bacterial species.⁵ We further speculate that this antibacterial defense mechanism may have developed at an early stage of evolution.

Recently, Sachais et al showed, with a monoclonal antibody (KKO), which recognizes PF4/heparin complexes, that these antibodies are able to induce clustering of PF4, even in the absence

of polyanions.³¹ In the present study, we show that PF4 binding to bacteria can be reduced depending on the composition of the polysaccharides of LPS. Some bacteria bind PF4 only weakly and could thereby escape the PF4/polyanion antibody-mediated defense mechanism. In this regard, it could be advantageous for the infected host if high-affinity anti-PF4/polyanion antibodies recognize PF4, even on pathogens that bind PF4 only weakly and then induce clustering of PF4 to augment binding of additional antibodies. This would help to opsonize also bacteria, which bind PF4 less efficiently (eg, by altering their LPS polysaccharide chain and to resist infection).

We identified lipid A of LPS as the binding site for PF4 by exploiting different LPS mutants of *S. enterica* sv Typhimurium, which differ in their sizes of the saccharide portion, including O-chain and core-oligosaccharides. Consecutive shortening of the LPS oligosaccharide increased the binding activity of PF4 to the LPS mutants. The mutant *S. enterica* sv Typhimurium SL1102 (*hldE543*), with only 2 Kdo residues attached to lipid A, displayed highest PF4 binding capacity. To test whether the lipid A part of LPS is sufficient for PF4 binding, we performed PF4 binding studies using the *waaA* mutant *E. coli* KPM121. We had to change bacteria species, as *E. coli* KPM121 is the only bacterial strain that is viable despite predominantly expressing only the lipid A precursor lipid IV_A.¹⁷ This strain showed strong PF4 binding activity, suggesting that Gram-negative bacteria sequester PF4 via lipid A of LPS. To further corroborate the validity of this experiment, we also assessed the *E. coli* K-12 wild-type strain BW30270 and the *E. coli* K-12 $\Delta waaC$ mutant KPM53 for their ability to bind PF4. As the results obtained with these strains were in good agreement with those obtained with

S enterica sv Typhimurium, we conclude that lipid A, as the most conserved part of LPS, is the main binding site for PF4 on Gram-negative bacteria.

Besides LPS, proteins are components of the outermost surface of Gram-negative bacteria. As these proteins can also be negatively charged,¹⁵ they may potentially contain additional binding sites for PF4. Our data on proteolytic treatment of *E coli* strains BW30270, KPM53, and KPM121 suggest that bacterial surface proteins do not have a major impact on binding of PF4. However, a contribution of proteins to PF4 binding cannot be excluded because we did not test whether the proteolytic treatment eliminated all surface-exposed proteins.

We further ruled out the possibility that expression of capsular polysaccharide may result in altered PF4 binding to the bacterial cells used in this study as the *E coli* K-12 strains do not express a capsule or the M-antigen (colanic acid) under the growth conditions used.^{32,33} Likewise, *S enterica* sv Typhimurium LT2 does not produce a capsule (K. E. Sanderson, *Salmonella* Genetic Stock Center, Calgary, AB, e-mail, May 11, 2012). Whether expression of a capsule affects PF4 binding needs to be investigated in future studies.

In confirmatory experiments assessing the interaction of PF4 with lipid A, we found that PF4 bound in a dose-dependent manner to immobilized lipid A but not to Kdo alone or immobilized Kdo₂-lipid A or LPS. In contrast, when Kdo₂-lipid A or LPS was added in excess to the fluid phase, both were able to inhibit PF4 binding to bacteria (Figure 4C). We assume that this discrepancy was probably the result of a steric hindrance. Kdo₂-lipid A and LPS can move freely in the fluid phase allowing the interaction of the lipid A part with PF4, whereas this is not possible for Kdo₂-lipid A or LPS immobilized on a solid phase.

Because of the strong positive charge of PF4 and the inhibitory effect of polymyxin B, the 2 negatively charged phosphate groups of lipid A are very likely responsible for the interaction with PF4. Indeed, MPLA had a lower PF4 binding capacity compared with lipid A (which is bisphosphorylated; Figure 4A) and showed a reduced capacity to inhibit PF4 binding to *E coli* KPM121 compared with lipid A (Figure 4C).

The lipid A moiety is the endotoxic moiety of LPS responsible for inducing endotoxic shock.³⁴ Thus, one role of PF4 might also be to protect from endotoxic shock, as has been shown for β_2 -glycoprotein I.³⁵ Lipid A also binds antimicrobial peptides, such as the bactericidal/permeability-increasing protein (BPI)^{36,37} and the cyclic lipopeptide polymyxin B, which interacts with the phosphate groups of lipid A.³⁸⁻⁴² In line with our other findings, BPI and polymyxin B inhibited PF4 binding to isolated lipid A (Figure 3B), further confirming that PF4 interacts with lipid A.

After identifying lipid A as the PF4 binding site, we asked the question whether this PF4-lipid A interaction also induces PF4/heparin-like epitopes to which anti-PF4/heparin antibodies can bind. Using PF4-coated *E coli* K-12 $\Delta waaA$ (KPM121) and $\Delta waaC$ (KPM53), we affinity purified anti-PF4/heparin antibodies from human serum by an adsorption-elution technique (Figure 5A). These antibodies did not only bind specifically to immobilized PF4/heparin complexes as tested by ELISA, but also mediated platelet activation in a functional assay for clinically relevant anti-PF4/heparin antibodies. This proves that lipid A and its biosynthetic precursor lipid IV_A are capable to induce neoepitopes on PF4 recognized by anti-PF4/heparin antibodies. Moreover, we show that opsonization of bacteria expressing only lipid A but

lacking LPS is enhanced when they were pretreated with PF4 and anti-PF4/heparin antibodies (Figure 5B).

We identified positively charged amino acids in the heparin binding site of PF4 (or the related chemokine IL-8, which also binds heparin⁴³ and has been reported to induce the production of antibodies in HIT patients^{44,45}), to be highly conserved in all vertebrates, including fish species. The interaction of PF4 and lipid A is inhibited by heparin (supplemental Figures 1 and 2, available on the *Blood* Web site; see the Supplemental Materials link at the top of the online article), suggesting that the amino acids known to contribute to heparin binding are also involved in binding to lipid A. This would be also compatible with our hypothesis of an ancient role of PF4 in an antibacterial host defense mechanism. On the other hand, one might consider as possible consequence of this "primitive mechanism of defense" that the highly variable O-antigens of LPS have significantly contributed to an efficient escape mechanism of the bacteria during evolution to evade the humoral response of the host.

Acknowledgments

The authors thank R. W. Woodard (University of Michigan, Ann Arbor, MI) for providing *E coli* KPM121; K. E. Sanderson (*Salmonella* Genetic Stock Center, Calgary, AB) for the *S enterica* sv Typhimurium strains; U. Dobrindt (University of Münster, Münster, Germany) for providing *E coli* anti-Ag43 antibodies; and N. Gisch (Forschungszentrum Borstel, Borstel, Germany) for helpful discussions about LPS chemical structures.

K.K. was supported by the Bundesministerium für Bildung und Forschung, Zentrum für Innovationskompetenz ZIK HIKE Förderkennzeichen (BMBF FKZ 03Z2CN12). This work was supported by the Deutsche Forschungsgemeinschaft (grants HA 3125/2-1 and 4-2, SFB/TRR34 project C10; S.H.).

Authorship

Contribution: K.K. designed and performed the bacterial experiments and ELISA and heparin-induced platelet activation tests, analyzed and interpreted the data, helped with the amino acid sequence survey, and wrote the manuscript; C.W. designed and performed the bacterial experiments, interpreted the data, helped with the amino acid sequence survey, and wrote the manuscript; S.B. performed the amino acid sequence survey; U.Z. purified and provided lipid A and Kdo₂-lipid A and revised the manuscript; U.M. constructed the *E coli* LPS mutants and revised the manuscript; A.G. reviewed the results and revised the manuscript; S.H. developed the concept, reviewed the results, and revised the manuscript; and all authors contributed to the study design and the data evaluation and approved the final version of the manuscript.

Conflict-of-interest disclosure: The authors declare no competing financial interests.

Correspondence: Sven Hammerschmidt, Ernst-Moritz-Arndt-Universität Greifswald, Interfakultäres Institut für Genetik und Funktionelle Genomforschung, Genetik der Mikroorganismen, Friedrich-Ludwig-Jahn-Strasse 15a, D-17487 Greifswald, Germany; e-mail: sven.hammerschmidt@uni-greifswald.de; and Andreas Greinacher, Ernst-Moritz-Arndt-Universität Greifswald, Institut für Immunologie und Transfusionsmedizin, Sauerbruchstraße, D-17475 Greifswald, Germany; e-mail: greinach@uni-greifswald.de.

References

- Diaco TG, Puri KD, Warnock RA, Springer TA, von Andrian UH. Platelet-mediated lymphocyte delivery to high endothelial venules. *Science*. 1996;273(5272):252-255.
- Elzey BD, Tian J, Jensen RJ, et al. Platelet-mediated modulation of adaptive immunity: a communication link between innate and adaptive immune compartments. *Immunity*. 2003;19(1):9-19.
- Tang YQ, Yeaman MR, Selsted ME. Antimicrobial peptides from human platelets. *Infect Immun*. 2002;70(12):6524-6533.
- Yeaman MR, Bayer AS. Antimicrobial peptides from platelets. *Drug Resist Updat*. 1999;2(2):116-126.
- Krauel K, Potschke C, Weber C, et al. Platelet factor 4 binds to bacteria, [corrected] inducing antibodies cross-reacting with the major antigen in heparin-induced thrombocytopenia. *Blood*. 2011;117(4):1370-1378.
- Fitzgerald JR, Foster TJ, Cox D. The interaction of bacterial pathogens with platelets. *Nat Rev Microbiol*. 2006;4(6):445-457.
- Yeaman MR. Bacterial-platelet interactions: virulence meets host defense. *Future Microbiol*. 2010;5(3):471-506.
- Rauova L, Poncz M, McKenzie SE, et al. Ultra-large complexes of PF4 and heparin are central to the pathogenesis of heparin-induced thrombocytopenia. *Blood*. 2005;105(1):131-138.
- Greinacher A, Gopinadhan M, Gunther JU, et al. Close approximation of two platelet factor 4 tetramers by charge neutralization forms the antigens recognized by HIT antibodies. *Arterioscler Thromb Vasc Biol*. 2006;26(10):2386-2393.
- Kelton JG, Sheridan D, Santos A, et al. Heparin-induced thrombocytopenia: laboratory studies. *Blood*. 1988;72(3):925-930.
- Reilly MP, Taylor SM, Hartman NK, et al. Heparin-induced thrombocytopenia/thrombosis in a transgenic mouse model requires human platelet factor 4 and platelet activation through FcγRIIIA. *Blood*. 2001;98(8):2442-2447.
- Hursting MJ, Pai PJ, McCracken JE, et al. Platelet factor 4/heparin antibodies in blood bank donors. *Am J Clin Pathol*. 2010;134(5):774-780.
- Greinacher A, Holtfreter B, Krauel K, et al. Association of natural anti-platelet factor 4/heparin antibodies with periodontal disease. *Blood*. 2011;118(5):1395-1401.
- van Winkelhoff AJ, Loos BG, van der Reijden WA, van der Velden U. Porphyromonas gingivalis, Bacteroides forsythus and other putative periodontal pathogens in subjects with and without periodontal destruction. *J Clin Periodontol*. 2002;29(11):1023-1028.
- Beveridge TJ. Structures of gram-negative cell walls and their derived membrane vesicles. *J Bacteriol*. 1999;181(16):4725-4733.
- Heinrichs DE, Yethon JA, Whitfield C. Molecular basis for structural diversity in the core regions of the lipopolysaccharides of Escherichia coli and Salmonella enterica. *Mol Microbiol*. 1998;30(2):221-232.
- Mamat U, Meredith TC, Aggarwal P, et al. Single amino acid substitutions in either YhD or MsbA confer viability to 3-deoxy-D-manno-oct-2-ulosonic acid-depleted Escherichia coli. *Mol Microbiol*. 2008;67(3):633-648.
- Mamat U, Schmidt H, Munoz E, et al. WaaA of the hyperthermophilic bacterium Aquifex aeolicus is a monofunctional 3-deoxy-D-manno-oct-2-ulosonic acid transferase involved in lipopolysaccharide biosynthesis. *J Biol Chem*. 2009;284(33):22248-22262.
- Rennemeier C, Hammerschmidt S, Niemann S, Inamura S, Zähringer U, Kehrel BE. Thrombospondin-1 promotes cellular adherence of gram-positive pathogens via recognition of peptidoglycan. *FASEB J*. 2007;21(12):3118-3132.
- Zähringer U, Salvatzi R, Wagner F, Lindner B, Ulmer AJ. Structural and biological characterization of a novel tetra-acyl lipid A from Escherichia coli F515 lipopolysaccharide acting as endotoxin antagonist in human monocytes. *J Endotoxin Res*. 2001;7(2):133-146.
- Juhl D, Eichler P, Lubenow N, Strobel U, Wessel A, Greinacher A. Incidence and clinical significance of anti-PF4/heparin antibodies of the IgG, IgM, and IgA class in 755 consecutive patient samples referred for diagnostic testing for heparin-induced thrombocytopenia. *Eur J Haematol*. 2006;76(5):420-426.
- Warkentin TE, Greinacher A. Laboratory testing for heparin-induced thrombocytopenia. In: Warkentin TE, Greinacher A, eds. *Heparin-induced Thrombocytopenia*. New York, NY: Informa Healthcare; 2007:227-238.
- Altschul SF, Madden TL, Schaffer AA, et al. Gapped BLAST and PSI-BLAST: a new generation of protein database search programs. *Nucleic Acids Res*. 1997;25(17):3389-3402.
- Liu D, Reeves PR. Escherichia coli K12 regains its O antigen. *Microbiology*. 1994;140(1):49-57.
- Handin RI, Cohen HJ. Purification and binding properties of human platelet factor four. *J Biol Chem*. 1976;251(14):4273-4282.
- Loscalzo J, Melnick B, Handin RI. The interaction of platelet factor four and glycosaminoglycans. *Arch Biochem Biophys*. 1985;240(1):446-455.
- Mayo KH, Ilyina E, Roongta V, et al. Heparin binding to platelet factor-4. An NMR and site-directed mutagenesis study: arginine residues are crucial for binding. *Biochem J*. 1995;312(2):357-365.
- Stuckey JA, St Charles R, Edwards BF. A model of the platelet factor 4 complex with heparin. *Proteins*. 1992;14(2):277-287.
- Ziporen L, Li ZQ, Park KS, et al. Defining an antigenic epitope on platelet factor 4 associated with heparin-induced thrombocytopenia. *Blood*. 1998;92(9):3250-3259.
- Zähringer U, Lindner B, Rietschel ET. Chemical structure of lipid A: recent methodical advances towards the complete structural analysis of a biologically active molecule. In: Brade H, Opal S, Vogel S, Morrison DC, eds. *Endotoxin in Health and Disease*. New York, NY: Marcel Dekker; 1999:93-114.
- Sachais BS, Litvinov RI, Yarovoi SV, et al. Dynamic antibody binding properties in the pathogenesis of HIT. *Blood*. 2012;120(5):1137-1142.
- Curtiss R 3rd. Biological containment and cloning vector transmissibility. *J Infect Dis*. 1978;137(5):668-675.
- Meredith TC, Mamat U, Kaczynski Z, Lindner B, Holst O, Woodard RW. Modification of lipopolysaccharide with colanic acid (M-antigen) repeats in Escherichia coli. *J Biol Chem*. 2007;282(11):7790-7798.
- Dixon DR, Darveau RP. Lipopolysaccharide heterogeneity: innate host responses to bacterial modification of lipid A structure. *J Dent Res*. 2005;84(7):584-595.
- Agar C, de Groot PG, Morgelin M, et al. Beta(2)-glycoprotein I: a novel component of innate immunity. *Blood*. 2011;117(25):6939-6947.
- Canny G, Levy O. Bactericidal/permeability-increasing protein (BPI) and BPI homologs at mucosal sites. *Trends Immunol*. 2008;29(11):541-547.
- Gazzano-Santoro H, Parent JB, Grinna L, et al. High-affinity binding of the bactericidal/permeability-increasing protein and a recombinant amino-terminal fragment to the lipid A region of lipopolysaccharide. *Infect Immun*. 1992;60(11):4754-4761.
- Daugelavicius R, Bakiene E, Bamford DH. Stages of polymyxin B interaction with the Escherichia coli cell envelope. *Antimicrob Agents Chemother*. 2000;44(11):2969-2978.
- Morrison DC, Jacobs DM. Binding of polymyxin B to the lipid A portion of bacterial lipopolysaccharides. *Immunochemistry*. 1976;13(10):813-818.
- Strimal S, Surolia N, Balasubramanian S, Surolia A. Titration calorimetric studies to elucidate the specificity of the interactions of polymyxin B with lipopolysaccharides and lipid A. *Biochem J*. 1996;315(2):679-686.
- Vaara M, Vaara T. Outer membrane permeability barrier disruption by polymyxin in polymyxin-susceptible and -resistant Salmonella typhimurium. *Antimicrob Agents Chemother*. 1981;19(4):578-583.
- Vaara M, Vaara T. Polycations as outer membrane-disorganizing agents. *Antimicrob Agents Chemother*. 1983;24(1):114-122.
- Witt DP, Lander AD. Differential binding of chemokines to glycosaminoglycan subpopulations. *Curr Biol*. 1994;4(5):394-400.
- Amiral J, Marfaing-Koka A, Wolf M, et al. Presence of autoantibodies to interleukin-8 or neutrophil-activating peptide-2 in patients with heparin-associated thrombocytopenia. *Blood*. 1996;88(2):410-416.
- Regnault V, de Maistre E, Carteaux JP, et al. Platelet activation induced by human antibodies to interleukin-8. *Blood*. 2003;101(4):1419-1421.

6.2 Paper II: Characterisation of the conformational Changes in Platelet Factor 4 induced by Polyanions: towards in vitro Prediction of Antigenicity

Characterisation of the conformational changes in platelet factor 4 induced by polyanions: towards *in vitro* prediction of antigenicity

Sven Brandt¹; Krystin Krauel^{1,2}; Kay E. Gottschalk³; Thomas Renné^{4,6}; Christiane A. Helm⁵; Andreas Greinacher^{2*}; Stephan Block^{1*}

¹ZIK HIKE – Zentrum für Innovationskompetenz „Humorale Immunreaktionen bei kardiovaskulären Erkrankungen“, Greifswald, Germany; ²Institut für Immunologie und Transfusionsmedizin, Greifswald, Germany; ³Institut für Experimentelle Physik, Universität Ulm, Germany; ⁴Department of Molecular Medicine and Surgery, Karolinska Institutet, Stockholm, Sweden; ⁵Institut für Physik, Ernst-Moritz-Arndt Universität, Greifswald, Germany; ⁶Institute for Clinical Chemistry and Laboratory Medicine, University Hospital Hamburg-Eppendorf, Hamburg, Germany

Summary

Heparin-induced thrombocytopenia (HIT) is the most frequent drug-induced immune reaction affecting blood cells. Its antigen is formed when the chemokine platelet factor 4 (PF4) complexes with polyanions. By assessing polyanions of varying length and degree of sulfation using immunoassay and circular dichroism (CD)-spectroscopy, we show that PF4 structural changes resulting in antiparallel β -sheet content >30% make PF4/polyanion complexes antigenic. Further, we found that polyphosphates (polyP-55) induce antigenic changes on PF4, whereas fondaparinux does not. We provide a model suggesting that conformational changes exposing antigens on PF4/polyanion complexes occur in the hairpin involving AA 32–38, which form together with C-terminal AA (66–70) of the adjacent PF4 monomer a continuous patch on the PF4 tetramer surface, explaining why only

tetrameric PF4 molecules express “HIT antigens”. The correlation of antibody binding in immunoassays with PF4 structural changes provides the intriguing possibility that CD-spectroscopy could become the first antibody-independent, *in vitro* method to predict potential immunogenicity of drugs. CD-spectroscopy could identify compounds during preclinical drug development that induce PF4 structural changes correlated with antigenicity. The clinical relevance can then be specifically addressed during clinical trials. Whether these findings can be transferred to other endogenous proteins requires further studies.

Keywords

Heparin-induced thrombocytopenia, platelet factor 4, GAGs, CD spectroscopy, antigenicity

Correspondence to:

Prof. Dr. med. Andreas Greinacher
Institut für Immunologie und Transfusionsmedizin
Sauerbruchstrasse
17475 Greifswald, Germany
Tel.: +49 3834 865482, Fax: +49 3834 865489
E-mail: greinach@uni-greifswald.de
or
Stephan Block, PhD
Applied Physics, Chalmers University of Technology
Fysikgränd 3, S-412 96 Gothenburg, Sweden
E-mail: block@physik.uni-greifswald.de, stephan.block@chalmers.se

Received: August 2, 2013

Accepted after major revision: January 20, 2014

Epub ahead of print: March 27, 2014

<http://dx.doi.org/10.1160/TH13-08-0634>

Thromb Haemost 2014; 112: 53–64

* Shared senior authorship.

Introduction

One of the major challenges for the development of new biotherapeutics is their potential immunogenicity (1, 2). Several drugs have failed when immune-mediated adverse effects became only obvious during phase III clinical trials (3, 4). Immunogenicity can be caused by the drug itself as a foreign protein as shown by recombinant hirudin (a leech derived protein) (5, 6), by conformational changes of endogenous proteins (induced during manufacturing or storing processes) as shown for erythropoietin (7), or by clustering of the protein as shown for interferon β (8, 9).

Currently, the most frequent immune-mediated adverse drug effect affecting blood cells is induced by the anticoagulant heparin (10). Polyanions (PAs) like heparin bind to the positively charged chemokine platelet factor 4 (PF4; CXCL4) (11–15) forming large complexes that are highly immunogenic (16, 17). The resulting

immunoglobulin G (IgG) antibodies can then trigger the adverse drug effect heparin-induced thrombocytopenia (HIT) (10, 18–22).

Although HIT has been actively studied for several decades, relatively little is known about the molecular mechanisms leading to the formation of antigenic structures to which the anti-PF4/heparin antibodies bind (23). As heparin can be replaced by other PAs without changing the antigenicity of the resulting PF4/PA complexes (23–25), it is widely accepted that the immunogenic epitopes are located on PF4. NMR measurements suggest that complex antigenicity is accompanied by structural changes of PF4 (27); however, there is no direct experimental proof for PA-induced changes in the secondary structure of PF4. Recently we observed by circular dichroism (CD) spectroscopy that PF4 undergoes a structural change if bound to certain PAs. Most interestingly, nucleic acid constructs that induced a conformational change of PF4 also induced anti-PF4/PA antibodies *in vivo* (26).

In this study, we now systematically characterise the structural changes of PF4 induced by binding to various PAs using CD spectroscopy and correlate these changes with the exposure of antigenic epitope(s) on PF4, i.e. allowing binding of anti-PF4/polyanion antibodies. We show that CD spectroscopy provides a potential *in vitro* tool to predict the potential of a PA to induce antigenic epitopes on PF4 and provide a model on the antigenic sites on PF4.

Materials and methods

Proteins and chemicals used were: Lyophilised, human platelet factor 4 (PF4) was isolated from platelets (Chromatec, Greifswald, Germany). Polyanions (PA): unfractionated heparin (UFH; Ratiopharm GmbH, Ulm, Germany), 2-O, 3-O desulfated heparin (ODSH; ParinGenix Inc., Weston, FL USA), reviparin (Clivarin 1750, Abbott GmbH & Co KG, Wiesbaden, Germany), fondaparinux (Arixtra 2.5 mg/0.5 mL, GlaxoSmithKline, Durham, NC, USA); hyaluronic acid, dextran sulfate; chondroitin sulfate A (Sigma-Aldrich, Munich, Germany) and polyphosphates of mean chain length 55 (polyP55; ICL Business Unit Bekaphos, Ladenburg, Germany).

Circular dichroism (CD) spectroscopy

Changes in the secondary structure of PF4 upon interaction with PAs were studied by recording far-UV CD spectra (200–260 nm) using a Chirascan CD spectrometer (Applied Photophysics, Leatherhead, UK). PF4 was dissolved in phosphate-buffered saline (PBS; pH 7.2; Invitrogen, Darmstadt, Germany) to final concentrations of 40 µg/ml (1.25 µmol/l) or 80 µg/ml (2.5 µmol/l). Complex formation was carried out at 20°C directly within the CD cuvette (Hellma, Müllheim, Germany). Each measurement started with a pure PF4 solution whose initial concentration was set to 40 µg/ml (cuvette path length = 10 mm) or 80 µg/ml (cuvette path length = 5 mm). Afterward, increasing amounts of a certain PA were sequentially added to the cuvette (leading to defined PF4/PA mixtures) and a CD spectrum was recorded for each mixing step. Additionally, buffer baselines, baselines of each PA concentration step (without PF4 in the solution) were recorded.

In the data analysis, the spectra of PF4 alone and of PF4/PA complexes were corrected for the baselines, path length, concentration, and number of amino acids to obtain the wavelength-dependent mean residue delta epsilon (MRDE) values of the PF4/PA complex. To estimate the secondary structure content of PF4, deconvolution of CD-spectra was carried out with CDNN (software, circular dichroism neural network) using a database of 33 reference proteins (28). In the deconvolution process calculations were adjusted for the moderate dilution of PF4 (due to addition of the PA solution).

Enzyme immunoassay (EIA)

PF4/PA EIA was performed with human sera of patients known to contain anti-PF4/heparin IgG verified by PF4/heparin EIA and heparin-induced platelet activation (HIPA) test as described (29) with some modifications. PF4 (20 µg/ml) was incubated (60 minutes [min] at room temperature [RT]) with rising concentrations of the PAs (as indicated in the figures) in coating buffer (0.05 M NaH₂PO₄, 0.1% NaN₃) to enable complex formation before coating wells of a microtiter plate (CovaLink, Nunc, Langenselbold, Germany) with 100 µl at 4°C overnight. Then plates were washed five times (0.15 M NaCl, 0.1% Tween 20, pH 7.5) and incubated (60 min, RT) with 100 µl patient serum (1:200 or 1:1,000 in 0.05 M NaH₂PO₄, 0.15 M NaCl, 7.5% goat normal serum, pH 7.5). Plates were washed five times and incubated with 100 µl peroxidase-conjugated anti-human IgG (1:20,000, Dianova, Hamburg, Germany). Afterward, plates were washed five times and incubated (10 min, RT) with 100 µl tetramethylbenzidine. The reaction was stopped with 100 µl 1 M H₂SO₄ and absorbance was measured at 450 nm.

Ethics

The use of human sera containing anti-PF4/heparin antibodies and obtaining whole blood from healthy volunteers was approved by the Greifswald ethics board.

Results

Changes in PF4 secondary structure due to interaction with UFH

► Figure 1 summarises the CD spectroscopic measurements on PF4/UFH complexes with defined molar ratios of PF4 and UFH. The concentration of PF4 was 40 or 80 µg/ml, respectively (1.25·10⁻⁶ M or 2.5·10⁻⁶ M), while the UFH concentration was stepwise increased from 0 to 107 µg/ml, which corresponds to a maximum UFH concentration of 0.35·10⁻³ M (per saccharide monomer). During the titration process, pronounced changes in the CD spectra are observed (► Figure 1A, B): (i) For UFH concentrations increasing from 0 to 6.9 µg/ml (2.2·10⁻⁵ M per saccharide monomer) the whole spectrum shifts upward, i.e. toward lower absolute ellipticity values. (ii) For a further concentration increase, this trend reverses (► Figure 1B). Excess of UFH leads to folding of PF4 towards its native conformation (► Figure 1A, B).

The spectrum of native PF4 shows two negative bands at 205 nm and 220 nm whose absolute values correspond to the α-helix content of the protein (30). The intensity of these bands changes for different UFH concentrations, indicating alterations in the secondary structure of PF4. Deconvolution of the CD spectra shows that complex formation of PF4 with UFH decreases the α-helix and β-turn content, which is balanced by an increase in antiparallel β-sheet content (► Figure 1C). For the remaining types of secondary structure, only insignificant changes are observed. Maximal changes are found for a UFH concentration of 6.9 µg/ml (at a PF4 concentration of 40 µg/ml), which corresponds to a stoichiometric

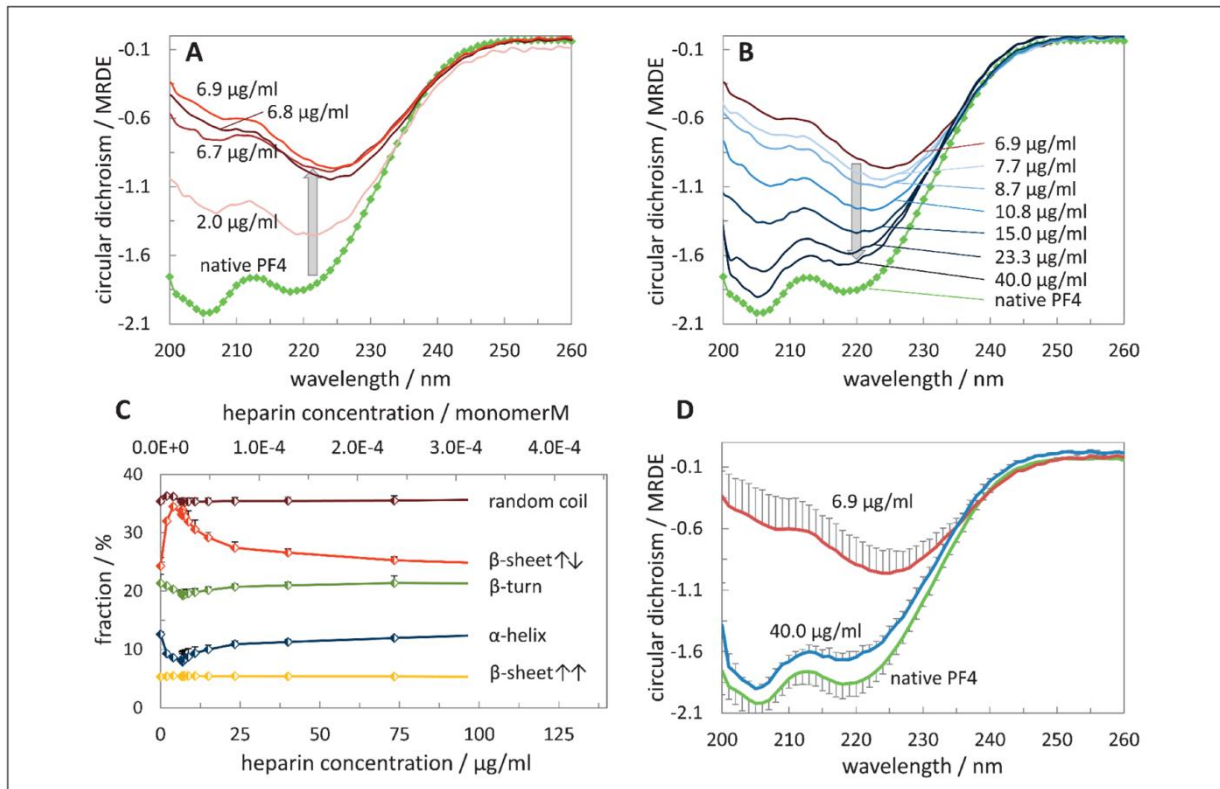


Figure 1: Binding to unfractionated heparin (UFH) changes the secondary structure of platelet factor 4 (PF4). CD spectra and secondary structure of PF4 in PF4/UFH complexes formed at various UFH concentrations as indicated (PF4 concentration = 40 µg/ml): A) – with increasing UFH concentration the CD spectra of PF4 shift to more positive ellipticity values, indicating changes in PF4 secondary structure, B) – with further increasing the UFH concentration, a return to a native-like state is observed, C) – decon-

volution of the PF4/heparin CD spectra shows an increase in antiparallel β -sheet content (β -sheet \uparrow), which is balanced by a decrease in α -helix and β -turn content, D) – comparison of CD spectra of native PF4 (green) and of the PF4/UFH complex, formed at a concentration of 6.9 µg/ml (red) or in excess of UFH (native-like folding state; blue). The error bars correspond to the standard deviation, taken from the results of $n = 3$ experiments.

metric ratio of 18 saccharide monomers bound to one PF4 tetramer. Additionally, ► Figure 1D shows that the CD spectrum of native PF4 and of the PF4/UFH complexes formed at 6.9 µg/ml and in excess of UFH = 40.0 µg/ml), albeit similar, still significantly differ from each other.

Correlation of PF4 structural changes and PF4/PA complex antigenicity

The changes in the secondary structure of PF4 observed with CD spectroscopy highly resemble the concentration dependence of PF4/UFH complex antigenicity obtained with the PF4/UFH EIA (29): (i) for low UFH concentrations, the antigenicity rises with increasing amount of UFH, (ii) at a certain concentration a maximum value is reached and (iii) a further increase in UFH concentration decreases the antigenicity of the PF4/UFH complex (24, 25).

Next we formed complexes of PF4 and various PAs in different concentrations, and assessed the structural changes of PF4 using

CD spectroscopy and PF4/PA complex antigenicity by anti-PF4/heparin antibody binding using EIA. The PAs differed in their chain length (N) and degree of sulfation per saccharide monomer (DS), which enables to control the PF4/PA complex antigenicity (23–25): 1. variation of chain length: UFH (broad molecular weight distribution [large polydispersity] with average molecular weight of approximately 12 kDa), the low-molecular-weight heparin reviparin (LMWH, cut-off size approximately 5 kDa; $N \sim 16$ saccharide monomers) and fondaparinux (pentasaccharide with a molecular weight of 1.7 kDa) and 2. variation of degree of sulfation: dextran sulfate ($DS=2-2.3$), UFH ($DS = 1-1.2$), 2-O, 3-O desulfated heparin (ODSH; $DS=0.6-0.8$), chondroitin sulfate A (chondSA; $DS=0.4-0.5$), hyaluronic acid ($DS=0$) and the polymer dextran ($DS=0$).

► Figure 2 compares the results of the EIA and the CD spectroscopic measurements for UFH, reviparin, ODSH, chondSA, fondaparinux and dextran sulfate. In this figure, the PA concentration c_{PA} (mg/ml) is divided by the PF4 tetramer concentration c_{PF4} (mg/ml): $c_{rel} = c_{PA}/c_{PF4}$. Moreover, we used only the antiparallel β -sheet

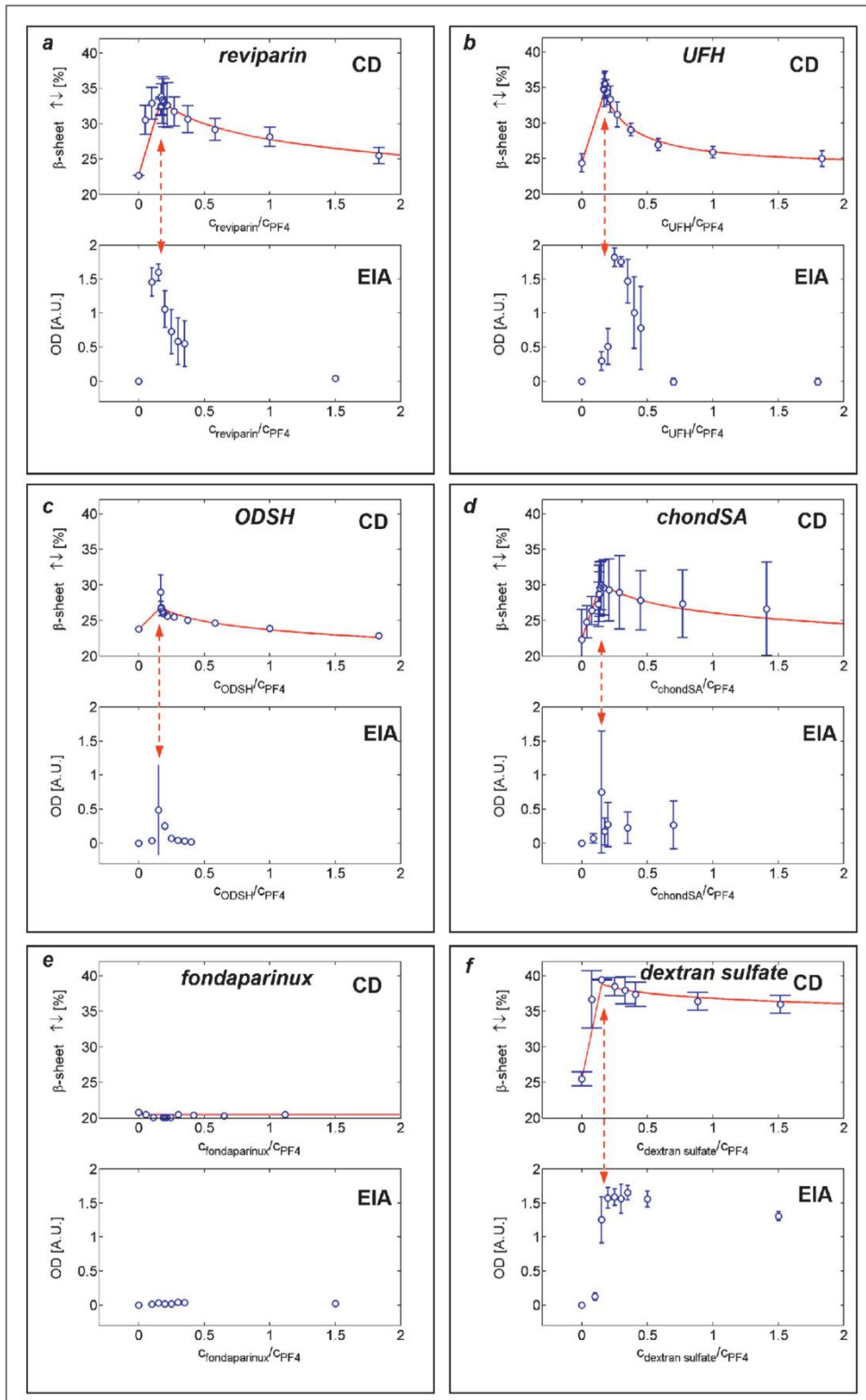


Figure 2: Comparison of PF4 structural changes and PF4/polyanion complex antigenicity obtained from CD spectroscopic and enzyme-immunoassay (EIA) measurements. A) Reviparin, B) unfractionated heparin (UFH), C) 2-O, 3-O desulfated heparin (ODSH), D) chondroitin sulfate A (chondSA), E) fondaparinux and F) dextran sulfate. The open circles give average values of OD (EIA) or antiparallel β -sheet content (CD spectroscopy) calculated from repetitions of these experiments, while the error bars correspond to the standard deviation (calculated from the results of $n = 3$ experiments using sera from 3 different patients with serologically confirmed HIT). In this figure, the PA concentration C_{PA} is normalised by the PF4 tetramer concentration C_{PF4} : $C_{rel} = C_{PA}/C_{PF4}$. Generally, changes in PF4 secondary structure observed with CD spectroscopy are qualitatively very similar to the concentration dependence of PF4/PA complex antigenicity.

content from the CD spectroscopic measurements as an indicator since (i) it is the only type of secondary structure, which is increased during the PF4/PA interaction, and (ii) the sum of changes of all other secondary structures is balanced by this value, which makes it a suitable measure for the overall change in PF4 secondary structure.

Again, complex antigenicity (binding of anti-PF4/heparin antibodies with an OD >1) was paralleled by pronounced PF4 structural changes (antiparallel β -sheet content >30%). These changes only occurred if both, chain length N and DS (per monosaccharide unit), exceed their limiting values, which was fulfilled by UFH, reviparin, and dextran sulfate (► Figure 2A, B, F). Reviparin induced (within experimental resolution) the same maximum PF4 structural change as did UFH (antiparallel β -sheet content up to ~35%). Moreover, the maximum structural change was observed for both PAs at a relative concentration of $c_{rel}=0.17$, which corresponded to UFH or reviparin concentrations of 6.9 $\mu\text{g/ml}$ at 40 $\mu\text{g/ml}$ PF4.

Dextran sulfate, which has a higher degree of sulfation than UFH, induced an antiparallel β -sheet content of up to 40% (► Figure 2F), but showed no complex dissolution in excess of the PA. The PF4 secondary structure was essentially not affected by a further increase in concentration, which was indicated by almost constant values in EIA and CD spectroscopy. Among all PAs investigated, complex formation with PF4 was irreversible only for dextran sulfate.

No structural changes of PF4 were observed for fondaparinux (low N [23]; cf. ► Figure 2E), hyaluronic acid and dextran (low DS [23]; see also Suppl. Figure 1 available online at www.thrombosis-online.com).

The DS of ODSH and chondroitin sulfate A (chondSA) are close to the critical DS , as reflected in our results: we observed for both PAs an antiparallel β -sheet content of up to 30%, which is less than the values observed for the highly antigenic PAs UFH (~35%), reviparin (~35%) and dextran sulfate (~40%) but significantly larger than for native PF4 (~23.5%). Accordingly, EIA measurements show that antigenicity of PF4/ODSH and PF4/chondSA complexes is smaller in comparison to PF4/UFH, PF4/reviparin and PF4/dextran sulfate complexes, as not all but only some of the sera containing anti-PF4/PA antibodies lead to a significant OD increase. Generally, we observed striking similarities between EIA and CD spectroscopy results. This implies a close correlation between PF4/PA complex antigenicity and changes in PF4 secondary structure induced by PAs. Hence, we plotted in ► Figure 3 the OD value of PF4/PA complexes versus the PF4 antiparallel β -sheet content. For this, we directly used the data from ► Figure 2 with one exception: As we noticed for UFH a discrepancy in peak positions for OD and antiparallel β -sheet content, we introduced a correction factor of 1.75 for the UFH concentration of the CD spectroscopic data, which brings both peak positions in agreement. This reduces the horizontal scattering of the data in ► Figure 3, but does not affect the main conclusion (discussed subsequently) as can be seen in an “uncorrected version” of this figure (see Suppl. Figure 2 available online at www.thrombosis-online.com).

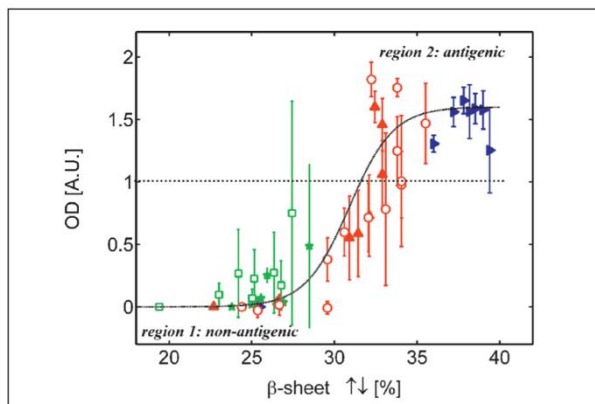


Figure 3: PF4/PA complex antigenicity correlates with changes in PF4 antiparallel β -sheet content. Correlation of antiparallel β -sheet content of PF4/PA complexes (as measured with CD spectroscopy) with the OD of the same complexes (as determined with EIA) for: (○) UFH, (▲) reviparin, (★) 2-O, 3-O desulfated heparin, (□) chondroitin sulfate A, (▶) dextran sulfate. Strong PF4/PA complex antigenicity (indicated by OD > 1) is accompanied by large changes of PF4 secondary structure (indicated by antiparallel β -sheet contents >30%). As we noticed for UFH a discrepancy in peak positions for OD and antiparallel β -sheet content (see Figure 2B), we introduced a correction factor of 1.75 for the UFH concentration of the CD spectroscopic data in this plot. An “uncorrected version” of this plot is given in the supporting material. The solid line gives the fit of Eq. 1 to the data.

For an antiparallel β -sheet content smaller than 30%, the corresponding EIA gives low OD values (<<1; region 1 in ► Figure 3). An increase in antiparallel β -sheet content above 30% causes a strong increase in OD (>1), which depends in first approximation linearly on the structural change (region 2 in ► Figure 3). This linear increase in OD has (within the experimental error) the same slope for all PAs.

PAs below the critical DS ($DS < 1$) are located only in region 1, which corresponds to a small but significant change in the PF4 secondary structure without turning the PF4/PA complex antigenic. Hence, region 1 corresponds to the non-antigenic region of ► Figure 3. Additionally, as only PAs forming antigenic PF4/PA complexes are able to enter region 2 (indicated by OD values >1), this region corresponds to the antigenic region.

Predicting PF4/PA complex antigenicity using CD spectroscopy

► Figure 3 implies a relationship between antiparallel β -sheet content and OD, which is captured by the sigmoid function (Eq. 1):

$$OD_{pred}(c_{rel}) = \frac{OD_{max}}{2} \cdot \left[1 + \tanh \left(\frac{2\Delta}{OD_{max}} \cdot \{ \beta_{\uparrow, \Delta}(c_{rel}) - \beta_{\uparrow, \Delta, 0} \} \right) \right]$$

Here, c_{rel} denotes as before the PA concentration c_{PA} (in mg/ml) normalised by the PF4 concentration c_{PF4} (in mg/ml), $c_{rel} = c_{PA}/c_{PF4}$, $OD_{pred}(c_{rel})$ gives the predicted/expected OD for a complex formed at c_{rel} , Δ is the slope in the *antigenic region*, $\beta_{\uparrow, \Delta}(c_{rel})$ is the antipar-

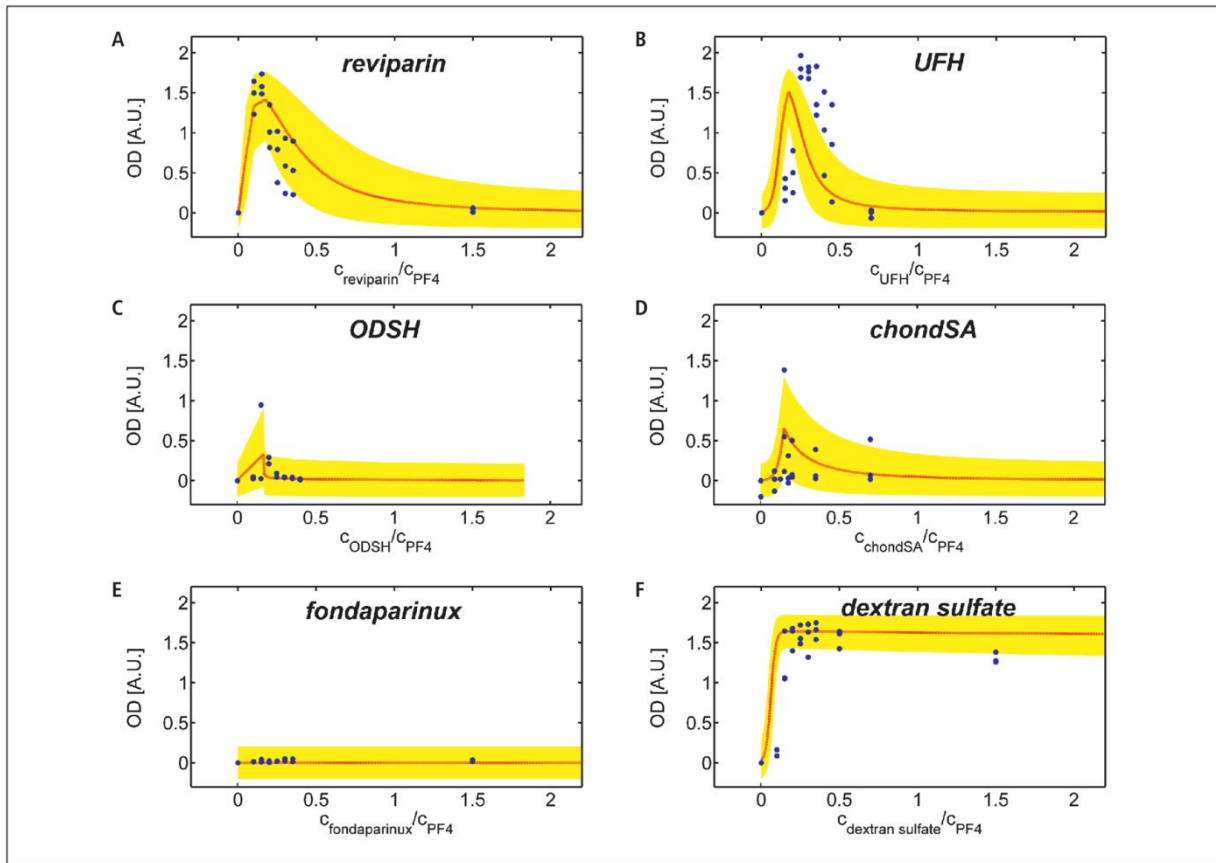


Figure 4: CD spectroscopy allows prediction of PA concentration dependent PF4/PA complex antigenicity. Comparison of OD values predicted from the CD spectroscopic measurements (red line and yellow areas) with the ones measured by EIA (blue dots). The red line is calculated according to Eq. 1 and translates the average value of PF4 antiparallel β -sheet content (see symbols in Figure 2) into an OD value of the PF4/PA complex in EIA measurements. The yellow areas are calculated in a similar way, but additionally account for measurement uncertainties in the determination of the secondary structure (see error bars in Figure 2). This means that from Eq. 1

(which is based on the correlation observed in Figure 3) we expect the data points of EIA measurements on PF4/PA complexes to be located within the yellow areas, which is indeed fulfilled for all PAs investigated (except UFH, see text for discussion). This shows that the antiparallel β -sheet content is quantitatively connected with the antigenicity of a PF4/PA complex. Moreover, results of EIA measurements can be predicted from CD spectroscopic measurements, i.e. CD spectroscopy in connection with Eq. 1 can be used to assess antigenicity of PF4/PA complexes.

allel β -sheet content at c_{rel} , while $\beta_{\uparrow,0}$ sets the point of inflection of Eq. 1 and has to be determined by fitting the data to Eq. 1. OD_{max} denotes the saturation OD value, which is reached for $\beta_{\uparrow} \gg \beta_{\uparrow,0}$. This model covers both aspects discussed before, i.e. all PAs exhibit the same slope Δ and a critical structural change (here accounted by $\beta_{\uparrow,0}$) has to be exceeded to induce a significant increase in OD. As Δ and OD_{max} can be extracted from ►Figure 3, the only adjustable parameter is $\beta_{\uparrow,0}$.

►Figure 4 compares OD values (predicted by applying Eq. 1 to CD spectroscopic data; red line and yellow area) with the ones measured by EIA (blue dots). For these calculations, we used the parameters $\Delta=0.3$ (for β in %; taken from the slope of the linear region in ►Figure 3) and $\beta_{\uparrow,0}=30.9\%$ (fitting parameter) for all PAs. The red line corresponds to Eq. 1 applied to the average value

$\langle \beta_{\uparrow} \rangle$ of the antiparallel β -sheet content β_{\uparrow} (as determined by CD spectroscopy; see ►Figure 2), while the yellow area accounts additionally for the fact that β_{\uparrow} can be resolved only within a certain measurement resolution $\Delta\beta_{\uparrow}$ (see error bars in ►Figure 2). The yellow areas correspond therefore to intervals, which are expected to contain the OD values measured by EIA.

►Figure 4 compares these OD “expectation” intervals (calculated using the CD spectroscopic data of ►Figure 2 and the average standard deviation $\Delta\beta_{\uparrow}=1.5\%$) with the results from the EIA measurements. For all PAs (except UFH), the majority of EIA data points (>85%) are located within the yellow areas, indicating that the change in antiparallel β -sheet content is converted by Eq. 1 into an indicator for complex antigenicity. However, as UFH exhibits its maximum OD at a different relative concentration c_{rel} than the

antiparallel β -sheet (see also ► Figure 2B), only very few EIA data points for PF4/UFH complexes hit the yellow area. If we introduce (in analogy to ► Figure 3) a correction factor for c_{rel} , almost all EIA data points are located in the yellow area (see Suppl. Figure 3 available online at www.thrombosis-online.com).

► Figure 4 shows that CD spectroscopy can be used to predict binding of anti-PF4/heparin antibodies to PF4/PA complexes (29). A PA can be regarded as non-antigenic if the yellow areas stay far below the threshold of OD=1.0 for all PA concentrations (► Figure 4E). It should be regarded as antigenic if the yellow area exceeds an OD of 1 (e.g. reviparin, UFH, and dextran sulfate; ► Figure 4A, B, F). In between, there might be the risk of forming weakly antigenic PF4/PA complexes, if the interval touches the antigenicity threshold (e.g. ODSH, chondroitin sulfate A; ► Figure 4C, D).

To generalise these findings, we applied CD spectroscopy to the polyphosphate polyP55 (mean chain length 55 monomers) and observed (► Figure 5) a strong increase in antiparallel β -sheet content as well as a strong increase in OD in the EIA. This shows that our approach is not restricted to PAs based on polysaccharides.

Discussion

In this study we establish a correlation between changes in PF4 secondary structure within PF4/PA complexes with the induction of antigenic epitope(s). This approach allows to calculate expectation intervals for anti-PF4/PA antibody binding (as expressed by OD values) solely using CD spectroscopic data. In the following, we use the term antigenicity to describe that a certain PA induces a change in PF4 which results in binding of known antibodies with anti-PF4/heparin specificity to the PF4/PA complexes.

To our knowledge, this is the first demonstration that antigenicity of a drug can be assessed without the necessity of *in vivo* studies or the use of antibodies obtained from immunized patients, or special monoclonal antibodies. This approach is of potential major relevance for drug development. Several classes of biotherapeutics are negatively charged, e.g. certain anti-cancer drugs (PI-88), or DNA- or RNA-based aptamers (26, 32).

Correlation between β -sheet formation and PF4/PA antigenicity

A critical chain length and a critical DS have to be exceeded by a PA to induce antigenic PF4/PA complexes: for polysaccharides, a critical chain length N_{crit} of ~12 monosaccharide units and a DS_{crit} of one sulfate group per saccharide monomer are frequently reported (23, 38, 39). Our measurements are in agreement with these results: non-antigenic PF4/PA complexes were formed if either the PA was too short (fondaparinux, $N=5$) or if the degree of sulfation was too low (dextran, $DS=0$; hyaluronic acid, $DS=0.5$) (23–25). For these PAs, no significant structural changes of PF4 were observed, while antigenic PF4/PA complexes were formed, if both, N_{crit} and DS_{crit} were simultaneously exceeded (UFH, reviparin, dextran sulfate). For these PAs, pronounced PF4 structural changes were observed.

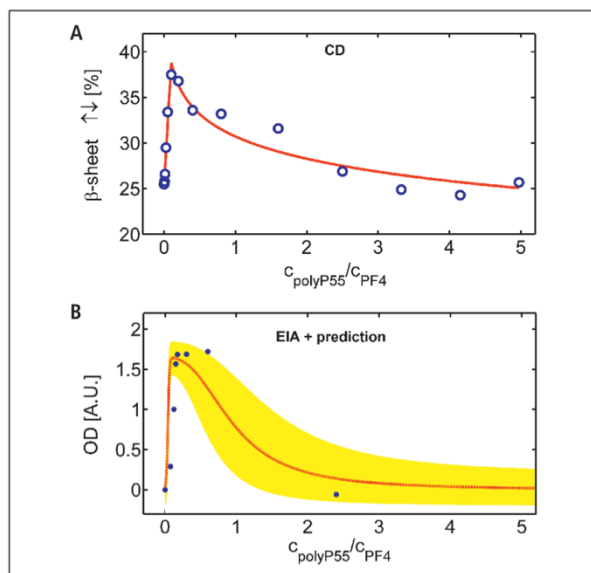


Figure 5: Polyphosphates form antigenic complexes with PF4. Comparison of PF4 structural changes and PF4/polyP55 antigenicity obtained from A) CD spectroscopic and B) EIA measurements. Similar to the PAs of Figure 2, one observes that changes in PF4 secondary structure (indicated by a strong increase in antiparallel β -sheet content; open circles in A) are accompanied by complex antigenicity (indicated by OD values far exceeding 1; dots in B). Moreover, B) compares OD values predicted from the CD spectroscopic measurements (red line and yellow area) with the ones measured by EIA (blue dots) for PF4/polyP55 complexes (see caption of Figure 4 and text for details). Again, the data points of the EIA measurements are mostly located within the expected (yellow) area, which shows that results of EIA measurements can be predicted from CD spectroscopy (using Eq. 1) also for PAs carrying phosphate groups.

Interestingly, among all PAs investigated only dextran sulfate showed no complex dissolution in excess of the PA (which is the usual observation for HIT-relevant PF4/PA complexes). As the main difference between dextran sulfate and the other PAs is mainly the higher (negative) line charge density, we assume that the electrostatic part of the PF4/PA-interaction is stronger for dextran sulfate than for the other PAs. However, we cannot fully rule out that also non-electrostatic effects (e.g. due to different monosaccharide conformation) might further stabilise the binding of PF4 to dextran sulfate.

The novelty here is the finding that the PF4 secondary structure can be altered by the interaction with PAs, without turning the PF4/PA complexes completely antigenic: The DS of ODSH and chondSA are close to the critical value of 1. These PAs induced smaller PF4 structural changes (antiparallel β -sheet content of max. 30% vs >35% for UFH) and not all sera in EIA led to a peak in OD for PF4/ODSH and PF4/chondSA complexes. Indeed, Joglekar et al. (40) showed that ODSH creates a very small risk of inducing immune reactions to PF4/ODSH complexes. Our interpretation of the more variable binding of the anti-PF4/PA antibodies to the complexes between PF4 and ODSH or chondroitin sulfate is

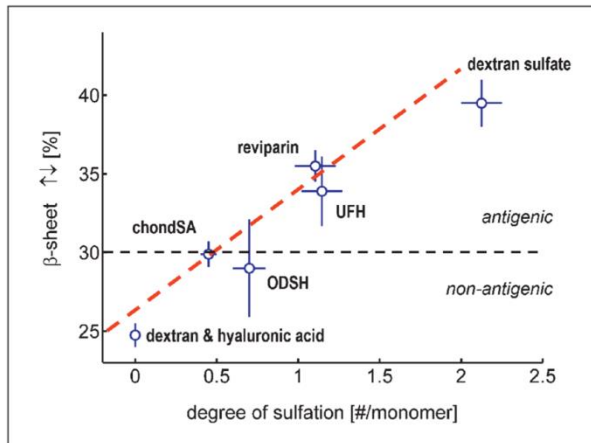


Figure 6: Maximum change in PF4 secondary structure correlates with the polyanion's degree of sulfation. Relation between degree of sulfation, DS, and maximum change in antiparallel β -sheet content for PF4/PA complexes as indicated. An almost linear increase in maximum structural change is observed.

that the epitope is expressed in a suboptimal way on the PF4/ODSH and PF4/chondroitin sulfate complexes, respectively. This indicates that the antibodies we used differ slightly, either in the binding sites they recognise on PF4 or in their affinity. Antibodies showing high affinity may still bind despite a less optimal expression of the conformation dependent neoepitope induced by the PA.

For all PAs tested we observed that the increase in antiparallel β -sheet content is balanced by a decrease in structures having α -helical or β -turn conformations. This suggests that the antiparallel β -sheet content might be indicative for the antigenicity of the PF4/PA complex, which was confirmed by correlating EIA and CD spectroscopic data.

Using these considerations it was possible to predict PF4/PA complex antigenicity solely from the antiparallel β -sheet content (as measured by CD spectroscopy; ► Figure 4). As the peak PA concentrations of both approaches coincide in all (except one) cases, we conclude that maximum antigenicity is obtained at a PA concentration that also induces maximum change in PF4 antiparallel β -sheet content. Exposure of HIT-relevant epitope(s) is only observed for PAs that also change the secondary structure of PF4. Hence, it is not sufficient to form a repetitive PF4 alignment on the PA chain, as we hypothesised in previous studies (16).

One might argue, whether the differences in the antibody binding capacity for the different PAs might be caused by the charge and/or length of the respective PA. We are relatively confident that the charge does not inhibit the access of an IgG to the epitopes, as complexes of PF4 with dextran sulfate and hypersulfated chondroitin sulfate show even better antibody binding than UFH (23). The length of the PA has an indirect impact on antibody binding as a certain chain length N_{crit} has to be exceeded to induce antigenic PF4/PA-complexes. The existence of N_{crit} led to the hypoth-

esis that at least two PF4 tetramers have to be connected by one PA chain to make the formed complex antigenic (16). Depending on the PAs N and DS , each PF4 tetramer occupies a certain amount of monomers on the PA chain, which limits the maximum number of PF4 tetramers that can be bound to a PA chain. However, a single chain must be able to bind at least two PF4 tetramers to induce epitope expression and antibody binding. That very long PAs (having the capability to bind many PF4 tetramers) do not mediate antibody binding to PF4 is likely not caused by charge related hindrance of antibody binding, but, as we have shown by systematic studies many years ago (25), this is more likely caused by wrapping of the PA around PF4 instead of bridging between PF4 molecules. As the PAs bind to the equatorial ring of positively charged amino acids, it should be sufficiently far away from the antibody binding site. Thus the length of the polyanion likely does not interfere with IgG binding, but influences it indirectly via saturation of all binding sites of PF4 which prevents formation of multimolecular complexes. These complexes seem to be essential for antigenicity and even the conformational changes in PF4 seem to be influenced by complex formation of several PF4 molecules.

This reasoning can be generalized to show that the changes in antibody binding of the different PF4/PA-complexes cannot be caused by steric or electrostatic inhibition of antibody access. A steric hindrance would be largest in the presence of highly charged PAs. Hence, in this case PF4/dextran sulfate- and PF4/polyP55-complexes should have the lowest antibody binding capacity, which is also not observed in the experiment. Therefore, we rule out that biophysical features of the PAs affect antibody access sterically or electrostatically unless a certain length is not exceeded. Our data rather show that PA binding to PF4 creates (a) new epitope(s) by inducing a change in PF4 secondary structure. These neoepitopes are likely also dependent on the close approximation of several PF4 tetramers. However, the latter is still speculative.

Up to now, we found deviations between CD spectroscopy and EIA only for UFH, while for the LMWH reviparin (which is chemically equivalent to UFH but exhibits a much narrower size distribution) a good agreement was obtained. As the chain length distribution of UFH is much broader with respect to the other PAs, we hypothesise that the discrepancy of the peak positions in CD spectroscopy and EIA are caused by the polydispersity of UFH.

It is evident from ► Figure 4 that the data from the CD spectroscopy can be used to predict whether a PA has a high likelihood to induce the binding sites for anti-PF4/PA antibodies for all less polydisperse PAs and hence, to get a measure for the PF4/PA complex antigenicity solely from CD spectroscopic measurements. The antigenicity threshold is reached at an antiparallel β -sheet content of approximately 30%, i.e. PAs inducing PF4 structural changes that exceed that threshold constitute antigenic PF4/PA complexes. A similar value is obtained if the dependence between degree of sulfation DS and maximum value of PF4 antiparallel β -sheet content is plotted for all PF4/PA complexes investigated and one regards that PF4/ODSH and PF4/chondSA complexes are at the antigenic threshold (► Figure 6).

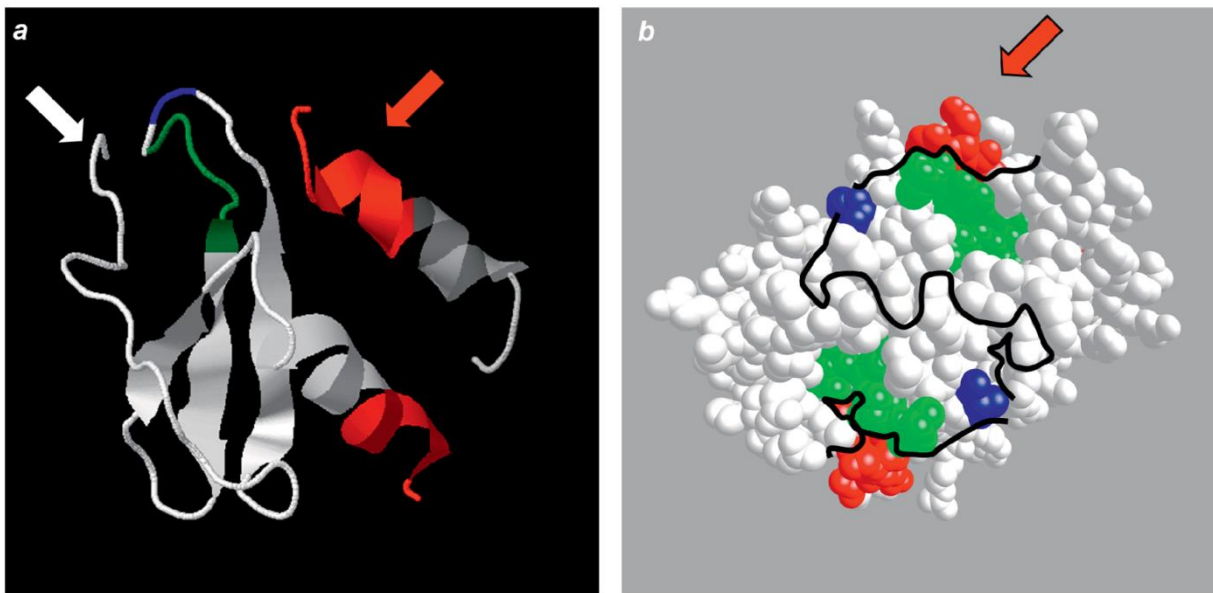


Figure 7: Structural model for the conformational changes of PF4 induced by PF4/polyanion complex formation. Molecular model of a) the secondary structure of a PF4 monomer (supplemented by the α -helix of the adjacent PF4 monomer) and b) the surface of a PF4 tetramer as determined by X-ray crystallographic measurements of Zhang et al. (46) (code 1RHP of the Brookhaven Protein Data Bank). The three curved, black lines in b) indicate the course of the interfaces between the four PF4 monomers that together form the homotetramer. The view axis in b) is perpendicular to the plane of the PF4 heparin binding site and shows that the majority of the amino acids (constituting the protein surface) belong to solely two monomers above the heparin binding side (while the remaining two

monomers form the majority of the surface on the opposite side). The two known HIT related epitopes (site 1 = amino acids 37–41: green structures; amino acid 34 belongs to site 2: blue structures) are located at a β -turn hair-pin. Both epitopes are neighbored by the C-terminal amino acids (amino acids 66–70: red arrow) and red structures in b) of the α -helix of the adjacent PF4 monomer (with respect to the plane defined by the heparin binding site) so that the epitopes and the C-terminal part of the α -helix form a continuous patch on the surface of the PF4 tetramer. Due to this interplay between neighbored PF4 monomers, this patch is only exposed if PF4 is in a tetrameric form.

While findings of *in vitro* experiments are largely compatible with our model, there is, however, a conflicting clinical observation in regard to fondaparinux. Patients receiving fondaparinux after major orthopaedic surgery developed anti-PF4/heparin antibodies (41). On the other hand, patients with acute HIT can be treated safely with fondaparinux. A potential explanation (42) might be that other polyanions, like heparan sulfate act together with fondaparinux as a feeder for PF4-complex formation (43) in large enough quantities for immunisation but in too low concentrations for inducing immune-complex mediated activation of platelets. This puzzling issue requires further investigations.

The almost complete lack of cross-reactivity of anti-PF4/heparin antibodies against PF4/danaparoid complexes is also compatible with our findings. First of all, danaparoid is mostly (>95%) a mixture of GAGs, whose degree of sulfation DS is generally smaller than the critical $DS_{crit} \sim 1$, which already indicates that (similar to ODSH and chondroitin sulfate A, chondSA) at most a very weak cross-reactivity is expected. Nevertheless, danaparoid also has a small content of highly sulfated heparin, which contributes to about 5% of the drug. This constituent of danaparoid with high affinity to antithrombin fully reacts with anti-PF4/heparin antibodies (44). However, due to the relatively low specific ac-

tivity of danaparoid much more danaparoid is given on a weight basis. While low molecular weight heparin has an anti-FXa activity of ~100 U/mg, the activity of danaparoid is only 15 U/mg. Both drugs are dosed according to the anti-FXa plasma levels, which are in therapeutic dose about 0.4 – 0.6 anti-FXaU/ml for danaparoid given as continuous infusion. Thus on a molecular basis there are about 6–7 times more PA molecules administered. We have shown that the mixture of 5% high antithrombin affinity drug plus 95% low antithrombin affinity material completely blocks platelet activation by HIT antibodies, which has more recently been further characterised by our group (44, 45).

Another issue, however, can be explained more easily. In some patients, typically suffering from severe HIT, it was observed that their sera contain antibodies that directly bind to PF4 (i.e. complex formation with polyanions like heparin is not necessary for these sera). As these antibodies bind to PF4 also in absence of polyanions, it is very likely that they recognise epitopes on PF4 that are not dependent on conformational changes of PF4. We can only speculate that these antibodies are created in parallel during the immune response against the PF4/heparin-complexes. Typically these antibodies, which react with PF4 in the absence of heparin, are present in sera showing a very high OD in the antigen assays

What is known about this topic?

- Platelet factor 4 (PF4) and polyanions like heparin form complexes. Some of these complexes are antigenic, i.e. they react with anti-PF4/heparin antibodies.
- Only PF4 tetramers can expose the antigen to which anti-PF4/heparin antibodies bind.
- It is unclear whether the epitope to which anti-PF4/heparin antibodies bind results from a conformational change of PF4 or from close approximation of two PF4 tetramers.
- Platelets contain polyphosphates in their dense granules

What does this paper add?

- The described method is the first to screen new drugs for their potential immunogenicity by inducing a conformational change in PF4.
- To the best of our knowledge this is the first report describing how a complex neoantigen is expressed on an endogenous protein resulting from a conformational change AND formation of densely packed proteins. This may serve as a model to better understand formation of autoantigens.
- It shows that the epitope recognised by HIT antibodies is induced by a change in the conformation of PF4 which requires both, binding of the polyanion and close approximation of two PF4 molecules, hereby combining two of the currently discussed models.
- Characterisation of the antigenic epitope as a composite epitope of the β -strands of one PF4-monomer and the α -helix of the adjacent monomer. This is the explanation for the long known empirical observation that only PF4 tetramers are able to expose the HIT antigen.
- The described method of CD spectroscopy can be used by all manufacturers of HIT antibody assays as an in-process quality control to identify optimal and/or false lots of PF4/heparin complexes.
- Polyphosphates interact strongly with PF4 and induce a conformational change in PF4.

and show very strong platelet activation in the functional assays. A similar mechanism is observed in post transfusion purpura, in which boosting of an immune response to the human platelet antigen (HPA)-1a results in formation of antibodies, which also bind to the HPA-1a negative autologous platelets of the patient (i.e. they behave like autoantibodies), causing severe thrombocytopenia. Also these sera react very strongly against the platelet glycoprotein IIb/IIIa in EIAs. Whether this is the well-known phenomenon of epitope spreading during the acute phase of B-cell stimulation or whether there is another underlying cause is currently unresolved.

Model of PF4 structural changes based on the CD spectroscopic data

X-ray diffraction studies performed on bovine and human PF4 showed that the PF4 monomer consists of a single α -helix (located at the C-terminus; amino acids (AA) 60–70), which is followed by three antiparallel β -sheet strands (AA 24–31, 39–44 and 49–53) (35, 46). Four β -turn structures connect the three β -sheet strands and the α -helix (►Figure 7A). The remaining part of PF4 (AA 1–19) adopts an unordered conformation.

As the axes of the α -helix and the β -sheet strands enclose an angle of approximately 45°, this configuration belongs to *class 2* in the nomenclature of Chou et al. (35, 47). The α -helix contains a cluster of four lysines, which are known to be a prerequisite for PF4 binding to heparin or other PAs. In its tetrameric form, the four α -helices and most of the positively charged AAs form a positively charged “ring” around the PF4 tetramer, which is expected to be the actual heparin binding site (46).

By analysing the binding capacity of anti-PF4/UFH antibodies to complexes made of UFH and mutations of PF4, the group of Dr. Poncz in Philadelphia located two different HIT-related epitopes (48, 49). Site-1 is located between the PF4 AAs 37–41, which are part of a β -turn hairpin structure connecting β -sheet strand 1 and 2 (green structures in ►Figure 7). This site is recognised by sera of approximately one third of PF4/PA antibodies (48). Site-2 involves the N-terminus (white arrow in ►Figure 7A) and at least AA 34 (blue structures in ►Figure 7) and is recognised by KKO, a HIT-like monoclonal antibody (50). Recently, it was shown that only those anti-PF4/UFH antibodies activate platelets which compete with KKO (51). This shows that site-2 constitutes or at least overlaps with an area that is recognised by a large fraction of anti-PF4/UFH antibodies and has therefore high clinical relevance (49). Interestingly, it seems that the C-terminal part of PF4 (AA 44–70) is not related to any epitope, as they are not recognised by anti-PF4/UFH antibodies (52) and as antibodies specific to these AAs do not compete with binding of anti-PF4/UFH antibodies to the PF4/UFH complex (48).

CD spectroscopy suggests that AAs adopting a β -turn or a α -helical secondary structure are transformed into an antiparallel β -sheet. As the anti-PF4/heparin antibody binding site-1 (AA 37–41) and parts of site-2 (AA 34) are directly located at the β -turn hairpin (AA 32–38), it is very likely that the structural changes occur in the vicinity of these sites. This is further supported by the length of the β -turns: Only the β -turn hairpin (AA 32–38) is long enough to allow a (partly) transition to antiparallel β -sheets, while the other β -turns are much shorter (making this transition rather unlikely).

The observation that epitope formation is accompanied by a structural change of the α -helix was unexpected as (i) it is currently believed that the C-terminal amino acids are not involved in HIT-related epitope formation (48, 52), and (ii) as the α -helix is located oppositely to the yet known epitopes in the PF4 monomer. However, modelling the PF4 dimer (as done by Zhang et al. [46]) indicates that the C-terminal AAs of the α -helix of one PF4 monomer (red arrow and red structures in ►Figure 7) are close to

site-1 and -2 of the adjacent PF4 monomer (green and blue structures in ►Figure 7). Hence, although there is a large distance between the α -helix and the known epitopes within a single PF4 monomer, these structures become closely placed in the PF4 dimer and tetramer.

This suggests that structural changes of the α -helix create (a) new epitope(s) which are directly neighboured to the known epitope(s) site-1 and -2, forming a large antigenic patch at the surface of PF4 (►Figure 7B). AAs 66–70 are involved in the expression of the epitope. These AAs are part of the α -helix of the native PF4, and neighbour the known epitopes on the PF4 surface. Therefore it is likely that they are part of the epitope. This interplay between antigenic structures of neighboured PF4 monomers explains the observation that the ability to form antigenic PF4/UHF complexes depends strongly on the ability of PF4 to form tetramers: complexes made of UHF and non-tetrameric PF4 (i.e. PF4 that is unable to form tetramers) showed a much lower antigenicity with respect to tetrameric PF4 (43). Hence, in its tetrameric form PF4 exposes four antigenic patches (two on each side of the plane defined by the heparin binding site), making these patches highly available for antibody binding regardless of the actual PF4 orientation within the PF4/PA complex.

Study limitations

Although the correlation between EIA and CD spectroscopy looks very promising, there are some limitations resulting from approximations done in this study. First of all, to measure antigenicity we used sera from three different patients only, which probably do not represent the full reactivity pattern of all anti-PF4/heparin antibodies. Moreover, we are aware that EIA typically does not exhibit a linear dependence from the amount of bound antibodies and that we cannot assume steady state binding of clinically-relevant anti-PF4/heparin antibodies from patient sera to PF4/PA-complexes, making a quantitative interpretation of the OD in terms of antigenicity challenging.

However, even using this relatively easy to apply “crude” approach, we get very reproducible results with various PAs. This strongly indicates that the system is stable and allows a robust assessment. Otherwise one would expect variable results, a wide range of reactivities and no clear correlation between the peak signals in the EIA and the CD spectroscopy at the same PA concentrations. Increasing the numbers of sera (for future experiments) and resolving the functional dependence between antibody binding capacity and OD in EIA might enhance the accuracy of the correlation and allow for even more precise *in vitro* assessment of PA antigenicity.

Conclusion

CD spectroscopy is found to be a powerful technique to monitor structural changes of PF4 caused by binding to various polyanions (PA). In all cases, exposure of HIT-relevant epitope(s) is only observed for PAs that also induce changes in PF4 secondary structure. A comparison of results of an immunoassay with CD spec-

Supplementary Material

In the Supplementary Material, which is available online at www.thrombosis-online.com, results of CD spectroscopic measurements on PF4/dextran and PF4/hyaluronic acid complexes are given. Moreover, versions of Figures 3 and 4B are supplied, which use no correction factor for the UHF data.

troscopic data showed that the extent of complex antigenicity correlates well with the magnitude of changes in PF4 secondary structure, and that a minimum structural change of PF4 is necessary to achieve PF4/PA complex antigenicity. These findings allowed us to calculate expectation intervals for complex antigenicity solely using CD spectroscopic data. To our knowledge, this is the first demonstration that the capability of drugs to induce antigenicity of PF4 can be assessed without the necessity of *in vivo* studies or the use of antibodies obtained from immunised patients specific for the antigens. Although shown only for PF4, our finding might be applicable to other proteins that also express epitopes upon changes in their secondary structure. This will be addressed in future studies.

Acknowledgement

S. Brandt, K. Krauel and S. Block were supported by the “Zentrum für Innovationskompetenz Humorale Immunreaktionen bei Kardiovaskulären Erkrankungen” (ZIK HIKE, Federal Ministry of Education and Research-BMBF FKZ 03Z2CN11 and FKZ 03Z2CN12). S. Block also acknowledges support by the European Social Fund (grant number UG 10 022). T. Renné acknowledges funding by Vetenskapsrådet (K2013–65X-21462–04–5), and the ERC StG-2012–311575.

Conflicts of interest

None declared.

References

1. Schellekens H. The immunogenicity of therapeutic proteins. *Discov Med* 2010; 49: 560–564.
2. Schellekens H. Bioequivalence and the immunogenicity of biopharmaceuticals. *Nat Rev Drug Discov* 2002; 1: 457–462.
3. Moreland LW, McCabe DP, Caldwell JR, et al. 3rd. Phase I/II trial of recombinant methionyl human tumor necrosis factor binding protein PEGylated dimer in patients with active refractory rheumatoid arthritis. *J Rheumatol* 2000; 27: 601–609.
4. Rau R, Sander O, van Riel P, et al. Intravenous human recombinant tumor necrosis factor receptor p55-Fc IgG1 fusion protein Ro 45–2081 (lenercapt): a double blind, placebo controlled dose-finding study in rheumatoid arthritis. *J Rheumatol* 2003; 30: 680–690.
5. Eichler P, Lubenow N, Strobel U, et al. Antibodies against lepirudin are polyspecific and recognize epitopes on bivalirudin. *Blood* 2004; 103: 613–616.
6. Greinacher A, Lubenow N, Eichler P. Anaphylactic and anaphylactoid reactions associated with lepirudin in patients with heparin-induced thrombocytopenia. *Circulation* 2003; 108: 2062–2065.

6. Appended papers

6.2 Paper II: PF4/PA

64 Brandt et al. Conformational changes in PF4 predict immunogenicity

7. Casadevall N, Nataf J, Viron B, et al. Pure red-cell aplasia and antierythropoietin antibodies in patients treated with recombinant erythropoietin. *N Engl J Med* 2002; 346: 469–475.
8. van Beers MMC, Sauerborn M, Gilli F, et al. Aggregated recombinant human interferon beta induces antibodies but no memory in immune tolerant transgenic mice. *Pharm Res* 2010; 27: 1812–1824.
9. Hemmer B, Stüve O, Kieser B, et al. Immune response to immunotherapy: the role of neutralising antibodies to interferon beta in the treatment of multiple sclerosis. *Lancet Neurol* 2005; 4: 403–412.
10. Arepally GM, Ortel TL. Clinical practice. Heparin-induced thrombocytopenia. *N Engl J Med* 2006; 355: 809–817.
11. Wolpe SD, Cerami A. Macrophage inflammatory protein-1 and protein-2 – members of a novel superfamily of cytokines. *Faseb J* 1989; 3: 2565–2573.
12. Huang SS, Huang JS, Deuel TF. Proteoglycan carrier of human-platelet factor-4 – isolation and characterisation. *J Biol Chem* 1982; 257: 1546–1550.
13. Kaplan KL, Broekman MJ, Chernoff A, et al. Platelet alpha-granule proteins: studies on release and subcellular localisation. *Blood* 1979; 53: 604–618.
14. Rucinski B, Niewiarowski S, James P, et al. Antiheparin proteins secreted by human platelets. purification, characterisation, and radioimmunoassay. *Blood* 1979; 53: 47–62.
15. Deuel TF, Keim PS, Farmer M, et al. Amino-acid sequence of human platelet factor 4. *PNAS* 1977; 74: 2256–2258.
16. Greinacher A, Gopinadhan M, Günther J-U, et al. Close approximation of two platelet factor 4 tetramers by charge neutralisation forms the antigens recognized by HIT antibodies. *Arterioscl Thromb Vasc Biol* 2006; 26: 2386–2393.
17. Rauova L, Poncz M, McKenzie SE, et al. Ultralarge complexes of PF4 and heparin are central to the pathogenesis of heparin-induced thrombocytopenia. *Blood* 2005; 105: 131–138.
18. Chong BH, Pitney WR, Castaldi PA. Heparin-induced thrombocytopenia – association of thrombotic complications with heparin-dependent IgG antibody that induces thromboxane synthesis and platelet-aggregation. *Lancet* 1982; 2: 1246–1249.
19. Amiral J, Bridey F, Dreyfus M, et al. Platelet factor-iv complexed to heparin is the target for antibodies generated in heparin-induced thrombocytopenia. *Thromb Haemost* 1992; 68: 95–96.
20. Warkentin TE, Greinacher A. Heparin-induced thrombocytopenia: recognition, treatment, and prevention. *Chest* 2004; 126: 311s–337s.
21. Cines D, Kaywin P, Bina M, et al. Heparin associated thrombocytopenia. *N Engl J Med* 1980; 303: 788–795.
22. Chong BH, Fawaz I, Chesterman CN, et al. Heparin induced thrombocytopenia: mechanism of interaction of the heparin dependent antibody with platelets. *Br J Haematol* 1989; 73: 235–240.
23. Alban S, Krauel K, Greinacher A. Role of Sulfated Polysaccharides in the Pathogenesis of Heparin-Induced Thrombocytopenia. In: *Heparin-Induced-Thrombocytopenia (Fundamental and Clinical Cardiology)*, 5th edition. LLC: Boca Raton, USA: Taylor and Francis Group; 2013: pp. 181–208.
24. Kelton JG, Smith JW, Warkentin TE, et al. Immunoglobulin-G from Patients with Heparin-Induced Thrombocytopenia Binds to a Complex of Heparin and Platelet Factor-4. *Blood* 1994; 83: 3232–3239.
25. Greinacher A, Alban S, Dummel V, et al. Characterisation of the structural requirements for a carbohydrate based anticoagulant with reduced risk of inducing the immunological type of heparin-associated thrombocytopenia. *Thromb Haemost* 1995; 74: 886–892.
26. Jaax ME, Krauel K, Marschall T, et al. Complex formation with nucleic acids and aptamers alters antigenic properties of platelet factor 4. *Blood* 2013; 122: 272–281.
27. Mikhailov D, Young HC, Linhardt RJ, et al. Heparin dodecasaccharide binding to platelet factor-4 and growth-related protein-alpha. *J Biol Chem* 1999; 274: 25317–25329.
28. Bohm G, Muhr R, Jaenicke R. Quantitative-analysis of protein far UV circular-dichroism spectra by neural networks. *Protein Engin* 1992; 5: 191–195.
29. Juhl D, Eichler P, Lubenow N, et al. Incidence and clinical significance of anti-PF4/heparin antibodies of the IgG, IgM, and IgA class in 755 consecutive patient samples referred for diagnostic testing for heparin-induced thrombocytopenia. *Eur J Haematol* 2006; 76: 420–426.
30. Sreerama N, Woody RW. Computation and Analysis of Protein Circular Dichroism Spectra. In: *Methods in Enzymology* 383. San Diego, CA: Elsevier Academic Press; 2004: pp. 318–351.
31. Krauel K, Pötschke C, Weber C, et al. Platelet factor 4 binds to bacteria-inducing antibodies cross-reacting with the major antigen in heparin-induced thrombocytopenia. *Blood* 2011; 117: 1370–1378.
32. Rosenthal MA, Rischin D, McArthur G, et al. Treatment with the novel anti-angiogenic agent PI-88 is associated with immune-mediated thrombocytopenia. *Ann Oncol* 2002; 13: 770–776.
33. Mayo KH, Barker S, Kuranda MJ, et al. Molten globule monomer to condensed dimer – role of disulfide bonds in platelet factor-iv folding and subunit association. *Biochemistry* 1992; 31: 12255–12265.
34. Villanueva GB, Allen N, Walz D. Circular-dichroism of platelet factor-4. *Arch Biochem Biophys* 1988; 261: 170–174.
35. Charles RS, Walz DA, Edwards BFP. The 3-dimensional structure of bovine platelet factor-4 at 3.0-Å resolution. *J Biol Chem* 1989; 264: 2092–2099.
36. Gans PJ, Lyu PC, Manning MC, et al. The helix-coil transition in heterogeneous peptides with specific side-chain interactions: theory and comparison with CD spectral data. *Biopolymers* 1991; 31: 1605–1614.
37. Chin D-H, Woody RW, Rohl CA, et al. Circular dichroism spectra of short, fixed-nucleus alanine helices. *PNAS* 2002; 99: 15416–15421.
38. Leroux D, Canépa S, Viskov C, et al. Binding of heparin-dependent antibodies to PF4 modified by enoxaparin oligosaccharides: evaluation by surface plasmon resonance and serotonin release assay. *J Thromb Haemost* 2012; 10: 430–436.
39. Petitou M, Hérault JP, Bernat A, et al. Synthesis of thrombin-inhibiting heparin mimetics without side effects. *Nature* 1999; 398: 417–422.
40. Joglekar MV, Quintana Diez PM, Marcus S, et al. Disruption of PF4/H multi-molecular complex formation with a minimally anticoagulant heparin (ODSH). *Thromb Haemost* 2012; 107: 717–725.
41. Warkentin TE, Cook RJ, Marder VJ, et al. Anti-platelet factor 4/heparin antibodies in orthopedic surgery patients receiving antithrombotic prophylaxis with fondaparinux or enoxaparin. *Blood* 2005; 106: 3791–3796.
42. Warkentin TE, Pai M, Sheppard JI, et al. Fondaparinux treatment of acute heparin-induced thrombocytopenia confirmed by the serotonin-release assay: a 30-month, 16-patient case series. *J Thromb Haemost* 2011; 9: 2389–2396.
43. Sachais BS, Litvinov RI, Yarovoi SV, et al. Dynamic antibody-binding properties in the pathogenesis of HIT. *Blood* 2012; 120: 1137–1142.
44. Greinacher A, Michels I, Mueller-Eckhardt C. Heparin-associated thrombocytopenia: the antibody is not heparin specific. *Thromb Haemost* 1992; 67: 545–549.
45. Krauel K, Füll B, Warkentin TE, et al. Heparin-induced thrombocytopenia – therapeutic concentrations of danaparoid, unlike fondaparinux and direct thrombin inhibitors, inhibit formation of platelet factor 4–heparin complexes. *J Thromb Haemost* 2008; 6: 2160–2167.
46. Zhang X, Chen L, Bancroft DP. Crystal-structure of recombinant human platelet factor-4. *Biochemistry* 1994; 33: 8361–8366.
47. Chou K-C, Nemethy G, Rumsey S, et al. Interactions between an alpha-helix and a beta-sheet energetics of alpha-beta-packing in proteins. *J Mol Bio* 1985; 186: 591–609.
48. Ziporen L, Li ZQ, Park KS, et al. Defining an antigenic epitope on platelet factor 4 associated with heparin-induced thrombocytopenia. *Blood* 1998; 92: 3250–3259.
49. Li ZQ, Liu W, Park KS, et al. Defining a second epitope for heparin-induced thrombocytopenia/thrombosis antibodies using KKO, a murine HIT-like monoclonal antibody. *Blood* 2002; 99: 1230–1236.
50. Arepally GM, Park KS, Kamei S, et al. Characterisation of a murine monoclonal antibody that mimics heparin-induced thrombocytopenia antibodies. *Blood* 2000; 95: 1533–1540.
51. Cuker A, Rux AH, Hinds JL, et al. Novel diagnostic assays for heparin-induced thrombocytopenia. *Blood* 2012; 120: 267.
52. Suh JS, Aster RH, Visentin GP. Antibodies from patients with heparin-induced thrombocytopenia/thrombosis recognize different epitopes on heparin: platelet factor 4. *Blood* 1998; 91: 916–922.

6.3 Paper III: Binding of anti-Platelet Factor 4/Heparin Antibodies depends on the
Thermodynamics of conformational Changes in Platelet Factor 4

Regular Article

THROMBOSIS AND HEMOSTASIS

Binding of antiplatelet factor 4/heparin antibodies depends on the thermodynamics of conformational changes in platelet factor 4

Martin Kreimann,¹ Sven Brandt,¹ Krystin Krauel,² Stephan Block,¹ Christiane A. Helm,³ Werner Weitschies,⁴ Andreas Greinacher,² and Mihaela Delcea¹

¹ZIK HIKE—Zentrum für Innovationskompetenz, Humorale Immunreaktionen bei Kardiovaskulären Erkrankungen, Greifswald, Germany; ²Institut für Immunologie und Transfusionsmedizin, Greifswald, Germany; ³Institut für Physik, Greifswald, Germany; and ⁴Institut für Pharmazie, Greifswald, Germany

Key Points

- Besides clustering, platelet factor 4/polyanion complexes require input of energy to become immunogenic.
- Minute differences in chain length determine the induction of antigenicity of PF4.

The chemokine platelet factor 4 (PF4) undergoes conformational changes when complexing with polyanions. This can induce the antibody-mediated adverse drug effect of heparin-induced thrombocytopenia (HIT). Understanding why the endogenous protein PF4 becomes immunogenic when complexing with heparin is important for the development of other negatively charged drugs and may also hint toward more general mechanisms underlying the induction of autoantibodies to other proteins. By circular dichroism spectroscopy, atomic force microscopy, and isothermal titration calorimetry we characterized the interaction of PF4 with unfractionated heparin (UFH), its 16-, 8-, and 6-mer subfractions, low-molecular-weight heparin (LMWH), and the pentasaccharide fondaparinux. To bind anti-PF4/heparin antibodies, PF4/heparin complexes require (1) an increase in PF4 anti-

parallel β -sheets exceeding $\sim 30\%$ (achieved by UFH, LMWH, 16-, 8-, 6-mer), (2) formation of multimolecular complexes (UFH, 16-, 8-mer), and (3) energy (needed for a conformational change), which is released by binding of ≥ 11 -mer heparins to PF4, but not by smaller heparins. These findings may help to synthesize safer heparins. Beyond PF4 and HIT, the methods applied in the current study may be relevant to unravel mechanisms making other endogenous proteins more vulnerable to undergo conformational changes with little energy requirement (eg, point mutations and post-translational modifications) and thereby them to become immunogenic. (*Blood*. 2014;00(00):1-8)

Introduction

Heparin, widely used clinically as a parenteral anticoagulant,¹⁻³ is a polyanion consisting of iduronic acid, glucuronic acid, and glucosamine residues carrying sulfate groups. Pharmaceutical heparin is obtained from porcine gut mucosa and, as biological material, is composed of polysaccharide chains with variable length. Degradation of unfractionated heparin (UFH) results in less polydisperse and smaller low-molecular-weight heparins (LMWHs). The pentasaccharide fondaparinux consists of the shortest sequence able to catalyze the activity of antithrombin. It was the first synthesized heparin approved for clinical use.⁴ Currently, several other heparin-based, synthesized polysaccharides are in preclinical development.^{5,6} Beside their anticoagulant activity, heparins have other biological effects including potential antitumor activity,⁷ which, however, differs depending on the chain length.⁷

Clinically, beside bleeding, heparin-induced thrombocytopenia (HIT) is the most important adverse effect of heparin.⁸ HIT is a life-threatening immune-driven adverse effect, which occurs in up to 3% of patients receiving UFH after major surgery.⁹ HIT is caused by antibodies that recognize platelet factor 4 (PF4), a CXC chemokine family protein, in ultralarge multimolecular complexes with heparin.¹⁰

Several of these pathogenic antibodies can bind to the multimolecular complexes of PF4 and heparin, forming immunocomplexes. When these PF4/heparin-immunoglobulin (Ig)G immunocomplexes bind to platelets, the Fc parts of the antibodies cross-link Fc γ IIa receptors on platelets, which induces platelet activation and aggregation.¹¹ This results in a prothrombotic state and an increased risk for new thrombosis.¹² Heparin-induced antibodies recognize an antigen exposed on PF4 at a certain PF4/heparin ratio,¹⁰ at which PF4 tetramers¹³ are forced into close approximation,¹⁴ accompanied by charge neutralization.¹⁴⁻¹⁶

Previously, we have shown, using circular dichroism (CD) spectroscopy in combination with an enzyme-linked immunosorbent assay (ELISA), that the antigenic site is a composite surface formed by ≥ 2 (or 3) PF4 monomers in a PF4 tetramer. Exposure of this antigenic site occurs when polyanions induce changes in the structure of PF4, resulting in an increase of the antiparallel β -sheet content in the PF4 secondary structure to more than $\sim 30\%$.¹⁷

Here we report the physicochemical characterization of complexes formed between PF4 and UFH, LMWH, or subfractions produced from unfractionated heparin with defined chain lengths (16- [HO16],

Submitted March 3, 2014; accepted August 12, 2014. Prepublished online as *Blood* First Edition paper, August 22, 2014; DOI 10.1182/blood-2014-03-559518.

The publication costs of this article were defrayed in part by page charge payment. Therefore, and solely to indicate this fact, this article is hereby marked "advertisement" in accordance with 18 USC section 1734.

The online version of this article contains a data supplement.

© 2014 by The American Society of Hematology

8- [HO08], and 6- [HO06] mer), as well as with synthetic fondaparinux (5-mer).⁴ We found that beside the conformational change of PF4 exposing >30% antiparallel β -sheets and formation of large PF4/heparin complexes, the enthalpy of binding (released heat) has to exceed a threshold value to provide the energy for the conformational change of PF4 required to expose the antigenic epitope. These findings may provide relevant aspects to understand the structure-function relationship for other biological functions of heparins derived drugs¹⁸ and may also underlie mechanisms making other endogenous proteins immunogenic.

Methods

Ethics

The use of human sera containing anti-PF4/heparin antibodies and human platelets and obtaining whole blood from healthy volunteers was approved by the Greifswald Ethics Board.

Reagents

Lyophilized human PF4 isolated from platelets: Chromatec (Greifswald, Germany); UFH Heparin-Natrium-25000 (Ratiopharm, Ulm, Germany); fondaparinux (Arixtra; GlaxoSmithKline, London, UK); LMWH reviparin (Clivarin 1750; Abbott GmbH, Wiesbaden, Germany); hospital pharmacy; heparin oligosaccharides 6-mer (HO06), 8-mer (HO08) and 16-mer (HO16); Iduron Ltd. (Manchester, UK). These heparin fractions are obtained by partial heparin lyase digestion followed by high-resolution gel filtration and show a defined length as determined by the manufacturer. However, their interaction with antithrombin (ie, their anticoagulant capacity) is not defined. The smaller the oligosaccharides become, the more disruption on the pentasaccharide structure that is required for antithrombin binding occur.

ELISA

PF4/heparin ELISA was performed as described¹⁹ with 3 samples of human sera of patients known to contain anti-PF4/heparin IgG antibodies verified by PF4/heparin ELISA and the heparin-induced platelet activation test.¹⁹ UFH, LMWH, and the defined length heparins were added in rising concentrations to PF4 to form the complexes before they were coated on a microtiter plate (as indicated in the figures; UFH: 0-14 $\mu\text{g/mL}$, HO16 and HO08: 0-11.7 $\mu\text{g/mL}$, HO06: 0-15 $\mu\text{g/mL}$, fondaparinux: 0-30 $\mu\text{g/mL}$). To verify the reactivity pattern, we then coated the PF4/defined length heparin complexes at the optimal concentration determined by the titration experiment and tested them with an additional panel of 14 samples of characterized sera from patients with serologically confirmed HIT. LMWH was assessed by the same method.¹⁷

CD spectroscopy

Changes in the secondary structure of PF4 on interaction with heparins were studied by recording far-UV CD spectra (200-260 nm) using a Chirascan CD spectrometer (Applied Photophysics, Leatherhead, UK) as previously described.¹⁷ PF4 was dissolved in phosphate-buffered saline (PBS; 155 mM NaCl, 1.54 mM KH_2PO_4 , 2.71 mM $\text{Na}_2\text{HPO}_4 \cdot 7 \text{H}_2\text{O}$, pH 7.2) to a final concentration of 80 $\mu\text{g/mL}$ (2.5 μM). Complex formation was carried out at 20°C directly in the CD cuvette (Hellma, Müllheim, Germany) with a 5-mm path length. Each measurement started with a pure PF4 solution. Subsequently, increasing amounts of the heparins (UFH, HO16, HO08, HO06, and fondaparinux) were added to the cuvette, and CD spectra were recorded for each PF4/heparin ratio. Buffer baselines and baselines of each heparin concentration step (ie, without PF4 in the solution) were recorded. In the data analysis, the spectra of PF4 alone and of PF4/heparin complexes were corrected for the baselines, path length, number of amino acids, and concentration to obtain the wavelength-dependent mean residue $\delta \epsilon$ values of the PF4/heparin complex. To estimate the secondary structure content of PF4, deconvolution of CD spectra was carried out with CDNN software using a database of 33 reference proteins.²⁰ LMWH was assessed by the same method.¹⁷

Atomic force microscopy

To characterize the structural features of the PF4/heparin complexes, atomic force microscopy (AFM) imaging in liquid was carried out using a BioScope II scanning probe microscope from Digital Instruments (Santa Barbara, CA). NanoScope 7.3 software was used to control the AFM, to set the imaging parameters, and for flattening of the images. Preformed PF4/heparin complexes (at the optimal ratios found by isothermal titration calorimetry [ITC]) were incubated on freshly cleaved mica for 10 seconds, followed by washing the mica surface with ultrapure water. For imaging, a few drops of ultrapure water were added on the mica with adsorbed samples. All samples were imaged in tapping mode at room temperature using silicon nitride cantilevers DNP-S (Veeco, Camarillo, CA) with a drive frequency of 8 to 14 kHz in water and a nominal curvature radius of 10 nm. AFM images of the PF4/heparin complexes and of their constituents were recorded. All experiments were repeated ≥ 3 times.

The height distribution of the AFM-imaged features was analyzed using a MatLab script (MathWorks, Natick, MA).^{21,22} Briefly, the script scans over the images identifying the highest points within a moving 17×17 rectangle (supplemental Figure 1), giving the position and maximum height of the samples adsorbed to mica. To avoid cross-talk with measurement noise, a 0.9-nm threshold (the standard deviation of the background noise in the AFM images) was used in this study. Height values were then merged and plotted into a semilogarithmic point histogram. As the typically observed height values were on the order of the tip curvature radius, tip convolution led to a strong lateral broadening of the observed structures. We therefore did not further analyze the lateral dimensions of the detected structures.

ITC

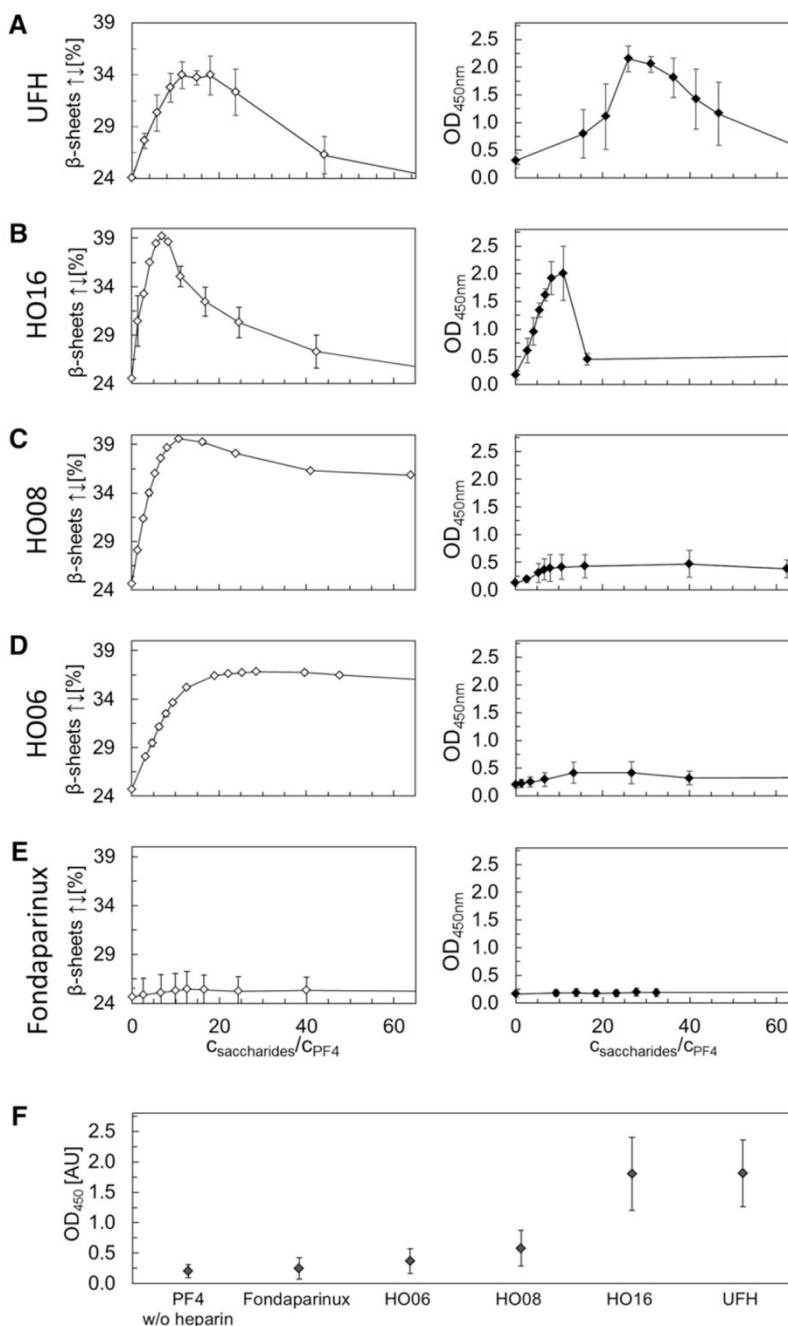
The different heparins and PF4 were separately dialyzed against PBS buffer at pH 7.4. ITC measurements were carried out using an iTC200 calorimeter (GE Healthcare Life Sciences). A PF4 solution (500-2470 $\mu\text{g/mL}$ [15.6-70 μM] in PBS) was added to the sample cell, and a solution of heparin (450-900 $\mu\text{g/mL}$ [37-500 μM]) was loaded into the injection syringe. For each experiment, a 60-second delay was followed by 19 injections of 1 μL of the titrant solution, spaced 240 seconds apart. The sample cell was stirred at 1000 rpm throughout and maintained at 25°C. Control titration was performed by injecting heparin into PBS buffer and subtracted prior to data analysis. The area under each peak of the resulting heat profile was integrated, normalized by the concentrations, and plotted against the molar ratio of heparin to PF4 using an Origin script supplied with the instrument (Origin 7; OriginLab Corporation). The resulting binding isotherms were fitted by nonlinear regression using the single-site model. The stoichiometry of the interaction ($n = c_{\text{Heparin}}/c_{\text{PF4}}$, where c is the concentration in moles per liter), the equilibrium constant (K_A), and the change in enthalpy (ΔH) were obtained during the fitting of all titration data. Equilibrium dissociation constants (K_D) were calculated as the reciprocal of K_A . The Gibbs free energy change (ΔG) was calculated with the equation $\Delta G = -RT \ln K_A$. All titrations were replicated to determine the experimental standard deviation for each parameter.

Results

Changes in the PF4 secondary structure by UFH, LMWH, and defined length heparins and binding of anti-PF4/heparin antibodies

We compared the structural changes of PF4 (quantified by CD spectroscopy) with anti-PF4/heparin antibody binding to PF4 (quantified by optical density [OD] changes in an ELISA at the wavelength 450 nm), when PF4 was incubated with increasing concentrations of UFH, 16-, 8-, 6-mer heparins, and fondaparinux. The CD data are given in the left panels and the corresponding ELISA results in the right panels of Figure 1; data obtained with LMWH are given in supplemental Figure 2. We always normalized the heparin concentration

Figure 1. Comparison of PF4 structural changes (antiparallel β -sheet content, determined by CD spectroscopy) and PF4/heparins antigenicity (OD obtained from EIA measurements) for (A) UFH, (B) HO16, (C) HO08, (D) HO06, and (E) fondaparinux as a function of molar ratio monosaccharides/PF4. The open and filled squares represent average values of antiparallel β -sheet content and OD values, respectively. Error bars correspond to the standard deviation (calculated from the results of $n = 3$ experiments). (F) EIA measurements for PF4 alone or in complex with fondaparinux, HO06, HO08, HO16, and UFH using a panel of 14 well-characterized sera containing anti-PF4/heparin antibodies. The filled squares represent average values of the maxima of the OD values. Error bars correspond to the standard deviation. Data for LMWH are given in supplemental Figure 2.



by the PF4 tetramer concentration (number of heparin monomers per PF4 tetramer), taking into account that the PF4 concentration slightly changed by adding heparin in the titrating experiments. Moreover, we plotted in Figure 1 only the antiparallel β -sheet content of PF4, which is indicative for the overall changes of the PF4 structure¹⁷ (supplemental Figure 3).

Figure 1 shows 3 different patterns of the PF4/polyanion complexes: (1) reversible increase in antiparallel β -sheets of PF4, paralleled by a reversible increase in anti-PF4/heparin antibody binding (complexes with UFH and HO16, Figure 1A-B; LMWH, supplemental Figure 2); (2) nonreversible increase in antiparallel β -sheets of PF4

and minimal binding of anti-PF4/heparin antibodies (complexes with HO08 and HO06; Figure 1C-D); and (3) no increase in antiparallel β -sheets and no anti-PF4/heparin antibody binding (complexes with pentasaccharide fondaparinux; Figure 1E). We then tested a panel of 14 well-defined sera containing anti-PF4/heparin antibodies, with the PF4/defined length heparin complexes at the optimal concentrations determined by titration, which gave the same results (Figure 1F).

The maximum increase in antiparallel β -sheets (34% for UFH; 34% for LMWH; 39% HO16; 40% for HO08; and 36% for HO06) was observed at distinct concentrations of each heparin preparation.

Due to the polydisperse (ie, variably sized) nature of UFH, it is impossible to define this on a molar basis. We therefore used an approach to take the mean MW of UFH 12 kDa, which corresponds to 39 monomers (saccharide monomers) per molecule. For consistency, the same approach was used for the heparin fragments.

In sharp contrast to all other heparins, no structural changes of PF4 and no anti-PF4/heparin antibody binding were observed for fondaparinux (Figure 1E), which is consistent with previous data.²³⁻²⁵

AFM morphological characterization of the complexes formed by PF4 with heparins of different chain length

The differences in anti-PF4/heparin antibody binding raised the question of whether the smaller heparins, albeit causing an increase in antiparallel β -sheets, form large complexes with PF4. We used tapping mode liquid AFM imaging to characterize the dependency between length of heparin and the size of the complexes formed with PF4.

We show the complexes that PF4 forms with 16, 8, 6-mer heparins and fondaparinux in Figure 2. PF4 forms ultralarge complexes (>20 nm) with the 16-mer (HO16) and the 8-mer (HO08) heparins (Figure 2C-D). The complexes formed by PF4 with HO16 and HO08 have a broad height distribution reaching up to 35 and 25 nm, respectively (Figure 2G). The 6-mer (HO06) and the 5-mer (fondaparinux) heparins formed small, if any, complexes with PF4 with heights in the range of 1 to 5 nm (Figure 2E-G). The complexes were similar to PF4 alone, which formed structures with a large height distribution (from 1 to 7 nm; supplemental Figure 4A,G).

When we tried to measure PF4/UFH complexes, we could not stably immobilize them on the mica surface. Most likely they were so large that they detached when we rinsed the surface. Consistently, in additional experiments with 300-second incubation time and gentle dipping instead of washing we found several large PF4/UFH complexes (data not shown).

We show the control experiment with UFH, 16, 8, 6-mer heparins, and fondaparinux adsorbed on mica surface alone in supplemental Figure 4B-F, where we found grains with average height of 1 to 2 nm.

Binding interaction between PF4 and UFH, LMWH, and defined chain length heparins: ITC study

We assessed the energetic characteristics of the interaction of PF4 with UFH, LMWH, and defined chain length heparins by ITC, which directly measures changes in heat that occur during complex formation.^{26,27} The upper panels of Figure 3 show the sequence of the titration, with each peak corresponding to the injection of the solution in the syringe, whereas the lower panels show the integrated heat plot as a function of heparin/PF4 tetramer ratio. The thermodynamic parameters are given in Table 1.

For all investigated heparins, the reaction with PF4 was exothermic (heat release; Figure 3), but 2 distinct reaction patterns occurred: (1) reactions with large heat release (enthalpy change) and (2) reactions with little heat release. PF4/UFH, PF4/LMWH, and PF4/HO16 complexes showed the largest heat release (Table 1; Figure 3A-C), whereas PF4/HO08 (Table 1; Figure 3D), PF4/HO06 (Table 1; Figure 3E), and PF4/fondaparinux complexes showed $\sim 60\%$, 30% , and $<20\%$ of the heat release of PF4/UFH complexes, respectively (Table 1; Figure 3F, please note the different scales in Figure 3).

We calculated relatively low values of equilibrium dissociation constant K_D for the complexes formed by PF4 with HO16 heparin ($0.05 \mu\text{M}$), LMWH ($0.09 \mu\text{M}$), and UFH ($0.14 \mu\text{M}$), indicating strong binding compared with the K_D for the complexes formed

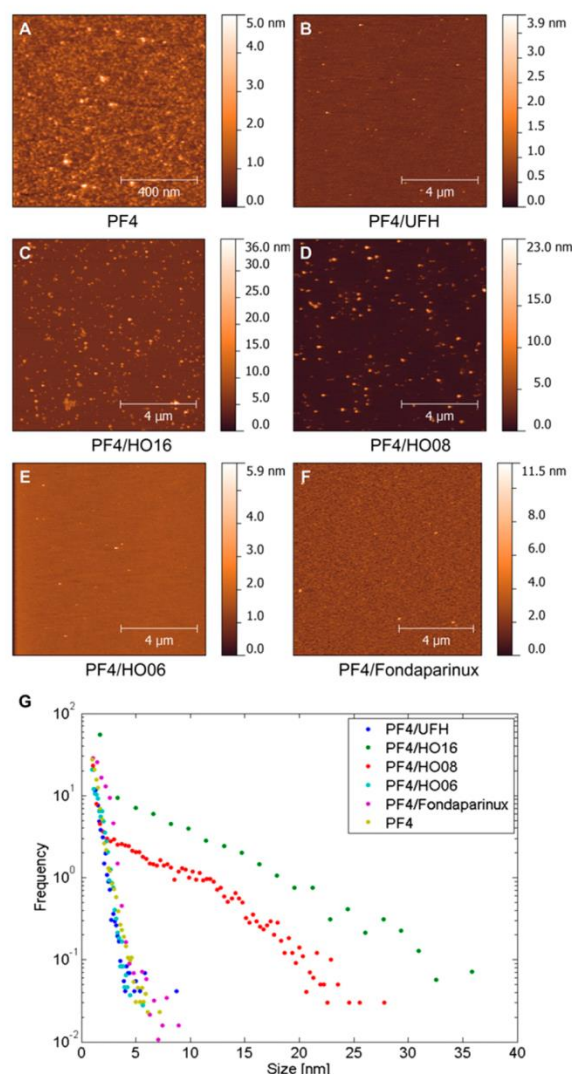


Figure 2. Representative liquid AFM tapping mode images of (A) PF4 alone and (B) PF4/UFH, (C) PF4/HO16, (D) PF4/HO08, (E) PF4/HO06, and (F) PF4/fondaparinux complexes on mica; the corresponding height histograms derived from all experiments are shown in G.

with short chain length heparins ($1.25 \mu\text{M}$ for PF4/fondaparinux complexes; $2.5 \mu\text{M}$ for PF4/HO06 complexes, and $0.2 \mu\text{M}$ for PF4/HO08 complexes).

The key finding of the thermodynamic studies is the change in randomness of the system (entropy, ΔS ; Table 1), which correlates very well with the binding capacity of the resulting PF4/heparin complexes for anti-PF4/heparin antibodies (as shown by ELISA). We give the enthalpy per PF4 molecule because this is the constant reaction partner in our experiments.

The calculated ΔS for the PF4/UFH complex and PF4/LMWH complex showed a negative value (-15.6 ± 4.1 and -11.5 ± 3.8 cal/mol/K, respectively, with respect to 1 PF4 molecule), ie, a considerable amount of energy released after PF4 binding was consumed by the conformational changes of the complexes (an alternative explanation is that hydrophobic functional groups move to the surface of PF4 coming into direct contact with water). A similar pattern (negative change in entropy, $\Delta S = -11.4 \pm 6.2$

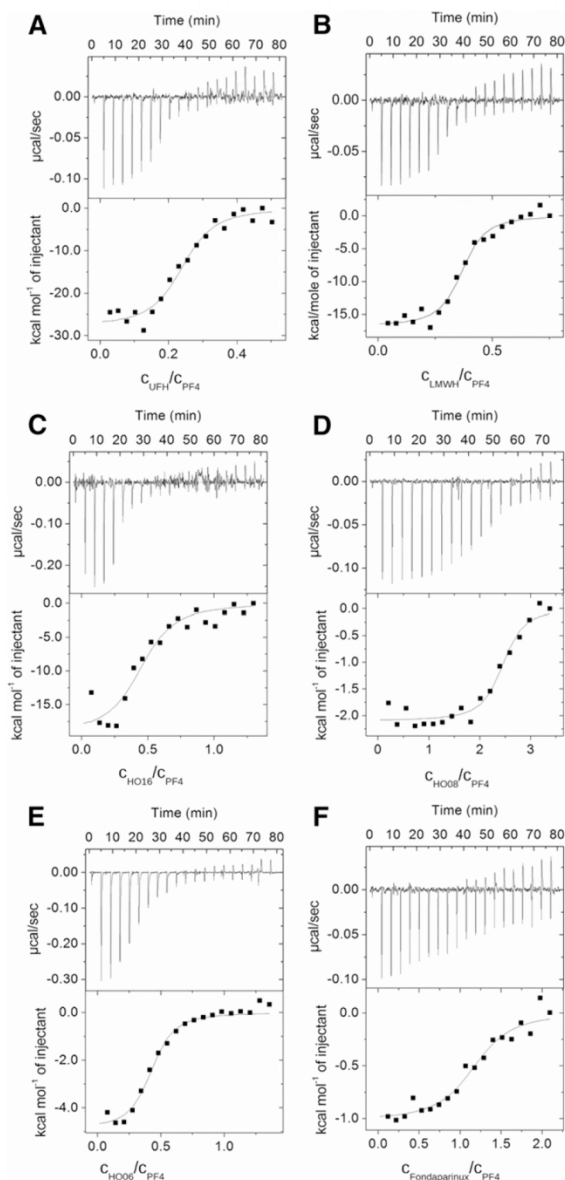


Figure 3. Representative binding isotherms for the titration of PF4 with defined chain length heparins. (Upper) Raw titration data and (lower) integrated heats as a function of the molar ratio of heparin/PF4 for (A) UFH, (B) LMWH, (C) HO16, (D) HO08, (E) HO06, and (F) fondaparinux.

cal/mol/K with respect to 1 mol PF4) was found for PF4/HO16 complexes. In contrast, complexes formed by PF4 with HO08, HO06, and fondaparinux showed a positive entropy change, ie,

binding of these heparins does not result in conformational changes of the PF4/heparin complexes that require additional energy.

Discussion

Our studies combining physicochemical characterization with assessment of anti-PF4/heparin antibody binding provide new insights into the interaction mechanism between PF4 and heparins. Using heparin fragments with defined length, we found that PF4/heparin complexes require the following characteristics to bind anti-PF4/heparin antibodies: induction of an increase in antiparallel β -sheets in PF4 exceeding $\sim 30\%$; formation of multimolecular complexes; and an amount of energy larger than -4000 cal/mol_{PF4}. This energy is required for the conformational changes in PF4 needed to expose the antigenic epitopes and is provided when heparins ≥ 11 -mers bind to PF4.

Although we confirm in this study that an increase in the antiparallel β -sheet content of PF4 $> 30\%$ is a requirement¹⁷ for binding of anti-PF4/heparin antibodies, it was a major surprise when we found that in complexes with HO08 and HO06, the antiparallel β -sheet content of PF4 increased clearly $> 34\%$ (ie, even more than in PF4/UFH complexes). It is well known that a critical heparin chain length of ~ 12 saccharide units is required to form PF4/polyanion complexes that express the antigen to which anti-PF4/heparin antibodies bind²⁸ and induce subsequent platelet activation.²⁴ 10-mer heparin fragments induce only weak recognition, and 8- and 6-mer heparin fragments are even less^{29,30} or nonreactive.²⁸ Consistent with these findings, anti-PF4/heparin antibodies did not (or only minimally) bind to PF4/HO08 and PF4/HO06 complexes in our study. Only fondaparinux neither increased the antiparallel β -sheet structures of PF4 nor facilitated binding of anti-PF4/heparin antibodies when complexed with PF4 (Figure 1). However, fondaparinux still binds to PF4 as shown by ITC, where interaction of PF4 with fondaparinux results in an exothermic reaction (ie, the enthalpy change is negative; Table 1; Figure 3E).

CD spectroscopy already gave a first hint that HO08 and HO06 form with PF4 different complexes than longer heparins. The typical reversible changes in the secondary structure of PF4 at high heparin concentrations were only seen for UFH, LMWH, and HO16, but not for HO08 and HO06. This feature, can, however, not be the only feature differentiating between PF4/polyanion complexes that bind anti-PF4/heparin antibodies and those that do not. Dextran sulfate also induces irreversible changes in the PF4 secondary structure but at the same time, anti-PF4/heparin antibodies bind strongly to PF4/dextran sulfate complexes.^{17,31}

We assumed that formation of multimolecular complexes is the requirement for anti-PF4/heparin antibody binding as already shown by us^{14,24,32} and others¹⁰ and that at minimum a 12-mer is required for formation of such large complexes.²⁸ Accordingly, we found by

Table 1. Thermodynamic parameters (calculated per mole PF4 tetramer) for the interaction of PF4 with UFH, HO16, LMWH, HO08, HO06, and fondaparinux at 25°C

Complexes	Enthalpy, ΔH (cal/mol)	Dissociation constant, K_D (μM)	Stoichiometry, n	Gibbs free energy, ΔG (cal/mol)	Entropy, ΔS (cal/mol/K)
PF4/UFH	-6682 ± 1150	0.14	0.24 ± 0.03	-2240 ± 80	-15.6 ± 4.1
PF4/HO16	-7260 ± 1365	0.05	0.42 ± 0.1	-3865 ± 489	-11.4 ± 6.2
PF4/LMWH	-6663 ± 906	0.09	0.36 ± 0.01	-3515 ± 136	-11.5 ± 3.8
PF4/HO08	-4240 ± 1467	0.20	1.93 ± 0.42	$-17\,148 \pm 635$	46.1 ± 23.3
PF4/HO06	-2071 ± 35	2.50	0.42 ± 0.04	-3190 ± 151	3.7 ± 0.5
PF4/fondaparinux	-1333 ± 57	1.25	1.30 ± 0.15	$-10\,415 \pm 404$	30.4 ± 1.4

The stoichiometry n is the molar ratio heparin molecule/PF4.

Table 2. Thermodynamic energies for the interaction of PF4 with UFH, LMWH, HO16, HO08, HO06, and fondaparinux at 25°C, calculated per mole of PF4 tetramers

Complexes	Enthalpy, ΔH (cal/mol)		Required enthalpy, ΔH_{req} (cal/mol)†
PF4/UFH	-6682 ± 1150	>*	-4673 ± 1238
PF4/HO16	-7260 ± 1365	>	-3415 ± 1865
PF4/LMWH	-6663 ± 906	>	-3450 ± 1140
PF4/HO08	-4240 ± 1467	\approx	$-3840 \pm 717\ddagger$
PF4/HO06	-2071 ± 35	<	$-3840 \pm 717\ddagger$
PF4/fondaparinux	-1333 ± 57	<	$-3840 \pm 717\ddagger$

*A comparison of the minimum required enthalpy with the measured enthalpy indicates if an antigenicity inducing conformational change (similar to UFH, LMWH, and HO16) is thermodynamically allowed ($\Delta H > \Delta H_{\text{req}}$), unlikely ($\Delta H \approx \Delta H_{\text{req}}$), or forbidden ($\Delta H < \Delta H_{\text{req}}$).

†The lower limit for the enthalpy required to drive antigenicity inducing conformational changes was estimated using TΔS by taking either the measured ΔS values (UFH, LMWH, HO16) or assuming ΔS = -12.8 cal/mol/K (for heparins labeled with ‡), which is the average of the entropy changes for UFH and HO16.

AFM that the size of PF4/fondaparinux and PF4/HO06 complexes did not differ largely from the size of PF4 alone (Figure 2). However, PF4/HO08 complexes were as large as PF4/HO16 complexes, and still anti-PF4/heparin antibodies did not bind to them. Thus, exposure of the antigen allowing binding of anti-PF4/heparin antibodies must require more than formation of multimolecular complexes between PF4 and a polyanion even if this induces a change in anti-parallel β -sheets of PF4 >30%.

These puzzling observations were further clarified by ITC, which measures the thermodynamic changes when PF4/polyanion complexes are formed. For all investigated heparins, heat was released on binding to PF4. However, longer heparins induced a higher heat release (negative change in enthalpy) compared with shorter heparins. Normalized per mole PF4 tetramers, the largest heat release (the highest negative values for enthalpy) was measured for the complexes formed by PF4 with UFH, LMWH, and HO16, whereas HO08, HO06, and fondaparinux (Tables 1 and 2) induced much less heat release when complexed with PF4. This is an unexpected finding for a mainly electrostatically mediated interaction.³³ The smaller heparin molecules should have been able to pack closer to the PF4 tetramers, thereby displacing more water molecules and consequently leading to an increased heat release.

By comparing the ELISA data with the ITC data, it became obvious that the heat release has to be stronger than approximately -4000 cal/mol_{PF4} to allow expression of the binding site for anti-PF4/heparin antibodies. In other words, this energy is needed to drive the structural changes in PF4 required for exposure of the neoantigens. This is hardly fulfilled by HO08, but not by HO06 and fondaparinux (Table 2).

We then extrapolated the change in enthalpy (heat release) of the different heparins, as shown graphically in Figure 4. The required change in enthalpy approaches the values of UFH and HO16 at a chain length of ~11 monosaccharide units. This excellently matches with empirically observed interaction patterns of PF4 with different heparins showing that ≥ 12 monosaccharides are necessary to induce anti-PF4/heparin antibody binding *in vitro*.²⁸⁻³⁰ This critical heparin chain length can therefore also be interpreted by the minimum chain length that is necessary to release enough energy to drive the PF4 conformational changes, which finally lead to epitope exposure.¹⁶

The CD experiments showed different patterns of the antiparallel β -sheet content of PF4 (Figure 1), which was reversible at higher concentrations when UFH, LMWH, and HO16 were added, but irreversible with HO08 and HO06. Likely, shorter heparins (HO08 and HO06, and presumably all heparins <11-mers) pack closely

around PF4 tetramers; thereby, each negative charge of the heparin chain finds positive binding partners on PF4. Larger heparins, however, are too long to just bind to one PF4 tetramer. Therefore, they likely bridge between two PF4 tetramers to find maximal binding partners to neutralize their negative charges. This requires close approximation and a conformational change that consumes energy. By adding more heparin, the long heparin molecules all compete for the positive binding sites on PF4. As already proposed in earlier studies,²⁴ this then results in disruption of the multimolecular complexes and reversal of the conformational change. In contrast, fondaparinux, HO06, and HO08 already form energetically favorable complexes with PF4, which will not be reversed by the addition of more fondaparinux, HO06, or HO08.

Our study has some limitations. We determined the structural changes of the PF4 molecule associated with exposure of the antibody binding site. Whether these changes are causative or indirectly related can only be determined when the structure of the binding site(s) for PF4/heparin antibodies is identified. This will require crystallization of PF4/heparin complexes together with an anti-PF4/heparin antibody. Although we did use typically reacting human anti-PF4/heparin antibodies, the panel of 14 human sera may not cover the entire spectrum of binding characteristics of human anti-PF4/heparin antibodies. In addition, the defined heparin fragments that we used are not characterized for their anticoagulatory potency. They are model substances and might show different physical characteristics, especially depending on the number of their sulfate groups. In the AFM experiments, we had technical difficulties to immobilize PF4/UFH complexes on the mica surface in the fluid phase, in contrast to previous experiments, in which we assessed PF4/heparin complexes by AFM on dried mica.¹⁴ Most likely, the PF4/UFH complexes are so large¹⁰ that they had been flushed away in the present fluid phase experiments. Consistent with this hypothesis, we found large PF4/UFH complexes in additional experiments (300-second incubation time and gentle dipping instead of washing; data not shown). In addition, the PF4/polyanion complexes we observed in the fluid phase were predominantly globular, similar to the complexes seen in TEM images of Rauova et al.¹⁰ We did not find ridge-like structures as previously described,¹⁴ which had a height of only about 2.9 nm and a length of up to 200 nm. These

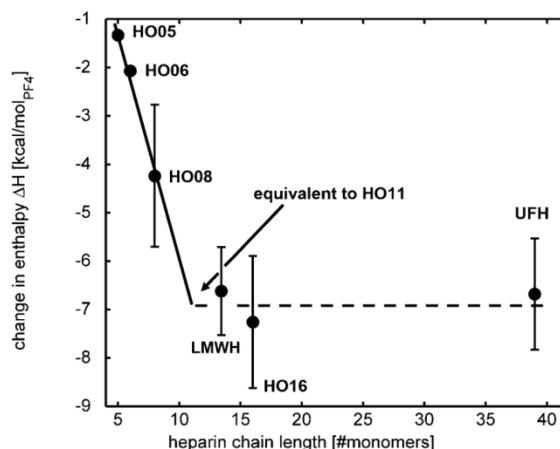


Figure 4. Dependence between change in enthalpy and heparin chain length. The change in enthalpy (circles, values taken from Table 2) increases with chain length and reaches the values of HO16 and UFH at a heparin chain length around 11 monosaccharides, which is close to the critical heparin chain length (=12) that has to be exceeded to form antigenic PF4/heparin complexes. The error bars for HO05 and HO06 are so small that they are hidden by the circles.

differences can be explained by the fact that measurements were carried out in liquid and tip convolution is much larger here than in the previous work. We also did not exclude the interaction of several polyanions with PF4, eg, endothelial cell heparin sulfate and the pentasaccharide, which may together induce conformational changes that likely happen in vivo and may be the explanation why fondaparinux can induce anti-PF4/heparin antibodies.³⁴

Our study shows for the first time that besides clustering, conformational changes of PF4 by a polyanion do not necessarily lead to the expression of the binding site for anti-PF4/heparin antibodies. This only occurs if binding of a polyanion to PF4 results in a conformational change that requires input of energy. Only then does PF4 expose structures to which the immune system reacts and that can therefore be seen as danger signal, eg, for labeling bacteria.³⁵ Thus, our biophysical methods may be applied to guide the development of synthetic heparins and other polyanion-based drugs, eg, aptamers,³⁶ that do not lead to expression of these danger signals, which results in an increased risk for heparin-induced thrombocytopenia.

Beyond HIT, understanding the conformational changes making PF4 immunogenic may be relevant for mechanisms underlying other autoimmune blood disorders and immune reactions to human recombinant proteins used as biotherapeutics. Many proteins that are the target of autoantibodies in hematology tend to cluster, eg, PF4 clusters with polyanions like heparin; platelet glycoprotein IIb/IIIa (target in immune thrombocytopenia) clusters in rafts³⁷; and ADAMTS13 (target in thrombotic thrombocytopenic purpura) may cluster on von Willebrand factor.³⁸ If in addition to clustering, these proteins undergo conformational changes, they may also trigger an immune response. In this regard, it is of interest that GPIIb/IIIa and ADAMTS13 have in common that their genes show many polymorphisms. Potentially, certain point mutation or post-translational modifications allow conformational changes critical for the immune system with less energy input.

In summary, biophysical methods allowed us to characterize the conformational changes, which the endogenous protein PF4 undergoes when it forms complexes with well-defined polyanions. Our findings may help to synthesize safer heparins. Beyond HIT, these methods may be relevant to unravel mechanisms that prone other endogenous proteins relevant in autoimmunity to become immunogenic.

Acknowledgments

The authors thank Dr Marco Marenchino (GE Healthcare) for valuable discussion and help with ITC data analysis and interpretation. This work was supported by the German Ministry of Education and Research within project FKZ 03Z2CN11. K.K. was supported by the Volkswagen Stiftung (Lichtenberg Professorship to Hansjörg Schwertz).

Authorship

Contribution: M.K. designed and carried out the ITC and AFM experiments, analyzed and interpreted the results, and wrote and reviewed the manuscript; S.B. designed and carried out the EIA and CD measurements, analyzed and interpreted the results, and reviewed the manuscript; K.K. discussed the results and reviewed the manuscript; S.B. supported the AFM experiments and participated in the thermodynamical interpretation of the data; C.A.H. discussed the results critically and reviewed the manuscript; W.W. discussed the results and reviewed the manuscript; A.G. provided the conceptual design of the experiments, provided critical review and discussion of results; and wrote the manuscript; M.D. provided the conceptual design of biophysical characterization of PF4-defined heparins complexes, designed the experiments, interpreted the results, and wrote and reviewed the manuscript; and all authors reviewed and approved the final version of the manuscript.

Conflict-of-interest disclosure: The authors declare no competing financial interests.

Correspondence: Andreas Greinacher, Institut für Immunologie und Transfusionsmedizin, Sauerbruchstrasse, 17475 Greifswald, Germany; e-mail: greinach@uni-greifswald.de; or Mihaela Delcea, ZIK HIKE-Zentrum für Innovationskompetenz, Humorale Immunreaktionen bei kardiovaskulären Erkrankungen, Ernst-Moritz-Armdt-Universität Greifswald, Fleischmannstrasse 42-44, 17489 Greifswald, Germany; e-mail: delceam@uni-greifswald.de.

References

- Mackman N. Triggers, targets and treatments for thrombosis. *Nature*. 2008;451(7181):914-918.
- Andersson LO, Barrowcliffe TW, Holmer E, Johnson EA, Sims GE. Anticoagulant properties of heparin fractionated by affinity chromatography on matrix-bound antithrombin III and by gel filtration. *Thromb Res*. 1976;9(6):575-583.
- Lane DA, Denton J, Flynn AM, Thunberg L, Lindahl U. Anticoagulant activities of heparin oligosaccharides and their neutralization by platelet factor 4. *Biochem J*. 1984;218(3):725-732.
- Walenga JM, Jeske WP, Samama MM, Frapaise FX, Bick RL, Fareed J. Fondaparinux: a synthetic heparin pentasaccharide as a new antithrombotic agent. *Expert Opin Investig Drugs*. 2002;11(3):397-407.
- Xu Y, Masuko S, Takiyuddin M, et al. Chemoenzymatic synthesis of homogeneous ultralow molecular weight heparins. *Science*. 2011;334(6055):498-501.
- Petitou M, Héroult JP, Bernat A, et al. Synthesis of thrombin-inhibiting heparin mimetics without side effects. *Nature*. 1999;398(6726):417-422.
- Mousa SA, Petersen LJ. Anti-cancer properties of low-molecular-weight heparin: preclinical evidence. *Thromb Haemost*. 2009;102(2):258-267.
- Greinacher A. Heparin-induced thrombocytopenia. *J Thromb Haemost*. 2009;7(Suppl 1):9-12.
- Warkentin TE, Levine MN, Hirsh J, et al. Heparin-induced thrombocytopenia in patients treated with low-molecular-weight heparin or unfractionated heparin. *N Engl J Med*. 1995;332(20):1330-1335.
- Rauova L, Poncz M, McKenzie SE, et al. Ultrahigh molecular weight complexes of PF4 and heparin are central to the pathogenesis of heparin-induced thrombocytopenia. *Blood*. 2005;105(1):131-138.
- Rauova L, Zhai L, Kowalska MA, Arepally GM, Cines DB, Poncz M. Role of platelet surface PF4 antigenic complexes in heparin-induced thrombocytopenia pathogenesis: diagnostic and therapeutic implications. *Blood*. 2006;107(6):2346-2353.
- Warkentin TE, Kelton JG. A 14-year study of heparin-induced thrombocytopenia. *Am J Med*. 1996;101(5):502-507.
- Sachais BS, Litvinov RI, Yarovi SV, et al. Dynamic antibody-binding properties in the pathogenesis of HIT. *Blood*. 2012;120(5):1137-1142.
- Greinacher A, Gopinadhan M, Günther JUG, et al. Close approximation of two platelet factor 4 tetramers by charge neutralization forms the antigens recognized by HIT antibodies. *Arterioscler Thromb Vasc Biol*. 2006;26(10):2386-2393.
- Suvarna S, Espinasse B, Qi R, et al. Determinants of PF4/heparin immunogenicity. *Blood*. 2007;110(13):4253-4260.
- Chudasama SL, Espinasse B, Hwang F, et al. Heparin modifies the immunogenicity of positively charged proteins. *Blood*. 2010;116(26):6046-6053.
- Brandt S, Krauel K, Gottschalk KE, et al. Characterization of the conformational changes in platelet factor 4 induced by polyanions: towards in-vitro prediction of antigenicity. *Thrombosis Haemostasis*. 2014;TH-13-08-0634.R2.
- Shastri MD, Peterson GM, Stewart N, Sohal SS, Patel RP. Non-anticoagulant derivatives of heparin for the management of asthma: distant dream or close reality? *Expert Opin Investig Drugs*. 2014;23(3):357-373.

19. Juhl D, Eichler P, Lubenow N, Strobel U, Wessel A, Greinacher A. Incidence and clinical significance of anti-PF4/heparin antibodies of the IgG, IgM, and IgA class in 755 consecutive patient samples referred for diagnostic testing for heparin-induced thrombocytopenia. *Eur J Haematol.* 2006;76(5):420-426.
20. Böhm G, Muhr R, Jaenicke R. Quantitative analysis of protein far UV circular dichroism spectra by neural networks. *Protein Eng.* 1992; 5(3):191-195.
21. Cornelsen M, Helm CA, Block S. Destabilization of polyelectrolyte multilayers formed at different temperatures and ion concentrations. *Macromolecules.* 2010;43(9):4300-4309.
22. Stranak V, Block S, Drache S, et al. Size-controlled formation of Cu nanoclusters in pulsed magnetron sputtering system. *Surf Coat Tech.* 2011;205(8-9):2755-2762.
23. Amiral J, Lormeau JC, Marfaing-Koka A, et al. Absence of cross-reactivity of SR90107A/ ORG31540 pentasaccharide with antibodies to heparin-PF4 complexes developed in heparin-induced thrombocytopenia. *Blood Coagul Fibrinolysis.* 1997;8(2):114-117.
24. Greinacher A, Alban S, Dummel V, Franz G, Mueller-Eckhardt C. Characterization of the structural requirements for a carbohydrate based anticoagulant with a reduced risk of inducing the immunological type of heparin-associated thrombocytopenia. *Thromb Haemost.* 1995;74(3): 886-892.
25. Ahmad S, Jeske WP, Walenga JM, et al. Synthetic pentasaccharides do not cause platelet activation by antiheparin-platelet factor 4 antibodies. *Clin Appl Thromb Hemost.* 1999;5(4): 259-266.
26. Laugel N, Betscha C, Winterhalter M, Voegel JC, Schaaf P, Ball V. Relationship between the growth regime of polyelectrolyte multilayers and the polyanion/polycation complexation enthalpy. *J Phys Chem B.* 2006;110(39):19443-19449.
27. Sperber BL, Cohen Stuart MA, Schols HA, Voragen AG, Norde W. Overall charge and local charge density of pectin determines the enthalpic and entropic contributions to complexation with β -lactoglobulin. *Biomacromolecules.* 2010;11(12): 3578-3583.
28. Visentin GP, Moghaddam M, Beery SE, McFarland JG, Aster RH. Heparin is not required for detection of antibodies associated with heparin-induced thrombocytopenia/thrombosis. *J Lab Clin Med.* 2001;138(1):22-31.
29. Amiral J, Bridey F, Wolf M, et al. Antibodies to macromolecular platelet factor 4-heparin complexes in heparin-induced thrombocytopenia: a study of 44 cases. *Thromb Haemost.* 1995; 73(1):21-28.
30. Greinacher A. Antigen generation in heparin-associated thrombocytopenia: the nonimmunologic type and the immunologic type are closely linked in their pathogenesis. *Semin Thromb Hemost.* 1995;21(1):106-116.
31. Greinacher A, Michels I, Mueller-Eckhardt C. Heparin-associated thrombocytopenia: the antibody is not heparin specific. *Thromb Haemost.* 1992;67(5):545-549.
32. Greinacher A, Pötzsch B, Amiral J, Dummel V, Eichner A, Mueller-Eckhardt C. Heparin-associated thrombocytopenia: isolation of the antibody and characterization of a multimolecular PF4-heparin complex as the major antigen. *Thromb Haemost.* 1994;71(2):247-251.
33. Capila I, Linhardt RJ. Heparin-protein interactions. *Angew Chem Int Ed Engl.* 2002;41(3):391-412.
34. Warkentin TE, Cook RJ, Marder VJ, et al. Anti-platelet factor 4/heparin antibodies in orthopedic surgery patients receiving antithrombotic prophylaxis with fondaparinux or enoxaparin. *Blood.* 2005;106(12):3791-3796.
35. Krauel K, Pötschke C, Weber C, et al. Platelet factor 4 binds to bacteria, [corrected] inducing antibodies cross-reacting with the major antigen in heparin-induced thrombocytopenia. *Blood.* 2011; 117(4):1370-1378.
36. Jaax ME, Krauel K, Marschall T, et al. Complex formation with nucleic acids and aptamers alters the antigenic properties of platelet factor 4. *Blood.* 2013;122(2):272-281.
37. Kasahara K, Kaneda M, Miki T, et al. Clot retraction is mediated by factor XIII-dependent fibrin- α IIb β 3-myosin axis in platelet sphingomyelin-rich membrane rafts. *Blood.* 2013; 122(19):3340-3348.
38. Kremer Hovinga JA, Lammle B. Role of ADAMTS13 in the pathogenesis, diagnosis, and treatment of thrombotic thrombocytopenic purpura. *Hematology Am Soc Hematol Educ Program.* 2012;2012:610-616.

6.4 Paper IV: Polyphosphate Chain Length determines the Antigenicity of the
Complexes formed with Platelet Factor 4 (PF4) and the binding of PF4 to Bacteria

Polyphosphate chain length determines the antigenicity of the complexes formed with platelet factor 4 (PF4) and the binding of PF4 to bacteria

Sven Brandt¹, Krystin Krauel², Miriam Jaax², Thomas Renné³, Christiane A. Helm⁴, Sven Hammer-schmidt⁵, Mihaela Delcea¹ and Andreas Greinacher²

¹ZIK HIKE – Center of innovative competence “Humoral Immune Responses in Cardiovascular Disease“, Greifswald, Germany;

²Institute for Immunology and Transfusion Medicine, Greifswald, Germany;

³Institute for Clinical Chemistry and Laboratory Medicine, University Hospital Hamburg-Eppendorf, Hamburg, Germany and Department of Molecular Medicine and Surgery, Karolinska Institutet, Stockholm, Sweden;

⁴Institute for Experimental Physics, Greifswald, Germany;

⁵Department Genetics of Microorganisms, Interfaculty Institute for Genetics and Functional Genomics, Greifswald, Germany

Corresponding authors:

Mihaela Delcea, PhD
ZIK HIKE - Ernst-Moritz-Arndt-Universität
Greifswald
Fleischmannstrasse 42-44
17489 Greifswald
Germany
Tel: +49-3834-8622343
Fax: +49-3834-8622341
e-mail: delceam@uni-greifswald.de

Prof. Dr. med. Andreas Greinacher, MD
Institut für Immunologie und Transfusionsmedizin
Sauerbruchstrasse
17475 Greifswald
Germany
Tel: +49-3834-865482
Skr: +49-3834-865479
Fax: +49-3834-865489
e-mail: greinach@uni-greifswald.de

Abstract

Polyphosphates (polyP) are one of the most ancient, conserved and enigmatic molecules in biology. These ubiquitous polymers are formed by phosphate (Pi) residues. They are procoagulant, prothrombotic, and pro-inflammatory and interfere with innate immune mechanisms. Here we demonstrate that defined chain length polyP (P45; P75) form, at specific stoichiometric ratios, complexes with platelet factor 4 (PF4 or CXCL4). PF4 is an evolutionary conserved chemokine, released from platelet α -granules binding to polyanionic lipid A on bacteria. This induces an antibody mediated bacterial host defense mechanism, which can be misdirected when PF4 and pharmacologic heparin form PF4/polyanion complexes thereby inducing the adverse drug reaction heparin-induced thrombocytopenia (HIT). We show by circular dichroism spectroscopy and isothermal titration calorimetry that PF4 changes its structure upon binding to polyP chain length (≥ 45 Pi) in a similar way as shown for PF4 in PF4/heparin complexes. Consequently, PF4/polyP complexes expose neoepitopes to which human anti-PF4/heparin antibodies obtained from HIT-patients bind. Most importantly, we show that polyP (≥ 45 Pi) enhance binding of PF4 to E. coli, hereby facilitating bacterial opsonization and, in the presence of human anti-PF4/polyanion antibodies, phagocytosis. This indicates a further biological role of polyP, i.e. enhancing an ancient bacterial immune defense mechanism.

Keywords: polyphosphates, platelet factor 4, protein structural changes, entropy, antigenicity, bacteria

Introduction

Inorganic polyphosphates (polyP) are ubiquitous polymers formed by phosphate (Pi) residues linked by phosphoanhydride bonds and one of the most ancient, conserved and enigmatic molecules in biology.¹⁻³

PolyP are of particular interest in hematology because they are secreted by activated platelets⁴⁻⁶ or mast cells⁷ and accumulate in many infectious microorganisms.⁸ It has been shown that polyP are procoagulant,^{6,9,10} prothrombotic,^{6,11} and pro-inflammatory.^{6,9,10} PolyP trigger clotting via the contact pathway,^{6,11,12} accelerate factor V activation,¹¹ enhance fibrin clot structure,^{13,14} and accelerate factor XI back-activation by thrombin.¹⁵ It has been recently shown that polyP dampen the innate immune response by suppressing complement, interfering therefore also with the complex relationship between coagulation and innate immunity.¹⁶

PolyP are stored in platelet dense granules together with calcium, ATP, ADP, and serotonin as polymers with a mean chain length of 60-100 Pi. They are secreted from procoagulant platelets and initiate thrombosis by contact activating FXII.⁶ Both synthetic platelet size polyP¹¹ and natural platelet derived polymers trigger coagulation in human plasma in a FXII-dependent manner.¹⁷ PolyP concentration in plasma ranges from 10-50 μ M, but due to phosphatases, polyP are unstable and have a half-life of about 90 min in plasma.^{11,13,18} Recently, it was found that polyP act as primordial chaperone stabilizing proteins in vivo helping them to withstand proteotoxic stress.²

Platelet factor 4 (PF4), a chemokine of the CXCL4 family released from alpha-granules during platelet activation,¹⁹⁻²¹ binds to polyanionic drugs e.g. heparin²²⁻²⁴ and exposes an epitope recognized by anti-PF4/heparin antibodies, leading to the prothrombotic adverse drug effect heparin-induced thrombocytopenia (HIT). PF4/polyanion complex formation is not restricted to sulfate groups in heparin; it may also occur through phosphate groups as shown for lipid A,²⁵ DNA and RNA.^{26,27}

As a (potential) part of the innate immune system, PF4 binds to the surface of bacteria, and when undergoing a conformational change, PF4 acts as a marker for pathogens to which anti-PF4/heparin antibodies bind, hereby enhancing phagocytosis of the pathogens by granulocytes.²⁸ Previously, we have shown that heparin increases the binding of PF4 to platelets at a certain molar ratio with binding being disrupted at very high heparin concentrations²⁹ which was also shown for bacterial surfaces.²⁸

More recently, we have shown that PF4 undergoes characteristic conformational changes when complexing with heparin, exposing the binding site for anti-PF4/heparin antibodies.³⁰

Here we report on the complex formation between PF4 and polyP with of defined two different mean chain lengths (45-, and 75-mer) and with triphosphate. We found that beside the conformational change of PF4 exposing approximately 40% antiparallel β -sheets, the PF4/polyP complexes cross-react with anti-PF4/heparin antibodies and undergo favorable entropic changes. We also show that polyP (≥ 45 Pi) influence the binding capacity of PF4 to Gram-negative *Escherichia coli* (*E. coli*) and – together with anti-PF4/polyanion antibodies – enhance bacterial phagocytosis by polymorphonuclear leukocytes in a concentration dependent manner. These findings may provide relevant aspects to understand the biological functions of polyP and give insights into their potential role as part of an ancient immune defense system recognizing bacteria.

Materials and Methods

Materials

Lyophilized, human platelet factor 4 (PF4) isolated from platelets was purchased from Chromatec GmbH (Greifswald, Germany). Sodium polyP of two different mean chain lengths (45, and 75 Pi per molecule) and triphosphate (P3) were obtained from BK Guilini (Ladenburg, Germany). Samples were dialyzed against phosphate buffered saline (PBS) with a pH of 7.4 (NaCl, KCl, KH_2PO_4 all purchased from Th. Geyer GmbH & Co KG, Renningen, Germany; Na_2HPO_4 from Merck KGaA, Darmstadt, Germany) in Slide-A-Lyzer dialysis cassettes (Thermo Scientific, 3 ml, 3500 MWCO, Schwerte, Germany).

Circular dichroism (CD) spectroscopy

Changes in the secondary structure of PF4 upon complex formation with polyP were investigated by Circular Dichroism (CD) spectroscopy using a Chirascan CD spectrometer (Applied Photophysics, Leatherhead, UK). Far-UV spectra (200-260 nm) were recorded for different molar ratios of polyP/PF4 ($c(\text{P}_i)/c(\text{PF}_4)=43\text{-}350$, as indicated in Figure 1) at 20°C using a 5 mm path length cuvette (110-QS, Hellma, Müllheim, Germany). Measurements were started with pure PF4 ($2.5 \cdot 10^{-6} \text{ M} = 80 \text{ } \mu\text{g/ml}$) diluted in PBS buffer and polyP concentration was subsequently increased. Baseline spectra of both PBS and polyP at the corresponding concentrations were subtracted and resulting spectra were corrected for concentration, number of amino acids, and path length to obtain mean residue delta epsilon (MRDE) values. The moderate dilution of PF4 was taken into account for the MRDE calculation. To illustrate the development of the two α -helical bands at 206 nm and 222 nm, the values of these bands were normalized with respect to the native spectrum (set as one) and the maximum change that was observed (set to zero) (Figure 1). Deconvolution of the CD data was carried out using CDNN (circular dichroism neural network) software using a database of 33 reference proteins.³¹

Enzyme immune assay (EIA)

PF4/polyP EIA was conducted with three human sera of patients who were immunized during treatment with heparin as described with some modifications.³² To enable complex formation PF4 ($6.25 \cdot 10^{-7} \text{ M} = 20 \text{ } \mu\text{g/ml}$) was incubated (RT, 1 h) with increasing concentrations of polyP ($0\text{-}1.556 \cdot 10^{-4} \text{ M}_m = 0\text{-}16 \text{ } \mu\text{g/ml}$) or coating buffer ($0.05 \text{ M NaH}_2\text{PO}_4$, $0.1\% \text{ NaN}_3$) before coating (4°C , overnight) wells of a microtiter plate (CovaLink, Nunc, Langenselbold, Germany) with $100 \text{ } \mu\text{l}$. Next day, plates were washed five times (0.15 M NaCl , $0.1\% \text{ Tween } 20$, pH 7.5) and incubated (RT, 1 h) with $100 \text{ } \mu\text{l}$ patient serum (1:300 or 1:1000 in $0.05 \text{ M NaH}_2\text{PO}_4$, 0.15 M NaCl , $7.5\% \text{ goat normal serum}$, Sigma G6767, pH 7.5). After washing five times, plates were incubated (RT, 1 h) with $100 \text{ } \mu\text{l}$ peroxidase-conjugated anti-human IgG (Dianova, Hamburg, Germany; 1:20000 in $0.05 \text{ M NaH}_2\text{PO}_4$, 0.15 M NaCl , $7.5\% \text{ goat normal serum}$). After five times washing, plates were incubated (RT, 10 min, dark) with $100 \text{ } \mu\text{l}$ tetramethylbenzidine (BD OptEIA TMB substrate, Heidelberg, Germany). The reaction was stopped with $100 \text{ } \mu\text{l H}_2\text{SO}_4$ and the absorbance was measured at 450 nm.

Isothermal titration calorimetry (ITC)

Isothermal titration calorimetry experiments were carried out at 25°C using a MicroCal iTC200 (GE Healthcare Life Sciences).^{33,34} PolyP and PF4 were prepared in PBS (pH 7.4). PF4 [$1.48 \cdot 10^{-5} \text{ M} = 472 \text{ } \mu\text{g/mL}$] was placed in the calorimeter cell and the syringe was loaded with triphosphate (P3 [$1.42 \cdot 10^{-3} \text{ M} = 500 \text{ } \mu\text{g/mL}$]) or polyP (P45 [$1.08 \cdot 10^{-4} \text{ M} = 500 \text{ } \mu\text{g/mL}$], P75 [$1.00 \cdot 10^{-4} \text{ M} = 750 \text{ } \mu\text{g/mL}$]). The measurement was started by injecting $0.4 \text{ } \mu\text{l}$ polyP, followed by 18 injections of $2 \text{ } \mu\text{l}$ at 1000 RPM with 240 seconds spacing time, low feedback, 5 seconds filtering period and the reference power to $6 \text{ } \mu\text{cal/sec}$. Calorimetric data were fitted to a One Set of Sites model with a non-linear regression to obtain the enthalpy (ΔH), stoichiometry (n), and the equilibrium constant (K_A) using Origin 7.0 SR4 software (OriginLab Cooperation, Northampton, USA). Equilibrium dissociation constants (K_D) were calculated as

the reciprocal of K_A . The Gibbs free energy change (ΔG) was calculated with the equation $\Delta G = -RT \ln K_A$ and the entropy (S) based on the relationship $\Delta G = \Delta H - T\Delta S$. The reported parameters are mean values of three independent measurements.

PF4 binding to bacteria

UV-inactivated and fluorescein (FITC) labeled 25 Gram-negative *Escherichia coli* (*E. coli* JM109-FITC) were incubated (30 min, 4°C) with biotinylated PF4 (20 µg/ml, diluted in PBS) alone or in the presence of different concentrations (0-40 µg/ml) of polyP. After washing with PBS/0.05% BSA (3000 g, 5 min, 4°C), bacteria were incubated (30 min, 4°C) with Streptavidin-PE Cy5.5 (BD Biosciences, Heidelberg, Germany) and washed as before. PF4 binding to the bacteria was analyzed by flow cytometry (Cytomics FC 500, Beckman Coulter). The binding activity was defined as the geometric mean fluorescence intensity multiplied by the percentage of labeled bacteria.

Phagocytosis assay

E. coli JM109 self-labeled with FITC 25 were incubated (30 min, 4°C) with PF4 (200 µg/mL) alone or in the presence of different concentrations (0.8-200 µg/mL) of P75. The washed samples (3000g, 5 minutes, 4°C) were incubated (30 min, 4°C) with human serum (1:50) of patients known to contain anti-PF4/heparin IgG antibodies ($n=3$). The sera had been heat-inactivated (56°C, 45 min) and pre-adsorbed with *E. coli* JM109 (non-PF4-coated; 15 min, 4°C; 4 times). Bacteria were washed again to remove unbound antibodies. Finally, a whole blood phagocytosis assay was performed as described²⁸ using pretreated bacteria.

Results

To investigate whether polyP induce changes in the secondary structure of PF4 we used CD spectroscopy. Triphosphate (P3) did not induce any changes in the CD signal of PF4 (Figure 1A), indicating that no alterations in the protein structure occurred. In contrast, PF4 showed pronounced structural changes when titrated with P45 (Figure 1B) and P75 (Figure 1C), respectively. The maximum changes observed in the CD signal were comparable and reached at similar concentrations (8 µg/mL = $1.7 \cdot 10^{-6}$ M for P45 and 6 µg/mL = $8.0 \cdot 10^{-7}$ M for P75). Absolute values of these two bands are proportional to the presence of α -helix content in the protein.^{35,36} In the bottom panels of Figure 1, the development of the bands normalized with respect to the maximum changes and the native spectrum are shown. The two bands shift to lower values during the titration having a minimum at a certain molar ratio, indicating the point of maximum structural changes. Deconvolution of the CD data confirmed a drop in α -helix in combination with a decrease in β -turn content (Figure S1). The decrease in both α -helix and in β -turn was balanced by a pronounced increase in antiparallel β -sheet exceeding 40% (Figure S1). The maximum structural changes are similar for PF4 in complex with P45 and P75 (an increase of ~15% in antiparallel β -sheet content), Figure 2B. The deconvolution of the CD data for the PF4/P3 complexes suggested no structural changes at any molar ratio (Figure 2B and Figure S1).

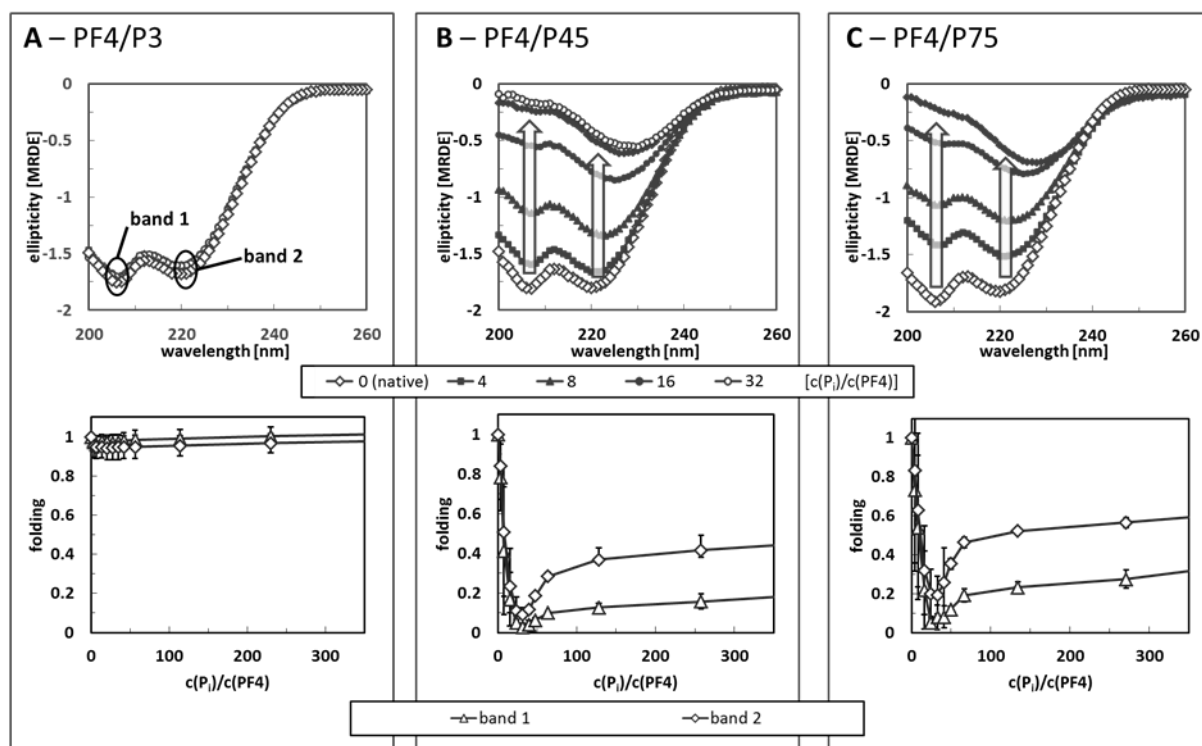


Figure 1: CD spectra of various $c(\text{Pi})/c(\text{PF}_4)$ molar ratios are shown, where $c(\text{Pi})$ and $c(\text{PF}_4)$ are the molar concentrations of phosphate monomers (Pi) and the PF₄ tetramer, respectively. PF₄ [2.5 μM = 80 $\mu\text{g}/\text{ml}$], was titrated with triphosphate P3 (A) and polyP P45 (B) and P75 (C), respectively. The top panels show the structural changes in the protein toward a maximum at a certain PF₄:polyP ratio, except for P3 where no changes were observed. The bottom panels show the normalized development of the two α -helix bands, indicated as band 1 and band 2 in the upper panel in Figure 1A.

Antibody binding to PF₄/polyP complexes and correlation with structural changes of PF₄

We further addressed the question whether the PF₄/polyP complexes can mimic the PF₄/heparin complexes by carrying out enzyme immunoassays (EIA) with sera of patients known to contain anti-PF₄/heparin antibodies (Figure 2A).

Previously, it was shown that binding of the antibodies to PF₄/heparin complexes depends on the molar ratio of the protein and the glycosaminoglycan.³² We therefore, formed complexes of PF₄ with increasing concentrations of polyP and assessed whether anti-PF₄/heparin antibodies obtained from patients who developed these antibodies during treatment with heparin, cross-react with PF₄/polyP complexes. No antibody binding was observed for the PF₄/P3 complexes at any molar ratio (Figure 2A, Δ). In contrast, the anti-PF₄/heparin antibodies recognized PF₄ in complex with P45 and P75 (Figure 2A, \square and \diamond). Only slight differences in structural changes of PF₄ in complex with P45 and P75 were observed by CD spectroscopy (Figure 2B), and in binding anti-PF₄/heparin antibodies to both complexes, PF₄/P75 and PF₄/P45 as determined by EIA. This shows that both P45 and P75 induce conformational changes in PF₄ thereby exposing the binding site for anti-PF₄/heparin antibodies. However, the PF₄/polyP molar ratio where the maximum antibody binding occurs, differs for P45 ($\text{P}_i/\text{PF}_4 \approx 27$) and P75 ($\text{P}_i/\text{PF}_4 = 48$). In addition, the maximum optical density at 450 nm for binding of anti-PF₄/heparin IgG antibodies to the PF₄/P75 complexes (OD 2.6) was higher than for the PF₄/P45 complexes (OD 1.5).

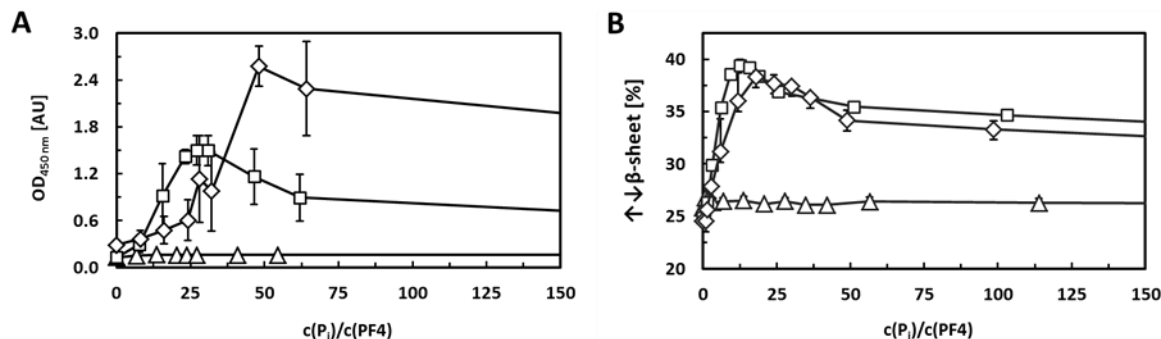


Figure 2: A – binding of three different sera containing anti-PF4/heparin antibodies to PF4/polyP complexes was assessed by enzyme immune assay (EIA) after coating of microtiter plates with various molar ratios of PF4 in complex with the triphosphate P3 (Δ) or with P45 (\square) or P75 (\diamond); **B** - conformational changes of PF4 in complex with P3 (Δ); P45 (\square); or P75 (\diamond) represented by antiparallel β -sheet content found by deconvolution of the CD data. For PF4/P3 complexes neither a change in antiparallel β -sheet, nor any antibody binding was observed over the whole concentration range. PF4 in complex with P45 or P75 showed an increase in antiparallel β -sheet up to approx. 40%. The change in OD at 450 nm reaches 1.50 ± 0.19 at a P45_i/PF4 ratio of ~ 27 and of 2.58 ± 0.25 at a P75_i/PF4 ratio of 48. The error bars represent the standard deviation of three independent CD measurements.

Thermodynamic characterization of PF4/polyP complexes

We further assessed the energetic characteristics of the PF4/polyP binding interactions using isothermal titration calorimetry (ITC) (Figure S2). The thermodynamic parameters are provided in Table 1. P45 and P75 polyP in complex with PF4 showed characteristic negative peaks, indicating an exothermic reaction (top panels in Figure S2B and Figure S2C). With the progression of titration, peaks become smaller suggesting saturation of the available binding sites on PF4. The area under the peaks was integrated to obtain the characteristic s-shaped curve (bottom panels in Figure S2B and Figure S2C). The titration of PF4 with P3 did not indicate interaction within the tested concentrations ($0 - 2.83 \cdot 10^{-5}$ M = 10 μ g/mL) and no thermodynamic parameters could be defined (n.d.). As expected from CD spectroscopy and EIA data, PF4 and polyP formed spontaneously complexes as indicated by negative values of the Gibbs free energy of binding (ΔG) calculated for P45 and P75 (Table 1 and Figure S3). The ΔG shows similar values (when calculated to a mole of polyP contributing to the reaction) for PF4/P45 and PF4/P75 complexes, respectively. The profile consisting of ΔG , enthalpy (ΔH), and entropy ($-\Delta S$) is different for the complex formation of PF4 with P45 and P75, respectively, (Table 1, Figure S3). PF4/P75 complex showed larger heat release (enthalpy change, $\Delta H = -7.06 \pm 0.33$ kcal/mol) than PF4/P45 complex ($\Delta H = -4.07 \pm 0.49$ kcal/mol), Table 1. This is consistent with the findings that anti-PF4/heparin antibodies bound differently to the two complexes as shown above.

Table 1: Thermodynamic parameters for the interaction of PF4 with P3, P45 and P75.

Complex	Enthalpy, ΔH^a [kcal/mol]	Enthalpy, ΔH^b [kcal/mol]	Dissociation constant ^b [M]	Stoichio- metry [polyP/PF4]	Gibbs Free Energy, ΔG^b [kcal/mol]	Entropy, $-T\Delta S^{*b}$ [kcal/mol]
PF4/P3	n.d.	n.d.	n.d.	n.d.	n.d.	n.d.
PF4/P45	-8.21±2.31	-4.07±0.49	$1.7 \cdot 10^{-7} \pm 6.7 \cdot 10^{-8}$	0.51±0.10	-9.25±0.22	1.04±2.47
PF4/P75	-16.6±0.46	-7.06±0.33	$8.4 \cdot 10^{-7} \pm 1.4 \cdot 10^{-7}$	0.43±0.01	-8.28±0.09	-8.36±0.55

Note: Change in enthalpy (ΔH) calculated: a) per mole of polyP chain or b) per mole of PF4 tetramer.

The calculated $-T\Delta S$ per mole of PF4 was negative for the PF4/P75 (-8.36 ± 0.55 kcal/mol/K), indicating that formation of PF4/P75 complexes is associated with favorable conformational changes and/or hydrophobic interactions. For PF4/P45 complexes, the change in entropy is close to zero (1.04 ± 2.47 kcal/mol per mole of polyP chain).

The dissociation constant of PF4 to P45 ($K_D = 1.7 \cdot 10^{-8}$ M) was found to be higher compared with the one of PF4 to P75 ($K_D = 8.4 \cdot 10^{-7}$ M) indicating lower affinity for the latter. The stoichiometry calculated for the PF4/P45 complex was 0.51 ± 0.1 P45/PF4 compared to 0.43 ± 0.01 P75/PF4, meaning that 2.36 PF4 bind per P75 molecule or 1.99 PF4 bind per P45 molecule. Therefore, ITC and CD spectroscopy show a similar stoichiometry: for P75, 31 P_i monomers bind to one PF4 compared to 48 from CD-spectroscopy. Fewer P_i monomers of P45 bind to one PF4: 23 or 24, respectively.

Binding of PF4 to bacteria in the presence of polyP

To investigate the influence of polyP on the binding of PF4 to bacterial surfaces, we used the well-characterized laboratory strain *Escherichia coli* (E. coli JM109). Bacteria were incubated with PF4 (20 $\mu\text{g/mL}$) and increasing concentrations of polyP (0–40 $\mu\text{g/mL}$) to obtain different PF4:polyP ratios. Flow cytometry measurements revealed the amount of PF4 bound to the bacterial surface as a function of polyP concentration. The short triphosphate P3 did not change the amount of PF4 bound to bacteria over a concentration range from 0–40 $\mu\text{g/mL}$. (Figure 3, Δ) In contrast polyP (P45 and P75) increased the amount of PF4 bound to the bacterial surface of E. coli (Figure 3, \square and \diamond). At higher concentrations P45 and P75 decreased PF4 binding.

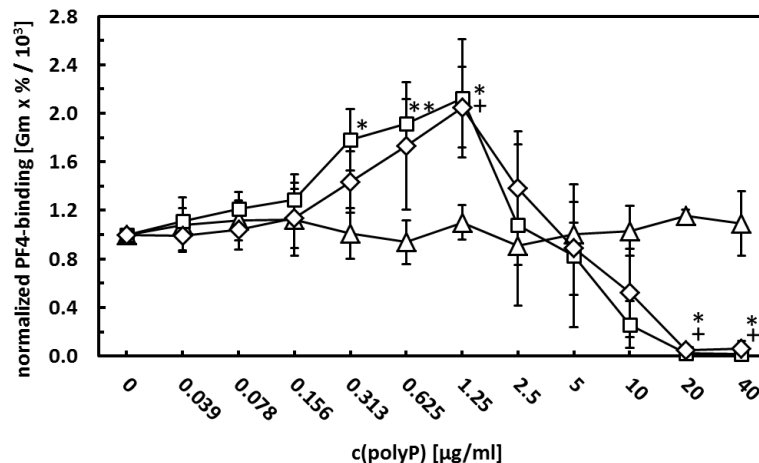


Figure 3: Binding of PF4 to *E. coli* as a function of polyP concentration (P3—Δ—, P45—□—, and P75—◇—) is shown. PF4 was incubated with bacteria and increasing concentrations of polyP and PF4 binding to bacteria was measured by flow cytometry. P45 and P75 increased PF4 binding to bacteria with a maximum at 1.25 µg/mL. At higher concentrations (>10 µg/ml) both, P45 and P75 inhibited PF4 binding to the bacterial surface. No significant changes could be observed for the triphosphate P3. (Significance levels: */+ - $p < 0.05$, **/++ - $p < 0.01$)

Phagocytosis of PF4/P75-coated *E. coli* incubated with anti-PF4/heparin antibodies by polymorphonuclear leukocytes

After showing that polyP can increase PF4 binding to bacteria, we analyzed whether polyP can also increase anti-PF4/heparin antibody-mediated bacterial phagocytosis by polymorphonuclear leukocytes (PMNs). Phagocytosis of *E. coli* increased by incubation with PF4 and anti-PF4/heparin antibody containing serum (Figure 4). Depending on the P75 concentration, the number of internalized bacteria increased with a maximum at 12.5 µg/mL and was inhibited at concentration higher than 50 µg/ml.

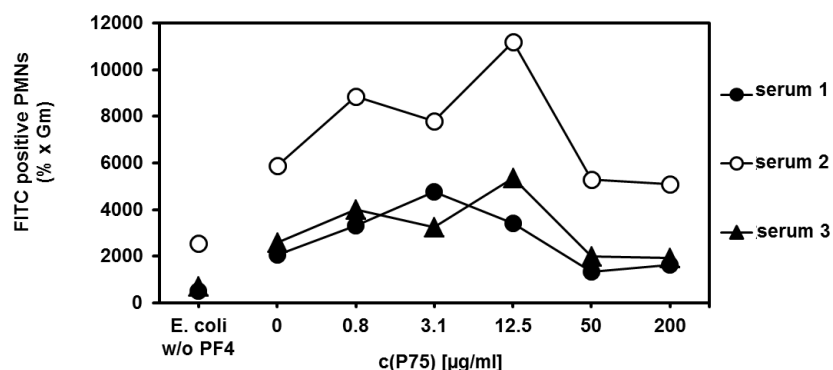


Figure 4: Phagocytosis of *E. coli* pretreated with PF4 or PF4/P75 complexes and anti-PF4/heparin antibody containing serum by polymorphonuclear leukocytes (PMNs) measured by flow cytometry. The figure shows the mean fluorescence intensity (MFI) multiplied by the percentage of FITC-positive PMNs as a measure for bacterial phagocytosis. Data are mean \pm SD of three independent experiments with three different sera and three different blood donors. (Significance levels: * $p < 0.05$)

Discussion

The main finding of this study is that polyP interact with the chemokine PF4, inducing a conformational change in PF4, which augments binding of anti-PF4/polyanion antibodies to PF4/polyP complexes on the bacterial surface. This identifies a new mechanism by which polyP contribute to an immune-mediated bacterial defense mechanism.²⁸

As we were interested in the role of platelet derived polyP, which contain polyP in the size range of 70-75 P_i⁴ or 60-100 P_i^{6,11} we selected polyP of 75-mer length for the primary experiment and a polyP 45-mer as well as a triphosphate to assess a potential impact of degradation of polyP by phosphatases. In accordance with previous data, which we obtained with carbohydrate based polyanions,^{24,30} and with nucleic acids,²⁶ only the longer polyP induced an increase in the antiparallel β -sheets exceeding 40% in the PF4 structure (45- and 75-mer polyP) and led to PF4/polyP complexes to which anti-PF4/heparin antibodies bound. Triphosphate (P3) was not able to induce conformational changes in the structure of PF4 and consistently, did not augment binding of anti-PF4/heparin antibodies. The short P3 did not even induce any signal in ITC when co-incubated with PF4. This shows that the changes in PF4 are not caused by addition of negative charges only but that the polyanion has to have a certain length. For polysaccharides, the critical length to induce conformational changes in PF4, which result in expression of the epitopes to which anti-PF4/heparin antibodies bind, is at about 10-12 carbohydrate units. For polyphosphates the critical length is between the triphosphate and the 45-mer. As released polyP is degraded (half-life of 1.5 to 2 hours),^{37,38} it was an interesting question, whether such smaller polyP molecules interfere with the positive charges on PF4, potentially acting as inhibitors of the interaction of longer polyP with PF4. This is obviously not the case for P45.

Polyphosphates increase PF4 binding to bacteria in a bell shaped curve (Figure 3). PF4 binds to lipid A, the basic structure of LPS on Gram negative bacteria even in the absence of polyP.²⁵ Addition of polyP increases binding of PF4 up to a concentration of 1.25 μ g/ml. At higher concentrations of polyP, PF4 binding decreases to the baseline and at concentrations above 5 μ g/mL, PF4 binding decreases below the baseline value. The explanation for this effect, which is similar to the one seen with sulfated carbohydrates and PF4 binding to platelets²⁹ and *E. coli*,²⁵ is the formation of complexes between polyP and PF4 at a certain stoichiometry. At higher concentrations, polyP saturates the positive PF4 binding sites, thereby inhibiting complex formation. At very high concentrations, polyP even competes with PF4 binding to lipid A, thereby decreasing PF4 binding to *E. coli* below the baseline values. Bacteria contain polyP³⁹ and release of polyP from bacteria might be a mechanism to counteract PF4 binding.

However, the optimal concentrations for PF4 binding to bacteria in vivo depend on both, the amount of PF4 and the amount of polyP, which may vary considerably depending on how many platelets are activated and release PF4.

Recently, Gray et al.² reported that polyP (45-1300 P_i units) stabilize proteins in vivo and protect a wide variety of proteins against stress-induced unfolding and aggregation in an ATP-independent manner. Our data obtained by CD spectroscopy and ITC clearly show that polyP also stabilize the conformation of PF4 which is important for bacterial host defense²⁸ in an ATP independent manner. This allows enhanced binding of anti-PF4/polyanion antibodies and increases phagocytosis of such opsonized pathogens by PMNs.

This let us to propose that polyP amplifies the host defense mechanism of PF4, which we have recently proposed after showing that PF4 binds to bacteria, forming complexes to which anti-PF4/heparin antibodies bind (Figure 5).

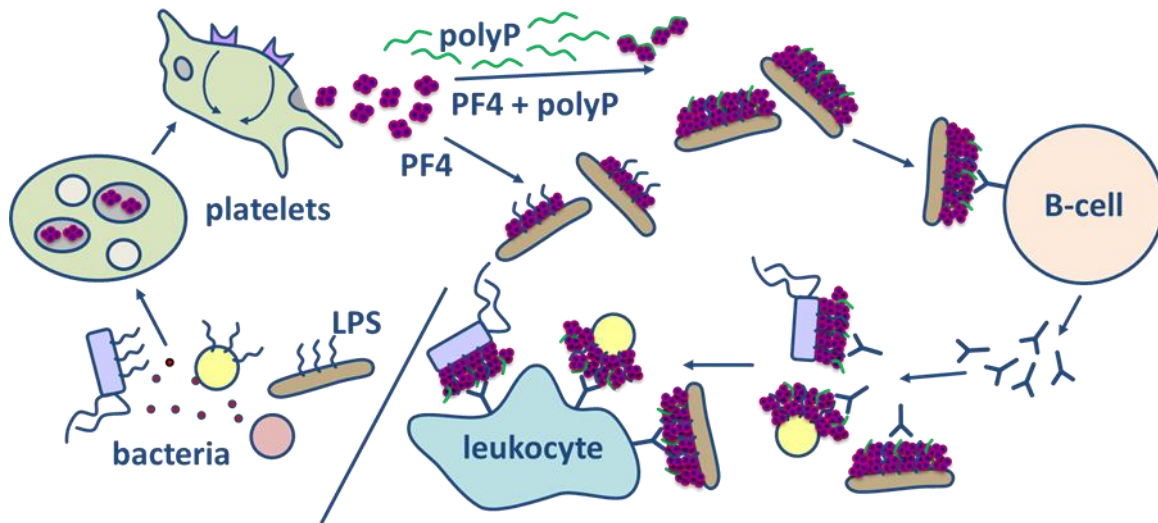


Figure 5: Schematic representation of the mechanism of how polyP mediate antibacterial host defense. Activated platelets release positively charged PF4 interacting with polyP at the bacterial surface. This generates antigenic PF4 clusters which initiate antibody production by B-cells. These antibodies can bind to all bacterial species which form PF4 clusters on their surface which facilitates phagocytosis.

As shown before, bacteria activate platelets by direct or indirect interaction.³⁸ This results in release of alpha granules which store PF4. PF4 then binds to lipid A (which consists of phosphate groups and glucosamine units) on the surface of Gram negative bacteria. This mechanism is now enhanced by polyP. Upon stronger platelet activation, not only alpha granules but also dense granules which store polyP are released. The polyP bind to PF4 and thereby enhance formation of multimolecular PF4/polyP complexes. This not only exposes additional binding sites for anti-PF4/polyanion antibodies, it makes PF4/polyP complexes also more accessible to anti-PF4/polyanion antibodies. PF4/polyanion complexes can reach a size >200 nm⁴⁰ in a linear form and a diameter of about 30 nm when they reach a globular form.^{30,41} The primary binding site of PF4 on Gram negative bacteria is lipid A,²⁵ the basic structure of LPS. The core structure of LPS has a height of 3.2 nm⁴² to which the O-antigen polysaccharide is attached, which is highly variable but may reach a length of 37 nm.⁴³ Thus IgG 1 antibodies, which have a height of ~8.5 nm,⁴⁴ bound to PF4 on lipid A may not extend their Fc part beyond the LPS cover impeding their recognition by Fc-receptors of leukocytes, while the Fc parts of antibodies bound to the larger PF4/polyP complexes are sterically completely free and can thereby better bind to Fc-receptors on granulocytes and macrophages.

We have observed in the EIA experiments, that anti-PF4/heparin antibodies gave a higher OD when PF4/P75 complexes were coated as compared to when PF4/P45 complexes were coated. A simple explanation for this might be that PF4/P75 complexes are larger and thereby allow more anti-PF4/heparin antibodies to bind than on the smaller PF4/P45 complexes. On the other hand, P75 did not enhance PF4 binding to bacteria more than P45. As platelet stored polyP are at least in the size range of P75 or longer, this in vitro difference between P45 and P75 observed in the EIA, likely has no major biological relevance.

In this regard, the well-established observation that patients whose platelets cannot store polyP due to a hereditary defect in platelet dense granule formation, typically suffer from colitis⁴⁵⁻⁴⁷ raises two potential

implications by which polyP may contribute to colitis. The first is disturbance of bacterial defense in the altered tissue of the colon which allows bacteria to invade, the other, however, is accumulation of PF4/polyP complexes in the tissue allowing activation of leukocytes, either directly or as immune-complexes when anti-PF4/heparin antibodies have bound.

In summary, our study provides a potential new biological function of polyP, i.e. augmentation of an immune mediated bacterial host defense mechanism. We show that polyP chain length influences the conformational changes induced in PF4 with polyP between 45- and 75-mers induce above 40% antiparallel β -sheets in PF4 and thereby, expose the binding site for anti-PF4/polyanion antibodies. We also show that polyP chain length influence the binding of PF4 to bacteria and its disruption from the bacterial surface. These findings may provide relevant aspects to understand the biological functions of polyP and give insights in their role as cofactor in an ancient immune system recognizing bacteria.

Acknowledgements

The authors would like to thank Dr. Marco Marenchino (GE Healthcare) for valuable discussion with ITC data interpretation. This work was supported by the German Ministry of Education and Research (BMBF) within the project FKZ 03Z2CN11. Krystin Krauel was supported by the Volkswagen Stiftung (Lichtenberg Professorship to Hansjörg Schwertz).

References

1. Achbergerova L, Nahalka J. Polyphosphate--an ancient energy source and active metabolic regulator. *Microb Cell Fact*. 2011;10:63.
2. Gray MJ, Wholey WY, Wagner NO, et al. Polyphosphate is a primordial chaperone. *Mol Cell*. 2014;53(5):689-699.
3. Rao NN, Gomez-Garcia MR, Kornberg A. Inorganic polyphosphate: essential for growth and survival. *Annual Review of Biochemistry*. 2009;78:605-647.
4. Ruiz FA, Lea CR, Oldfield E, Docampo R. Human platelet dense granules contain polyphosphate and are similar to acidocalcisomes of bacteria and unicellular eukaryotes. *Journal of Biological Chemistry*. 2004;279(43):44250-44257.
5. Herzberg MC, Krishnan LK, Macfarlane GD. Involvement of Alpha(2)-Adrenoceptors and G-Proteins in the Modulation of Platelet Secretion in Response to Streptococcus-Sanguis. *Critical Reviews in Oral Biology & Medicine*. 1993;4(3-4):435-442.
6. Muller F, Mutch NJ, Schenk WA, et al. Platelet polyphosphates are proinflammatory and procoagulant mediators in vivo. *Cell*. 2009;139(6):1143-1156.
7. Moreno-Sanchez D, Hernandez-Ruiz L, Ruiz FA, Docampo R. Polyphosphate Is a Novel Pro-inflammatory Regulator of Mast Cells and Is Located in Acidocalcisomes. *Journal of Biological Chemistry*. 2012;287(34):28435-28444.
8. Kornberg A, Rao NN, Ault-Riche D. Inorganic polyphosphate: A molecule of many functions. *Annual Review of Biochemistry*. 1999;68:89-125.
9. Morrissey JH. Polyphosphate: a link between platelets, coagulation and inflammation. *International Journal of Hematology*. 2012;95(4):346-352.

6. Appended papers
6.4 Paper IV: PF4/polyP

10. Morrissey JH, Choi SH, Smith SA. Polyphosphate: an ancient molecule that links platelets, coagulation, and inflammation. *Blood*. 2012;119(25):5972-5979.
 11. Smith SA, Mutch NJ, Baskar D, Rohloff P, Docampo R, Morrissey JH. Polyphosphate modulates blood coagulation and fibrinolysis. *Proceedings of the National Academy of Sciences of the United States of America*. 2006;103(4):903-908.
 12. Smith SA, Choi SH, Davis-Harrison R, et al. Polyphosphate exerts differential effects on blood clotting, depending on polymer size. *Blood*. 2010;116(20):4353-4359.
 13. Smith SA, Morrissey JH. Polyphosphate enhances fibrin clot structure. *Blood*. 2008;112(7):2810-2816.
 14. Mutch NJ, Engel R, de Willige SU, Philippou H, Ariens RAS. Polyphosphate modifies the fibrin network and down-regulates fibrinolysis by attenuating binding of tPA and plasminogen to fibrin. *Blood*. 2010;115(19):3980-3988.
 15. Choi SH, Smith SA, Morrissey JH. Polyphosphate is a cofactor for the activation of factor XI by thrombin. *Blood*. 2011;118(26):6963-6970.
 16. Wat JM, Foley JH, Krisinger MJ, et al. Polyphosphate suppresses complement via the terminal pathway. *Blood*. 2014;123(5):768-776.
 17. Nickel KF, Spronk HM, Mutch NJ, Renne T. Time-dependent degradation and tissue factor addition mask the ability of platelet polyphosphates in activating factor XII-mediated coagulation. *Blood*. 2013;122(23):3847-3849.
 18. Smith SA, Morrissey JH. Polyphosphate as a general procoagulant agent. *Journal of Thrombosis and Haemostasis*. 2008;6(10):1750-1756.
 19. Wolpe SD, Cerami A. Macrophage Inflammatory Protein-1 and Protein-2 - Members of a Novel Superfamily of Cytokines. *Faseb Journal*. 1989;3(14):2565-2573.
 20. Huang SS, Huang JS, Deuel TF. Proteoglycan Carrier of Human-Platelet Factor-4 - Isolation and Characterization. *Journal of Biological Chemistry*. 1982;257(19):1546-1550.
 21. Deuel TF, Keim PS, Farmer M, Heinrikson RL. Amino-Acid Sequence of Human Platelet Factor 4. *Proceedings of the National Academy of Sciences of the United States of America*. 1977;74(6):2256-2258.
 22. Rucinski B, Niewiarowski S, James P, Walz DA, Budzynski AZ. Antiheparin Proteins Secreted by Human Platelets - Purification, Characterization, and Radioimmunoassay. *Blood*. 1979;53(1):47-62.
 23. Kaplan KL, Broekman MJ, Chernoff A, Lesznik GR, Drillings M. Platelet Alpha-Granule Proteins - Studies on Release and Subcellular-Localization. *Blood*. 1979;53(4):604-618.
 24. Brandt S, Krauel K, Gottschalk KE, et al. Characterisation of the conformational changes in platelet factor 4 induced by polyanions: towards in vitro prediction of antigenicity. *Thromb Haemost*. 2014;112(1).
 25. Krauel K, Weber C, Brandt S, et al. Platelet factor 4 binding to lipid A of Gram-negative bacteria exposes PF4/heparin-like epitopes. *Blood*. 2012;120(16):3345-3352.
 26. Jaax ME, Krauel K, Marschall T, et al. Complex formation with nucleic acids and aptamers alters antigenic properties of platelet factor 4. *Blood*. 2013.
 27. Lo YM, Zhang J, Leung TN, Lau TK, Chang AM, Hjelm NM. Rapid clearance of fetal DNA from maternal plasma. *Am J Hum Genet*. 1999;64(1):218-224.
 28. Krauel K, Potschke C, Weber C, et al. Platelet factor 4 binds to bacteria, [corrected] inducing antibodies cross-reacting with the major antigen in heparin-induced thrombocytopenia. *Blood*. 2011;117(4):1370-1378.
-

29. Krauel K, Furl R, Warkentin TE, et al. Heparin-induced thrombocytopenia - therapeutic concentrations of danaparoid, unlike fondaparinux and direct thrombin inhibitors, inhibit formation of platelet factor 4-heparin complexes. *Journal of Thrombosis and Haemostasis*. 2008;6(12):2160-2167.
30. Kreimann M, Brandt S, Krauel K, et al. Interaction between Platelet Factor 4 and Heparins: Thermodynamic determines expression of the binding site for Anti-Platelet Factor 4/Heparin Antibodies. *Blood*, 2014 Aug 22; doi: blood-2014-03-559518.
31. Bohm G, Muhr R, Jaenicke R. Quantitative-Analysis of Protein Far Uv Circular-Dichroism Spectra by Neural Networks. *Protein Engineering*. 1992;5(3):191-195.
32. Juhl D, Eichler P, Lubenow N, Strobel U, Wessel A, Greinacher A. Incidence and clinical significance of anti-PF4/heparin antibodies of the IgG, IgM, and IgA class in 755 consecutive patient samples referred for diagnostic testing for heparin-induced thrombocytopenia. *European Journal of Haematology*. 2006;76(5):420-426.
33. Wiseman T, Williston S, Brandts JF, Lin LN. Rapid Measurement of Binding Constants and Heats of Binding Using a New Titration Calorimeter. *Analytical Biochemistry*. 1989;179(1):131-137.
34. Freire E, Mayorga OL, Straume M. Isothermal Titration Calorimetry. *Analytical Chemistry*. 1990;62(18):A950-A959.
35. Toumadje A, Alcorn SW, Johnson WC. Extending Cd Spectra of Proteins to 168 Nm Improves the Analysis for Secondary Structures. *Analytical Biochemistry*. 1992;200(2):321-331.
36. Sreerama N, Woody RW. Computation and analysis of protein circular dichroism spectra. *Numerical Computer Methods*, Pt D. 2004;383:318-351.
37. Lorenz B, Leuck J, Kohl D, Muller WE, Schroder HC. Anti-HIV-1 activity of inorganic polyphosphates. *J Acquir Immune Defic Syndr Hum Retrovirol*. 1997;14(2):110-118.
38. Lorenz B, Schroder HC. Mammalian intestinal alkaline phosphatase acts as highly active exopolyphosphatase. *Biochim Biophys Acta*. 2001;1547(2):254-261.
39. Whitehead MP, Eagles L, Hooley P, Brown MR. Most bacteria synthesize polyphosphate by unknown mechanisms. *Microbiology*. 2014;160(Pt 5):829-831.
40. Greinacher A, Gopinadhan M, Gunther JUG, et al. Close approximation of two platelet factor 4 tetramers by charge neutralization forms the antigens recognized by HIT antibodies. *Arteriosclerosis Thrombosis and Vascular Biology*. 2006;26(10):2386-2393.
41. Rauova L, Poncz M, McKenzie SE, et al. Ultralarge complexes of PF4 and heparin are central to the pathogenesis of heparin-induced thrombocytopenia. *Blood*. 2005;105(1):131-138.
42. Qiao S, Luo Q, Zhao Y, Zhang XC, Huang Y. Structural basis for lipopolysaccharide insertion in the bacterial outer membrane. *Nature*. 2014;511(7507):108-111.
43. Strauss J, Burnham NA, Camesano TA. Atomic force microscopy study of the role of LPS O-antigen on adhesion of E. coli. *J Mol Recognit*. 2009;22(5):347-355.
44. Tan YH, Liu M, Nolting B, Go JG, Gervay-Hague J, Liu GY. A nanoengineering approach for investigation and regulation of protein immobilization. *ACS Nano*. 2008;2(11):2374-2384.
45. Salvaggio HL, Graeber KE, Clarke LE, Schlosser BJ, Orlow SJ, Clarke JT. Mucocutaneous Granulomatous Disease in a Patient With Hermansky-Pudlak Syndrome. *JAMA Dermatol*. 2014.
46. Seward SL, Jr., Gahl WA. Hermansky-Pudlak syndrome: health care throughout life. *Pediatrics*. 2013;132(1):153-160.
47. Mora AJ, Wolfsohn DM. The management of gastrointestinal disease in Hermansky-Pudlak syndrome. *J Clin Gastroenterol*. 2011;45(8):700-702.

6.5 Paper V: Complex Formation with Nucleic Acids and Aptamers alters the antigenic Properties of Platelet Factor 4

Regular Article

THROMBOSIS AND HEMOSTASIS

Complex formation with nucleic acids and aptamers alters the antigenic properties of platelet factor 4

Miriam E. Jaax,¹ Krystin Krauel,^{1,2} Thomas Marschall,³ Sven Brandt,² Julia Gansler,⁴ Birgitt Füllr,¹ Bettina Appel,³ Silvia Fischer,⁴ Stephan Block,² Christiane A. Helm,⁵ Sabine Müller,³ Klaus T. Preissner,⁴ and Andreas Greinacher¹

¹Institut für Immunologie und Transfusionsmedizin, ²Zentrum für Innovationskompetenz Humorale Immunreaktionen bei kardiovaskulären Erkrankungen, and ³Institut für Biochemie, Ernst-Moritz-Arndt-Universität, Greifswald, Germany; ⁴Institut für Biochemie, Fachbereich Medizin, Justus-Liebig-Universität, Giessen, Germany; and ⁵Institut für Physik, Ernst-Moritz-Arndt-Universität, Greifswald, Germany

Key Points

- PF4 binds to nucleic acids and thereby exposes the epitope to which anti-PF4/heparin antibodies bind.
- PF4/apptamer complexes can induce an immune response resembling heparin-induced thrombocytopenia.

The tight electrostatic binding of the chemokine platelet factor 4 (PF4) to polyanions induces heparin-induced thrombocytopenia, a prothrombotic adverse drug reaction caused by immunoglobulin G directed against PF4/polyanion complexes. This study demonstrates that nucleic acids, including aptamers, also bind to PF4 and enhance PF4 binding to platelets. Systematic assessment of RNA and DNA constructs, as well as 4 aptamers of different lengths and secondary structures, revealed that increasing length and double-stranded segments of nucleic acids augment complex formation with PF4, while single nucleotides or single-stranded polyA or polyC constructs do not. Aptamers were shown by circular dichroism spectroscopy to induce structural changes in PF4 that resemble those induced by heparin. Moreover, heparin-induced anti-human-PF4/heparin antibodies cross-reacted with human PF4/nucleic acid and PF4/apptamer complexes, as shown by an enzyme immunoassay and a functional platelet activation assay.

Finally, administration of PF4/44mer-DNA protein C aptamer complexes in mice induced anti-PF4/apptamer antibodies, which cross-reacted with murine PF4/heparin complexes. These data indicate that the formation of anti-PF4/heparin antibodies in postoperative patients may be augmented by PF4/nucleic acid complexes. Moreover, administration of therapeutic aptamers has the potential to induce anti-PF4/polyanion antibodies and a prothrombotic diathesis. (*Blood*. 2013;122(2):272-281)

Introduction

The chemokine platelet factor 4 (PF4) is released from platelet α -granules during platelet activation¹ and binds, due to its high positive charge, to many negatively charged polyanions, including heparin. PF4 forms large multimolecular complexes with heparin that are highly immunogenic.^{2,3} The resulting immunoglobulin G (IgG) antibodies are the cause of heparin-induced thrombocytopenia (HIT), a prothrombotic adverse drug effect.⁴ In HIT, multimolecular complexes composed of PF4, heparin, and anti-PF4/heparin IgG cross-link platelet Fc γ IIa receptors,⁵ triggering platelet activation, microparticle formation, and thrombin generation, with ~50% of affected patients developing thrombosis.⁶

Recently, we showed that PF4 binds to polyanions on the surface of bacteria, thereby forming multimolecular complexes that are recognized by human anti-PF4/heparin antibodies. More specifically, we identified the PF4 binding site on gram-negative bacteria as the phosphate groups of lipid A.⁷ Based on this observation, we hypothesized that nucleic acids might also form multimolecular complexes with PF4 because they also expose multiple negatively charged phosphate groups. This idea was fostered by previous findings that salmon sperm DNA could substitute heparin in HIT-IgG-induced platelet activation.⁸

Plasma levels of extracellular nucleic acids are regulated by prompt nuclease degradation and renal clearance, resulting in their short half-life (4-30 minutes),⁹ with a slightly longer half-life for DNA than for RNA. In healthy individuals, extracellular nucleic acid concentrations in plasma range from 0 to >1000 ng/mL.¹⁰ However, under pathological conditions, cell-free nucleic acids can be generated from the breakdown of bacteria and viruses, tissue damage, cell apoptosis, and the release from blood cells such as the formation of neutrophil extracellular traps. Plasma levels of extracellular nucleic acids can rise up to 2000 μ g/mL.^{11,12}

With the recent introduction of aptamers, small DNA/RNA constructs designed as therapeutic oligonucleotides,¹³ the interaction of nucleic acids and PF4 becomes more relevant from a drug safety perspective. In this study, we characterized the structural features of RNA and DNA molecules, as well as aptamers, that are relevant for complex formation with PF4. We also demonstrated by circular dichroism (CD) spectroscopy that nucleic acids cause conformational changes in PF4 similar to those induced by heparin, and we showed that PF4/apptamer complexes can be highly immunogenic.

Submitted January 15, 2013; accepted April 21, 2013. Prepublished online as *Blood* First Edition paper, May 14, 2013; DOI 10.1182/blood-2013-01-478966.

M.E.J. and K.K. are equal first authors to this study, and K.T.P. and A.G. are equal last authors to this study.

There is an Inside *Blood* commentary on this article in this issue.

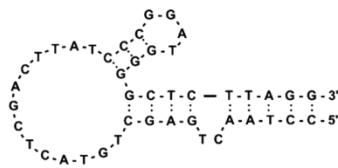
The publication costs of this article were defrayed in part by page charge payment. Therefore, and solely to indicate this fact, this article is hereby marked "advertisement" in accordance with 18 USC section 1734.

The publisher or recipient acknowledges right of the US government to retain a nonexclusive, royalty-free license in and to any copyright covering the article.

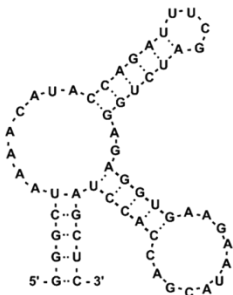
A Aptamers

5'-G-G-T-T-G-G-T-G-T-G-G-T-T-G-G-3'

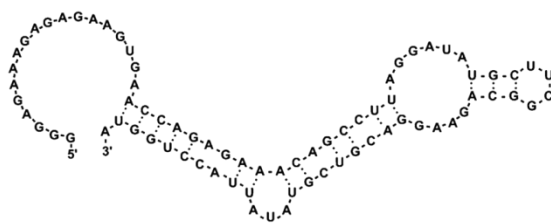
15mer-DNA thrombin aptamer¹



44mer-DNA protein C aptamer¹



57mer-RNA tetracycline aptamer²



77mer-RNA FMN aptamer²

D Linear double-stranded

5'-A-A-G-A-A-T-A-C-G-A-C-C-A-C-C-T-A-G-C-T-C-3'
3'-T-T-C-T-T-A-T-G-C-T-G-G-T-G-G-A-T-C-G-A-G-5'

21mer-double-stranded DNA¹

F Others

cellular RNA⁴

**Nucleotides (Deoxyribonucleotide-triphosphates:
ATP, CTP, GTP, TTP)**⁵

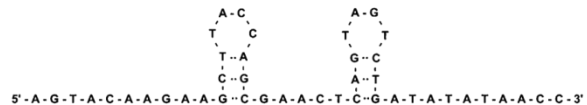
B Non – and minimally structured constructs

5'-G-T-T-A-A-T-T-A-T-C-3'

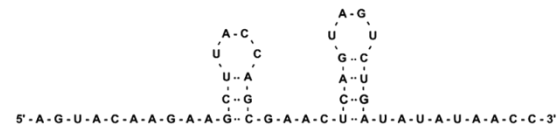
10mer-single-stranded DNA¹

5'-A-G-A-A-T-A-C-G-A-C-C-A-C-C-A-T-A-G-C-T-C-3'

21mer-single-stranded DNA¹



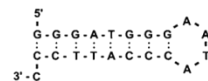
45mer-double stem-loop DNA¹



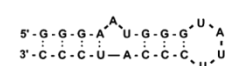
45mer-double stem-loop RNA I³

C

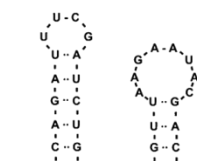
Complex structured constructs



21mer-hairpin DNA¹



21mer-hairpin RNA³



45mer-double stem-loop RNA II³

E Linear homopolymer constructs

[C-C-C-C-C-C-C-C-C-C]₅
45mer-polyC¹

[A-A-A-A-A-A-A-A-A-A]₅
45mer-polyA¹

Methods

Platelets and sera

Platelet-rich plasma was prepared from 10 mL hirudinized whole blood (10 µg/mL lepirudin; Pharmion, Hamburg, Germany) obtained from healthy blood donors (120 g, 20 minutes, 30°C). Platelets were isolated by gel filtration as described in Krauel et al¹⁴ and adjusted to 50 × 10⁹/L in Tyrode buffer (137 mM sodium chloride, 2.7 mM potassium chloride, 2 mM

magnesium chloride × 6 water, 2 mM calcium chloride × 2 water, 12 mM sodium bicarbonate, 0.4 mM sodium phosphate monobasic, 0.4% bovine serum albumin [BSA], and 0.1% glucose, pH 7.2). Sera containing anti-PF4/heparin antibodies were leftovers from clinical specimens used for laboratory diagnosis of HIT.

Nucleic acids and aptamers

Sequences and sources of aptamers and nucleic acid compounds are given in Figure 1. Secondary structures were calculated by the mfold RNA and

Figure 1. The structures of aptamers, DNA and RNA constructs, and nucleotides are shown. Indicated compounds used in this study are¹ (A-E) chemically synthesized by a commercial supplier (PURIMEX, Grebenstein, Germany),² (A) enzymatically transcribed in vitro from oligonucleotide templates using T7 RNA polymerase,³ (B and C) chemically synthesized in house using the phosphoramidite method (Gene Assembler Special, Pharmacia Biotech, Freiburg, Germany),⁴ (F) isolated from mouse vascular smooth muscle cells using an extraction kit (Sigma, Munich, Germany) or the DNAzol reagent (Invitrogen, Groningen, The Netherlands),⁵ or (F) purchased from Fermentas (St. Leon-Rot, Germany).

mfold DNA database of the University of Albany (NY, <http://mfold.rna.albany.edu/?q=mfold>). The single-stranded 15mer-DNA thrombin aptamer targets thrombin¹⁵; the 44mer-DNA protein C aptamer inhibits activated protein C¹⁶; the 57mer-RNA tetracycline aptamer binds tetracycline¹⁷; and the 77mer-RNA flavin mononucleotide (FMN) aptamer is an artificial FMN-responsive catalytic RNA.¹⁸ Cellular RNA and DNA were isolated from mouse vascular smooth muscle cells using an extraction kit (Sigma, Munich, Germany) or the DNAzol reagent (Invitrogen, Groningen, The Netherlands).

Binding of biotinylated RNA to PF4

Microtiter plates were coated with 50- μ L solutions of PF4 or BSA (each at 10 μ g/mL) in 100 mM sodium carbonate (pH 9.5) at 4°C for 20 hours, then washed and blocked (Tris-buffered saline, 3% BSA; 2 hours). Different concentrations of biotinylated RNA (0.78–25 μ g/mL), prepared from isolated cellular RNA using the Psoralen-PEO-Biotin reagent (Thermo Fisher Scientific [Pierce], Rockford, NY), were allowed to bind at 22°C for 2 hours, followed by 3 washes with Tris-buffered saline. Bound biotinylated RNA was detected using peroxidase-conjugated streptavidin (Dako, Glostrup, Denmark) and the immunopure 3,3',5,5'-tetramethylbenzidine substrate kit (Pierce). In competition experiments, increasing concentrations of biotinylated RNA were mixed with unlabeled RNA, DNA, or heparin (each at 300 μ g/mL) before binding assays were performed. To confirm that PF4 was not removed from the plate upon heparin addition, surface-coated PF4 was quantified by dot blot analysis and densitometry.

Influence of nucleic acids on PF4 binding to platelets

The impact of nucleic acids on the binding of human platelet-derived PF4 (25 μ g/mL) (ChromaTec, Greifswald, Germany) to gel-filtered platelets (50 000/ μ L) was assessed by flow cytometry (Cytomics FC 500; Beckman Coulter, Krefeld, Germany) using a polyclonal fluorescein isothiocyanate-labeled rabbit anti-human PF4 antibody (Dianova, Marl, Germany),¹⁴ in the absence or presence of unfractionated heparin (UFH; activity ~150 IU/mg; Braun, Melsungen, Germany) or different nucleic acid compounds (0.08–640 μ g/mL; Figure 1). In parallel, RNA samples were treated with ribonuclease A (RNase A) (100 μ g/mL, 90 minutes, 37°C) (Fermentas, St. Leon-Rot, Germany) before addition to the respective test solution to document RNA dependency. Antibody binding was quantified by geometric mean fluorescent intensity.

PF4/nucleic acid EIA

Binding of human anti-PF4/heparin IgG to PF4/nucleic acid complexes was assessed by enzyme immunoassay (EIA)¹⁹ using microtiter plates (Nunc, Langensfeld, Germany) coated (16 hours; 4°C) with preformed PF4/polyanion complexes: PF4 (20 μ g/mL) preincubated (1 hour, room temperature) with either UFH as the positive control (3.33 μ g/mL), 15mer-DNA thrombin aptamer, 44mer-DNA protein C aptamer, 57mer-RNA tetracycline aptamer, or 77mer-RNA FMN aptamer in concentrations ranging from 1.25 to 80 μ g/mL. To find the optimal stoichiometric ratios for complex formation, we first titrated selected aptamers in the presence of a constant PF4 concentration in the EIA. As the control for specific antibody binding, UFH (660 μ g/mL) was added to disrupt PF4/polyanion complexes and to inhibit antibody binding.

Platelet activation assay

Platelet activation by human anti-PF4/polyanion antibodies was assessed by the heparin-induced platelet activation assay, as described in Warkentin and Greinacher,²⁰ using 0.2 μ g/mL heparin (positive control: riviparin; Abbott GmbH & Co KG, Wiesbaden, Germany), deoxynucleotidetriphosphates (0.05–1000 μ g/mL), 21mer-double-stranded DNA (0.05–1000 μ g/mL), 21mer-hairpin DNA (0.05–1000 μ g/mL), cellular RNA (0.05–5 μ g/mL), 15mer-DNA thrombin aptamer (0.5–40 μ g/mL), 44mer-DNA protein C aptamer (0.05–1000 μ g/mL), 57mer-RNA tetracycline aptamer (0.5–5 μ g/mL), and 77mer-RNA FMN-ribozyme (0.5–5 μ g/mL). To find the optimal concentrations for platelet activation, titration with the respective nucleic acid constructs in the heparin-induced platelet activation test with 1 or 2 sera was

performed, and then additional sera were assessed using this concentration. Specificity of platelet activation was confirmed by its inhibition using high concentrations of heparin (660 μ g/mL), which disrupts PF4/polyanion complexes,²¹ as well as the monoclonal antibody IV.3 (2.5 μ g/mL; LGC Promochem, Wesel, Germany), which blocks Fc γ IIa receptor-mediated platelet activation.²²

CD spectroscopy of PF4/polyanion complexes

Conformational changes of PF4 (40 μ g/mL) were measured by far-UV CD spectroscopy (200–260 nm; Chirascan CD spectrometer; Applied Photophysics, Leatherhead, United Kingdom) at increasing concentrations of heparin (6.66–73.33 μ g/mL), or 44mer-DNA protein C aptamer (0.31–40 μ g/mL) in a 101-QS quartz precision cell (path length: 10 mm) (Hellma, Muellheim, Germany). Baseline spectra of phosphate-buffered saline, heparin, and 44mer-DNA protein C aptamer were subtracted to estimate secondary structures of the respective PF4/heparin or PF4/apptamer complexes (CDNN CD Spectra Deconvolution Software).²³

Immunization of mice by PF4/apptamer complexes

C57BL/6 mice (8–10 weeks of age; Charles River Laboratories Europe, Kisslegg, Germany) were anesthetized (2% xylazine/10% ketamine) and immunized as described in Suvarna et al²⁴ with recombinant murine PF4 (mPF4) (ChromaTec, Greifswald, Germany), 44mer-DNA protein C aptamer, mPF4/44mer-DNA protein C aptamer complexes (each at 200 μ g/mL), or complexes of mPF4 (200 μ g/mL) and heparin (33 μ g/mL) in a final volume of 100 μ L via retroorbital injection daily for 5 days. After another 10 days, blood was withdrawn and serum was analyzed for anti-mPF4/apptamer or anti-mPF4/heparin antibodies, respectively, by EIA using mPF4/heparin and mPF4/44mer-DNA protein C aptamer complexes as antigens.

Ethics

All blood donors gave informed consent. The use of antibodies from leftovers of clinical diagnostic material was approved by the ethical board of Greifswald University. The animal studies were performed and approved according to the regulations of Greifswald University.

Statistical analysis

Binding of biotinylated RNA to PF4 in the presence of competing polyanions was compared using paired samples Student *t* test. The significance of differences in the impact on PF4 binding to platelets between nucleic acids was tested by analysis of variance and paired samples Student *t* test (RNase experiment). Reduction of antibody binding in the PF4/polyanion immunoassays after the heparin inhibition step was assessed by paired samples Student *t* test. Murine immune responses to mPF4/44mer-DNA protein C aptamer complexes and mPF4 were compared by Wilcoxon 2-sample test. The significance level was .05.

Results

RNA binds to PF4

The binding of RNA to PF4 was assessed using biotinylated RNA, which bound to PF4 in a saturable manner, reaching a maximum at 6.25 μ g/mL (Figure 2). High concentrations of unlabeled RNA, DNA, or heparin decreased the binding of biotinylated RNA to PF4, with heparin showing the strongest inhibitory effect, followed by RNA and DNA. This indicates charge-dependent binding of RNA to PF4.

RNA and DNA enhance PF4 binding to platelets

Next we assessed the interaction of PF4 and different nucleic acid constructs with gel-filtered platelets by flow cytometry, as previously described in Krauel et al¹⁴ for PF4-polysaccharide-platelet

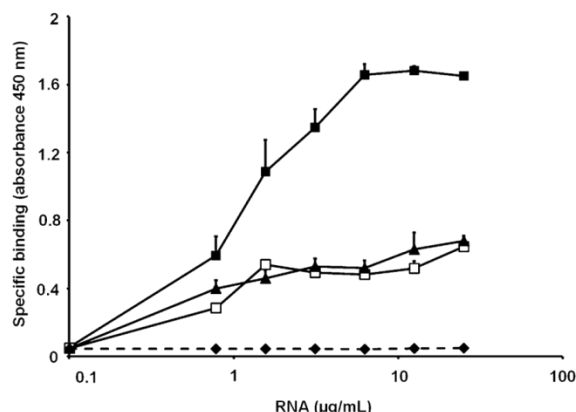


Figure 2. The graph shows the binding of biotinylated RNA to PF4 and the influence of competitors. The binding of increasing doses of biotinylated RNA to surface-coated PF4 was performed in the absence (■) or presence of excess DNA (▲), nonbiotinylated RNA (□), or heparin (◆). Values represent mean \pm standard deviation (SD) of 3 independent experiments.

interactions. To analyze the structure-function relationship, RNA and DNA constructs of different length and structural complexity were tested. Figure 3 shows the influence of these constructs on PF4 binding to the platelet surface, whereby baseline binding was defined as PF4 binding to platelets in the absence of nucleic acids. Heparin, the prototype compound for PF4-polyanion interaction, increased PF4 binding to platelets in a dose-dependent manner, represented by a bell-shaped curve with a maximal 4.44-fold increase (± 0.15 , shown as the gray curve in Figure 3A-D).

Cellular RNA exhibited a similar effect on PF4 binding to platelets as heparin, with a maximal 3.69-fold increase (± 1.09 ; Figure 3A) at $0.63 \mu\text{g/mL}$. This was almost completely abrogated by pretreatment with RNase A (1.25-fold increase ± 0.29 ; $P = .0037$, $n = 3$; Figure 3A).

Enhancement of PF4 binding to the platelet surface by DNA or RNA was dependent on the size of the nucleic acid construct: shorter constructs (10mer–single-stranded DNA; 21mer–hairpin RNA) showed a weaker effect and required higher concentrations than longer constructs (45mer–double-stem-loop RNA II; Figure 3B). RNA compounds appeared to have a stronger effect on PF4 binding than DNA homologs, as exemplified by the 45mer–double-stem-loop RNA I, which induced binding of more PF4 to platelets, compared with the 45mer–double-stem-loop DNA ($P < .0001$; Figure 3C), although both 45mers had the same nucleotide sequence (RNA, however, contained uridine and ribose instead of thymidine and deoxyribose).

In contrast to the structured 45mers, the unpaired homopolymers 45mer–polyA and 45mer–polyC, or single nucleotides, did not promote PF4 binding to platelets (Figure 3C). Furthermore, the influence of 3 DNA 21mers with distinct secondary structures (Figure 1B-D) on PF4 binding was analyzed: the 21mer–double-stranded DNA showed the strongest enhancement on PF4 binding to platelets ($P < .0001$; Figure 3D), while the 2 single-stranded constructs were far less effective. PF4 binding increased with the structural complexity of the nucleic acid construct (compare 21mer–hairpin vs 21mer–single-stranded DNA, $P < .0001$; Figure 3D), indicating that interactions of nucleic acids with PF4 were not only charge dependent but determined by their conformation.

Aptamers enhance PF4 binding to platelets

We then investigated the influence of 4 different aptamers (Figure 1A) on PF4 binding to the platelet surface. All 4 aptamers enhanced

PF4 binding to gel-filtered platelets; however, maximal PF4 binding in each case occurred at different concentrations of the respective aptamer: the 57mer–RNA tetracycline aptamer (2.48-fold increase ± 0.63 ; Figure 4A) and the 77mer–RNA FMN aptamer (2.07-fold increase ± 0.52 ; Figure 4B) induced maximal PF4 binding to platelets at similar concentrations ($0.63 \mu\text{g/mL}$). However, maximal enhancement of PF4 binding by these aptamers was lower than that induced by heparin. The 44mer–DNA protein C aptamer induced maximal enhancement of PF4 binding (2.59-fold increase ± 0.35) at a greater than 10-fold higher concentration of $5 \mu\text{g/mL}$ (Figure 4C), whereas the short 15mer–DNA thrombin aptamer enhanced PF4 binding only at very high concentrations (at $320 \mu\text{g/mL}$: 3.57-fold increase ± 1.1 ; Figure 4D).

Aptamer-induced changes in PF4 resemble those induced by heparin

The impact of nucleic acids on the secondary structure of PF4 was analyzed using CD spectroscopy. The 44mer–DNA protein C aptamer was used due to its nuclease resistance. Although changes in the PF4 structure induced by complex formation with the 44mer–DNA protein C aptamer were similar to those induced by heparin, the most pronounced alterations of PF4 were observed at broader ranges of 44mer–DNA protein C aptamer ($5\text{--}20 \mu\text{g/mL}$) compared with that seen with heparin ($6.9\text{--}7.2 \mu\text{g/mL}$; Figure 5A).

Deconvolution of the spectra of PF4 obtained after the addition of $5 \mu\text{g/mL}$ 44mer–DNA protein C aptamer or $6.9 \mu\text{g/mL}$ heparin showed an increase in anti-parallel β sheet content from 24.2% to 34.3% for heparin and to 35.8% for the 44mer–DNA protein C aptamer. This refolding was balanced by a decrease of the α helix fraction from 12.2% to 8.9% (heparin) and to 8.1% (44mer–DNA protein C aptamer) and a decrease in the β -turn fraction from 22.8% to 19.8% (heparin) and 20.5% (44mer–DNA protein C aptamer). Parallel β sheet and random coil content did not change significantly.

Human anti-PF4/heparin antibodies bind to PF4/nucleic acid complexes

To assess whether complex formation between aptamers and PF4 also results in exposure of the same epitopes as on PF4/heparin complexes, we tested human sera known to contain anti-PF4/heparin IgG by EIA. Antibody binding to PF4/heparin (positive control) resulted in a mean optical density (OD) of 1.130 ± 0.143 . Anti-PF4/heparin antibodies bound differently to complexes formed by PF4 and distinct aptamers. They reacted only very weakly with PF4/15mer–DNA thrombin aptamer complexes (at $40 \mu\text{g/mL}$: mean OD: 0.431 ± 0.064 ; Figure 5D) but strongly with PF4/44mer–DNA protein C aptamer complexes over a broad concentration range ($5\text{--}30 \mu\text{g/mL}$ aptamer per $20 \mu\text{g/mL}$ PF4; mean OD: 1.098 ± 0.140 ; Figure 5D). Binding was significantly reduced by the addition of high concentrations of heparin (mean OD: 0.593 ± 0.203 , $P < .0001$; Figure 5D). (Marked inhibition of antibody binding against PF4/polyanion complexes at high concentrations of heparin is a characteristic feature of anti-PF4/polyanion antibody binding.)

Less pronounced binding was observed with PF4/57mer–RNA tetracycline aptamer complexes (at $20 \mu\text{g/mL}$: mean OD: 0.819 ± 0.115 ; Figure 5D) and PF4/77mer–RNA FMN aptamer complexes (at $10 \mu\text{g/mL}$: mean OD: 0.910 ± 0.190 ; Figure 5D). Control sera did not react with any PF4/nucleic acid complexes (OD range: $0.02\text{--}0.28$, $n = 11$, data not shown in the figure).

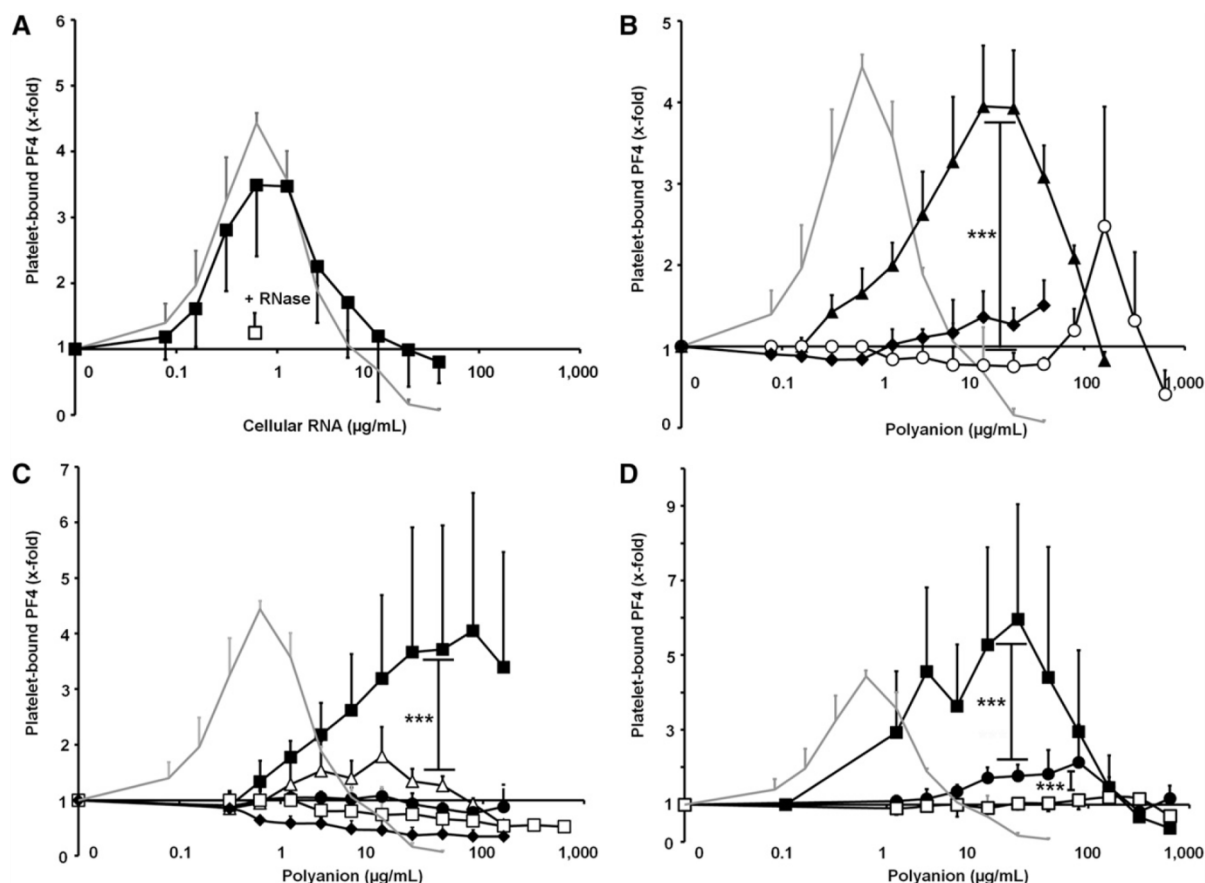


Figure 3. The influence of differently structured nucleic acid compounds on PF4 binding to platelets is shown. (For details of the nucleic acid constructs, please compare with Figure 1B-F.) Enhancement of PF4 binding is expressed as the x-fold increase compared with PF4 binding to platelets in buffer only. Heparin (gray line) was used as the positive control. (A) PF4 binding to platelets was performed in the presence of increasing doses of cellular RNA (■). Pretreatment with RNase A (□) significantly reduced PF4 binding to platelets ($P = .0037$). (B) PF4 binding to platelets was evaluated in the presence of increasing doses of nucleic acids with different lengths: 45mer-double-stem-loop RNA II (▲), 21mer-hairpin RNA (○), and 10mer-single-stranded DNA (◆). (C) PF4 binding to platelets was performed with increasing doses of 45mer-nucleic acid compounds, comprising different structures: 45mer-double stem-loop RNA I (■), 45mer-double stem-loop DNA (△), 45mer-polyA (●), 45mer-polyC (◆), and single nucleotides (□). (D) PF4 binding to platelets was measured in the presence of increasing doses of double-stranded vs single-stranded 21mer-DNA compounds: 21mer-double-stranded DNA (■), 21mer-hairpin DNA (●), and 21mer-single-stranded DNA (□). Enhancement of PF4 binding is expressed as the x-fold increase of PF4 binding compared with platelets in buffer only. Negative values indicate detachment of PF4 from the platelet surface below the baseline value. All data represent mean \pm SD of 3 independent experiments. *** $P < .001$.

Human anti-PF4/heparin antibodies induce platelet activation in the presence of nucleic acids and aptamers

Among 29 human sera that caused platelet activation in the presence of heparin, 18 (62.1%) also caused platelet activation in the presence of nucleic acids. These 18 sera induced platelet aggregation in the presence of all nucleic acid constructs, including aptamers, but not in the presence of buffer. Mean lag time to platelet activation was slightly longer for the nucleic acid constructs (12.69 ± 2.84 minutes) than for heparin (10.73 ± 6.27 minutes), with only minor differences between the single constructs (Figure 5B). Mean reactivity with donor platelets (ie, the platelets of how many donors reacted) was also lower for the nucleic acids (85.31%) than for heparin (93.22%), with the 15mer-DNA thrombin aptamer showing the lowest reactivity (Figure 5C). Platelet aggregation was consistently inhibited by high concentrations of heparin as well as by the monoclonal antibody IV.3.²² In contrast to heparin, the nucleic acid constructs induced platelet aggregation over a wide concentration range (0.005-100 $\mu\text{g/mL}$). Consistent with what is known from heparin, very high concentrations of nucleic acids exceeding 1000 $\mu\text{g/mL}$ inhibited

platelet aggregation. None of the control sera ($n = 9$) induced platelet activation in the presence of heparin or any nucleic acid construct.

PF4/aptamer complexes induce anti-PF4/polyanion antibodies in vivo

In mice, mPF4/44mer-DNA protein C aptamer complexes induced a strong and robust immune response within 15 days in all animals (median OD: 2.39, range: 1.96-2.61, $n = 5$; Figure 5E). These antibodies cross-reacted against mPF4/heparin complexes (median OD: 1.73, range 1.10-2.13, $n = 5$; Figure 5E). Mice immunized with mPF4/heparin complexes (positive control) showed an immune response against mPF4/heparin complexes (median OD: 1.58, range: 0.61-2.76, $n = 7$). Injection of the aptamer alone did not induce antibody formation with the exception of 1 animal (median OD: 0.20, range: 0.10-1.39; Figure 5E). Immunization with mPF4 alone also caused an immune response (median OD: 0.84, range: 0.32-2.52; Figure 5E), but this was significantly weaker than the immunization induced by mPF4/44mer-DNA protein C aptamer complexes

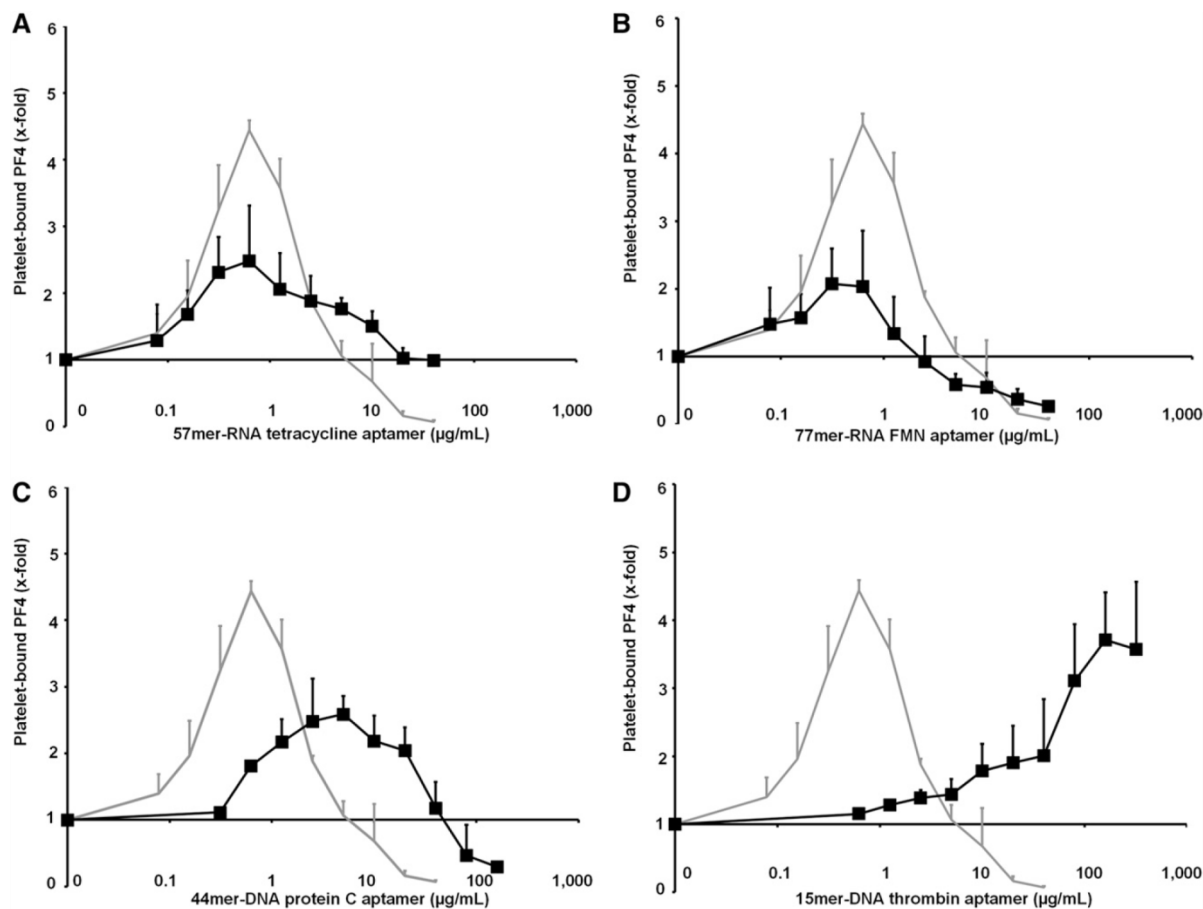


Figure 4. The influence of aptamers on PF4 binding to platelets is shown. (For details of aptamer structure, please compare with Figure 1A.) The following 4 aptamers (■) were tested in increasing doses for promoting PF4 binding to platelets in comparison with heparin (gray line) as the positive control: (A) 57mer-RNA tetracycline aptamer, (B) 77mer-RNA FMN aptamer, (C) 44mer-DNA protein C aptamer, and (D) 15mer-DNA thrombin aptamer. All data represent mean \pm SD of 3 independent experiments. The figures indicate that PF4 binding to platelets correlates with the length and the size of double-stranded domains of the aptamers.

($P = .015$). The reason for an immune response to mPF4 alone is most likely the formation of some mPF4 autoaggregates resembling mPF4/aptamer complexes, as mPF4 tends to form spontaneous complexes in buffers with low salt concentrations (unpublished observations of our group). Antibody binding was always inhibited by the addition of high concentrations of heparin.

Discussion

In this study, we demonstrated a charge- and structure-related interaction between PF4 and nucleic acids and we characterized the functional properties of these multimolecular complexes. Nucleic acids induced structural changes in the PF4 molecule similar to those typically observed in PF4/heparin complexes. These structural changes resulted in the exposure of neoepitopes that were recognized by a subset of platelet-activating anti-PF4/heparin antibodies. Moreover, PF4/aptamer complexes induced antibodies in mice, which cross-reacted with PF4/heparin complexes.

It is well known that PF4 forms complexes with polyanions other than heparin, such as dextran sulfate, pentosan polysulfate, polyvinyl sulfonate, hypersulfated chondroitin sulfate, and PI-88 (investigational antiangiogenic drug).²⁵⁻²⁷ The formation of epitopes

on these complexes that are recognized by anti-PF4/heparin antibodies is dependent on critical structural features of the polyanions, for example, charge density,^{26,28,29} length,^{26,28} and charge clustering, such as those that occur on branched polysaccharides.²⁶ Nucleic acids express charged oxygens (O^-) of phosphate groups that are spaced 0.5 to 0.7 nm apart.^{30,31} These dimensions are similar to the known critical charge density of sulfated polysaccharides, in which sulfates are spaced about 0.5 nm apart along the carbohydrate backbone.²⁷ Thus, the surface-exposed phosphate residues in RNA and DNA compounds most likely serve as binding partners for PF4. In fact, polysaccharides in which sulfate groups were substituted by phosphates were demonstrated to bind to PF4, indicating strong PF4-phosphate interaction.²⁷ Moreover, the phosphate groups of lipid A as a component of lipopolysaccharide also interact with PF4.⁷

Besides charge density, the size of nucleic acids appears to be critical for enhancing the binding of PF4 on the platelet surface. Longer constructs augmented PF4 binding to platelets (Figure 3B), while single nucleotides added at the same concentration did not. Similarly, disaccharides do not bind to PF4, and the synthetic pentasaccharide, fondaparinux, binds only weakly to PF4.^{32,33}

Although nucleic acids seem to share some similarities with heparins in regard to their polyanion character, the structure-function relationships for interactions between PF4 and nucleic acids appear to be more complicated. Other than heparins, nucleic acids can fold

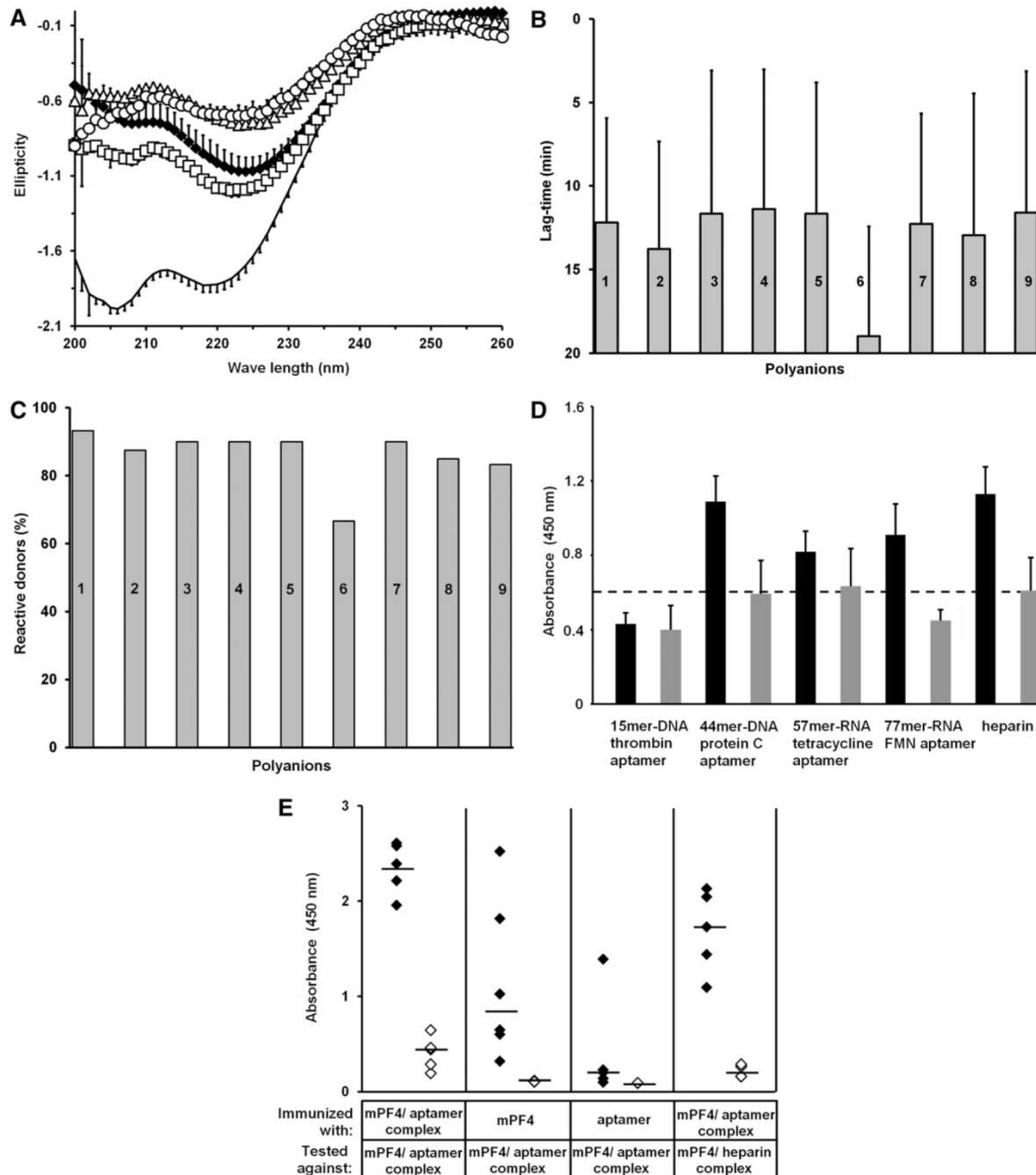


Figure 5. Aptamer-induced changes in PF4 lead to expression of PF4/heparin-like epitopes. (A) Shown are structural changes in PF4 induced by the 44mer-DNA protein C aptamer. Changes in the CD pattern of PF4 (20 µg/mL) are shown in the absence (n = 4, black line) or presence of either heparin (n = 3, 6.9 µg/mL, ♦) or 44mer-DNA protein C aptamer at different doses (n = 2 each, 2.5 µg/mL, □; 5 µg/mL, Δ; 20 µg/mL, ○). Note that the changes in PF4 spectra are rather similar, regardless whether heparin or the aptamer was used. All data represent mean ± SD of n independent experiments. Each experiment consists of at least 5 measurements. (B-C) Human anti-PF4/heparin antibodies induce platelet activation in the presence of nucleic acids and aptamers. (B) Mean lag time until aggregation of donor platelets (at least n = 15 for each polyanion) and (C) reactivity of donor platelets expressed as the percentage of all tested donor platelets were analyzed in the presence of different anti-PF4/heparin antibody-containing sera (at least 4 for each polyanion) and either riviparin (0.2 µg/mL, bar 1), cellular RNA (0.5 µg/mL, bar 2), 21mer-double-stranded DNA (0.5 µg/mL, bar 3), 21mer-hairpin DNA (0.5 µg/mL, bar 4), 44mer-DNA protein C aptamer (8 µg/mL, bar 5), 57mer-RNA tetracycline aptamer (5 µg/mL, bar 6), or 77mer-RNA FMN-ribozyme (2.5 µg/mL, bar 7). Except for the short 15mer-DNA thrombin aptamer, which induces platelet aggregation after 19.0 ± 0.67 minutes and only in 66.6% of all donors, lag time and reactivity of platelets show only minor differences between the constructs. (D) The graph shows the binding of anti-PF4/heparin antibodies to PF4/aptamer complexes. Anti-PF4/heparin antibodies bind to complexes generated with 20 µg/mL PF4 and either 44mer-DNA protein C aptamer (20 µg/mL, n = 9), 57mer-RNA tetracycline aptamer (10 µg/mL, n = 4), 77mer-RNA FMN aptamer (10 µg/mL, n = 4), or heparin (3.3 µg/mL, n = 9, black bars), while no binding to complexes of PF4 and the 15mer-DNA thrombin aptamer (0.5 µg/mL, n = 4) occurred. Gray bars show the inhibition of binding by high heparin (660 µg/mL). All data represent mean ± SD of at least 4 independent experiments. (E) Shown is the immune response to PF4/aptamer complexes in mice. Mice were immunized with either mPF4/44mer-DNA protein C aptamer complexes (n = 5), mPF4 alone (n = 6), or 44mer-DNA protein C aptamer alone (n = 6), and the binding of antibodies from the respective sera to mPF4/44mer-DNA protein C aptamer complexes as well as mPF4/heparin complexes was assessed by EIA in the absence (♦) or presence (○) of 660 µg/mL heparin. Median values are marked by black lines.

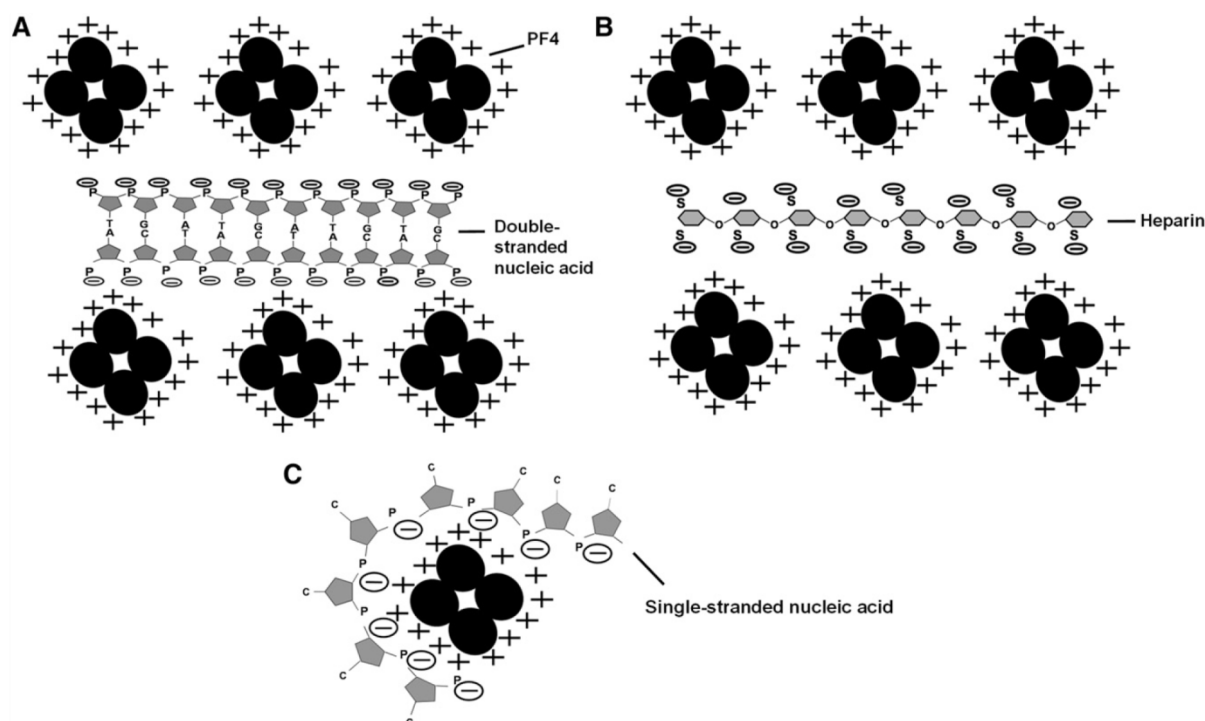


Figure 6. A schematic model of complex formation between PF4 and nucleic acids is shown. (A) The basic amino acid residues (+) in the PF4 tetramer interact with the negatively charged phosphate groups (–) in double-stranded nucleic acids, thereby forming large multimolecular complexes. (B) PF4 binds to the negatively charged sulfate groups (–) on both sides of the heparin molecule, resulting in the formation of large multimolecular complexes. (C) Due to their high flexibility, single-stranded nucleic acids potentially wrap around PF4 tetramers, thereby inhibiting the formation of large, multimolecular complexes with PF4.

into highly organized structures, for example, those exhibiting spatial clustering of negative charges. While several RNA and DNA constructs formed complexes with PF4, the linear homopolymers 45mer-polyA and 45mer-polyC did not (Figure 3), although they were above the critical length and showed a high charge density. Thus, double-stranded domains within nucleic acids seem to be important for binding to PF4. This is in line with our recent observations that double-stranded hairpin-forming, but not single-stranded, nucleic acid oligomers are also potent activators of the intrinsic coagulation pathway by interacting with the RNA-binding cofactor high molecular weight kininogen.³⁴

Figure 6 depicts a simplified model of the interaction between PF4 and nucleic acids: the negatively charged phosphate residues along the backbone of double-stranded nucleic acids bind to PF4, just as PF4 binds to the sulfate groups of heparin (Figure 6A-B). In contrast, due to their higher flexibility and the loose spatial arrangement of negative charges, single-stranded nucleic acids are more likely to wrap around 1 PF4 tetramer instead of bridging several PF4 tetramers (Figure 6C). This is mediated by interactions of their phosphate groups with positively charged amino acid residues of PF4, as it has already been described for polysaccharides comprising >34 sugar units.³⁵

However, the molecular interactions are likely more complex, and certain conformations of nucleic acids appear to be more prone than others to forming multimolecular complexes with PF4. One example is the reactivity of the 44mer-DNA protein C aptamer vs the 77mer-RNA FMN aptamer. Although the latter is much longer and has more double-stranded segments (Figure 1A), anti-PF4/heparin antibodies bound somewhat more strongly to PF4/44mer-protein C aptamer complexes (Figure 5D).

Our data raise further questions beyond the scope of the current study. It remains unclear why only about 60% of the anti-PF4/heparin antibodies that induced platelet activation in the presence of heparin also caused platelet activation in the presence of nucleic acids. Even more puzzling is our observation that those sera that induced platelet activation in the presence of nucleic acids did so with most nucleic acids, independent of whether these strongly enhanced PF4 binding to the platelet surface or not. In the absence of a 3-dimensional model of the structural changes of PF4 induced by different nucleic acids, we can only speculate that the nucleic acids may expose different epitopes than heparins do.

Another hypothetical explanation could be based on the recent studies of Sachais et al,³⁶ showing that the monoclonal antibody KKO, but not another anti-PF4 monoclonal antibody, is also able to induce oligomerization of PF4 in the absence of heparin, suggesting that some anti-PF4/heparin antibodies are capable of promoting further formation of their own antigen.³⁷ Following this concept, sera causing platelet activation in the presence of nucleic acids might contain antibodies that, like KKO, can cross-link PF4 molecules. In this case, the negative charge of nucleic acids would initiate antigen formation by allowing close approximation of PF4 molecules, which would be sufficient for further oligomerization of PF4 by such anti-PF4/heparin antibodies. Unfortunately, we cannot readily test these hypotheses experimentally due to the polyclonal nature of human antibodies.

Despite these unresolved issues, our study provides an explanation for why patients with major tissue damage develop increased levels of anti-PF4/heparin antibodies compared with patients with minor tissue damage.³⁸ Increased concentrations of cell-free plasma DNA (1–2 µg/mL) have been found in various clinical conditions,

including trauma,³⁹ cancer,⁴⁰ and infections,⁴¹ correlating with the severity of trauma or infection.^{11,41} However, due to their short plasma half-life, elevated RNA/DNA plasma levels return to baseline within a few hours after tissue damage. Yet this might be sufficient to induce an immune response, as also single and minimal applications of heparin have been shown to be sufficient for the induction of HIT.⁴² Cellular RNA and DNA released by the tissue trauma might complex with PF4, potentially enhancing the immune response against PF4/heparin complexes. In vivo formation of PF4/nucleic acid complexes may also explain the formation of anti-PF4/heparin antibodies in patients after major orthopedic surgery even in the absence of heparin,⁴³⁻⁴⁵ as well as the relatively high frequency of antibodies in critically ill patients.⁴⁶ In addition, formation of PF4/nucleic acid complexes might be another explanation for the reported cases of "spontaneous HIT," because all patients who suffered from a HITlike thromboembolic disorder, despite no previous heparin administration, suffered from infections⁴⁵ or had undergone major orthopedic surgery.⁴⁴

Finally, our findings might be of relevance for the recognition of unwanted effects of therapeutic oligonucleotides such as aptamers or antisense RNA. The PF4/44mer-DNA protein C aptamer complexes induced a strong immune response in mice, and these complexes are recognized by anti-PF4/heparin antibodies. The resulting antibodies cross-reacted with PF4/heparin complexes, indicating that therapeutic aptamers (with a long plasma half-life) could potentially induce an immune response toward PF4/polyanion complexes. To date, there are no reported cases of HITlike adverse effects under treatment with therapeutic aptamers, and we are not aware of thrombotic complications in the ongoing trials using aptamers. Yet clinical data are still sparse, as the only approved therapeutic aptamer, pegaptanib, an RNA aptamer targeting vascular endothelial growth factor, is administered intravitreally and systemic concentrations are very low.⁴⁷ Moreover, thromboembolic complications occurring under pegaptanib are considered to be a class effect of antivascular endothelial growth factor drugs.⁴⁸ Beyond this, it should be considered that heparin is much more immunogenic when given to patients with major proinflammatory states, such as following surgery⁴⁹ or major trauma.³⁸ Thus, studies of aptamer administration in healthy volunteers could be expected to underestimate the anti-PF4/apptamer immune response that could occur in patients. The evaluation of the anti-PF4/polyanion immune response within clinical studies is a far more sensitive marker of evaluating the potential of a given aptamer for inducing serious adverse effects than is monitoring for thrombocytopenia and thrombosis.

While induction of an immune reaction resembling typical HIT may be rather unlikely due to the usually low plasma concentrations of aptamers, a strong antibody response to PF4/apptamer complexes may result in an immune reaction resembling "delayed onset HIT,"⁵⁰ an autoimmune-like syndrome in which strongly reactive anti-PF4/polyanion antibodies activate platelets and induce thrombosis even in the absence of heparin. Yet various aptamers differ considerably

in their structure and are often chemically modified, which may interfere with their binding to PF4. Using the methods described in this study, it should be possible to screen aptamers for their potential interaction with PF4. We suggest that clinical trials of aptamers or other therapeutic nucleic acid constructs should include screening for the development of anti-PF4/apptamer antibodies and potential clinical features of HIT as part of their safety end points.

Acknowledgments

The authors thank Professor Dr Bernd Pötzsch and Dr Müller (Institut für Experimentelle Hämatologie und Transfusionsmedizin, University of Bonn, Germany) for kindly providing the 44mer-DNA protein C aptamer.

This work was supported by the Gerhard-Domagk-Program of the Medical School, University of Greifswald (M.E.J.) and by the Zentrum für Innovationskompetenz Humorale Immunreaktionen bei kardiovaskulären Erkrankungen (ZIK HIKE, Federal Ministry of Education and Research, BMBF FKZ 03Z2CN12 and FKZ 03Z2CN11) (K.K., S. Brandt, and S. Block). Part of the work was supported by the Excellence-cluster Cardio-pulmonary system (ECCPS) and grant FI 543/2-2 from the Deutsche Forschungsgemeinschaft (Bonn, Germany) (K.T.P. and S.F.).

Authorship

Contribution: M.E.J. designed and performed the in vitro experiments and wrote the manuscript; K.K. designed the study, supervised the experiments, reviewed and interpreted the results, and revised the manuscript; B.F. performed and supervised the mouse experiments and interpreted the results; T.M. and B.A. designed and synthesized the nucleic acid constructs and reviewed the results; S. Brandt, S. Block, and C.A.H. performed the CD spectroscopy experiments and reviewed and interpreted the results; S.F. and J.G. isolated the cellular RNA, performed the preliminary experiments on PF4-RNA interaction, and reviewed the manuscript; S.M. designed the nucleic acid constructs and reviewed the results and the manuscript; K.T.P. created the hypothesis of PF4-nucleic acid interaction, designed the experiments on RNA, and wrote the manuscript; A.G. developed the hypothesis of PF4-apptamer interaction, designed the experiments, reviewed the results, and wrote the manuscript; and all authors reviewed and approved the final version of the manuscript.

Conflict-of-interest disclosure: The authors declare no competing financial interests.

Correspondence: Andreas Greinacher, Institut für Immunologie und Transfusionsmedizin, Universitätsmedizin, Ernst-Moritz-Armdt-Universität Greifswald, Sauerbruchstrasse, D-17475 Greifswald, Germany; e-mail: greinach@uni-greifswald.de.

References

1. Kaplan KL, Broekman MJ, Chernoff A, Lesznik GR, Drillings M. Platelet alpha-granule proteins: studies on release and subcellular localization. *Blood*. 1979;53(4):604-618.
2. Greinacher A, Gopinadhan M, Günther JU, et al. Close approximation of two platelet factor 4 tetramers by charge neutralization forms the antigens recognized by HIT antibodies. *Arterioscler Thromb Vasc Biol*. 2006;26(10):2386-2393.
3. Rauova L, Poncz M, McKenzie SE, et al. Ultralarge complexes of PF4 and heparin are central to the pathogenesis of heparin-induced thrombocytopenia. *Blood*. 2005;105(1):131-138.
4. Arepally GM, Ortel TL. Clinical practice. Heparin-induced thrombocytopenia. *N Engl J Med*. 2006;355(8):809-817.
5. Warkentin TE, Chong BH, Greinacher A. Heparin-induced thrombocytopenia: towards consensus. *Thromb Haemost*. 1998;79(1):1-7.
6. Warkentin TE, Greinacher A, Koster A, Lincoff AM. Treatment and prevention of heparin-induced thrombocytopenia: American College of Chest Physicians Evidence-Based Clinical Practice Guidelines (8th Edition). *Chest*. 2008;133(6 Suppl):340S-380S.

6. Appended papers

6.5 Paper V: PF4/aptamer

7. Krauel K, Weber C, Brandt S, Zähringer U, Mamat U, Greinacher A, Hammerschmidt S. Platelet factor 4 binding to lipid A of Gram-negative bacteria exposes PF4/heparin-like epitopes. *Blood*. 2012;120(16):3345-3352.
8. Anderson GP. Insights into heparin-induced thrombocytopenia. *Br J Haematol*. 1992;80(4):504-508.
9. Lo YM, Zhang J, Leung TN, Lau TK, Chang AM, Hjelm NM. Rapid clearance of fetal DNA from maternal plasma. *Am J Hum Genet*. 1999;64(1):218-224.
10. Mitra I, Nair NK, Mishra PK. Nucleic acids in circulation: are they harmful to the host? *J Biosci*. 2012;37(2):301-312.
11. Lam NY, Rainer TH, Chan LY, Joynt GM, Lo YM. Time course of early and late changes in plasma DNA in trauma patients. *Clin Chem*. 2003;49(8):1286-1291.
12. Kikuchi Y, Rykova EY, eds. Extracellular Nucleic Acids. In: Gross HJ, Bujnicki JM, eds. *Nucleic Acids and Molecular Biology*. Vol 25. Berlin: Springer-Verlag; 2010.
13. Ni X, Castaneres M, Mukherjee A, Lupold SE. Nucleic acid aptamers: clinical applications and promising new horizons. *Curr Med Chem*. 2011;18(27):4206-4214.
14. Krauel K, Füll B, Warkentin TE, Weitschies W, Kohlmann T, Sheppard JI, Greinacher A. Heparin-induced thrombocytopenia—therapeutic concentrations of danaparoid, unlike fondaparinux and direct thrombin inhibitors, inhibit formation of platelet factor 4-heparin complexes. *J Thromb Haemost*. 2008;6(12):2160-2167.
15. Bock LC, Griffin LC, Latham JA, Vermaas EH, Toole JJ. Selection of single-stranded DNA molecules that bind and inhibit human thrombin. *Nature*. 1992;355(6360):564-566.
16. Müller J, Isermann B, Dücker C, et al. An exosite-specific ssDNA aptamer inhibits the anticoagulant functions of activated protein C and enhances inhibition by protein C inhibitor. *Chem Biol*. 2009;16(4):442-451.
17. Suess B, Hanson S, Berens C, Fink B, Schroeder R, Hillen W. Conditional gene expression by controlling translation with tetracycline-binding aptamers. *Nucleic Acids Res*. 2003;31(7):1853-1858.
18. Strohhach D, Novak N, Müller S. Redox-active riboswitching: allosteric regulation of ribozyme activity by ligand-shape control. *Angew Chem Int Ed Engl*. 2006;45(13):2127-2129.
19. Juhl D, Eichler P, Lubenow N, Strobel U, Wessel A, Greinacher A. Incidence and clinical significance of anti-PF4/heparin antibodies of the IgG, IgM, and IgA class in 755 consecutive patient samples referred for diagnostic testing for heparin-induced thrombocytopenia. *Eur J Haematol*. 2006;76(5):420-426.
20. Warkentin TE, Greinacher A. Laboratory Testing for Heparin-Induced Thrombocytopenia. In: Warkentin TE, Greinacher A, eds. *Heparin-Induced Thrombocytopenia*. New York, NY: Informa Healthcare; 2007:227-238.
21. Greinacher A, Pötzsch B, Amiral J, Dummel V, Eichner A, Mueller-Eckhardt C. Heparin-associated thrombocytopenia: isolation of the antibody and characterization of a multimolecular PF4-heparin complex as the major antigen. *Thromb Haemost*. 1994;71(2):247-251.
22. Kelton JG, Sheridan D, Santos A, et al. Heparin-induced thrombocytopenia: laboratory studies. *Blood*. 1988;72(3):925-930.
23. Böhm G, Muhr R, Jaenicke R. Quantitative analysis of protein far UV circular dichroism spectra by neural networks. *Protein Eng*. 1992;5(3):191-195.
24. Suvanna S, Qi R, Arepally GM. Optimization of a murine immunization model for study of PF4/heparin antibodies. *J Thromb Haemost*. 2009;7(5):857-864.
25. Alban S, Franz G. Gas-liquid chromatography-mass spectrometry analysis of anticoagulant active curdlan sulfates. *Semin Thromb Hemost*. 1994;20(2):152-158.
26. Greinacher A, Alban S, Dummel V, Franz G, Mueller-Eckhardt C. Characterization of the structural requirements for a carbohydrate based anticoagulant with a reduced risk of inducing the immunological type of heparin-associated thrombocytopenia. *Thromb Haemost*. 1995;74(3):886-892.
27. Visentin GP, Moghaddam M, Beery SE, McFarland JG, Aster RH. Heparin is not required for detection of antibodies associated with heparin-induced thrombocytopenia/thrombosis. *J Lab Clin Med*. 2001;138(1):22-31.
28. Leroux D, Canépa S, Viskov C, et al. Binding of heparin-dependent antibodies to PF4 modified by enoxaparin oligosaccharides: evaluation by surface plasmon resonance and serotonin release assay. *J Thromb Haemost*. 2012;10(3):430-436.
29. Petitou M, Héroult JP, Bernat A, Driguez PA, Duchaussoy P, Lormeau JC, Herbert JM. Synthesis of thrombin-inhibiting heparin mimetics without side effects. *Nature*. 1999;398(6726):417-422.
30. Schneider B, Patel K, Berman HM. Hydration of the phosphate group in double-helical DNA. *Biophys J*. 1998;75(5):2422-2434.
31. Saenger W. *Principles of Nucleic Acid Structure*. Berlin: Springer-Verlag; 1984.
32. Savi P, Chong BH, Greinacher A, et al. Effect of fondaparinux on platelet activation in the presence of heparin-dependent antibodies: a blinded comparative multicenter study with unfractionated heparin. *Blood*. 2005;105(1):139-144.
33. Weimann G, Lubenow N, Selleng K, Eichler P, Albrecht D, Greinacher A. Glucosamine sulfate does not crossreact with the antibodies of patients with heparin-induced thrombocytopenia. *Eur J Haematol*. 2001;66(3):195-199.
34. Gansler J, Jaax M, Leiting S, Appel B, Greinacher A, Fischer S, Preissner KT. Structural requirements for the procoagulant activity of nucleic acids. *PLoS ONE*. 2012;7(11):e50399.
35. Stuckey JA, St Charles R, Edwards BF. A model of the platelet factor 4 complex with heparin. *Proteins*. 1992;14(2):277-287.
36. Sachais BS, Litvinov RI, Yarovoi SV, et al. Dynamic antibody-binding properties in the pathogenesis of HIT. *Blood*. 2012;120(5):1137-1142.
37. Greinacher A, Krauel K, Jensch I. HIT-antibodies promote their own antigen. *Blood*. 2012;120(5):930-931.
38. Lubenow N, Hinz P, Thomaschewski S, et al. The severity of trauma determines the immune response to PF4/heparin and the frequency of heparin-induced thrombocytopenia. *Blood*. 2010;115(9):1797-1803.
39. Lo YM, Rainer TH, Chan LY, Hjelm NM, Cocks RA. Plasma DNA as a prognostic marker in trauma patients. *Clin Chem*. 2000;46(3):319-323.
40. Jahr S, Hentze H, Englisch S, Hardt D, Fackelmayer FO, Hesch RD, Knippers R. DNA fragments in the blood plasma of cancer patients: quantitations and evidence for their origin from apoptotic and necrotic cells. *Cancer Res*. 2001;61(4):1659-1665.
41. Huttunen R, Kuparinen T, Jylhävä J, et al. Fatal outcome in bacteremia is characterized by high plasma cell free DNA concentration and apoptotic DNA fragmentation: a prospective cohort study. *PLoS ONE*. 2011;6(7):e21700.
42. Gettings EM, Brush KA, Van Cott EM, Hurford WE. Outcome of postoperative critically ill patients with heparin-induced thrombocytopenia: an observational retrospective case-control study. *Crit Care*. 2006;10(6):R161.
43. Jay RM, Warkentin TE. Fatal heparin-induced thrombocytopenia (HIT) during warfarin thromboprophylaxis following orthopedic surgery: another example of 'spontaneous' HIT? *J Thromb Haemost*. 2008;6(9):1598-1600.
44. Pruthi RK, Daniels PR, Nambudiri GS, Warkentin TE. Heparin-induced thrombocytopenia (HIT) during postoperative warfarin thromboprophylaxis: a second example of postorthopedic surgery 'spontaneous' HIT. *J Thromb Haemost*. 2009;7(3):499-501.
45. Warkentin TE, Makris M, Jay RM, Kelton JG. A spontaneous prothrombotic disorder resembling heparin-induced thrombocytopenia. *Am J Med*. 2008;121(7):632-636.
46. Levine RL, Hergenroeder GW, Francis JL, Miller CC, Hursting MJ. Heparin-platelet factor 4 antibodies in intensive care patients: an observational seroprevalence study. *J Thromb Thrombolysis*. 2010;30(2):142-148.
47. Drolet DW, Nelson J, Tucker CE, et al. Pharmacokinetics and safety of an anti-vascular endothelial growth factor aptamer (NX1838) following injection into the vitreous humor of rhesus monkeys. *Pharm Res*. 2000;17(12):1503-1510.
48. Costagliola C, Agnifili L, Arcidiacono B, et al. Systemic thromboembolic adverse events in patients treated with intravitreal anti-VEGF drugs for neovascular age-related macular degeneration. *Expert Opin Biol Ther*. 2012;12(10):1299-1313.
49. Warkentin TE, Sheppard JA, Sigouin CS, Kohlmann T, Eichler P, Greinacher A. Gender imbalance and risk factor interactions in heparin-induced thrombocytopenia. *Blood*. 2006;108(9):2937-2941.
50. Rice L, Attisha WK, Drexler A, Francis JL. Delayed-onset heparin-induced thrombocytopenia. *Ann Intern Med*. 2002;136(3):210-215.

6.6 Paper VI: Anti–Protamine-Heparin Antibodies: Incidence, clinical Relevance, and Pathogenesis

Plenary Paper

THROMBOSIS AND HEMOSTASIS

Anti-protamine-heparin antibodies: incidence, clinical relevance, and pathogenesis

Tamam Bakchoul,¹ Heike Zöllner,¹ Jean Amiral,² Simon Panzer,³ Sixten Selleng,¹ Thomas Kohlmann,⁴ Sven Brandt,⁵ Mihaela Delcea,⁵ Theodore E. Warkentin,⁶ Ulrich J. Sachs,⁷ and Andreas Greinacher¹

¹Institute for Immunology und Transfusion Medicine, Ernst-Moritz-Arndt University Greifswald, Germany; ²Hyphen BioMed, Neuville sur Oise, France; ³Department for Blood Group Serology and Transfusion Medicine, Medical University Vienna, Austria; ⁴Institute for Community Medicine, and ⁵Center for Innovation Competence, Humoral Immune Response in Cardiovascular Diseases (ZIK HIKE), Ernst-Moritz-Arndt University Greifswald, Germany; ⁶Department of Pathology and Molecular Medicine, and Department of Medicine, McMaster University, Hamilton, Ontario, Canada; and ⁷Institute for Clinical Immunology und Transfusion Medicine, Justus Liebig University Giessen, Germany

Key Points

- Immunization against protamine/heparin complexes was frequently observed in patients undergoing cardiac surgery.
- Platelet-activating anti-protamine-heparin antibodies are a potential risk factor for early postoperative thrombosis and thrombocytopenia.

Protamine, which is routinely used after cardiac surgery to reverse the anticoagulant effects of heparin, is known to be immunogenic. Observing patients with an otherwise unexplained rapid decrease in platelet count directly after protamine administration, we determined the incidence and clinical relevance of protamine-reactive antibodies in patients undergoing cardiac-surgery. In vitro, these antibodies activated washed platelets in a FcγRIIIa-dependent fashion. Using a nonobese diabetic/severe combined immunodeficiency mouse model, those antibodies induced thrombocytopenia only when protamine and heparin were present but not with protamine alone. Of 591 patients undergoing cardiopulmonary bypass surgery, 57 (9.6%) tested positive for anti-protamine-heparin antibodies at baseline and 154 (26.6%) tested positive at day 10. Diabetes was identified as a risk factor for the development of anti-protamine-heparin antibodies. In the majority of the patients, these antibodies were transient and titers decreased substantially after 4 months ($P < .001$). Seven patients had platelet-activating, anti-protamine-heparin antibodies at baseline and showed a greater and more prolonged decline in platelet counts compared with antibody-negative patients ($P = .003$). In addition, 2 of those patients experienced early arterial thromboembolic complications vs 9 of 584 control patients (multivariate analysis: odds ratio, 21.58; 95% confidence interval, 2.90-160.89; $P = .003$). Platelet-activating anti-protamine-heparin antibodies show several similarities with anti-platelet factor 4-heparin antibodies and are a potential risk factor for early postoperative thrombosis. (*Blood*. 2013;121(15):2821-2827)

Introduction

Protamine, a positively charged DNA-binding protein purified from salmon sperm, is administered as protamine sulfate to neutralize the anticoagulant activity of heparin (eg, after cardiopulmonary bypass surgery)¹⁻⁵ and as a stabilizer of insulin.⁶ Protamine is immunogenic, and anti-protamine antibodies are found in patients treated with insulin.^{6,7} We found anti-protamine-heparin antibodies in patients undergoing cardiac surgery,^{8,9} and Chudasama et al showed high immunogenicity of protamine-heparin complexes in a mouse model.¹⁰ Some of these features resemble immunogenicity of complexes between heparin and positively charged platelet factor 4 (PF4), which are well known to induce the causative antibodies of heparin-induced thrombocytopenia, a prothrombotic adverse drug reaction.^{5,11}

After observing patients with acute thrombocytopenia, which was more pronounced than typically expected after cardiopulmonary bypass surgery because of dilution and consumption, we systematically addressed the presence and potential clinical relevance of anti-protamine-heparin antibodies in patients undergoing cardiopulmonary

bypass surgery, and characterized the interaction of these antibodies with platelets. We found that platelet-activating anti-protamine-heparin antibodies, present at the time of protamine application, are associated with more pronounced thrombocytopenia and may be a risk factor for early thromboembolic complications in patients undergoing cardiac surgery.

Materials and methods

Patients and sera

The index patient raising suspicion for protamine-induced complications had been referred for laboratory assessment of heparin-induced thrombocytopenia. To define the frequency of anti-protamine-heparin antibodies at the time of cardiac surgery, and the formation of anti-protamine-heparin antibodies after cardiopulmonary bypass, we investigated serum samples of a previously reported cohort of 591 patients undergoing cardiopulmonary bypass surgery.¹²

Submitted October 11, 2012; accepted January 2, 2013. Prepublished online as *Blood* First Edition paper, January 16, 2013; DOI 10.1182/blood-2012-10-460691.

There is an Inside *Blood* commentary on this article in this issue.

The publication costs of this article were defrayed in part by page charge payment. Therefore, and solely to indicate this fact, this article is hereby marked "advertisement" in accordance with 18 USC section 1734.

© 2013 by The American Society of Hematology

Samples were obtained preoperatively (day 0), day 6 and day 10 postoperatively, and from a subgroup 120 days postoperatively, and were stored at -80°C until use. All patients had received protamine to neutralize heparin given during surgery. All patients had been screened for PF4/heparin antibodies. All thromboembolic complications were objectively documented at diagnosis and had already been adjudicated in the aforementioned study, and only then we assessed the patients in a blinded fashion for protamine-reactive antibodies.

Clinical diagnoses were identified according to the patient hospital chart information. Diabetes was defined as either use of hyperglycemic agents or other data according to outpatient records. Hypertension was defined as a systolic blood pressure of more than 140 mm Hg, a diastolic blood pressure of more than 90 mm Hg, or use of antihypertensive therapy at the time of hospital admission. Previous myocardial infarction was defined as either self-reported history or electrocardiographic evidence at hospital admission. Congestive heart failure (CHF) was defined according to outpatient reports or current manifestations suggestive of CHF and impaired heart ejection fraction on echocardiography. Peripheral vascular disease was defined as self-reported history or other data according to outpatient reports.

Serological studies

In vitro, we assessed anti-protamine and anti-protamine-heparin IgG antibodies by enzyme immunoassay (EIA) using microtiter plates coated with protamine sulfate (20 $\mu\text{g}/\text{mL}$; Sigma-Aldrich, Munich, Germany) in a phosphate buffer (pH 7.5) or with protamine-heparin complexes (a mixture of 20 $\mu\text{g}/\text{mL}$ of protamine sulfate with an excess of unfractionated heparin). In both cases, plates were saturated with goat serum. Bound antibodies were detected by goat anti-human IgG (cutoff value, 0.50; optical density [OD], 450 nm).

As a "functional" (platelet activation) assay, we used the heparin-induced platelet activation assay (HIPA)¹³ with minor modifications. Serum was incubated with washed platelets of 4 donors (tested individually) under 6 test conditions: (1) buffer, (2) protamine (2 $\mu\text{g}/\text{mL}$), (3) heparin (0.2 IU/mL), (4) protamine (2 $\mu\text{g}/\text{mL}$) and heparin (0.2 IU/mL), (5) protamine (2 $\mu\text{g}/\text{mL}$) and heparin (100 IU/mL), and (6) protamine (2 $\mu\text{g}/\text{mL}$) and heparin (0.2 IU/mL) and the Fc γ IIa receptor-blocking monoclonal antibody IV.3 (10 $\mu\text{g}/\text{mL}$) (final concentrations). Platelet aggregation with at least 2 platelet donors' suspensions in the presence of protamine (or protamine and 0.2 IU/mL of heparin), but not buffer or heparin alone, was deemed positive. Laboratory personnel were blinded to the patients' clinical data. Serial samples from individual patients were assessed in parallel to avoid interassay variation.

Anti-PF4-heparin antibodies were investigated by an in-house PF4-heparin assay¹⁴ and the HIPA test.¹³ The index patient was assessed by two EIAs for PF4-heparin antibodies: (1) Asserachrom HPIA (Diagnostica Stago, Asnières, France) and (2) GTI-IgG (Gen-Probe GTI Diagnostics, Brookfield, WI), and an EIA that is also able to detect anti-IL8 and anti-NAP2 antibodies,¹⁵ and by HIPA.

Animal model

We assessed the biologic effects of anti-protamine-heparin antibodies in a nonobese diabetic/severe combined immunodeficiency (NOD/SCID) mouse model.^{16,17} Human platelets supplemented with heparin (0.6 IU/mL), protamine (6 $\mu\text{g}/\text{mL}$), heparin (0.6 IU/mL) and protamine (6 $\mu\text{g}/\text{mL}$), or buffer were injected into NOD/SCID mice (The Jackson Laboratory, Bar Harbor, Maine). After 30 minutes (baseline), the IgG fraction of anti-protamine-heparin antibody-positive sera (or controls) was intraperitoneally injected. Survival of human platelets in the mouse circulation and their activation status were assessed (platelet count; CD62p expression) after 60, 120, and 300 minutes. Platelet activation dependency on platelet Fc γ IIa receptors was investigated using IV.3 F(ab)₂-fragments.

Structural studies

Changes in the secondary structure of protamine on interaction with heparin were studied by circular dichroism spectroscopy in a 5-mm cuvette (Hellma, Müllheim, Germany) using far UV circular dichroism spectra. Wavelength between 185 and 260 nm were recorded using a Chirascan circular dichroism spectrometer (Applied Photophysics, Leatherhead, UK). Protamine (60 $\mu\text{g}/\text{mL}$)

was incubated with increasing heparin concentrations at 20°C . Spectra of protamine and protamine-heparin complexes were corrected for baselines, path length, and concentrations to obtain wavelength-dependent mean residue $\delta \epsilon$ values of the protamine-heparin complexes.

Statistical analysis

Statistical analyses were performed using GraphPad prism 5. Nonparametric tests were used when data failed to follow a normal distribution. Platelet counts and early postsurgery thrombotic complications were compared in relationship to antibody status. Analysis-of-covariance models to assess the association between antibody status and thromboembolic complications or platelet count were performed by multiple linear regression analysis using SPSS version 20 software (SPSS, Chicago, IL). Models were adjusted for the presence diabetes, hypertension, previous myocardial infarction, CHF, and peripheral vascular disease. Group comparison was performed using the Wilcoxon rank-sum test, and the Fisher exact test with categorical variables. All analyses were 2-tailed; a *P* value of $< .05$ was assumed to represent statistical significance.

Ethics

This prospective study has been approved by the ethical committee of the Ernst-Moritz-Arndt University; all patients gave informed consent in accordance with the Declaration of Helsinki. The animal studies were approved by the local authorities.

Results

Index patient

A 50-year-old man underwent mitral valve replacement/aortic valve reconstruction with heparin anticoagulation for cardiopulmonary bypass; the protamine platelet count after protamine administration decreased abruptly from $100 \times 10^9/\text{L}$ to $26 \times 10^9/\text{L}$. Thereafter, platelet counts increased to $88 \times 10^9/\text{L}$ (day 6). As cardiac function did not recover, the patient was scheduled for a cardiac-assist device placement. Protamine was given again after the cardiopulmonary bypass procedure, and the platelet count again decreased abruptly from $80 \times 10^9/\text{L}$ to $31 \times 10^9/\text{L}$. Heparin was replaced by argatroban because of suspected heparin-induced thrombocytopenia, with platelet count recovery. However, on postoperative day 7, the patient tested negative for anti-PF4-heparin antibodies in the serum (2 immunoassays and a heparin-induced platelet activation test) and anti-IL8 and anti-NAP2 antibodies (1 immunoassay and 1 functional assay). However, he tested strongly positive for the presence of protamine and heparin on the anti-protamine-heparin immunoassay and functional assay (a preoperative blood sample was not available for testing).

Anti-protamine and anti-protamine-heparin antibodies in 591 patients undergoing cardiac surgery

In this cohort study, 591 patients were enrolled, of whom 14 (2.4%) tested positive for anti-protamine IgG antibodies (only protamine-coated) before surgery (mean OD, 0.96 ± 0.55). By day 6, an additional 16 (2.8%) of 578 patients seroconverted to an OD of more than 0.5 (mean OD, 1.13 ± 0.61); by day 10, an additional 19 (3.3%) of 578 patients had seroconverted (mean OD, 1.46 ± 0.76) (Figure 1). Three patients no longer had seropositivity ($n = 1$ until day 6; $n = 2$ until day 10). In total, 46 (8.0%) of 578 patients tested positive for anti-protamine IgG at day 10 postsurgery.

However, an even greater number of patients tested positive for anti-protamine-heparin IgG antibodies (protamine-heparin complexes coated): 57 (9.6%) of 591 tested positive at baseline (mean

6. Appended papers

6.6 Paper VI: PS/heparin

BLOOD, 11 APRIL 2013 • VOLUME 121, NUMBER 15

CLINICAL RELEVANCE OF ANTI-PROTAMINE-HEPARIN IgG 2823

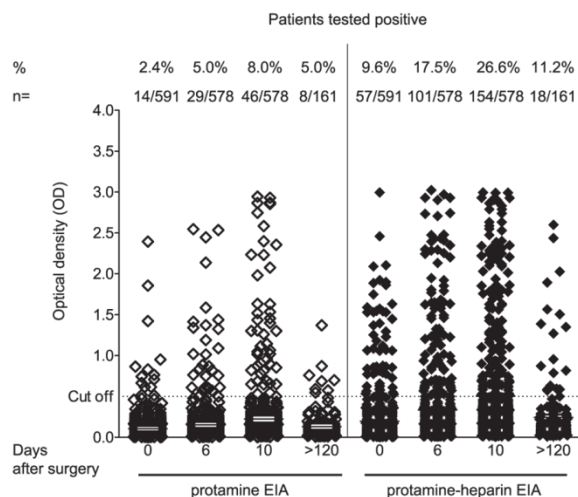


Figure 1. Prevalence of anti-protamine and anti-protamine-heparin antibodies in patients undergoing cardiac surgery at different time points. Binding of IgG to either protamine (left) or protamine-heparin complexes (right panel) was assessed by EIA in patients undergoing cardiopulmonary bypass ($n = 591$) before surgery (day 0) and at day 6 and day 10 after surgery. In a subgroup of 161 patients, a follow-up sample was available more than 120 days after surgery.

OD, 1.15 ± 0.55), 52 (9.0%) of 578 seroconverted (mean OD, 1.35 ± 0.74) at day 6, and 154 patients (26.6%) tested positive (mean OD, 1.47 ± 0.78) by day 10 (Figure 1). Twenty patients no longer seropositivity ($n = 8$ until day 6; $n = 12$ until day 10).

In the functional assay (Figure 2), 24 (15.6%) of the anti-protamine-heparin IgG-positive sera induced platelet activation in the presence of protamine. The reaction was enhanced (shortened lag time) when 0.2 IU/mL of heparin were added (median, 25 minutes [range, 5–40 minutes] vs 14 minutes [range, 5–35 minutes]; $P = .047$). Platelet activation was inhibited by 100 IU/mL of heparin and by the FcγIIa receptor-blocking IV.3 antibody. None of the sera reacted in the presence of buffer, but 5 sera reacted weakly in the presence of heparin. Interestingly, all but 2 of the platelet-activating sera showed

increased binding to protamine-heparin (mean OD, 2.08 ± 0.74) compared with protamine alone (mean OD, 1.88 ± 0.96 ; $P = .025$).

Only 1 of 24 sera that activated platelets in the presence of protamine-heparin also showed the typical pattern found in heparin-induced thrombocytopenia,¹⁸ that is, activation of platelets in the presence of 0.2 IU/mL of heparin within 30 minutes (indicated by the open circle in Figure 2). Of the 154 patients with anti-protamine-heparin IgG antibodies, 97 (63.0%) also tested positive for anti-PF4-heparin IgG.

Association of platelet-activating anti-protamine-heparin antibodies with postoperative outcomes

In patients with IgG antibodies against protamine-heparin, a history of diabetes was identified as a risk factor for preoperative seropositivity (62.0% vs 36.5%; $P < .001$). Unfortunately, we did not have available the specific type of treatment the patients had received before hospital admission (insulin or oral hypoglycemic agents). No significant difference was observed regarding a history of hypertension (100% vs 90.4%; $P = .221$), previous myocardial infarction (6% vs 12.4%; $P = .346$), or peripheral vascular disease (14.0% vs 17.4%; $P = .635$) (Table 1).

As protamine is given near the end of surgery, patients with platelet-activating protamine-reactive IgG antibodies present before surgery might be at higher risk for adverse outcomes. Indeed, the 7 patients with platelet-activating, anti-protamine-heparin antibodies before surgery showed a more pronounced and prolonged decrease in platelet counts compared with the 50 patients with non-platelet-activating anti-protamine-heparin antibodies (Figure 3). Of note, the platelet count course in patients with nonactivating anti-protamine-heparin antibodies did not differ significantly from that in antibody-negative patients (Figure 3). Analysis of covariates and adjustment of the risk to the presence of diabetes, hypertension, previous myocardial infarction, and peripheral vascular disease showed that patients with platelet-activating anti-protamine-heparin antibodies had significantly lower postoperative platelet counts than those with nonactivating anti-protamine-heparin antibodies and those testing negative for such antibodies ($P = .004$; $P = .005$, respectively).

The most important clinical finding is that 7 patients with platelet-activating anti-protamine-heparin antibodies at baseline had an

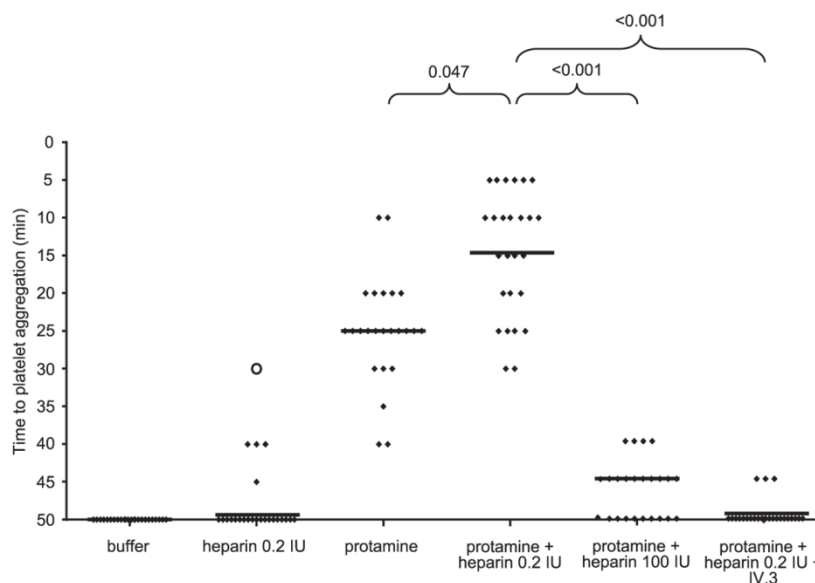


Figure 2. Serological characterization of anti-protamine-heparin antibodies: anti-protamine-heparin antibodies are capable of platelet activation in a heparin-dependent manner via cross-linking FcγIIa receptors. Heat-inactivated sera from patients with anti-protamine-heparin antibodies were incubated with washed platelets in the presence of buffer, heparin (0.2 IU/mL), and protamine (2 μg/mL) with or without heparin (0.2 IU/mL). Inhibition studies were performed with protamine plus high heparin (100 IU/mL) or protamine (2 μg/mL) plus heparin (0.2 IU/mL) in the presence of FcγIIa receptor-blocking antibody (IV.3). Platelet aggregation was determined by change in turbidity of the suspension and assessed every 5 minutes, as described.¹³

Table 1. Demographics of 591 patients who received protamine during cardiopulmonary bypass surgery

Patient characteristics	Total no. of patients: 591 (100%)	Status of protamine-heparin IgG-antibodies at baseline			P value
		No antibodies (n = 534; 90.4%)	Non-platelet-activating antibodies (n = 50; 8.4%)	Platelet-activating antibodies (n = 7; 1.2%)	
Age (y)	67.5 ± 9.5	67.5 ± 9.7	67.6 ± 7.6	72.3 ± 8.7	.414
Female sex (%)	162 (27.4)	145 (27.2)	16 (32.0)	1 (14.3)	.688
Body mass index	29.0 ± 4.6	28.9 ± 4.6	30.3 ± 4.3	28.9 ± 4.1	.281
Diabetes (%)	233 (39.4)	195 (36.5)	31 (62.0)	7 (100)	< .001
Hypertension (%)	539 (91.2)	483 (90.4)	50 (100.0)	6 (85.7)	.221
Previous myocardial infarction (%)	70 (11.8)	66 (12.4)	3 (6.0)	1 (14.3)	.346
Congestive heart failure (%)	5 (0.8)	2 (0.4)	3 (6.0)	0 (0)	.001
Peripheral vascular disease (%)	102 (17.3)	93 (17.4)	7 (14.0)	2 (28.6)	.635

increased risk for early thromboembolic complications. In 2 (28.6%) of these 7 patients, arterial occlusions developed (symptomatic early coronary bypass occlusion in 1 patient, diagnosed at day 2; and stroke in the other patient, diagnosed at day 3), compared with 9 thromboembolic events occurring by day 7 in the remaining 584 (1.5%) of 591 patients (odds ratio, 25.6; 95% confidence interval, 4.37-149.59; $P = .006$). After adjustment for the presence of diabetes, arterial hypertension, previous myocardial infarction, CHF, and peripheral vascular disease at baseline by use of logistic regression analysis, platelet-activating protamine-heparin antibodies remained an independent risk factor for early thromboembolic complications (odds ratio, 21.58; 95% confidence interval, 2.90-160.89; $P = .003$). In all 11 patients with thromboembolic complications after surgery, heparin-induced thrombocytopenia had been ruled out by a negative test result for platelet-activating anti-PF4-heparin antibodies (HIPA), although 2 patients tested weakly positive for PF4-heparin IgG antibodies at day 6 (OD, 0.53; and OD, 0.82). These 2 patients had no platelet-activating protamine-heparin antibodies. Neither mortality nor hospital length of stay differed between the groups.

Persistence of anti-protamine-heparin antibodies

Of the 161 patients in our long-term follow-up study, 43 (26.7%) tested positive for anti-protamine-heparin antibodies at day 10, but only 18 (11.2%) continued to test positive on EIA after more than 120 days of follow-up ($P < .001$). These 18 patients also had considerably decreased OD ($P < .001$; Figure 1); of these, 12 (66%) had diabetes.

In vivo characterization of anti-protamine-heparin antibodies (animal model)

In the NOD/SCID mouse model (Figure 4), the addition of protamine and heparin together with anti-protamine-heparin IgG strongly decreased platelet survival rate to 23% (range, 20%-28%), whereas destruction of human platelets was only minimally enhanced by anti-protamine-heparin IgG in the presence of protamine alone (platelet survival rate, 77%; range, 71%-80%). Platelet destruction was largely inhibited by FcγIIa-inhibiting IV.3 F(ab)₂-fragments (platelet survival rate, 65%; range, 45%-70%). No enhanced platelet clearance was observed by the administration of IgG from healthy donors in the

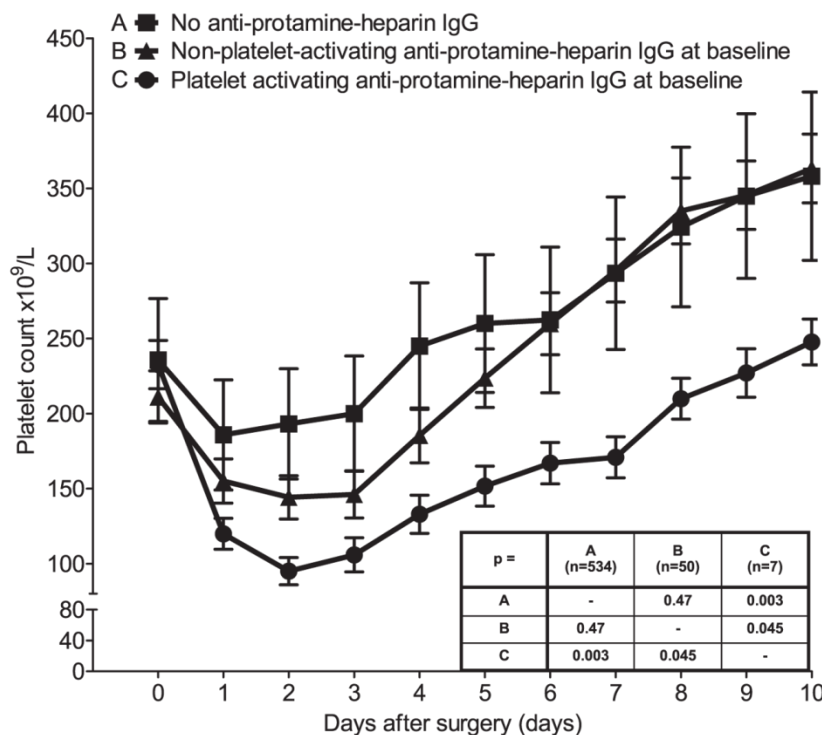
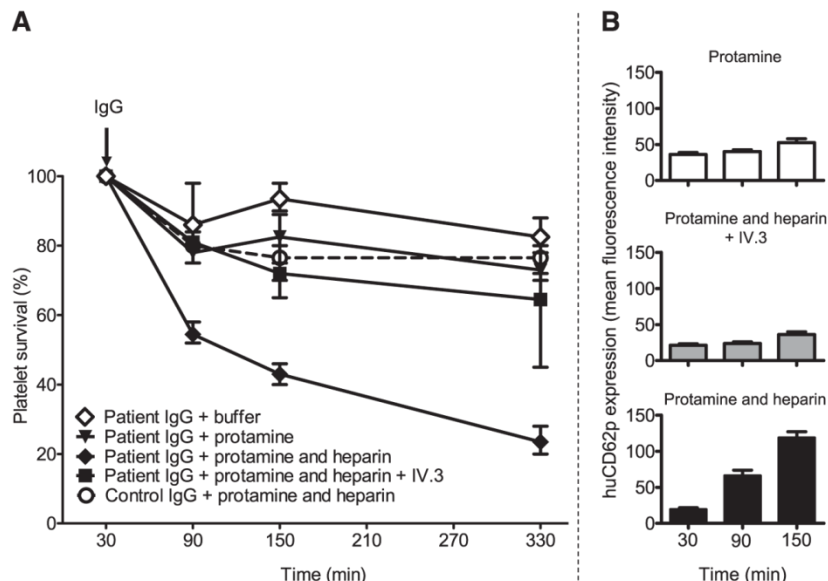


Figure 3. Platelet counts of patients after cardiopulmonary bypass. Patients were grouped depending on the presence of anti-protamine-heparin antibodies (absent, group A [n = 534]) and the capability of these antibodies to activate platelets in vitro (non-platelet-activating anti-protamine-heparin antibodies, group B [n = 50]; platelet-activating anti-protamine-heparin antibodies, group C [n = 7]). The means of platelet counts at the corresponding day after surgery are plotted. The insert table shows the P values comparing the different platelet count curves with each other.

Figure 4. Anti-protamine-heparin antibodies cause platelet activation and destruction in vivo in a heparin-dependent manner via cross-linking the FcγIIa receptor. Human platelets supplemented with protamine, or protamine-heparin, or protamine-heparin and F(ab)₂ fragments of the FcγIIa-inhibiting monoclonal antibody IV.3, or buffer were injected retro-orbitally into NOD/SCID mice. After 30 minutes (baseline), the number of circulating human platelets was estimated (100%), and the IgG fractions of patient sera containing anti-protamine-heparin antibodies (or the IgG fraction from healthy control participants) were injected intraperitoneally. The percentage survival of human platelets was measured after 60, 120, and 300 minutes. Results are shown as a median (range) of experiments performed with anti-protamine-heparin antibodies obtained from 7 patients after CPB (A). Expression of the platelet activation marker human CD62p was estimated at 30, 60, and 120 minutes after platelet injection (B). The control IgG fraction did not cause platelet elimination (A, open circles and dashed line) and minor expression of CD62p (median fluorescence intensity, 40; range, 35-46) at 120 minutes after platelet injection in the presence of protamine-heparin (not shown).



presence of protamine and heparin (platelet survival rate, 76%; range, 72%-80%) (Figure 4). Platelet counts were compared at 330 minutes after injection of anti-protamine-heparin IgG.

Decreased platelet survival rate by anti-protamine-heparin antibodies was associated with platelet activation (Figure 4, right panel). The platelet activation marker human CD62p at 150 minutes was much higher expressed in the presence of patient IgG and protamine and heparin (median fluorescence intensity, 117; range, 100-140; 84% of human platelets were positive) compared with protamine alone (median fluorescence intensity, 48; range, 45-68, $P = .028$; 32% of human platelets were positive). Platelet activation by patient IgG was inhibited by IV.3 F(ab)₂-fragments (median fluorescence intensity, 35; range, 30-45; $P = .029$; 43% of human platelets were positive). In the presence of buffer and anti-protamine-heparin IgG, huCD62p expression was minimal (median fluorescence intensity, 25; range, 18-28; 12% of human platelets were positive). Control IgG did not increase CD62p expression on circulating platelets either in the presence of buffer (median fluorescence intensity, 34; range, 30-45) or protamine alone (median fluorescence intensity, 36.5; range, 30-42), or protamine and heparin (median fluorescence intensity, 40; range, 35-46).

Characterization of protamine-heparin complexes

In circular dichroism spectroscopy, the spectrum of protamine showed a negative band at 198 nm, which is usually attributed to the presence of random coil structures (Figure 5). Increasing heparin concentrations decreased the ellipticity values, indicating a decrease in the respective secondary structure content on a qualitative level.

Discussion

This study shows that the preoperative presence of platelet-activating anti-protamine-heparin antibodies in cardiac surgery using heparin anticoagulation during cardiopulmonary bypass with protamine neutralization is associated with early and prolonged postoperative thrombocytopenia and indicates that these antibodies may also be associated with an increased risk for arterial thrombosis. This finding

bears several similarities to heparin-induced thrombocytopenia: both disorders are characterized by IgG class antibodies that activate platelets through FcγIIa receptors; both are associated with thrombocytopenia; and both heparin and protamine administration in association with cardiac surgery are associated with very high frequencies (25%-50%) of subsequent, but transient, formation of anti-PF4-heparin and anti-protamine-heparin antibodies, respectively. However, a major clinical difference exists between protamine-induced thrombocytopenia and heparin-induced thrombocytopenia: whereas protamine-induced thrombocytopenia seems to be associated with early-onset thrombocytopenia and, potentially, with early thrombotic events (as a consequence of antibodies already detectable at the time of surgery), heparin-induced thrombocytopenia more commonly causes thrombocytopenia and thrombosis at 1 to 2 weeks after surgery

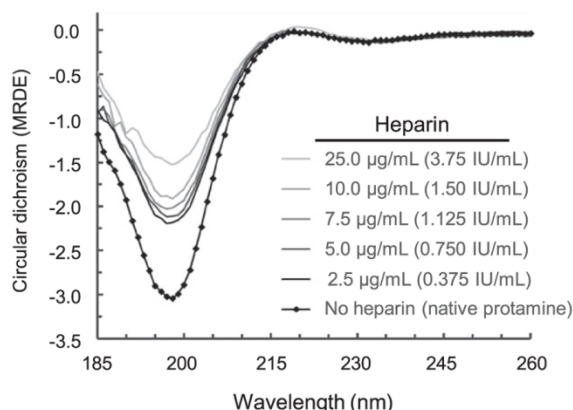


Figure 5. Changes in the secondary structure of protamine upon interaction with heparin. The complex formation was carried out at 20°C directly within the circular dichroism cuvette and was recorded using far UV circular dichroism spectra (185-260 nm) with a Chirascan circular dichroism spectrometer. The spectra of protamine and of protamine-heparin complexes were corrected for the baselines, path length, and concentration to obtain the wavelength-dependent mean residue ellipticity values of the protamine-heparin complexes. Note that increasing heparin concentrations decreased the ellipticity values, indicating a decrease in the respective secondary structure content on a qualitative level.

because of newly formed antibodies that become detectable beginning ~5 days after surgery.^{19,20}

Although we found that 26.6% of patients tested positive for anti-protamine-heparin antibodies at day 10 after cardiac surgery, which is similar to findings reported by Lee et al²¹ and Pouplard et al,²² only a small subset of these antibodies seem to be clinically relevant. As with heparin-induced thrombocytopenia, anti-protamine-heparin antibodies of IgG class with platelet-activating properties evince greater pathogenicity than do non-platelet-activating anti-protamine-heparin antibodies, particularly when present before surgery. The preoperative presence of these antibodies is associated with a more pronounced decrease in postsurgery platelet counts and might even be associated with an increased risk for new arterial thrombotic complications. In our study, 7 patients (1.2%) had these platelet-activating antibodies present before cardiac surgery, of whom early symptomatic bypass graft reocclusion developed in the first patient (day 2) and the other patient experienced a thrombotic stroke (confirmed at day 3). Although such findings may indicate that these antibodies are a risk factor for early thrombotic complications after cardiac surgery, our study does not establish a definite association because of the overall small number of patients affected. In the studies of Lee et al²¹ and Pouplard et al,²² the protamine-heparin IgG antibodies were not associated with an increased risk for new thrombosis. However, in these studies, the analyses were not stratified for platelet-activating antibodies at baseline. Thus, the clinical effects of the platelet-activating antibodies might have been obscured by the presence of many non-platelet-activating protamine-heparin antibodies, a phenomenon also well known in heparin-induced thrombocytopenia.

An increased risk for early postoperative thrombotic complications would present a contrast to the clinical picture of heparin-induced thrombocytopenia after cardiac surgery. To date, immediate and very early thrombotic complications attributable to the preoperative presence of platelet-activating anti-PF4-heparin antibodies has not been reported, perhaps because of a protective anticoagulant effect of the high amounts of heparin given at cardiac surgery. In contrast, for patients with anti-protamine-heparin antibodies, the platelet-activating effects of these antibodies coincide with an abrupt neutralization of the anticoagulant effects of heparin by administration of protamine.

Our observation of a prolonged decrease in platelet counts in patients with platelet-activating anti-protamine-heparin IgG antibodies raises more questions. Protamine has a short half-life (~5 minutes).^{23,24} As protamine is not a circulating endogenous protein like PF4, it is unlikely that a mechanism similar to the one observed in delayed-onset HIT²⁵ (ie, cross-reactivity of PF4-heparin antibodies with PF4 bound to glycosaminoglycans²⁶) is also the cause for prolonged thrombocytopenia in patients with protamine-heparin antibodies. It is also unlikely that the antibodies cross-react with epitopes of proteins other than protamine. However, protamine-heparin complexes circulate much longer than protamine alone, as shown by a rebound of the anticoagulant activity of heparin frequently seen several hours after protamine application.²⁷ Also, protamine attached to platelet surfaces may circulate longer or is even taken up into platelet α granules such as abciximab and is later reexposed.²⁸ Another possibility to explain this observation is that protamine-heparin-antibody complexes bind to megakaryocytes and thereby impair megakaryocytopoiesis, as shown for antibodies dependent on the glycoprotein IIb-IIIa antagonist, eptifibatide.²⁹ These theoretical considerations require further study.

In view of the high immunization rate and a prevalence of ~4% of platelet-activating anti-protamine-heparin antibodies at day 10 after surgery, the transience of anti-protamine-heparin IgG antibodies is an important finding of our study. Most patients who tested strongly positive at day 10 after surgery tested negative in the follow-up

sample taken at more than 120 days after surgery, and the remaining positive samples had a lower OD (Figure 1). Thus, if the patient requires a second cardiac procedure after several months or years, the anti-protamine-heparin antibodies will have likely disappeared, allowing safe subsequent exposure to protamine. The transience of anti-protamine-heparin antibodies resembles that reported for antibodies implicated in heparin-induced thrombocytopenia.³⁰ However, if there is subsequent exposure to protamine in patients who still have circulating platelet-activating anti-protamine-heparin antibodies, a risk for thrombotic complications might still be present.

We also provide further insights into the pathogenesis of thrombocytopenia and thrombotic complications induced by anti-protamine-heparin antibodies. These antibodies cause intravascular platelet activation via the platelet Fc γ IIa receptor, both in vitro and in vivo (mouse model). This mechanism also resembles the well-characterized platelet activation pathway induced by anti-PF4-heparin IgG. Of potential relevance for diabetic patients requiring (protamine-containing) insulin products, intravascular platelet activation was only induced by anti-protamine-heparin antibodies, and only if both protamine and heparin were given together. This is also fully consistent with the observed risk for early arterial thrombosis in patients with platelet-activating antibodies at the time of combined heparin and protamine exposure. Cardiopulmonary bypass itself has prothrombotic and hypercoagulable effects that are likely enhanced by concomitant anti-protamine-heparin antibody-mediated platelet activation, thereby increasing the overall risk for acute arterial thrombosis.

Protamine is purified from salmon sperm, and immunization against protamine can occur in patients with fish allergy^{1,31,32} and in diabetic patients treated with protamine-containing insulin preparations.^{6,33} In addition, men who have undergone vasectomy develop antibodies against protamine.^{7,8,31,34} A limitation of our study was that we did not have available the types of antidiabetic treatment the patients received before hospital admission (insulin or oral hypoglycemic agents), and whether the patients had undergone vasectomy. Therefore, we can only describe the association of diabetes with an increased risk for development of these antibodies. Nevertheless, it is tempting to hypothesize that protamine in insulin preparations may enhance the risk for formation of anti-protamine-heparin antibodies, but the anti-protamine antibodies seem to differ from those against protamine-heparin complexes. Only a subset of antibodies reacting with protamine-heparin complexes also bound to protamine alone, and in our mouse model, the antibodies required both protamine and heparin to cause platelet activation and thrombocytopenia. Protamine forms immunogenic macromolecular complexes with heparin,¹⁰ and we show by circular dichroism spectroscopy that protamine changes its conformation when complexed with heparin. Thus, heparin binding likely induces neoepitopes on protamine. Despite the similarities between the immune responses to protamine-heparin and PF4-heparin, the epitope(s) recognized by platelet-activating anti-protamine-heparin antibodies seem to differ from those recognized by platelet-activating anti-PF4-heparin antibodies: only one of the activating anti-protamine-heparin antibodies caused platelet activation in the presence of heparin alone, which would be a typical reaction pattern for PF4-heparin-reactive antibodies.

We have recently shown that anti-PF4-heparin antibodies potentially resemble an ancient bacterial host defense mechanism, by which a danger signal epitope is expressed when the positively charged protein PF4 binds to bacterial polyanions or heparin.³⁵⁻³⁷ Protamine seems to be another example of such a mechanism, which may indicate that this type of rapid, but transient, immune reaction toward conformationally altered proteins might be more common than anticipated.

Although our study, together with the recent observations of others (Lee et al²¹ and Pouplard et al²²), shows that anti-protamine-heparin antibodies are frequent and are potentially clinically relevant, additional multicenter prospective studies are required to further define the prevalence and clinical consequences of anti-protamine-heparin antibodies. Our study provided the laboratory tools to identify these patients, to differentiate among the various types of anti-protamine antibodies (particularly the pathogenic platelet-activating anti-protamine-heparin antibodies), and to obtain a suitable animal model to further study the pathogenesis of such antibodies.

Acknowledgments

The authors gratefully acknowledge the excellent technical support of Jessica Bagemühl, Ulrike Strobel, Annika Krautwurst, Olivia Heidecke, and Astrid Giptner.

This study was supported by the German Federal Ministry for Education and Research (CAN04/006, ZIK-HIKE FKZ 03Z2CN11,

03Z2CN12) and the “Forschungsverbund Molekulare Medizin” of the Ernst-Moritz-Arndt-University Greifswald.

H.Z. is a PhD candidate, and this study is submitted in partial fulfillment of the requirement for a PhD.

Authorship

Contribution: T.B., U.J.S., and A.G. designed the study; M.D., S.B., H.Z., J.A., and T.B. performed the experiments; S.P., S.S., J.A., T.B., and H.Z. collected the data; H.Z., T.K., A.G., T.E.W., and T.B. analyzed and interpreted the data; T.B., S.P., S.S., T.E.W., and A.G. interpreted the data and wrote the manuscript.

Conflict-of-interest disclosure: The authors declare no competing financial interests.

Correspondence: Andreas Greinacher, Institute for Immunology und Transfusion Medicine, Ernst-Moritz-Arndt-University Greifswald, Sauerbruchstrasse, 17475 Greifswald, Germany; e-mail: greinach@uni-greifswald.de.

References

- Kimmel SE, Sekeres MA, Berlin JA, et al. Adverse events after protamine administration in patients undergoing cardiopulmonary bypass: risks and predictors of under-reporting. *J Clin Epidemiol*. 1998;51(1):1-10.
- Bull BS, Korpman RA, Huse WM, et al. Heparin therapy during extracorporeal circulation. I. Problems inherent in existing heparin protocols. *J Thorac Cardiovasc Surg*. 1975;69(5):674-684.
- Deykin D. Regulation of heparin therapy. *N Engl J Med*. 1972;287(7):355-356.
- Deykin D. Current concepts: the use of heparin. *N Engl J Med*. 1969;280(17):937-938.
- Arepally GM, Ortel TL. Clinical practice. Heparin-induced thrombocytopenia. *N Engl J Med*. 2006;355(8):809-817.
- Ellerhorst JA, Comstock JP, Nell LJ. Protamine antibody production in diabetic subjects treated with NPH insulin. *Am J Med Sci*. 1990;299(5):298-301.
- Nell LJ, Thomas JW. Frequency and specificity of protamine antibodies in diabetic and control subjects. *Diabetes*. 1988;37(2):172-176.
- Bakchoul T, Giptner A, Krautwurst A, et al. In vivo animal model of drug-induced thrombocytopenia: the clinical relevance of anti-protamine sulfate antibodies. *J Thromb Haemost*. 2011;9(S2):.
- Amiral J, Peyrafitte M, Vissac A. Association of protamine sulfate antibodies with “Pseudo-HIT” in heparin treated patients. *Haemostaseologie*. 2009; PP4.4-9:A65 (Abstract).
- Chudasama SL, Espinasse B, Hwang F, et al. Heparin modifies the immunogenicity of positively charged proteins. *Blood*. 2010;116(26):6046-6053.
- Greinacher A. Heparin-induced thrombocytopenia. *J Thromb Haemost*. 2009;7(Suppl 1):9-12.
- Selleng S, Malowsky B, Itterman T, et al. Incidence and clinical relevance of anti-platelet factor 4/heparin antibodies before cardiac surgery. *Am Heart J*. 2010;160(2):362-369.
- Greinacher A, Michels I, Kiefel V, et al. A rapid and sensitive test for diagnosing heparin-associated thrombocytopenia. *Thromb Haemost*. 1991;66(6):734-736.
- Juhl D, Eichler P, Lubenow N, et al. Incidence and clinical significance of anti-PF4/heparin antibodies of the IgG, IgM, and IgA class in 755 consecutive patient samples referred for diagnostic testing for heparin-induced thrombocytopenia. *Eur J Haematol*. 2006;76(5):420-426.
- Prechel M, Hilby A, Walenga J. Cross reactivity of heparin-induced PF4 antibodies with heparin-bound IL-8. In: Proceedings from the American Society of Hematology; December 6-9, 2008; San Francisco, CA. Abstract 3429. [Abstract]
- Boylan B, Chen H, Rathore V, et al. Anti-GPVI-associated ITP: an acquired platelet disorder caused by autoantibody-mediated clearance of the GPVI/FcγR3a complex from the human platelet surface. *Blood*. 2004;104(5):1350-1355.
- Bakchoul T, Boylan B, Sachs UJ, et al. Blockade of maternal anti-HPA-1a-mediated platelet clearance by an HPA-1a epitope-specific F(ab') in an in vivo mouse model of alloimmune thrombocytopenia. *Transfusion*. 2009;49(2):265-270.
- Greinacher A, Ittermann T, Bagemühl J, et al. Heparin-induced thrombocytopenia: towards standardization of platelet factor 4/heparin antigen tests. *J Thromb Haemost*. 2010;8(9):2025-2031.
- Warkentin TE. How I diagnose and manage HIT. *Hematology Am Soc Hematol Educ Program*. 2011;2011:143-149.
- Warkentin TE, Greinacher A. Heparin-induced thrombocytopenia and cardiac surgery. *Ann Thorac Surg*. 2003;76(2):638-648.
- Lee GM, Welsby IJ, Phillips Bute B, et al. High incidence of antibodies to protamine and protamine/heparin complexes in patients undergoing cardiopulmonary bypass [published online ahead of print Feb 19, 2013]. *Blood*. doi: 10.1182/blood-2012-11-469130.
- Pouplard C, Leroux D, Rolin J, et al. Incidence of antibodies to protamine/heparin complexes in cardiac surgery patients and impact on platelet activation in vitro and clinical outcome. In: Proceedings of the American Society of Hematology; December 10-13, 2011; San Diego, CA. Abstract 2217. [Abstract]
- Butterworth J, Lin YA, Prielipp R, et al. The pharmacokinetics and cardiovascular effects of a single intravenous dose of protamine in normal volunteers. *Anesth Analg*. 2002;94(3):514-522.
- Butterworth J, Lin YA, Prielipp RC, et al. Rapid disappearance of protamine in adults undergoing cardiac operation with cardiopulmonary bypass. *Ann Thorac Surg*. 2002;74(5):1589-1595.
- Warkentin TE, Kelton JG. Delayed-onset heparin-induced thrombocytopenia and thrombosis. *Ann Intern Med*. 2001;135(7):502-506.
- Rauova L, Hirsch JD, Greene TK, et al. Monocyte-bound PF4 in the pathogenesis of heparin-induced thrombocytopenia. *Blood*. 2010;116(23):5021-5031.
- Subramaniam P, Skillington P, Tatoulis J. Heparin-rebound in the early postoperative phase following cardiopulmonary bypass. *Aust N Z J Surg*. 1995;65(5):331-333.
- Nurden P, Poujol C, Durrieu-Jais C, et al. Labeling of the internal pool of GP IIb-IIIa in platelets by c7E3 Fab fragments (abciximab): flow and endocytic mechanisms contribute to the transport. *Blood*. 1999;93(5):1622-1633.
- Greinacher A, Fuerl B, Zinke H, et al. Megakaryocyte impairment by epifibatide-induced antibodies causes prolonged thrombocytopenia. *Blood*. 2009;114(6):1250-1253.
- Warkentin TE, Kelton JG. Temporal aspects of heparin-induced thrombocytopenia. *N Engl J Med*. 2001;344(17):1286-1292.
- Collins C, O'Donnell A. Does an allergy to fish pre-empt an adverse protamine reaction? A case report and a literature review. *Perfusion*. 2008;23(6):369-372.
- Knappe JT, Schuller JL, de Haan P, et al. An anaphylactic reaction to protamine in a patient allergic to fish. *Anesthesiology*. 1981;55(3):324-325.
- Nell LJ, Hulbert C, Arem R, et al. Factors affecting the insulin autoantibody ELISA. *Autoimmunity*. 1989;2(4):299-309.
- Levy JH, Schwieger IM, Zaidan JR, et al. Evaluation of patients at risk for protamine reactions. *J Thorac Cardiovasc Surg*. 1989;98(2):200-204.
- Greinacher A. Oposites attract. *Blood*. 2010;115(3):440-441.
- Krauel K, Pötschke C, Weber C, et al. Platelet factor 4 binds to bacteria, [corrected] inducing antibodies cross-reacting with the major antigen in heparin-induced thrombocytopenia. *Blood*. 2011;117(4):1370-1378.
- Krauel K, Weber C, Brandt S, et al. Platelet factor 4 binding to lipid A of Gram-negative bacteria exposes PF4/heparin-like epitopes. *Blood*. 2012;120(16):3345-3352.

7. References

1. Krauel K, Weber C, Brandt S, et al. Platelet factor 4 binding to lipid A of Gram-negative bacteria exposes PF4/heparin-like epitopes. *Blood*. 2012;120(16):3345-3352.
2. Slungaard A. Platelet factor 4: a chemokine enigma. *The International Journal of Biochemistry & Cell Biology*. 2005;37(6):1162-1167.
3. Zucker MB, Katz IR. Platelet factor 4: production, structure, and physiologic and immunologic action. *Proceedings of the Society for Experimental Biology and Medicine*. 1991;198(2):693-702.
4. Deutsch E, Johnson SA, Seegers WH. Differentiation of certain platelet factors related to blood coagulation. *Circulation Research*. 1955;3(1):110-115.
5. Maione TE, Gray GS, Petro J, et al. Inhibition of angiogenesis by recombinant human platelet factor-4 and related peptides. *Science*. 1990;247(4938):77-79.
6. Wang Z, Huang H. Platelet factor-4 (CXCL4/PF-4): an angiostatic chemokine for cancer therapy. *Cancer Letters*. 2013;331(2):147-153.
7. Clark-Lewis I, Dewald B, Geiser T, Moser B, Baggiolini M. Platelet factor 4 binds to interleukin 8 receptors and activates neutrophils when its N terminus is modified with Glu-Leu-Arg. *Proceedings of the National Academy of Sciences of the United States of America*. 1993;90(8):3574-3577.
8. Deuel TF, Senior RM, Chang D, Griffin GL, Henrikson RL, Kaiser ET. Platelet factor 4 is chemotactic for neutrophils and monocytes. *Proceedings of the National Academy of Sciences of the United States of America*. 1981;78(7):4584-4587.
9. Senior RM, Griffin GL, Huang JS, Walz DA, Deuel TF. Chemotactic activity of platelet alpha granule proteins for fibroblasts. *Journal of Cell Biology*. 1983;96(2):382-385.
10. Greinacher A, Potzsch B, Amiral J, Dummel V, Eichner A, Mueller-Eckhardt C. Heparin-associated thrombocytopenia: isolation of the antibody and characterization of a multimolecular PF4-heparin complex as the major antigen. *Thrombosis and Haemostasis*. 1994;71(2):247-251.
11. Greinacher A. Heparin-induced thrombocytopenia. *Journal of Thrombosis and Haemostasis*. 2009;7 Suppl 1:9-12.
12. Warkentin TE, Levine MN, Hirsh J, et al. Heparin-induced thrombocytopenia in patients treated with low-molecular-weight heparin or unfractionated heparin. *New England Journal of Medicine*. 1995;332(20):1330-1335.
13. Rauova L, Poncz M, McKenzie SE, et al. Ultralarge complexes of PF4 and heparin are central to the pathogenesis of heparin-induced thrombocytopenia. *Blood*. 2005;105(1):131-138.
14. Schütt C, Bröker B. Grundwissen Immunologie. Vol. 3: Spektrum Akademischer Verlag; 2011.
15. Kelton JG, Sheridan D, Santos A, et al. Heparin-induced thrombocytopenia: laboratory studies. *Blood*. 1988;72(3):925-930.
16. Chudasama SL, Espinasse B, Hwang F, et al. Heparin modifies the immunogenicity of positively charged proteins. *Blood*. 2010;116(26):6046-6053.
17. Visentin GP, Ford SE, Scott JP, Aster RH. Antibodies from patients with heparin-induced thrombocytopenia/thrombosis are specific for platelet factor 4 complexed with heparin or bound to endothelial cells. *Journal of Clinical Investigation*. 1994;93(1):81-88.
18. Greinacher A. Heparin-induced thrombocytopenia: Frequency and pathogenesis. *Pathophysiology of Haemostasis and Thrombosis*. 2006;35(1-2):37-45.
19. Greinacher A, Gopinadhan M, Gunther JUG, et al. Close approximation of two platelet factor 4 tetramers by charge neutralization forms the antigens recognized by HIT antibodies. *Arteriosclerosis, Thrombosis, and Vascular Biology*. 2006;26(10):2386-2393.
20. Warkentin TE, Greinacher A. Heparin-induced thrombocytopenia: Recognition, treatment, and prevention. *Chest*. 2004;126(3):311s-337s.

21. Rauova L, Zhai L, Kowalska MA, Arepally GM, Cines DB, Poncz M. Role of platelet surface PF4 antigenic complexes in heparin-induced thrombocytopenia pathogenesis: diagnostic and therapeutic implications. *Blood*. 2006;107(6):2346-2353.
22. Warkentin TE, Kelton JG. A 14-year study of heparin-induced thrombocytopenia. *American Journal of Medicine*. 1996;101(5):502-507.
23. Ziporen L, Li ZQ, Park KS, et al. Defining an antigenic epitope on platelet factor 4 associated with heparin-induced thrombocytopenia. *Blood*. 1998;92(9):3250-3259.
24. Sachais BS, Litvinov RI, Yarovoi SV, et al. Dynamic antibody-binding properties in the pathogenesis of HIT. *Blood*. 2012;120(5):1137-1142.
25. Suvarna S, Espinasse B, Qi R, et al. Determinants of PF4/heparin immunogenicity. *Blood*. 2007;110(13):4253-4260.
26. Krauel K, Potschke C, Weber C, et al. Platelet factor 4 binds to bacteria, [corrected] inducing antibodies cross-reacting with the major antigen in heparin-induced thrombocytopenia. *Blood*. 2011;117(4):1370-1378.
27. Jaax ME, Krauel K, Marschall T, et al. Complex formation with nucleic acids and aptamers alters antigenic properties of platelet factor 4. *Blood*. 2013.
28. Brandt S, Krauel K, Gottschalk KE, et al. Characterisation of the conformational changes in platelet factor 4 induced by polyanions: towards in vitro prediction of antigenicity. *Thrombosis and Haemostasis*. 2014;112(1).
29. Krauel K, Potschke C, Weber C, et al. Platelet factor 4 binds to bacteria-inducing antibodies cross-reacting with the major antigen in heparin-induced thrombocytopenia. *Blood*. 2011;117(4):1370-1378.
30. Mikhailov D, Young HC, Linhardt RJ, Mayo KH. Heparin dodecasaccharide binding to platelet factor-4 and growth-related protein- α - Induction of a partially folded state and implications for heparin-induced thrombocytopenia. *Journal of Biological Chemistry*. 1999;274(36):25317-25329.
31. Munoz EM, Linhardt RJ. Heparin-binding domains in vascular biology. *Arteriosclerosis, Thrombosis, and Vascular Biology*. 2004;24(9):1549-1557.
32. Juhl D, Eichler P, Lubenow N, Strobel U, Wessel A, Greinacher A. Incidence and clinical significance of anti-PF4/heparin antibodies of the IgG, IgM, and IgA class in 755 consecutive patient samples referred for diagnostic testing for heparin-induced thrombocytopenia. *European Journal of Haematology*. 2006;76(5):420-426.
33. Kreimann M, Brandt S, Krauel K, et al. Interaction between Platelet Factor 4 and Heparins: Thermodynamic determines expression of the binding site for Anti-Platelet Factor 4/Heparin Antibodies. *Blood*. 2014;subitted(submitted).
34. Strauss J, Burnham NA, Camesano TA. Atomic force microscopy study of the role of LPS O-antigen on adhesion of *E. coli*. *Journal of Molecular Recognition*. 2009;22(5):347-355.
35. Mittra I, Nair NK, Mishra PK. Nucleic acids in circulation: are they harmful to the host? *Journal of Biosciences*. 2012;37(2):301-312.
36. Kikuchi Y, Rykova EY, P.P. L, V.V. V. Extracellular Nucleic Acids - Chapter 7 - Circulating Nucleic Acids in Health and Disease. In: Gross HJ, J.M. B, eds. *Extracellular Nucleic Acids*. Vol. 25. Berlin: Springer Science & Business Media; 2010:244.
37. Lam NY, Rainer TH, Chan LY, Joynt GM, Lo YM. Time course of early and late changes in plasma DNA in trauma patients. *Clinical Chemistry*. 2003;49(8):1286-1291.
38. Lo YM, Zhang J, Leung TN, Lau TK, Chang AM, Hjelm NM. Rapid clearance of fetal DNA from maternal plasma. *American Journal of Human Genetics*. 1999;64(1):218-224.
39. Ni X, Castanares M, Mukherjee A, Lupold SE. Nucleic Acid Aptamers: Clinical Applications and Promising New Horizons. *Current Medicinal Chemistry*. 2011;18(27):4206-4214.

40. Kimmel SE, Sekeres MA, Berlin JA, Goldberg LR, Strom BL. Adverse events after protamine administration in patients undergoing cardiopulmonary bypass: risks and predictors of under-reporting. *Journal of Clinical Epidemiology*. 1998;51(1):1-10.
41. Bull BS, Korpman RA, Huse WM, Briggs BD. Heparin therapy during extracorporeal circulation. I. Problems inherent in existing heparin protocols. *The Journal of Thoracic and Cardiovascular Surgery*. 1975;69(5):674-684.
42. Deykin D. Current Concepts - Use of Heparin. *New England Journal of Medicine*. 1969;280(17):937-&.
43. Arepally GM, Ortel TL. Clinical practice. Heparin-induced thrombocytopenia. *New England Journal of Medicine*. 2006;355(8):809-817.
44. Ellerhorst JA, Comstock JP, Nell LJ. Protamine antibody production in diabetic subjects treated with NPH insulin. *American Journal of the Medical Sciences*. 1990;299(5):298-301.
45. Nell LJ, Thomas JW. Frequency and specificity of protamine antibodies in diabetic and control subjects. *Diabetes*. 1988;37(2):172-176.
46. Bloch DP. A catalog of Sperm Histones - Chapter 5: Histones of Sperm: Springer-Verlag US; 1969.
47. Roque A, Ponte I, Suau P. Secondary structure of protamine in sperm nuclei: an infrared spectroscopy study. *Bmc Structural Biology*. 2011;11.
48. Awotwe-Otoo D, Agarabi C, Keire D, et al. Physicochemical Characterization of Complex Drug Substances: Evaluation of Structural Similarities and Differences of Protamine Sulfate from Various Sources. *American Association of Pharmaceutical Scientists Journal*. 2012;14(3):619-626.
49. Voet D, Voet JG. Biochemistry. Vol. 4th Edition; 2011.
50. Kaplan KL, Broekman MJ, Chernoff A, Lesznik GR, Drillings M. Platelet Alpha-Granule Proteins - Studies on Release and Subcellular-Localization. *Blood*. 1979;53(4):604-618.
51. Witt DP, Lander AD. Differential binding of chemokines to glycosaminoglycan subpopulations. *Current Biology*. 1994;4(5):394-400.
52. Jordan RE, Oosta GM, Gardner WT, Rosenberg RD. The kinetics of hemostatic enzyme-antithrombin interactions in the presence of low molecular weight heparin. *Journal of Biological Chemistry*. 1980;255(21):10081-10090.
53. Olson ST, Bjork I, Sheffer R, Craig PA, Shore JD, Choay J. Role of the antithrombin-binding pentasaccharide in heparin acceleration of antithrombin-proteinase reactions. Resolution of the antithrombin conformational change contribution to heparin rate enhancement. *Journal of Biological Chemistry*. 1992;267(18):12528-12538.
54. Conrad HE. Heparin-binding proteins; chapter 7: Antithrombin, the Prototypic Heparin-Binding Protein: Eslevier; 1998.
55. Arepally GM, Ortel TL. Heparin-induced thrombocytopenia. *New England Journal of Medicine*. 2006;355(8):809-817.
56. Warkentin TE, Greinacher A, Koster A, Lincoff AM, American College of Chest P. Treatment and prevention of heparin-induced thrombocytopenia: American College of Chest Physicians Evidence-Based Clinical Practice Guidelines (8th Edition). *Chest*. 2008;133(6 Suppl):340S-380S.
57. Warkentin TGA. Heparin-induced Thrombocytopenia (Fundamental and Clinical Cardiology). Vol. 5. USA: Taylor and Francis Group; 2013.
58. Alban S, Krauel K, Greinacher A. Role of Sulfated Polysaccharides in the Pathogenesis of Heparin-Induced Thrombocytopenia. In: Heparin-Induced-Thrombocytopenia (Fundamental and Clinical Cardiology). Vol. 5: Boca Raton, USA: Taylor and Francis Group; 2013.
59. Bakchoul T, Zollner H, Amiral J, et al. Anti-protamine-heparin antibodies: incidence, clinical relevance, and pathogenesis. *Blood*. 2013;121(15):2821-2827.
60. Wagner I, Musso H. New Naturally-Occurring Amino-Acids. *Angewandte Chemie-International Edition*. 1983;22(11):816-828.
61. Jakubke HDSN. Peptides from A-Z - A Concicse Encyclopedia: Wiley-VCH; 2008.

-
62. Hertweck C. Biosynthesis and Charging of Pyrrolysine, the 22nd Genetically Encoded Amino Acid. *Angewandte Chemie-International Edition*. 2011;50(41):9540-9541.
 63. Zhang D, Milan S. Medical Biometrics - Second International Conference: Springer; 2010.
 64. Anfinsen CB. Principles That Govern Folding of Protein Chains. *Science*. 1973;181(4096):223-230.
 65. Levinthal C. Are There Pathways for Protein Folding. *Journal De Chimie Physique Et De Physico-Chimie Biologique*. 1968;65(1):44-&.
 66. Berezovsky IN, Trifonov EN. Loop fold structure of proteins: Resolution of Levinthal's paradox. *Journal of Biomolecular Structure & Dynamics*. 2002;20(1):5-6.
 67. Trifonov EN, Berezovsky IN. Evolutionary aspects of protein structure and folding. *Current Opinion in Structural Biology*. 2003;13(1):110-114.
 68. Zhang XH, Chen LQ, Bancroft DP, Lai CK, Maione TE. Crystal-Structure of Recombinant Human Platelet Factor-4. *Biochemistry*. 1994;33(27):8361-8366.
 69. Tunnacliffe A, Majumdar S, Yan B, Poncz M. Genes for beta-thromboglobulin and platelet factor 4 are closely linked and form part of a cluster of related genes on chromosome 4. *Blood*. 1992;79(11):2896-2900.
 70. Poncz M, Surrey S, LaRocco P, et al. Cloning and characterization of platelet factor 4 cDNA derived from a human erythroleukemic cell line. *Blood*. 1987;69(1):219-223.
 71. Deuel TF, Keim PS, Farmer M, Heinrikson RL. Amino-Acid Sequence of Human Platelet Factor 4. *Proceedings of the National Academy of Sciences of the United States of America*. 1977;74(6):2256-2258.
 72. Rucinski B, Niewiarowski S, James P, Walz DA, Budzynski AZ. Antiheparin Proteins Secreted by Human Platelets - Purification, Characterization, and Radioimmunoassay. *Blood*. 1979;53(1):47-62.
 73. Stcharles R, Walz DA, Edwards BFP. The 3-Dimensional Structure of Bovine Platelet Factor-4 at 3.0-Å Resolution. *Journal of Biological Chemistry*. 1989;264(4):2092-2099.
 74. Mayo KH, Roongta V, Ilyina E, et al. Nmr Solution Structure of the 32-Kda Platelet Factor-4 Elr-Motif N-Terminal Chimera - a Symmetrical Tetramer. *Biochemistry*. 1995;34(36):11399-11409.
 75. Mayo KH, Chen MJ. Human-Platelet Factor-4 Monomer Dimer Tetramer Equilibria Investigated by H-1-Nmr Spectroscopy. *Biochemistry*. 1989;28(24):9469-9478.
 76. Handin RI, Cohen HJ. Purification and Binding Properties of Human Platelet Factor 4. *Journal of Biological Chemistry*. 1976;251(14):4273-4282.
 77. Mayo KH, Ilyina E, Roongta V, et al. Heparin-Binding to Platelet Factor-Iv - an Nmr and Site-Directed Mutagenesis Study - Arginine Residues Are Crucial for Binding. *Biochemical Journal*. 1995;312:357-365.
 78. Stuckey JA, Charles RS, Edwards BFP. A Model of the Platelet Factor-Iv Complex with Heparin. *Proteins-Structure Function and Genetics*. 1992;14(2):277-287.
 79. Rabellino EM, Levene RB, Leung LL, Nachman RL. Human megakaryocytes. II. Expression of platelet proteins in early marrow megakaryocytes. *Journal of Experimental Medicine*. 1981;154(1):88-100.
 80. McLaren KM, Holloway L, Pepper DS. Human platelet factor 4 and tissue mast cells. *Thrombosis Research*. 1980;19(1-2):293-297.
 81. McKay DJ, Renaux BS, Dixon GH. Rainbow trout protamines. Amino acid sequences of six distinct proteins from a single testis. *European Journal of Biochemistry*. 1986;158(2):361-366.
 82. Sakai M, Fujii-Kuriyama Y, Saito T, Muramatsu M. Closely related mRNA sequences of protamines in rainbow trout testis. *Journal of Biochemistry*. 1981;89(6):1863-1868.
 83. States JC, Connor W, Wosnick MA, Aiken JM, Gedamu L, Dixon GH. Nucleotide sequence of a protamine component CII gene of *Salmo gairdnerii*. *Nucleic Acids Research*. 1982;10(15):4551-4563.
 84. Gill TA, Singer DS, Thompson JW. Purification and analysis of protamine. *Process Biochemistry*. 2006;41(8):1875-1882.
-

85. Nelson DL, Cox MC. Lehninger - Principles of Biochemistry. Vol. 6th. New York: W.H. Freeman and Company; 2013.
86. Fraser JRE, Laurent TC, Laurent UBG. Hyaluronan: Its nature, distribution, functions and turnover. *Journal of Internal Medicine*. 1997;242(1):27-33.
87. Lee S, Raw A, Yu L, et al. Scientific considerations in the review and approval of generic enoxaparin in the United States. *Nature Biotechnology*. 2013;31(3):220-226.
88. Mulloy B, Gray E, Barrowcliffe TW. Characterization of unfractionated heparin: comparison of materials from the last 50 years. *Thrombosis and Haemostasis*. 2000;84(6):1052-1056.
89. Harris EN, Weigel JA, Weigel PH. The human hyaluronan receptor for endocytosis (HARE/Stabilin-2) is a systemic clearance receptor for heparin. *Journal of Biological Chemistry*. 2008;283(25):17341-17350.
90. Gray E, Mulloy B, Barrowcliffe TW. Heparin and low-molecular-weight heparin. *Thrombosis and Haemostasis*. 2008;99(5):807-818.
91. Xu Y, Cai C, Chandarajoti K, et al. Homogeneous low-molecular-weight heparins with reversible anticoagulant activity. *Nature Chemical Biology*. 2014.
92. Petitou M, van Boeckel CA. A synthetic antithrombin III binding pentasaccharide is now a drug! What comes next? *Angewandte Chemie-International Edition*. 2004;43(24):3118-3133.
93. Al Dieri R, Wagenvoort R, van Dedem GW, Beguin S, Hemker HC. The inhibition of blood coagulation by heparins of different molecular weight is caused by a common functional motif--the C-domain. *Journal of Thrombosis and Haemostasis*. 2003;1(5):907-914.
94. European_Directorate_for_Quality_of_Medicines-Council_of_Europe_(COE). European Pharmacopoeia 6th Edition. Europe: European Pharmacopoeia (Pharmacopoea Europaea, Ph. Eur.); 2008, 2041-2042.
95. Melnikova I. The anticoagulants market. *Nature Reviews Drug discovery*. 2009;8(5):353-354.
96. Harder S. Renal Profiles of Anticoagulants. *Journal of Clinical Pharmacology*. 2012;52(7):964-975.
97. Zhang ZQ, Weiwer M, Li BYZ, Kemp MM, Daman TH, Linhardt RJ. Oversulfated chondroitin sulfate: Impact of a heparin impurity, associated with adverse clinical events, on low-molecular-weight heparin preparation. *Journal of Medicinal Chemistry*. 2008;51(18):5498-5501.
98. Kennedy TP, Walenga J. Administering 2-O desulfated heparin or 2-O, 3-O desulfated heparin; does not produce platelet activation in the presence of serum containing HIT antibodies. Vol. CA2585640A1; 2008.
99. Fryer A, Huang YC, Rao G, et al. Selective O-desulfation produces nonanticoagulant heparin that retains pharmacological activity in the lung. *Journal of Pharmacology and Experimental Therapeutics*. 1997;282(1):208-219.
100. Rao NV, Argyle B, Xu XY, et al. Low anticoagulant heparin targets multiple sites of inflammation, suppresses heparin-induced thrombocytopenia, and inhibits interaction of RAGE with its ligands. *American Journal of Physiology-Cell Physiology*. 2010;299(1):C97-C110.
101. Walenga J, Kennedy TP. 2-O, 3-O DESULFATED HEPARIN FOR THE TREATMENT OF HEPARIN-INDUCED THROMBOCYTOPENIA (HIT) SYNDROME. In: Paringenix IT, AZ 85711 (US) ed. EUROPEAN PATENT SPECIFICATION. Vol. EP 1 807 095 B1. GB; 2005.
102. Walenga JM, Jeske WP, Bara L, Samama MM, Fareed J. Biochemical and pharmacologic rationale for the development of a synthetic heparin pentasaccharide. *Thrombosis Research*. 1997;86(1):1-36.
103. Walenga JM, Jeske WP, Samama MM, Frapaise FX, Bick RL, Fareed J. Fondaparinux: a synthetic heparin pentasaccharide as a new antithrombotic agent. *Expert Opin Investig Drugs*. 2002;11(3):397-407.
104. Weitz JI, Linkins LA. Beyond heparin and warfarin: the new generation of anticoagulants. *Expert Opin Investig Drugs*. 2007;16(3):271-282.

-
105. Monfort J, Pelletier JP, Garcia-Giralt N, Martel-Pelletier J. Biochemical basis of the effect of chondroitin sulphate on osteoarthritis articular tissues. *Ann Rheum Dis*. 2008;67(6):735-740.
 106. Barnhill JG, Fye CL, Williams DW, Reda DJ, Harris CL, Clegg DO. Chondroitin product selection for the glucosamine/chondroitin arthritis intervention trial. *J Am Pharm Assoc (2003)*. 2006;46(1):14-24.
 107. Volpi N. Oral bioavailability of chondroitin sulfate (Condrosulf) and its constituents in healthy male volunteers. *Osteoarthritis Cartilage*. 2002;10(10):768-777.
 108. Rankin JC, Jeanes A. Evaluation of the Periodate Oxidation Method for Structural Analysis of Dextran. *Journal of the American Chemical Society*. 1954;76(17):4435-4441.
 109. Dimler RJ, Wolff IA, Sloan JW, Rist CE. Interpretation of Periodate Oxidation Data on Degraded Dextran. *Journal of the American Chemical Society*. 1955;77(24):6568-6573.
 110. Lindberg B, Svensson S. Structural Studies on Dextran from *Leuconostoc Mesenteroides* Nr1 B-512. *Acta Chemica Scandinavica*. 1968;22(6):1907-&.
 111. Bovey FA. Enzymatic Polymerization .1. Molecular Weight and Branching during the Formation of Dextran. *Journal of Polymer Science*. 1959;35(128):167-182.
 112. Senti FR, Hellman NN, Ludwig NH, et al. Viscosity, Sedimentation, and Light-Scattering Properties of Fractions of an Acid-Hydrolyzed Dextran. *Journal of Polymer Science*. 1955;17(86):527-546.
 113. Katchalsky A. Polyelectrolytes + Their Biological Interactions. *Biophys J*. 1964;4(1sp):9-&.
 114. Kitajima S, Takuma S, Morimoto M. Histological analysis of murine colitis induced by dextran sulfate sodium of different molecular weights. *Exp Anim*. 2000;49(1):9-15.
 115. Hirono I, Kuhara K, Yamaji T, Hosaka S, Golberg L. Carcinogenicity of dextran sulfate sodium in relation to its molecular weight. *Cancer Lett*. 1983;18(1):29-34.
 116. Larm O, Lindberg B, Svensson S. Studies on Length of Side Chains of Dextran Elaborated by *Leuconostoc-Mesenteroides* Nr1 B-512. *Carbohydrate Research*. 1971;20(1):39-&.
 117. Reed RK, Lilja K, Laurent TC. Hyaluronan in the Rat with Special Reference to the Skin. *Acta Physiologica Scandinavica*. 1988;134(3):405-411.
 118. Shu XZ, Ghosh K, Liu YC, et al. Attachment and spreading of fibroblasts on an RGD peptide-modified injectable hyaluronan hydrogel. *Journal of Biomedical Materials Research Part A*. 2004;68A(2):365-375.
 119. Meyer K, Hobby GL, Chaffee E, Dawson MH. The Hydrolysis of Hyaluronic Acid by Bacterial Enzymes. *Journal of Experimental Medicine*. 1940;71(2):137-146.
 120. Scott JE. Supramolecular Organization of Extracellular-Matrix Glycosaminoglycans, In vitro and in the Tissues. *Federation of American Societies For Experimental Biology Journal*. 1992;6(9):2639-2645.
 121. Lewis SL, Dirksen SR, Heitkemper MM, Bucher L, Camera IM. Medical Surgical Nursing. Vol. 8: Elsevier; 2010.
 122. Pasteur L. On the viscous fermentation and the butyrous fermentation. *Bulletin de la Société Chimique de France*. 1861;11(11):30-31.
 123. Vink H. Precision Measurements of Osmotic Pressure in Concentrated Polymer Solutions. *European Polymer Journal*. 1971;7(10):1411-&.
 124. Staat RH, Gawronsk Th, Schachte Cf. Detection and Preliminary Studies on Dextranase-Producing Microorganisms from Human Dental Plaque. *Infection and Immunity*. 1973;8(6):1009-1016.
 125. Achbergerova L, Nahalka J. Polyphosphate--an ancient energy source and active metabolic regulator. *Microbial Cell Factories*. 2011;10:63.
 126. Gray MJ, Wholey WY, Wagner NO, et al. Polyphosphate is a primordial chaperone. *Molecular Cell*. 2014;53(5):689-699.
 127. Rao NN, Gomez-Garcia MR, Kornberg A. Inorganic polyphosphate: essential for growth and survival. *Annual Review of Biochemistry*. 2009;78:605-647.
-

128. Ruiz FA, Lea CR, Oldfield E, Docampo R. Human platelet dense granules contain polyphosphate and are similar to acidocalcisomes of bacteria and unicellular eukaryotes. *Journal of Biological Chemistry*. 2004;279(43):44250-44257.
129. Herzberg MC, Krishnan LK, Macfarlane GD. Involvement of Alpha(2)-Adrenoceptors and G-Proteins in the Modulation of Platelet Secretion in Response to Streptococcus-Sanguis. *Critical Reviews in Oral Biology & Medicine*. 1993;4(3-4):435-442.
130. Muller F, Mutch NJ, Schenk WA, et al. Platelet polyphosphates are proinflammatory and procoagulant mediators in vivo. *Cell*. 2009;139(6):1143-1156.
131. Moreno-Sanchez D, Hernandez-Ruiz L, Ruiz FA, Docampo R. Polyphosphate Is a Novel Pro-inflammatory Regulator of Mast Cells and Is Located in Acidocalcisomes. *Journal of Biological Chemistry*. 2012;287(34):28435-28444.
132. Kornberg A, Rao NN, Ault-Riche D. Inorganic polyphosphate: A molecule of many functions. *Annual Review of Biochemistry*. 1999;68:89-125.
133. Morrissey JH. Polyphosphate: a link between platelets, coagulation and inflammation. *International Journal of Hematology*. 2012;95(4):346-352.
134. Morrissey JH, Choi SH, Smith SA. Polyphosphate: an ancient molecule that links platelets, coagulation, and inflammation. *Blood*. 2012;119(25):5972-5979.
135. Smith SA, Mutch NJ, Baskar D, Rohloff P, Docampo R, Morrissey JH. Polyphosphate modulates blood coagulation and fibrinolysis. *Proceedings of the National Academy of Sciences of the United States of America*. 2006;103(4):903-908.
136. Smith SA, Choi SH, Davis-Harrison R, et al. Polyphosphate exerts differential effects on blood clotting, depending on polymer size. *Blood*. 2010;116(20):4353-4359.
137. Smith SA, Morrissey JH. Polyphosphate enhances fibrin clot structure. *Blood*. 2008;112(7):2810-2816.
138. Mutch NJ, Engel R, de Willige SU, Philippou H, Ariens RAS. Polyphosphate modifies the fibrin network and down-regulates fibrinolysis by attenuating binding of tPA and plasminogen to fibrin. *Blood*. 2010;115(19):3980-3988.
139. Choi SH, Smith SA, Morrissey JH. Polyphosphate is a cofactor for the activation of factor XI by thrombin. *Blood*. 2011;118(26):6963-6970.
140. Smith SA, Morrissey JH. Polyphosphate as a general procoagulant agent. *Journal of Thrombosis and Haemostasis*. 2008;6(10):1750-1756.
141. Whitman WB, Coleman DC, Wiebe WJ. Prokaryotes: The unseen majority. *Proceedings of the National Academy of Sciences of the United States of America*. 1998;95(12):6578-6583.
142. Fredrickson JK, Zachara JM, Balkwill DL, et al. Geomicrobiology of high-level nuclear waste-contaminated vadose sediments at the Hanford Site, Washington State. *Applied and Environmental Microbiology*. 2004;70(7):4230-4241.
143. Gram C. Ueber die isolirte Färbung der Schizomyceten in Schnitt- und Trockenpräparaten. *Fortschritte der Medicin*. 1884;2(6):185-189.
144. Tzeng YL, Datta A, Kolli VK, Carlson RW, Stephens DS. Endotoxin of Neisseria meningitidis composed only of intact lipid A: inactivation of the meningococcal 3-deoxy-D-manno-octulosonic acid transferase. *Journal of Bacteriology*. 2002;184(9):2379-2388.
145. Hershberger C, Binkley SB. Chemistry and metabolism of 3-deoxy-D-mannooctulosonic acid. I. Stereochemical determination. *Journal of Biological Chemistry*. 1968;243(7):1578-1584.
146. Raetz CR, Whitfield C. Lipopolysaccharide endotoxins. *Annual Review of Biochemistry*. 2002;71:635-700.
147. Benno Y, Sawada K, Mitsuoka T. The Intestinal Microflora of Infants - Composition of Fecal Flora in Breast-Fed and Bottle-Fed Infants. *Microbiology and Immunology*. 1984;28(9):975-986.
148. Yoshioka H, Iseki K, Fujita K. Development and Differences of Intestinal Flora in the Neonatal-Period in Breast-Fed and Bottle-Fed Infants. *Pediatrics*. 1983;72(3):317-321.

149. Hudault S, Guignot J, Servin AL. Escherichia coli strains colonising the gastrointestinal tract protect germfree mice against Salmonella typhimurium infection. *Gut*. 2001;49(1):47-55.
150. Reid G, Howard J, Gan BS. Can bacterial interference prevent infection? *Trends in Microbiology*. 2001;9(9):424-428.
151. Bentley R, Meganathan R. Biosynthesis of Vitamin-K (Menaquinone) in Bacteria. *Microbiological Reviews*. 1982;46(3):241-280.
152. Messing J, Crea R, Seeburg PH. A System for Shotgun DNA Sequencing. *Nucleic Acids Research*. 1981;9(2):309-321.
153. Rennemeier C, Hammerschmidt S, Niemann S, Inamura S, Zahringer U, Kehrel BE. Thrombospondin-1 promotes cellular adherence of Gram-positive pathogens via recognition of peptidoglycan. *Federation of American Societies For Experimental Biology Journal*. 2007;21(12):3118-3132.
154. Sneath G. Circular Dichroism - Principles and Applications. New York: Weinheim Wiley-VCH; 1994.
155. Greenfield NJ. Using circular dichroism spectra to estimate protein secondary structure. *Nature Protocols*. 2006;1(6):2876-2890.
156. Sreerama N, Woody RW. Estimation of protein secondary structure from circular dichroism spectra: Comparison of CONTIN, SELCON, and CDSSTR methods with an expanded reference set. *Analytical Biochemistry*. 2000;287(2):252-260.
157. Bohm G, Muhr R, Jaenicke R. Quantitative-Analysis of Protein Far Uv Circular-Dichroism Spectra by Neural Networks. *Protein Engineering*. 1992;5(3):191-195.
158. Whitmore L. WBA. DichroWeb. http://dichroweb.cryst.bbk.ac.uk/html/userguide_algorithms.shtml.
159. Freire E, Mayorga OL, Straume M. Isothermal Titration Calorimetry. *Analytical Chemistry*. 1990;62(18):A950-A959.
160. Christen J, Izatt RM, Hansen LD, Partridge FA. Entropy Titration. A Calorimetric Method for Determination of ΔG , ΔH , and ΔS from a Single Thermometric Titration. *Journal of Physical Chemistry*. 1966;70(6):2003-&.
161. Freyer MW, Lewis EA. Isothermal titration calorimetry: experimental design, data analysis, and probing macromolecule/ligand binding and kinetic interactions. *Methods Cell Biol*. 2008;84:79-113.
162. Wiseman T, Williston S, Brandts JF, Lin LN. Rapid Measurement of Binding Constants and Heats of Binding Using a New Titration Calorimeter. *Analytical Biochemistry*. 1989;179(1):131-137.
163. Record MT, Jr., Lohman ML, De Haseth P. Ion effects on ligand-nucleic acid interactions. *Journal of Molecular Biology*. 1976;107(2):145-158.
164. Mascotti DP, Lohman TM. Thermodynamics of single-stranded RNA binding to oligolysines containing tryptophan. *Biochemistry*. 1992;31(37):8932-8946.
165. Laugel N, Betscha C, Winterhalter M, Voegel JC, Schaaf P, Ball V. Relationship between the growth regime of polyelectrolyte multilayers and the polyanion/polycation complexation enthalpy. *Journal of Physical Chemistry B*. 2006;110(39):19443-19449.

Image Sources

Figure 3.0.1 B: Prof. Wright (Weber State University)

http://classconnection.s3.amazonaws.com/229/flashcards/3132229/jpg/control_spot_-1_large-141058E43F81380024E.jpg

Figure 3.1.1: Wadsworth Center (New York state department of health)

<http://www.wadsworth.org/databank/ecoli.htm>

8. Statutory Declaration

Hiermit erkläre ich, dass diese Arbeit bisher von mir weder an der Mathematisch-Naturwissenschaftlichen Fakultät der Ernst-Moritz-Arndt-Universität Greifswald noch einer anderen wissenschaftlichen Einrichtung zum Zwecke der Promotion eingereicht wurde.

Ferner erkläre ich, dass ich diese Arbeit selbständig verfasst und keine anderen als die darin angegebenen Hilfsmittel und Hilfen benutzt und keine Textabschnitte eines Dritten ohne Kennzeichnung übernommen habe.

9. Curriculum Vitae

Sven Brandt

born August 21st 1982 in Rostock

married, one child

since May 2010	Scientific researcher and PhD student at ZIK HIKE in the Nanostructure group in Greifswald <ul style="list-style-type: none">- poster & talk: 3rd International Meeting "Conformational transitions in macromolecular interactions" 2014 – Halle- talk: DPG 2013 – Regensburg- poster: DPG 2012 – Berlin- talk: MPI summerschool 2012 – Lecce/Italy
July 2009 to April 2010	Scientific researcher at the Kiel Neurology Hospital <ul style="list-style-type: none">- talk: International Group Meeting Neurology – Gargnano/Italy
October 2008 to June 2009	Diploma thesis at the NRL (Neurodegeneration Research Lab) in Rostock - "Investigations of intracerebral electrodes for deep brain stimulation (DBS) – application, optimization and simulation"
March 2007 to October 2008	Student assistant at the company NeuroProof GmbH in Rostock-Warnemünde - remedy testing on neuronal networks cultured on multi electrode arrays
October 2003 to June 2009	Studies of biological sciences at the University of Rostock <ul style="list-style-type: none">- main subject: animal physiology (focus on neurobiology)- biological minor subjects: bio-systems technology, microbiology- non biological minor subject: molecular neuropathology
August 1993 to July 2002	Abitur at the Ernst Barlach Gymnasium in Rostock

Publications:

Platelet factor 4 binding to lipid A of Gram-negative bacteria exposes PF4/heparin-like epitopes

Krystin Krauel, Claudia Weber, Sven Brandt, Ulrich Zähringer, Uwe Mamat, Andreas Greinacher, Sven Hammerschmidt
Blood, 2012 Oct 18;120(16):3345-52

Anti-protamine-heparin antibodies: incidence, clinical relevance, and pathogenesis

Tamam Bakchoul, Heike Zöllner, Jean Amiral, Simon Panzer, Sixten Selleng, Thomas Kohlmann, Sven Brandt, Mihaela Delcea, Theodore E. Warkentin, Ulrich J. Sachs, Andreas Greinacher
Blood, 2013 Apr 11;121(15):2821-7

Vaccination with anti-idiotypic antibody ganglidiomab mediates a GD2-specific anti-neuroblastoma immune response

Holger N. Lode, Manuela Schmidt, Diana Seidel, Nicole Huebener, Diana Brackrock, Matthias Bleeke, Daniel Reker, Sven Brandt, Hans-Peter Müller, Christiane A. Helm, Nikolai Siebert
Cancer Immunology and Immunotherapy, 2013 Jun;62(6):999-1010

Complex formation with nucleic acids and aptamers alters the antigenic properties of platelet factor 4

Miriam E. Jaax, Krystin Krauel, Thomas Marschall, Sven Brandt, Julia Gansler, Birgitt Füll, Bettina Appel, Silvia Fischer, Stephan Block, Christiane A. Helm, Sabine Müller, Klaus T. Preissner, Andreas Greinacher
Blood, 2013 Jul 11;122(2):272-81

Characterization of the Conformational Changes in Platelet Factor 4 Induced By Polyanions: Towards In-Vitro Prediction of Antigenicity

Sven Brandt, Krystin Krauel, Kay E. Gottschalk, Thomas Renné, Christiane A. Helm, Andreas Greinacher, Stephan Block
Thrombosis Haemostasis 2014; 112: 53-64

Interaction between Platelet Factor 4 and Heparins: Thermodynamics determines Conformational Changes required for binding of Anti-Platelet Factor 4/Heparin Antibodies

Martin Kreimann, Sven Brandt, Stephan Block, Krystin Krauel, Andreas Greinacher, Mihaela Delcea
Blood, 2014 Aug 22; doi: 10.1182/blood-2014-03-559518

Polyphosphate chain length determines the antigenicity of the complexes formed with platelet factor 4 (PF4) and the binding of PF4 to bacteria

Sven Brandt, Krystin Krauel, Miriam Jaax, Thomas Renné, Christiane Helm, Sven Hammerschmidt, Mihaela Delcea, Andreas Greinacher
submitted to Blood

Evolution and Characterization of Aptamers targeting Platelet Factor 4

Thomas Marschall, Sven Brandt, Martin Kreimann, Sonja Petkovic, Jennifer Frommer, Bettina Appel, Andreas Greinacher, Mihaela Delcea, Sabine Müller
in preparation

Acknowledgement

First of all, I am grateful to my family for endless inspiration, especially Katharina for having a different view on many things and supporting me in stressful times. I also thank Karl for mostly sleeping well at night. Many thanks also to my parents for their funding and support during studies, without you this thesis would not have been possible.

My sincere gratitude to:

- Prof. Kay E. Gottschalk for giving me the opportunity to work on the subject and for providing me a comfortable start at ZIK HIKE,
- Prof. Christiane A. Helm for taking over the supervision of my thesis and her physical input and support during writing,
- Prof. Andreas Greinacher for countless inspiring ideas,
- Dr. Stephan Block for all the input letting me have a different view on many results,
- Dr. Mihaela Delcea for supervision, giving me the opportunity to write my own papers, although the first one took quite long and for helping with the writing of thesis,
- Dr. Krystin Krauel for her introducing me into several techniques and for answering many many questions,
- Dr. Stephan Schultz and Jan Wesche for many scientific and non-scientific discussions,
- and finally Dr. Hans-Peter Müller for endless conversations about *God and the world of proteins*.

I also place on record, my sense of gratitude to one and all who, directly and indirectly, have lent their helping hand for this thesis.